NOVEL NEAR-INFRARED ABSORBING DYES

by

Stephen Nigel Corns

Submitted in accordance with the
requirements for the degree of
Doctor of Philosophy

Department of Colour Chemistry and Dyeing
University of Leeds
October 1990

To Mum, Dad and Paul

ACKNOWLEDGEMENTS

I wish to sincerely thank Dr J. Griffiths for his valuable advice, assistance, and encouragement (and wry sarcasm!) throughout the course of this work.

I also would like to thank Professor D. M. Lewis for allowing this work to be undertaken in his Department. My thanks are also extended to the members of the Technical and Academic staff of the Department for their friendship and assistance given during my University life.

I also wish to thank my friends, especially Ian, both in Leeds and in Lancashire for the valuable contributions they have made to my life.

Special thanks must be reserved for my parents who have, without question, always helped, and actively supported me throughout my entire education, culminating with their appreciable assistance in the preparation of this text

Finally, my thoughts turn to my great friend and inspiration, the late Mr Len Dixon, to whom I owe so many thanks for his invaluable contributions towards the content of this thesis. You are sadly missed.

SYNOPSIS

New near-infrared absorbing donor-acceptor chromophores have been investigated by varying the electron donating and accepting strength of the two halves of the molecule within wide limits. The dihydroperimidine, perimidine, Michler's ethylene and 1-decyl-2(1H)-methyl-benz[c,d]indolium iodide residues were examined as donor residues, and these were coupled to 4-nitrobenzenediazonium chloride to give monoazo dyes. The λ_{max} values of these gave a qualitative indication of relative electron donor strengths, and the 1-ethyl-2-methylperimidine azo dyes proved to be the most bathochromic, being blue in colour. The dyes were amongst the most bathochromic monoazo dyes yet prepared containing the 4-nitrophenylazo residue.

The N-alkyl-3-cyano-6-hydroxy-4-methyl-2-pyridone system was investigated as a potentially powerful electron acceptor system, and the 5-formyl and 5-nitroso derivatives were condensed with Michler's ethylene and 1-decyl-2(1H)-methyl-benz[c,d]indolium iodide to give new donor-acceptor dyes. The aza dyes prepared from the nitroso compounds proved to be the most bathochromic in accord with PMO theory and many were near-infrared absorbing.

A series of near-infrared absorbing squarylium dyes with narrow, intense absorption bands at about 800nm were obtained by reacting squaric acid with 2,2-disubstituted dihydroperimidines. The first dyes of this type possessed poor organic solvent solubilities but, through modification of the 2,2-substituents of the dihydroperimidines it was possible to obtain squarylium dyes with good organic solvent solubility, this being a much sought after property of infrared dyes. Other squarylium dyes were obtained by the reaction of squaric acid with 1-ethyl-2-methylperimidine, Michler's ethylene and 1-decyl-2(1H)-methyl-benz[c,d]indolium iodide. The latter two dyes absorbed in the infrared region at 809 and 900nm respectively in toluene.

A modified procedure for the synthesis of croconic acid was developed, which enables the acid to be obtained in the anhydrous form readily. Reaction of croconic acid with 3-hydroxy-N,N-dialkylanilines afforded highly bathochromic dyes (λ_{max} ca. 830nm). Reaction with 1- decyl-2(1H)-methyl benz[c,d]indolium iodide gave a croconium dye that absorbed beyond 1000nm. The reaction of 8-hydroxyjulolidine with croconic acid was particularly interesting as it occurred readily at room temperature. Thus it was possible to undertake a kinetic study of mechanistic aspects of the condensation reaction between croconic acid and arylamines. The results indicated that the optimum reaction conditions involved using a low proportion of an alcohol in a non-polar aprotic solvent in the presence of a weak acid catalyst.

Dyes were also obtained from the reaction of various electrophilic chlorine-substituted compounds with electron-donor aromatic residues, thus giving new donor-acceptor dyes, several of which were near-infrared absorbing with low molecular masses and good organic solvent solubilities. The dyes were, however, strongly coloured due to their broad absorption bands which extended well into the visible region.

The thermal and photochemical stabilities of representative examples of all the infrared dye classes prepared in this work have been examined, using standard procedures.

CONTENTS

LIST OF TABLES

LIST OF FIGURES

1. A SURVEY OF DEVELOPMENTS IN NEAR-INFRARED ABSORBING DYES.

1.1 INTRODUCTION

Since Perkin's discovery of Mauveine in 1856 research in dye chemistry has been intensive and has made many significant advances. In recent years however, the focus of effort has, notably, moved away from the traditional areas of coloration of textiles and other polymer substrates into new high technology fields. It is in the latter sphere that near-infrared absorbing dyes, ie. dyes that absorb light beyond 700nm, find greatest use. Although infrared dyes have been known for many years their uses in traditional areas were, and still are severely restricted. This is because light absorbed by a dye beyond about 750nm is invisible to the human eye and so infrared dyes are undetectable to the observer.

For many high technology applications the absorption spectrum of an infrared dye should show ideally minimal absorption between 400-700nm (the visible region) and possess a narrow intense absorption band (ε_{max} greater than 20,000 $lmol^{-1}cm^{-1}$) at the desired point beyond 700nm (Fig. 1).

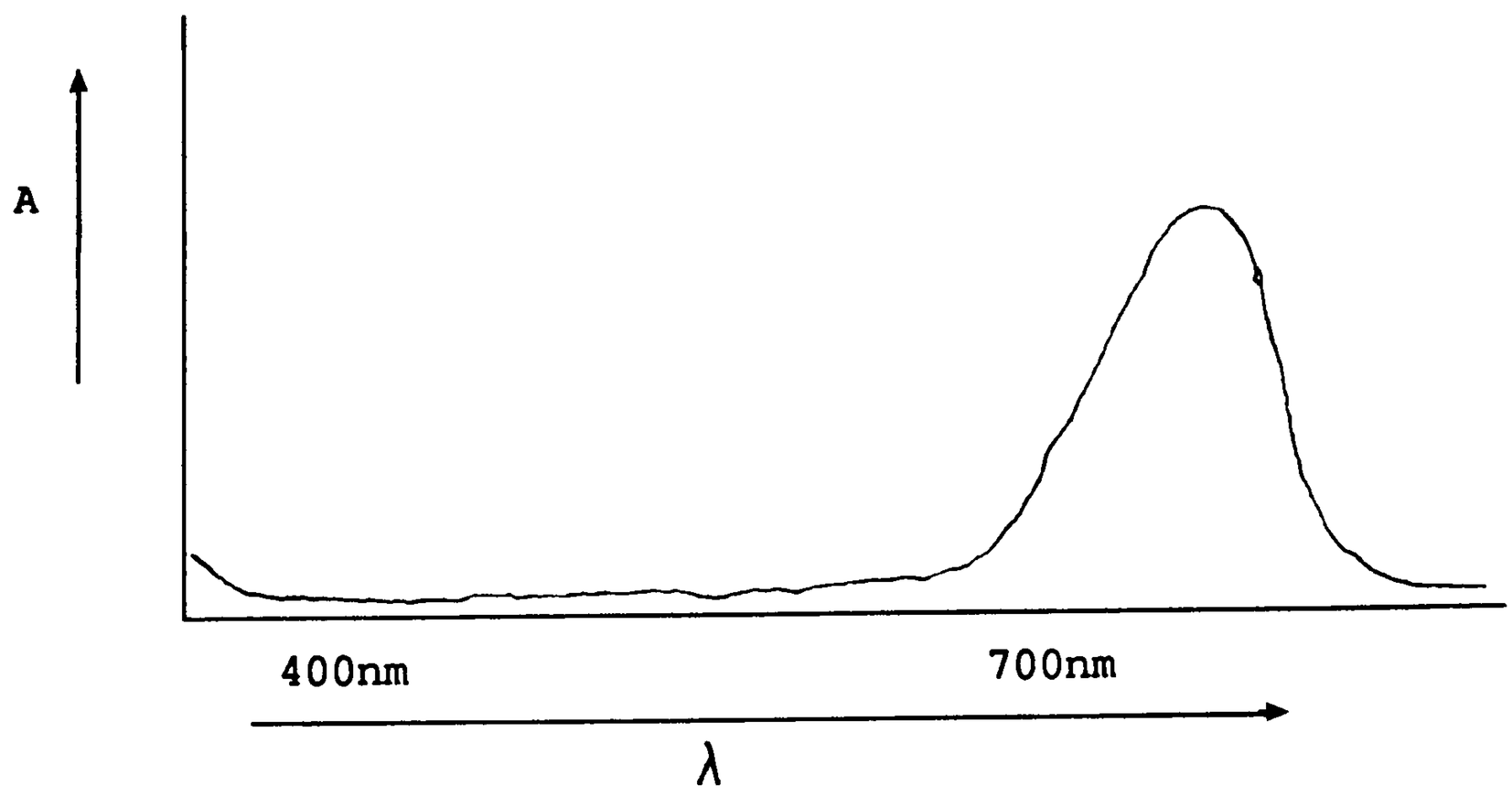

A = Absorbance

λ = Wavelength

Fig. 1: Idealised uv-visible absorption curve for an infrared dye.

Such demands on a dye chromophore severely limits the π-electron structure of the molecule. Thus the energy gap between the highest occupied molecular orbital (HOMO) and lowest unoccupied molecular orbital (LUMO) must be very narrow (150KJmol^{-1} or less). At the same time other possible transitions (eg. HOMO-1 ⟶ LUMO and HOMO ⟶ LUMO+1) must be sufficiently high in energy to avoid absorption of visible light (ideally greater than 300KJmol^{-1}), (Fig. 2).

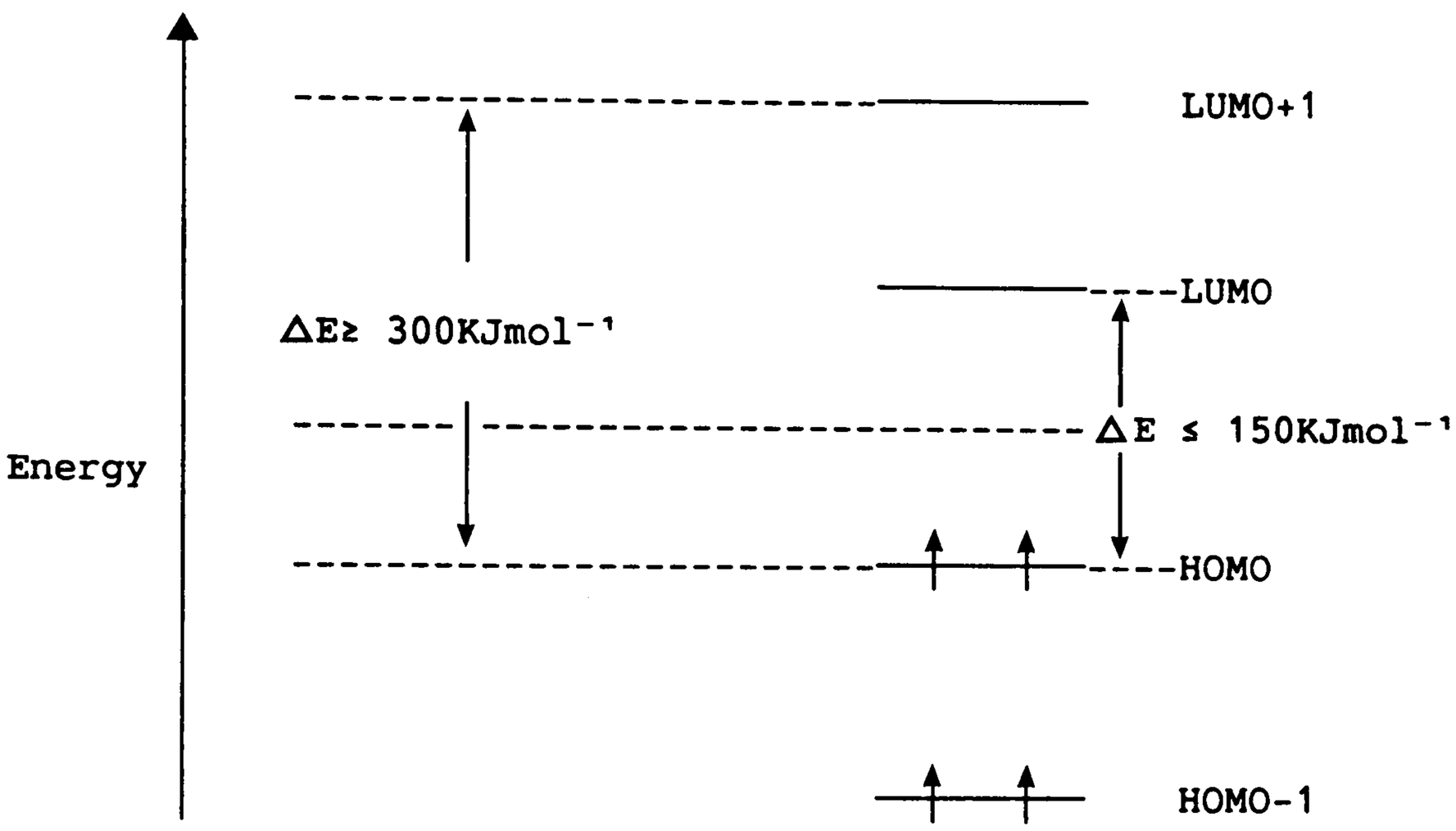

Fig.2 : Disposition of molecular orbitals for a typical i.r. dye.

In order to obtain a π-electron structure with such characteristics it is necessary either to modify traditional dye chromophores or to develop completely new dye chromogens, and to aid the chemist in this quest the PPP-molecular orbital theory[1,2] has been developed specifically for the investigation of colour-structure relationships[3]. Therefore, the theory can now be applied quantitatively to the design of dye chromophores in order to predict their colour and colour-related properties.

The major dye classes that give rise to infrared absorbing dyes are:-

i. Cyanine-type dyes.

ii. Donor-acceptor chromogens

iii. Metal complex dyes.

Each of these classes can be subdivided further.

As indicated, the near-infrared dyes have many uses in high technology but also find applications in more everyday technologies. Some typical uses include:-

i. Solar screens (eg. car windscreens/windows etc.).

ii. Laser screens (eg. military uses; protective goggles etc.).

iii. Solar heating (eg. salt water evaporation; horticultural plastics).

iv. Optical data storage systems.

v. Thermal imaging processes.

vi. Infrared camouflage.

vii. Security printing.

viii. Machine-readable systems.

ix. Laser dyes (infrared fluorescent).

Synthetic developments in the main infrared dye classes will now be reviewed.

1.2 CYANINE-TYPE NEAR-INFRARED DYES.

1.2.1 General Characteristics

The cyanine dyes were the first class of synthetic dye to be discovered, the first example being (1), discovered by Greville Williams in 1856[4] although its structure was not determined until several years later[5].

The cyanines permit perhaps the simplest way of obtaining systems

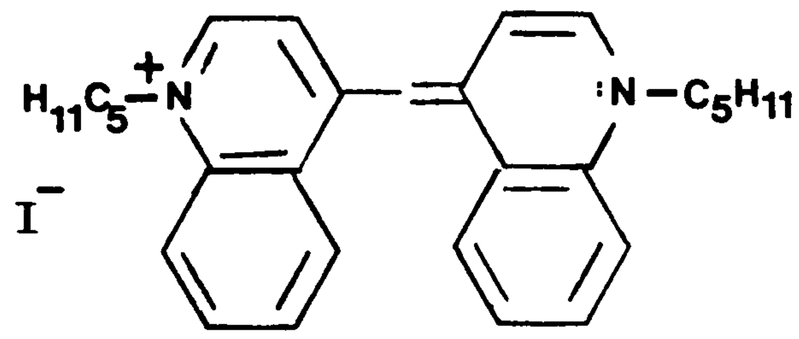

(1)

that absorb well into the near-infrared region of the spectrum, and were in fact the first to be developed for this purpose. Commercially cyanines have been used for a long time as photographic sensitisers and they have been the subject of much research[3,6-10].

A cyanine type chromogen can be defined as any conjugated system that is isoconjugate with an odd-alternant hydrocarbon, and that can be represented by at least two equivalent resonance forms, eg. (2a), (2b) or (2c). The true cyanines are cations as in (2a; X=N) whereas (2b) is representative of the oxonols (Y=0). The free radicals (2c) are of theoretical interest only.

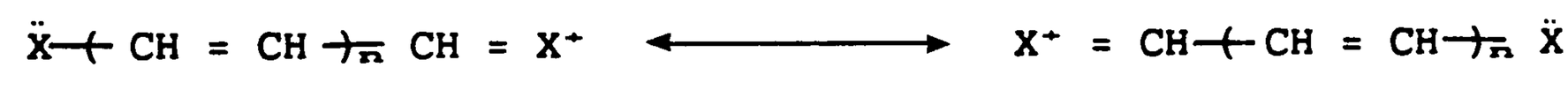

(2a)

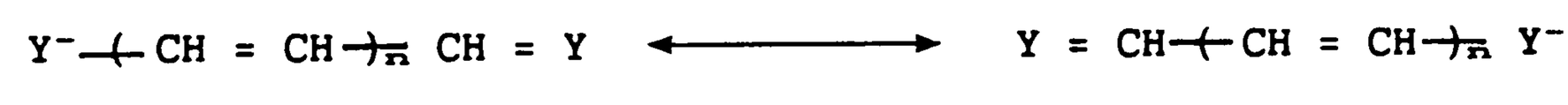

(2b)

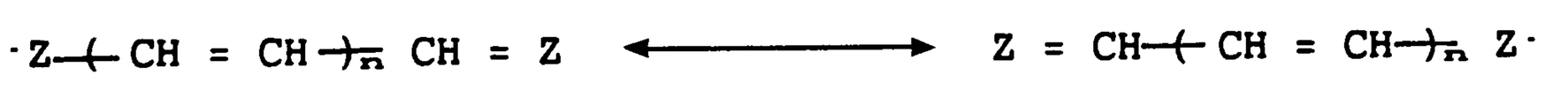

(2c)

As such systems have several resonance forms, a high degree of bond uniformity will prevail along the conjugated chains.

Cyanine-type dyes where the terminal groups are identical [as in (2a), (2b) and (2c)] show non-convergent displacements of the visible absorption band with increasing chain length. Thus increasing the number of vinylene groups increases the λ_{max} of the dye by the same amount for each additional vinylene group. This is termed the

"vinylene shift" and experimentally is found to be about 100nm (Fig. 3).

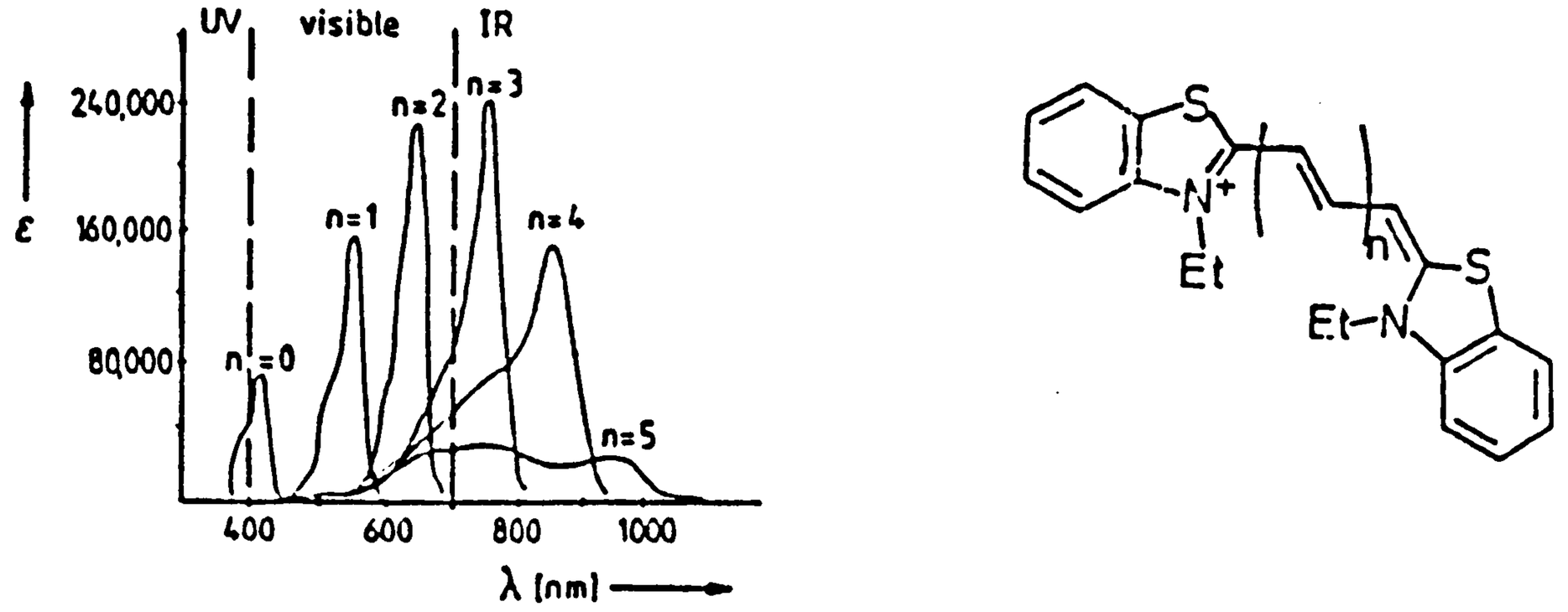

Fig. 3: Absorption spectra for symmetrical cyanine dyes

Cyanine dyes possess high extinction coefficients that initially increase with increasing chain length (up to ca. 250,000). However as the chain length increases (particularly beyond n = 5) there is a general flattening of the absorption curve accompanied with a significant decrease in extinction coefficient (Fig. 3). Thus even the very long chain dyes absorb visible light and so retain visible colour, which for some applications can be a disadvantage. As it is usual for there to be at least 5 double bonds in a cyanine-type system in order to obtain infrared absorption it is doubtful that a truly colourless infrared dye of this class will ever be developed.

If the two terminal groups in the cyanine-type system are of differing basicities, for example (3), a non-symmetrical distribution of electron density will be present in the molecule. Therefore, even though such a system is isoconjugate with an odd-alternant

(3)

hydrocarbon, and has several resonance forms, a significant amount of bond alternation may actually be present[3,7]. As a consequence a convergent displacement of the λ_{max} value occurs as the number of vinylene groups, n, increases. Thus it is much more difficult to achieve infrared absorption.

Cyanine-type dyes can be subdivided chemically into several categories, namely:-

a) True cyanines.

b) Di- and triphenylmethane.

c) Pyrylium and thiopyrylium.

d) Oxonols.

1.2.2 The True Cyanines

By strict definition, a cyanine dye is one that possesses terminal quinoline residues, but this definition has been broadened and now encompasses any cyanine-type system that contains terminal nitrogen atoms, ie. (4).

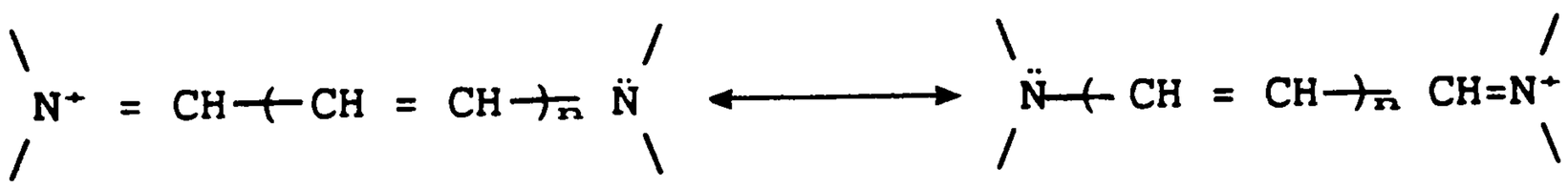

(4)

Table 1 lists typical examples of cyanine dyes. From this Table it can be appreciated that dye (5a) is yellow in hue but by adding a vinyl group the magenta coloured dye (5b) is obtained. This shift in λ_{max} illustrates the vinylene shift concept. If dyes (5b) and (5c) are considered it can be seen that by choice of appropriate terminal groups sizeable red shifts can be effected. These two particular dyes

also show the importance that extrachromophoric conjugation can play in shifting absorption maxima to longer wavelengths. In this case the alkyl pyridinium dye (5b) is magenta whereas the alkyl quinolinium dye (5c) is blue.

Table 1: Examples of cyanine dyes[11,12]

Structure	λ_{max}/nm
(5a)[11] 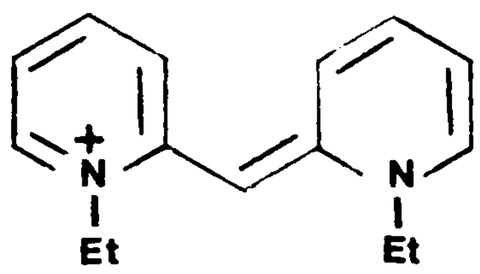	480 (ethanol)
(5b)[12] 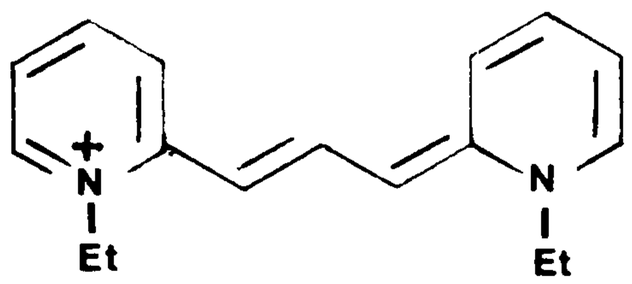	558 (ethanol) 562 (methanol)
(5c)[12] 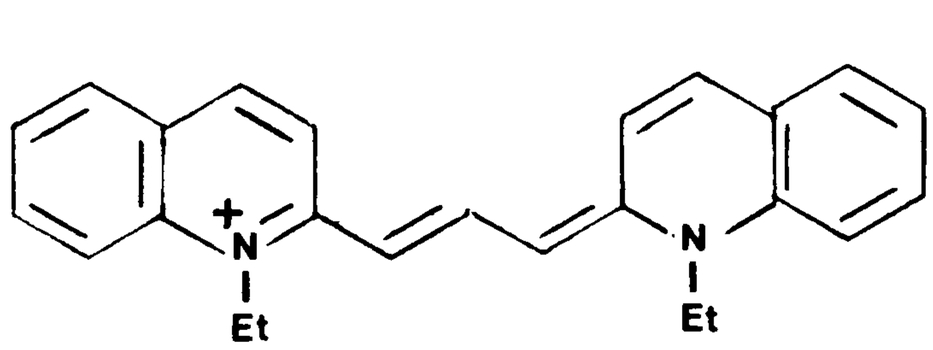	604 (methanol)

Although, for reasons that have previously been discussed in Section 1.2.1 cyanine dyes are generally poor potential infrared absorbers. They are nevertheless of commercial importance and some examples are given in Table 2.

It is worth noting that dyes (8; n=2) and (8; n=3), Table 2, are analogues of dye (5c), Table 1, but now absorb in the near-infrared region of the spectrum due to their greater conjugation.

Table 2: Some commercially important infrared absorbing dyes[13]

Structure	n	λ_{max}/nm
(6) 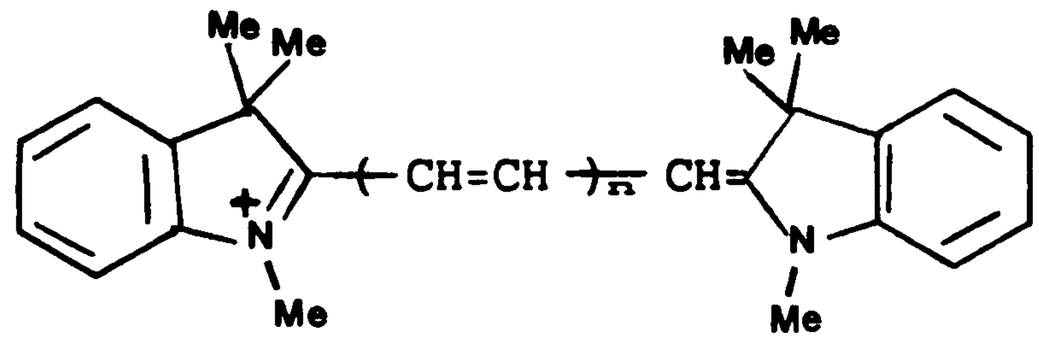	2	641[a]
	3	741[a]
(7) 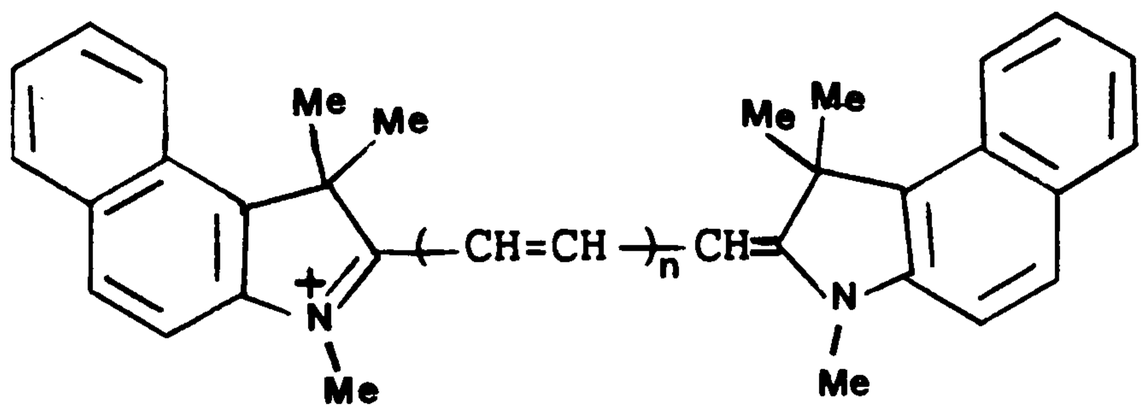	1	782[b]
(8) 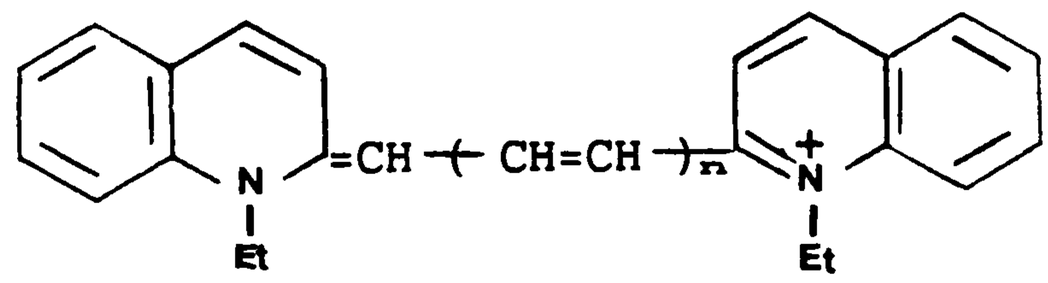	2	708[a]
	3	810[a]
(9) 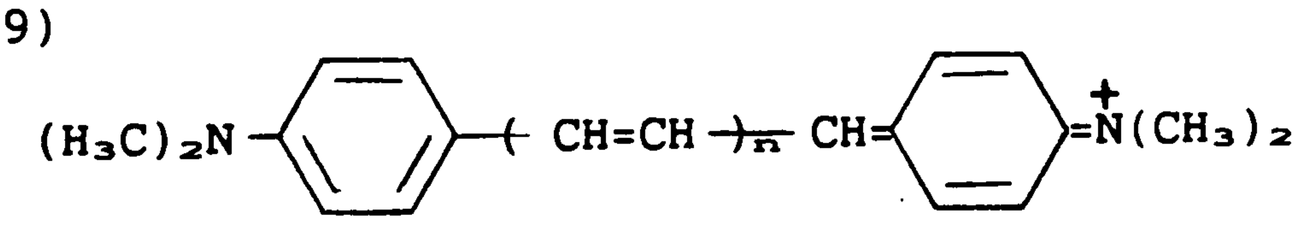	2	790[c]
	3	883[c]

(a) - measured in ethanol
(b) - measured in acidic ethanol
(c) - measured in acetic acid

1.2.3 Di- and Triphenylmethane Dyes

Triphenylmethane dyes such as Malachite Green (10) and Crystal Violet (11) are an old class of cationic cyanine-type dye.

The analogous diphenylmethane dyes, lacking the third phenyl ring are of no value as near-infrared absorbers, and will not be discussed further.

Several techniques have been developed for displacing

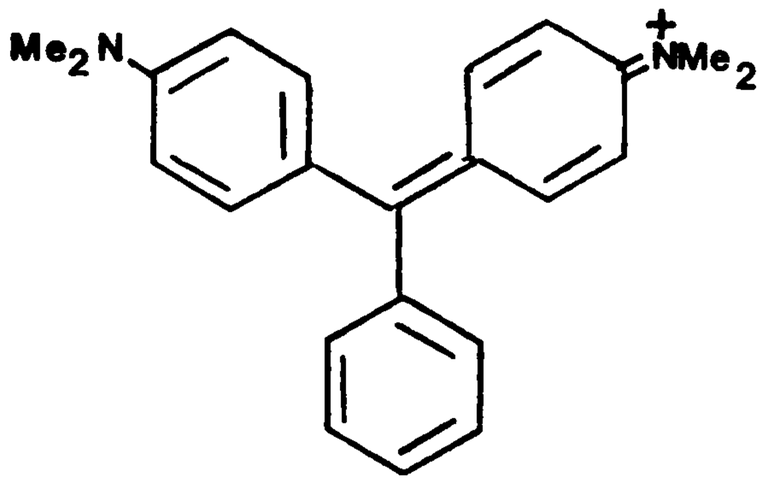

(10)

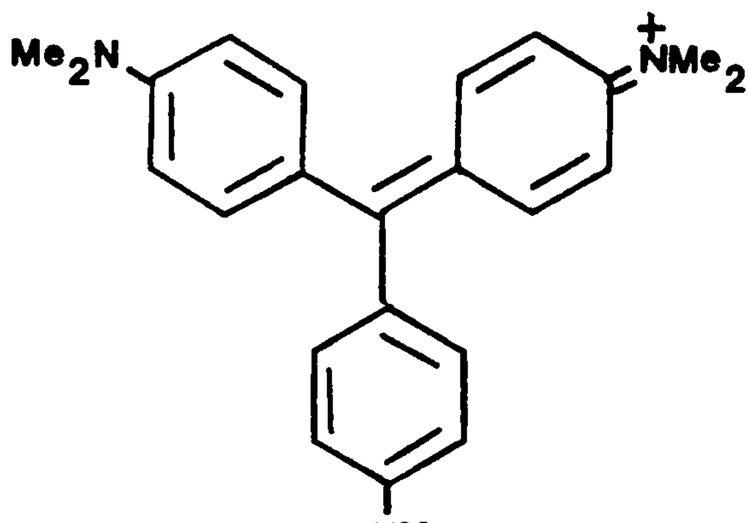

(11)

absorption maxima of triphenylmethane dyes into the near-infrared region of the spectrum.

In 1954, Barker[14] discovered that if two of the phenyl rings in such a system are additionally conjugated by means of a 2,2'-bridging bond (12) then an enormous bathochromic shift is induced in the molecule. This particular fluorene analogue of Malachite Green

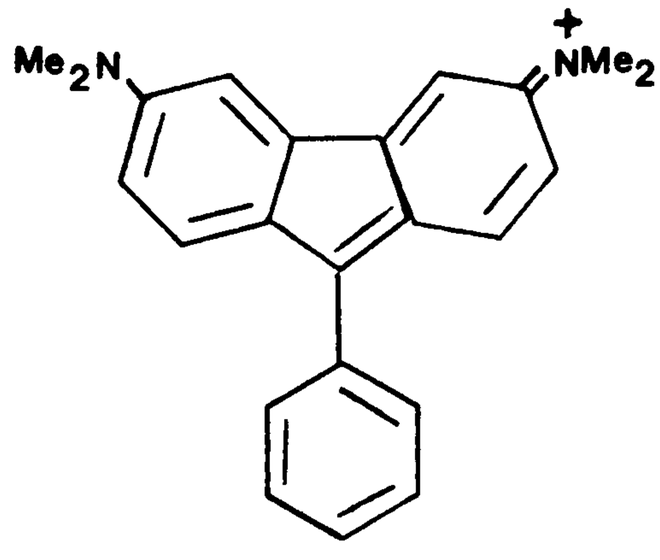

(12)

absorbs at 850 and 955nm in 98% acetic acid whereas Malachite Green (10) itself shows absorption bands at 490 and 656nm.

A different way of enhancing the conjugation of triphenylmethane dyes was realised by Akiyama and co-workers[15], which involves introducing an acetylenic link into the resonating system, as in (13). As a consequence, steric crowding between the <u>ortho</u> hydrogens of the phenyl groups is removed and conjugation is also increased. The size

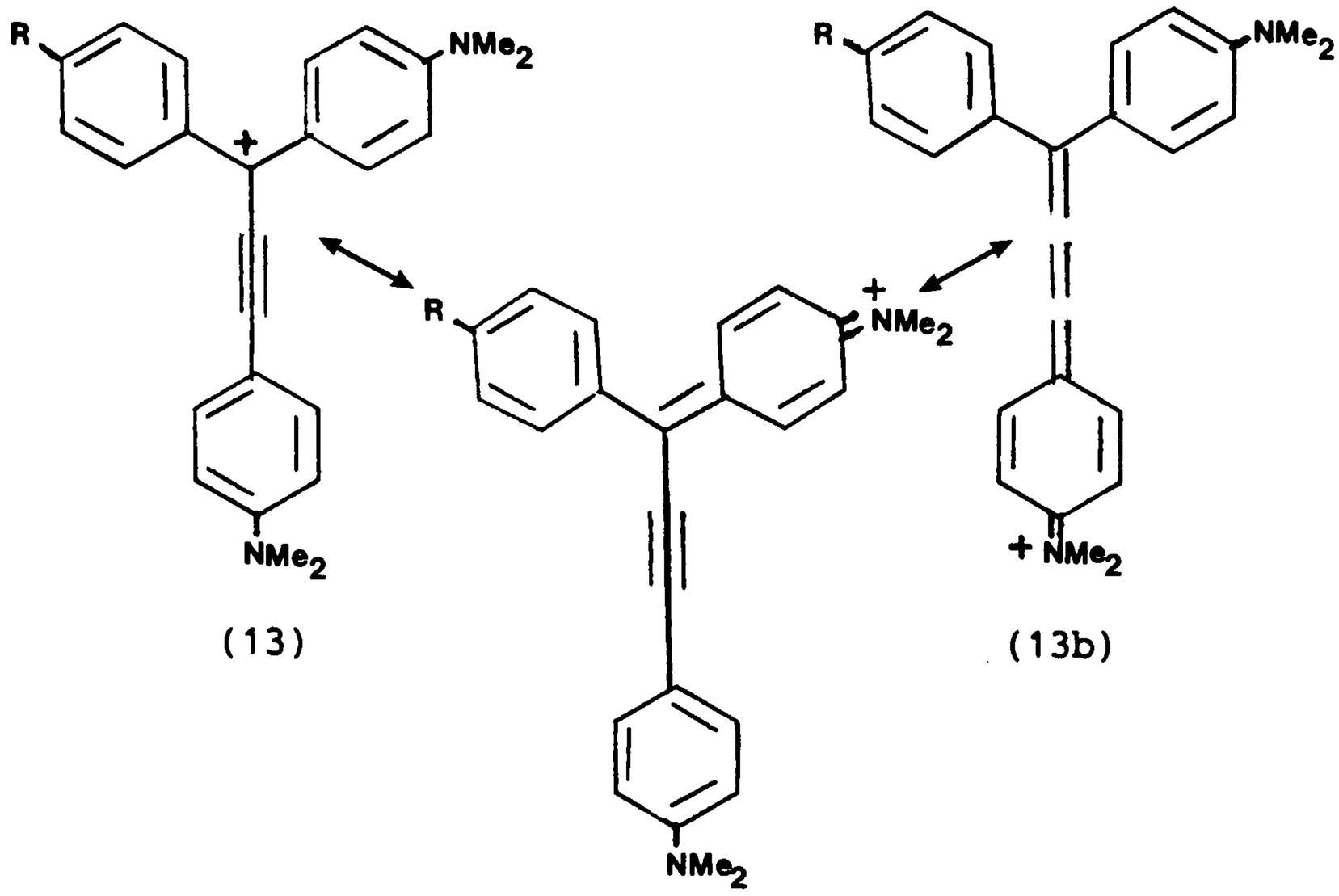

(13)

(13a)

(13b)

of the bathochromic shift seems to indicate that as well as quinoid resonance (13a) allene-quinoid resonance (13b) is present. For example, whereas the ethynologue of Malachite Green (13; R = H) absorbs at 727nm in dichloromethane, the analogous dye (14) with a double bond absorbs at 656nm[16]. The ethynologue of Crystal Violet (13; R = $N(CH_3)_2$) absorbs at 663nm in dichloromethane compared to 598nm for the parent dye (11)[17-21].

A significant red shift can also be imparted to triphenylmethane

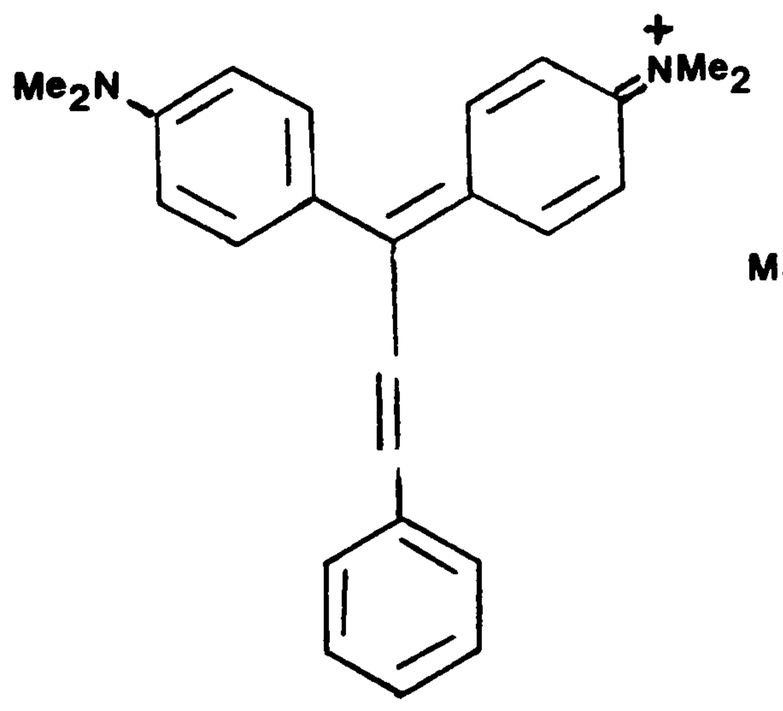

λ_{max} = 656nm

(14)

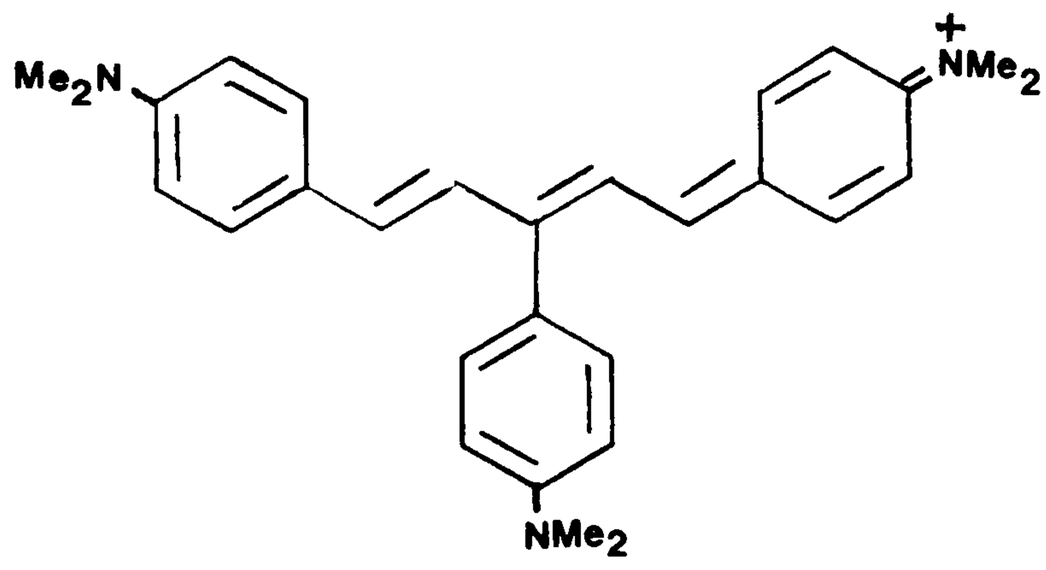

λ_{max} = 770nm (acetic acid)

(15)

dyes by extending the conjugation in other directions through the system. Thus extending the branches of the parent structure of Malachite Green (10) and Crystal Violet (11) produces more bathochromic dyes [(14) and (15) respectively].

Bathochromic shifts are also obtained if one of the phenyl rings in the triphenylmethane residue is replaced by a naphthalene ring. So the two Crystal Violet analogues (16) and (17) absorb at 623.5nm and 613nm respectively in acetic acid[3]. From the absorption maxima of

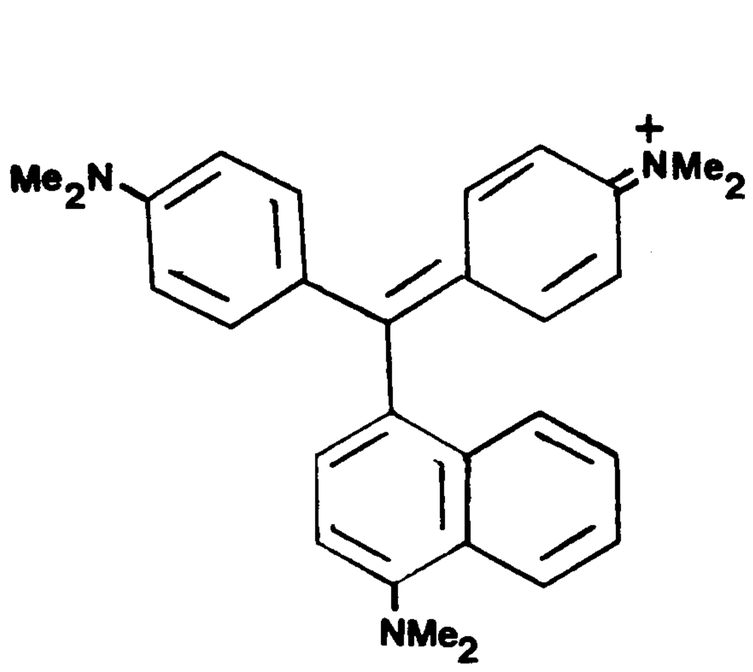

(16)

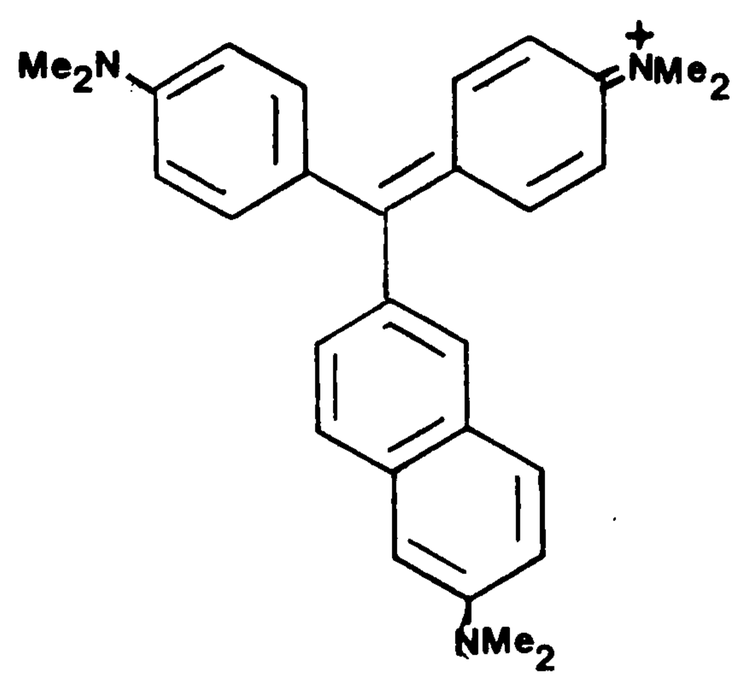

(17)

(16) and (17) it is apparent that conjugation is more effective through the 1,4-positions than the 2,6-positions of the naphthalene systems.

Both concepts of planarity and extended conjugation are used in (18) to effect infrared absorption.

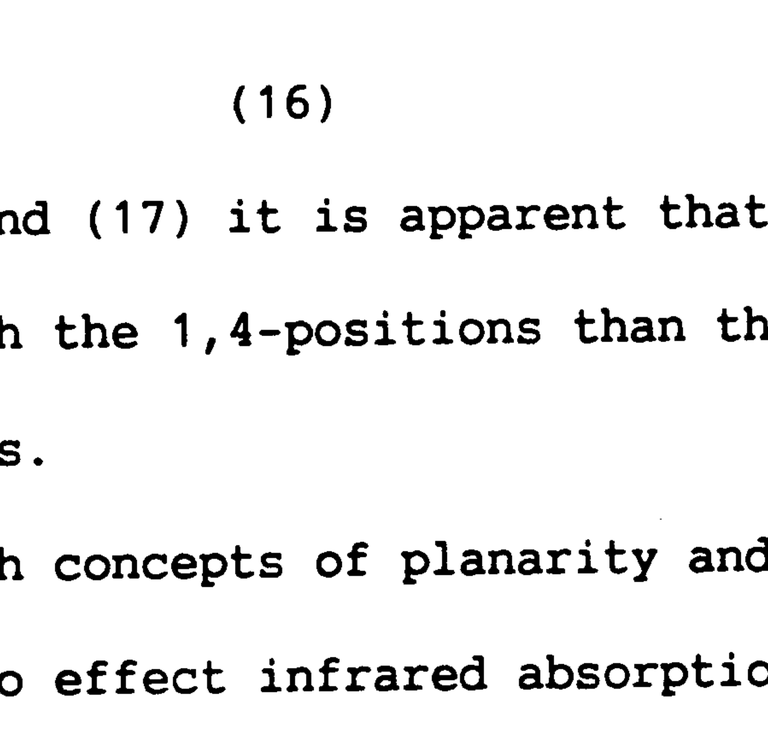

(18)

λ_{max} = 814nm (acetic acid)

Although triphenylmethane dyes are far more photo-stable than the cyanine dyes (by a factor of 100) they are similar in that the infrared absorbing derivatives still show visible absorption. Thus a truly colourless triphenylmethane dye has yet to be synthesised.

1.2.4 Pyrylium and Thiopyrylium Dyes

The pyrylium dye (19) is very bathochromic considering the relatively small number of double bonds between the terminal oxygen atoms[22]. Such a large bathochromic shift is even more surprising when

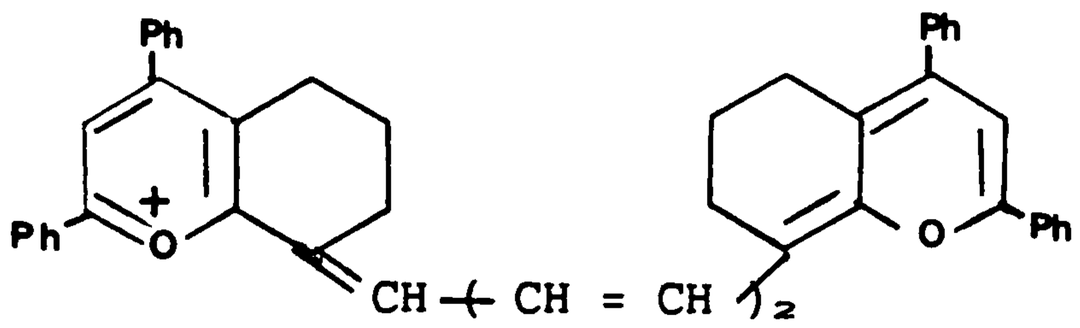

λ_{max} = 1040nm, ε_{max} = 125,000 (CH_2Cl_2)

(19)

Dewar's rules are considered. These rules predict that, as the oxygen atoms present in the pyrylium system are both more electronegative than nitrogen and are at starred positions, the resultant dye should be more hypsochromic than the cyanine analogue. In practice this is not found to be the case and the pyryliums absorb at longer wavelengths. Presumably the increased reluctance of oxygen to carry a positive charge compared to nitrogen causes a greater degree of electron symmetry to prevail in the pyrylium system with the result that the dyes are more bathochromic.

Drexhage[22] assessed the relative stabilities of a series of pyrylium dyes by irradiating samples dissolved in 1,2-dichloroethane with the light source of a Cary Model 14 spectrophotometer that was equipped with a suitable filter to eliminate light below 650nm. The

relative stabilities of the dyes are compared in Table 3 using dye (20a) as a reference structure.

Table 3: Pyrylium cationic dyes[22]

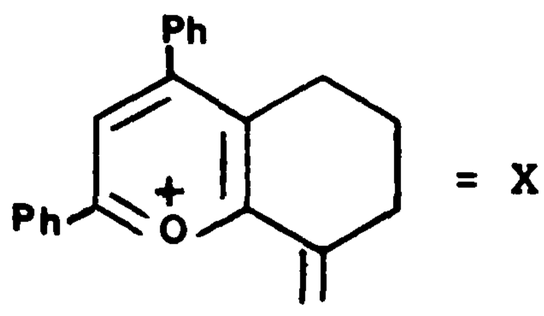

= X

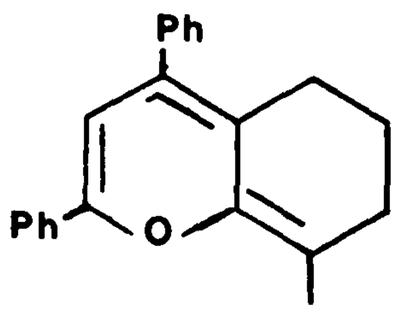

= Y

Dye structure	λ_{max}/nm(CH_2Cl_2)	ε_{max}($x10^{-3}$)	Relative stability
(20a) X = CH–(–CH = CH–)$_2$ Y	1040	125	1
(20b) 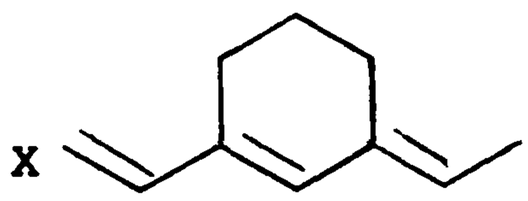	1090	140	76
(20c) 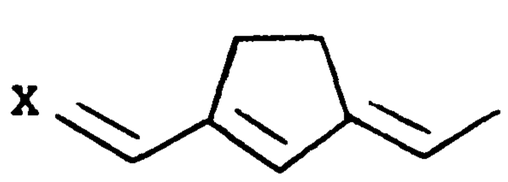	1138	70	37
(20d) 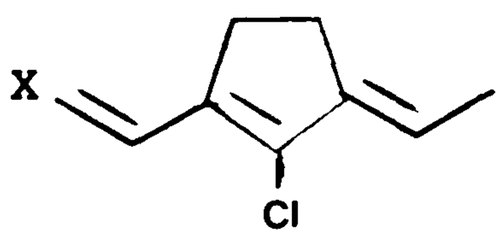	1145	143	178

Comparison of dyes (20a) and (20b) in Table 3 shows that incorporation of a cyclic residue into the centre of cyanine systems effects a significant bathochromic shift and enhances dye stability. This is due to the reduction in flexibility of the chain caused by the cyclic system and the protection of the carbon atoms of the unsaturated bridge from electron deficient species such as peroxide radicals. It is apparent that dyes containing 5-membered rings absorb at longer wavelengths than those with 6-membered rings, but sometimes suffer a reduction in extinction coefficients and stability.

Dye (20d) absorbs at even longer wavelengths, as predicted by Dewar's rules, due to the attachment of an electron withdrawing chlorine atom at an unstarred position.

Thiopyrylium dyes, eg.(21)[23], are the sulphur analogues of pyrylium

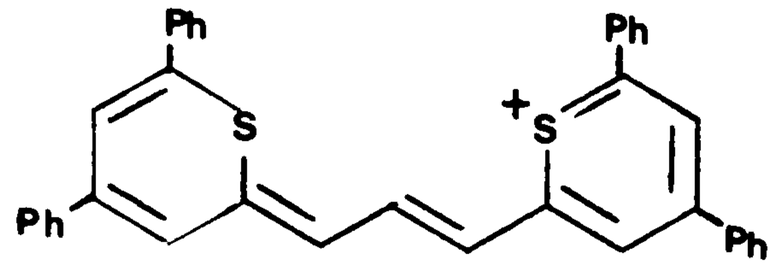

λ_{max} = ca. 780nm

(21)

dyes, and tend to absorb at longer wavelengths than their oxygen counterparts (Table 4)[22] due to the lowering of the energy gap between HOMO and LUMO orbitals.

Table 4: A comparison of analogous pyrylium and thiopyrylium dyes[22]

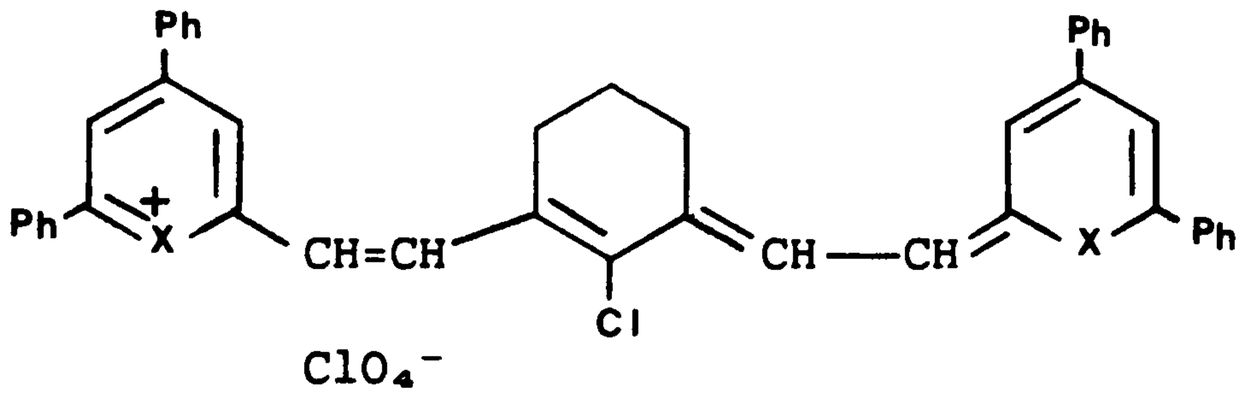

Dye	X	λ_{max}/nm (CH_2Cl_2)	ε_{max}($x10^{-3}$)
(22a)	O	1072	107.0
(22b)	S	1160	105.0

Thiopyrylium dyes are also far more stable than their pyrylium analogues. For instance, when subjected to the same test as the dyes in Table 3, dye (22b) was found to be at least 25 times more stable than dye (22a). This is readily explained by the fact that sulphur is less electronegative than oxygen and so will accommodate the

inherent positive charge more easily which, in turn stabilises the dye to a greater degree.

Several mixed pyrylium-thiopyrylium dyes with both sulphur and oxygen terminal groups in the same molecule have been prepared[24], a recent example being (23)[25]. Although this dye possesses a secondary

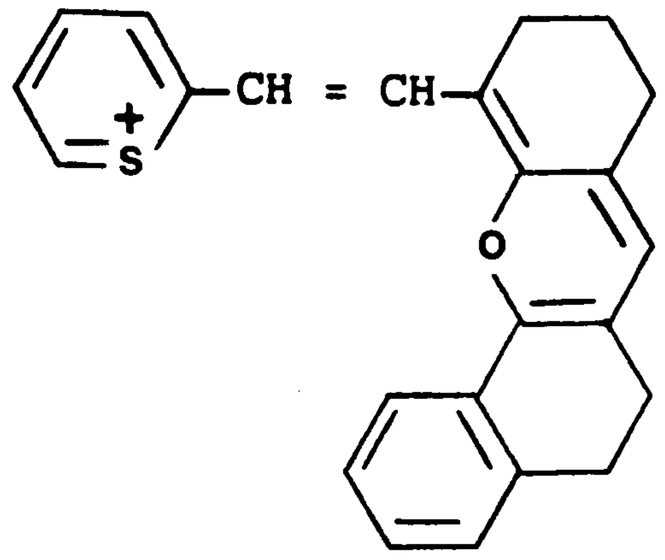

(23)

visible absorption band, giving it a yellow colour, it also has infrared bands at 744 and 824nm in acetonitrile, with extinction coefficients of 53,000 and 65,000 $lmol^{-1}cm^{-1}$ respectively.

1.2.5 The Oxonol Dyes

Oxonols are anionic cyanine-type dyes of the general formula (2b; Y=O). They are relatively unstable, their stability decreasing as the number of vinylene groups, n, increases. Hence, with a few notable exceptions, they are not of any great practical value [26].

Studies have shown that acyclic oxonols absorb at about 60nm less than their cyanine equivalents[27]. Heterocyclic oxonols tend to absorb at much longer wavelengths than those of the acyclic series. For example (24; n = 0) absorbs at 585nm and (24; n = 1) at 650nm[27].

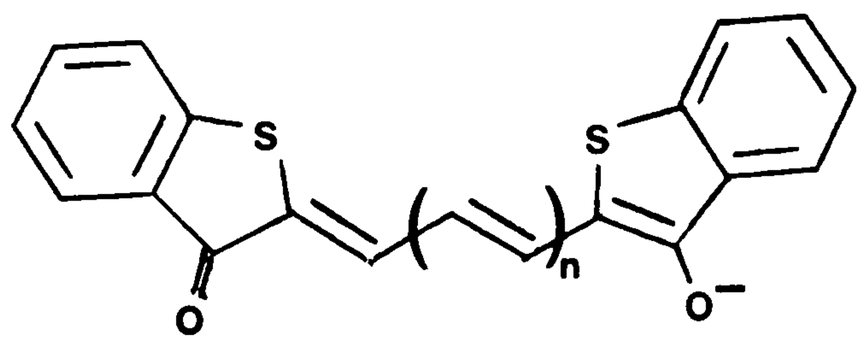

(24)

As with the other classes of cyanine-type dyes discussed, the non-symmetrical oxonols show convergent behaviour as 'n' increases, whereas the symmetrical dyes are non-convergent.

1.3 DONOR-ACCEPTOR CHROMOGENS

1.3.1 General Characterisation

With the exception of polycyclic quinones and phthalocyanines all commercially important organic colorants can be classed as donor-acceptor systems of one form or another.

Two broad classes of donor-acceptor chromogen can be envisaged, namely donor-simple acceptor systems and donor-complex acceptor systems[3]. It is from the latter category that the near-infrared absorbing donor-acceptor systems so far developed come from. These infrared dyes can be further subdivided into the following categories:-

a. Quinone dyes.

b. Azo dyes.

c. "Methine" and related dyestuffs.

d. Oxocarbon dyes (squarylium and croconium dyes).

These classes of near-infrared absorbing dyes will be surveyed.

1.3.2 Quinone Dyes

The known near-infrared absorbing quinone dyes are derived from 1,4-naphthoquinone (25) and 9,10-anthraquinone (26).

The first near-infrared absorbing quinone dye (27) was synthesised by Griffiths and Chu[28]. This dye had an absorption maximum of 759nmn in acetone and is prepared by the reaction of 5-amino-2,3-dicyano-1,4-naphthoquinone with aniline in ethanol. The red shift shown by this dye was somewhat unexpected but PPP-MO calculations confirmed the

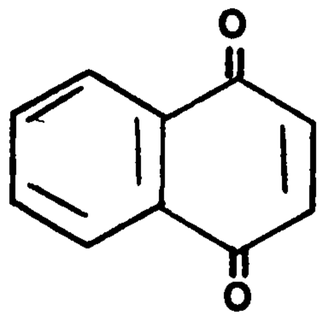

(25)

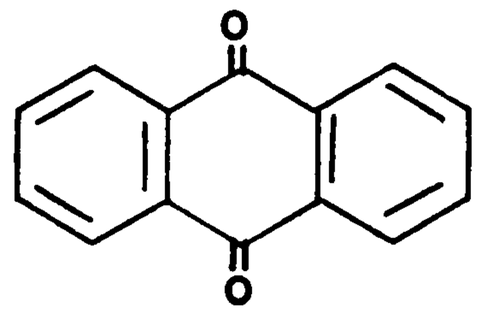

(26)

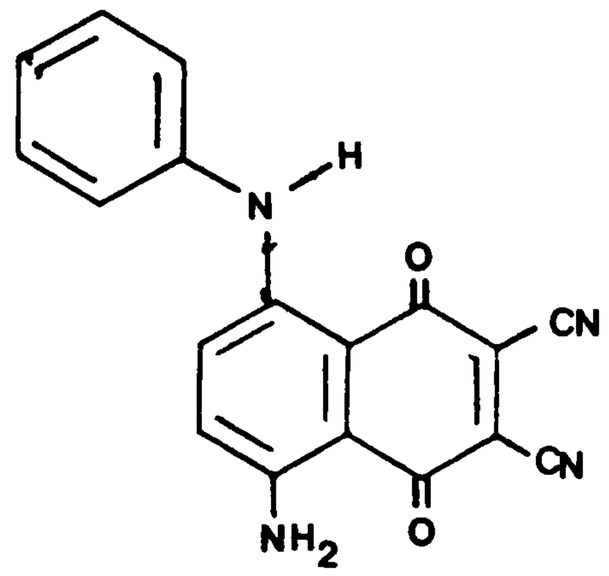

(27)

highly bathochromic nature of the system.

More recently research into the near-infrared absorbing quinone dyes has been intense[29.30]. Matsuoka and co-workers developed naphthoquinone infrared dyes of the type (28)[31.32]. In an

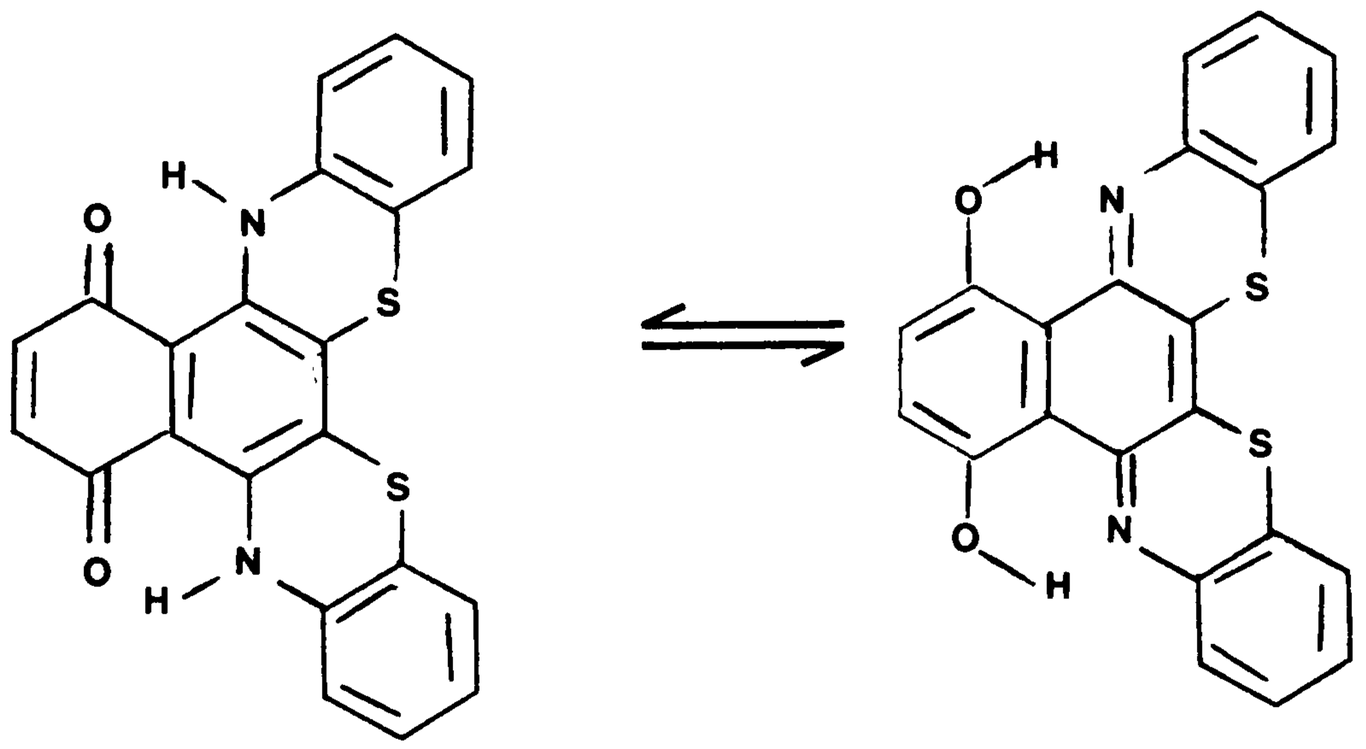

(a) (b)

(28)

investigation of the tautomerism of these dyes they concluded that the tautomerism was mainly influenced by the nature and position of the substituents and also the polarity of the solvent. For example, with (28), the dye existed predominantly as the quinone tautomer (28a) in

dimethylformamide, but in benzene the quinoneimine tautomer (28b) was more dominant. The analogue (29) was obtained in the quinoneimine form shown, and is of course incapable of tautomerism.

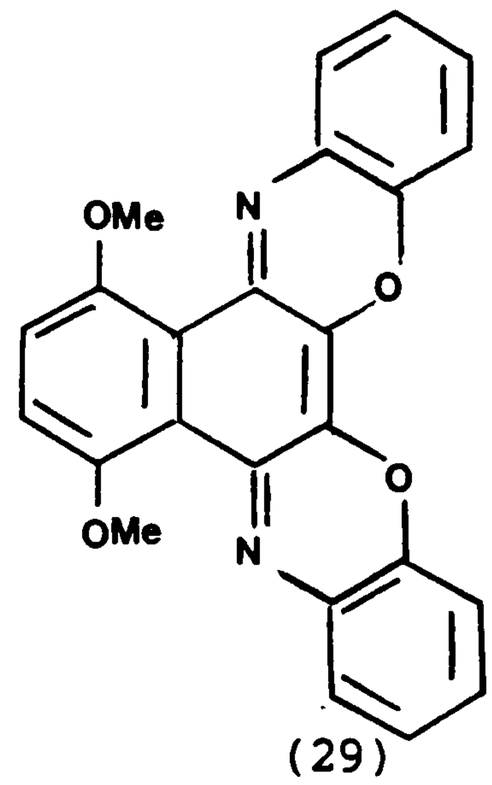

(29)

Dye (28), which absorbs at 728nm in benzene, was synthesised by reacting 2,3-dichloronaphthazarin (30) with potassium 2-aminobenzenethiolate (31). Oxidation of (28) by the action of hydrogen peroxide in acetic acid gave (32) which was yellowish brown in colour and absorbed at 827nm, Scheme 1.

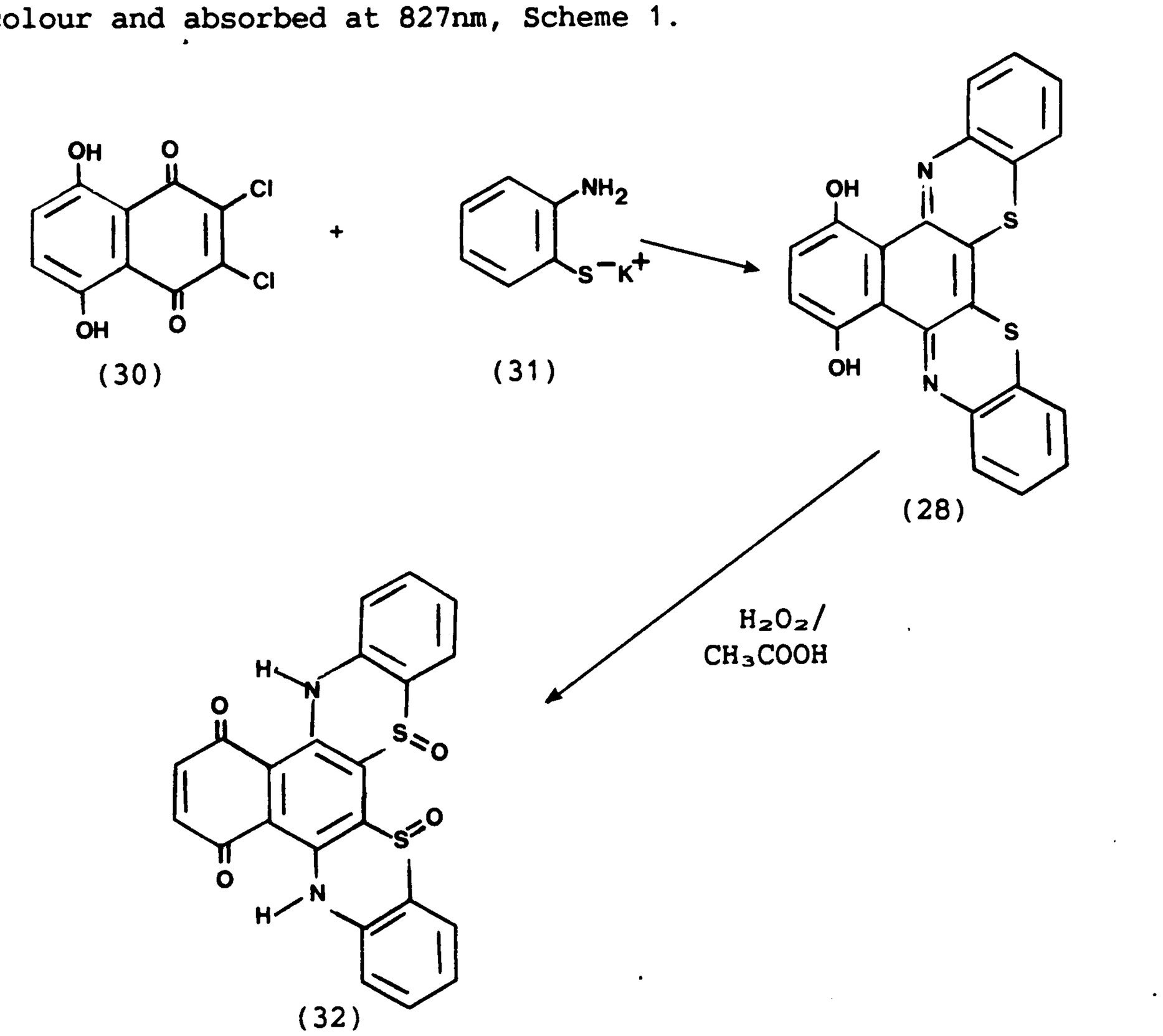

Scheme 1

Near-infrared absorbing 1,4-naphthoquinone dyes find use in optical data storage media, as they are relatively stable and have a good reflectivity in the solid state.

A series of dyes of type (27) [including (33), which absorbs at 765nm in acetonitrile] have been patented for use in near-infrared absorbing pigments[33].

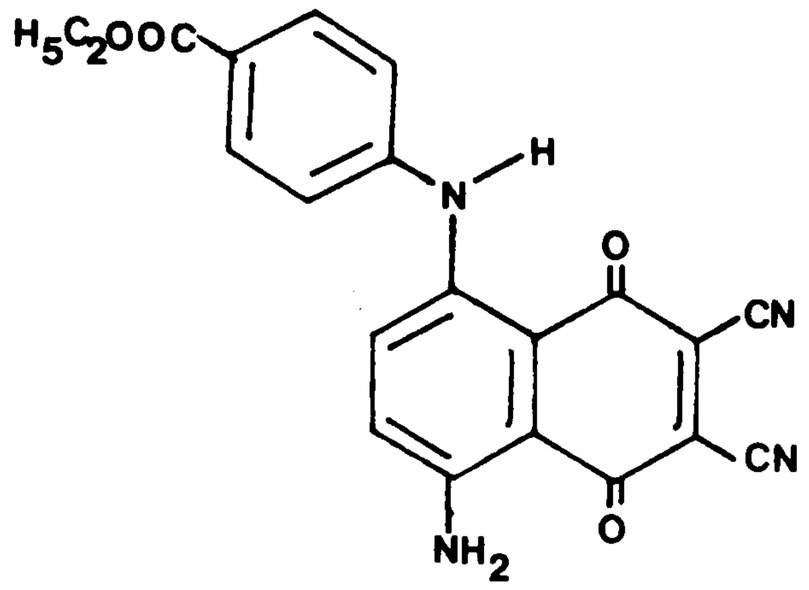

(33)

The deposition of ultrathin films containing the near-infrared absorbing 1,4-naphthoquinone dye (34) has recently been investigated for optical recording[34]. This dye contains a long n-alkyl chain and

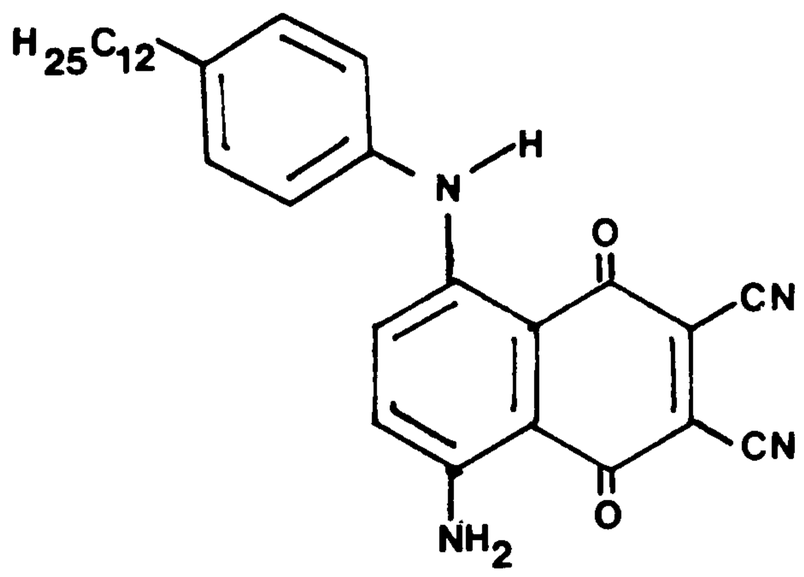

(34)

consequently at a suitable solvent/aqueous interface a Langmuir-Blodgett (monolayer) film is deposited. This film can then be transferred to an appropriate substrate and, for example can be written on with a laser with high sensitivity. Furhermore, whilst the dye absorbs at 775nm in chloroform a remarkable bathochromic shift to 960nm was observed for the aggregated form.

The first near-infrared absorbing anthraquinone dyes were developed

by Matsuoka et al. The anthraquinone analogues of dye (28) are made in a similar manner to that shown in Scheme 1 except that 2,3-dibromoquinizarin is used instead of (30)[35]. The resultant dye (35)

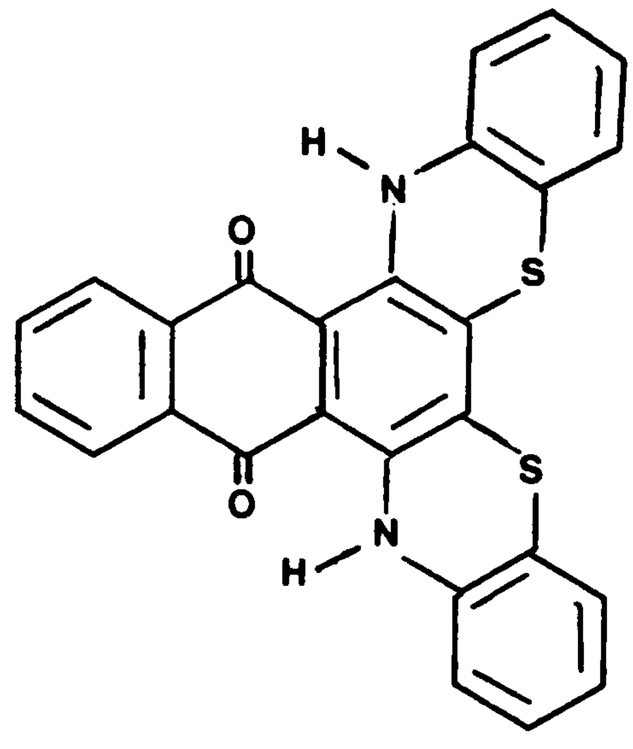

(35)

absorbs at 712nm in chloroform. The selenium analogue of (35) has also been prepared and has a λ_{max} of 720nm in chloroform[36].

In the quest for black mixtures of dyes with good ordering properties in liquid crystals Matsumoto et al discovered a new class of anthraquinones of the general formula (36)[37]. Dyes of this type

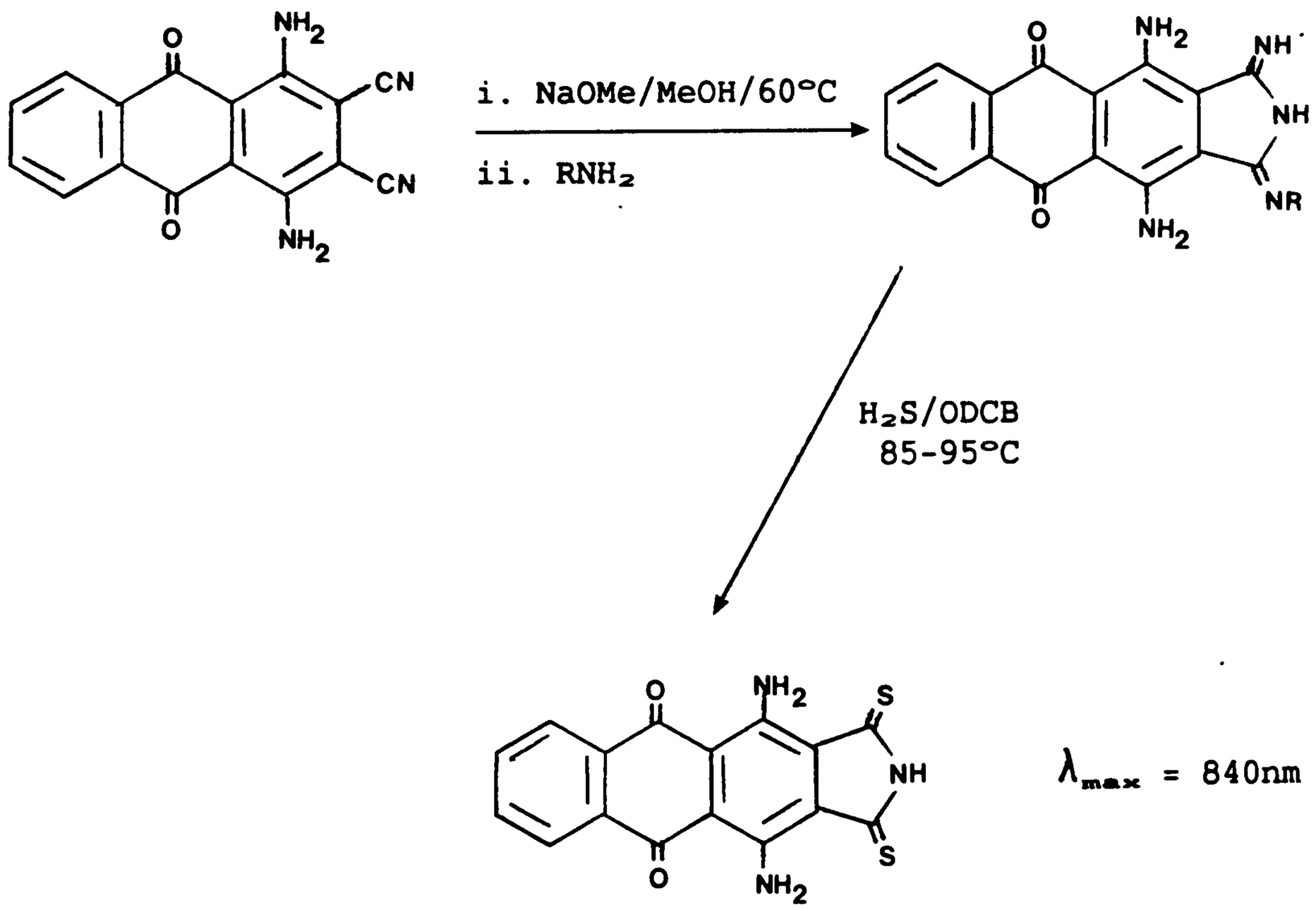

(36)

Scheme 2

have also since been patented for dyeing polyester fibres in light greenish blue shades which impart to the textile an increased ability to absorb solar energy and accumulate heat[38]. They can be prepared as shown in Scheme 2. The bathochromic shift due to the sulphur atoms is notable since the related imides (37) are blue with λ_{max} ca. 600-650nm.

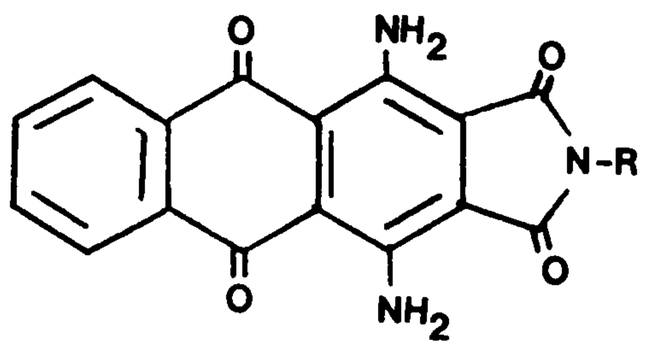

(37)

1.3.3 Azo Dyes

Azo chemistry originated from the work of Peter Griess who, in 1858, discovered the diazotisation of picramic acid[39]. From these fortuitous beginnings the azo dyes have become indisputably the most important single class of colorants, and well over 50% of all commercially important dyestuffs contain the azo linkage.

In view of their importance and the vast amount of research that the azo dyes have attracted, it is rather surprising that very few examples of near-infrared absorbing azo dyes are known and even these were only developed very recently.

If a generalised monoazo structure (38) is considered where D is one or more donor groups, X and Y are carbocyclic or heterocyclic ring

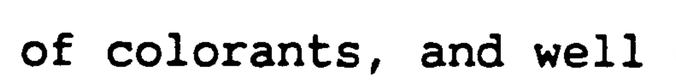

(38)

systems and A is one or more acceptor groups, then on excitation electrons flow from the donor part (D_n——X—) to the acceptor part (—Y—A_m) of the molecule via the conjugated (-N═N-) bridge. Therefore any modification to the dye structure that lowers the

ionisation potential of the donor part, or increases the electron affinity of the acceptor part will induce a bathochromic shift into the dye. There are several ways of achieving this, namely,

i. increasing the electron donor/acceptor strength of D/A respectively;

ii. increasing the number of groups D and/or A;

iii. varying the positions of attachment of groups D and/or A relative to the point of attachment of the azo groups;

iv. using heterocyclic instead of carbocyclic ring systems;

v. increasing the size and conjugation of the molecule.

Table 5[40,41] illustrates how, in considering only the acceptor part

Table 5: Comparison of monoazo dyes by varying acceptor substituents and acceptor ring 'Y'[40,41]

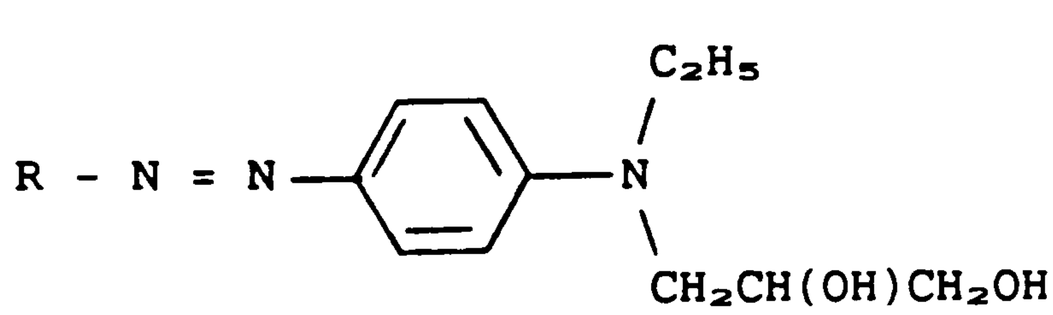

Structure	R	λ_{max}/nm (methanol)
(39a)[41]	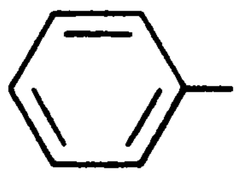	420
(39b)[41]	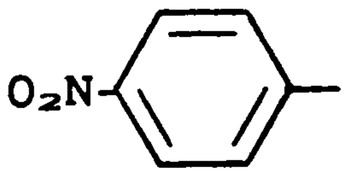	495
(39c)[41]	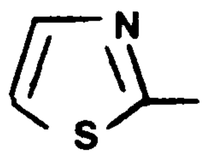	502
(39d)[40]	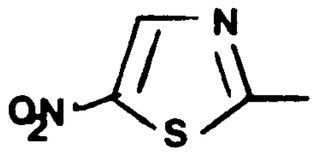	593
(39e)[40]	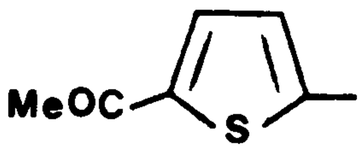	605

of the molecule, several of the above principles can be used to effect bathochromic shifts. Thus by comparing (39a) with (39b) and (39c) with (39d) it can be seen how the incorporation of a suitably placed nitro group can cause a shift to longer wavelength. Comparison of (39a) with (39c) and (39b) with (39d) shows how the thiazole system is more bathochromic than a phenyl ring. A further shift to longer wavelength can be obtained if a thiophene ring with additional acceptor groups is used instead of the thiazole residue as in (39e) relative to (39d).

Even though these principles have long been established it was not until 1986 that Griffiths and Bello published the first paper describing near-infrared absorbing monoazo dyes[42]. The dyes were prepared as shown in Scheme 3. Thus 2-amino-4-chloro-5-formyl

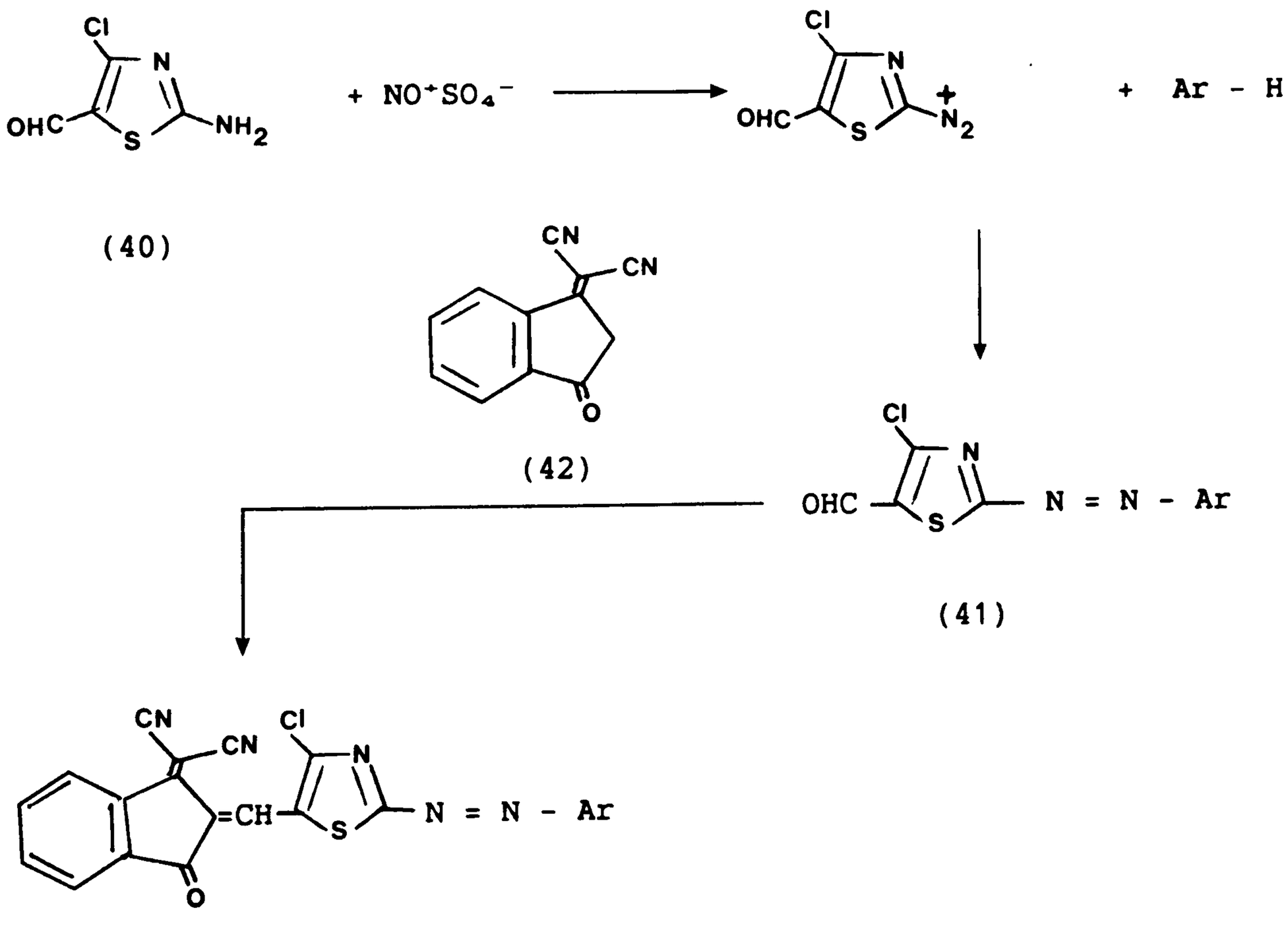

Scheme 3

thiazole (40) was diazotised in nitrosyl sulphuric acid and coupled to the appropriate arylamine (Ar-H) to give the

intermediate dyes (41). Condensation of (41) with 3-dicyanomethyleneindan-1-one (42) gave the near-infrared absorbing dyes (43). The absorption characteristics of some typical examples are shown in Table 6.

Table 6: Near-infrared absorbing monoazo dyes[42]

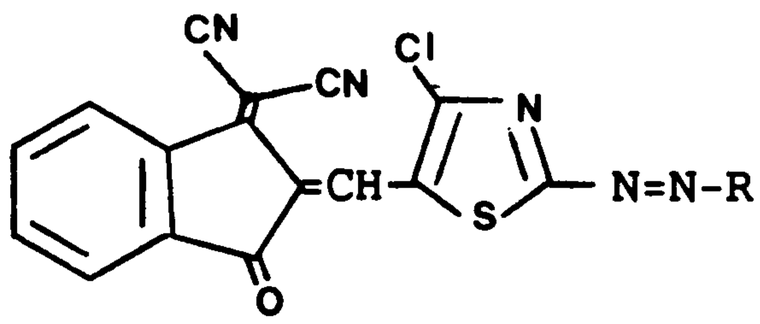

(43)

Structure	R	λ_{max}/nm (CH_2Cl_2)	ε_{max}/lmol^{-1}cm^{-1} (CH_2Cl_2)
(43a)	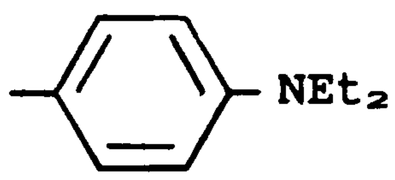	700	67,800
(43b)	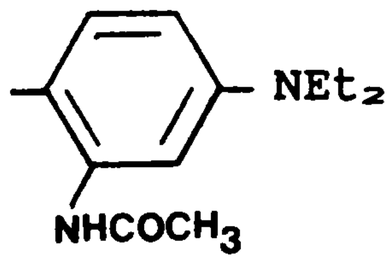	710	74,700
(43c)	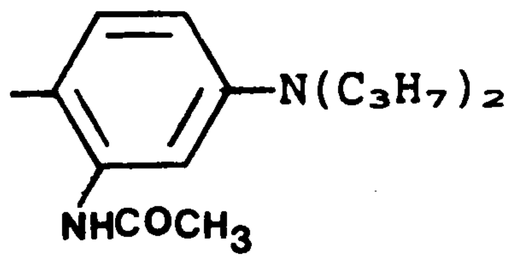	716	74.000
(43d)	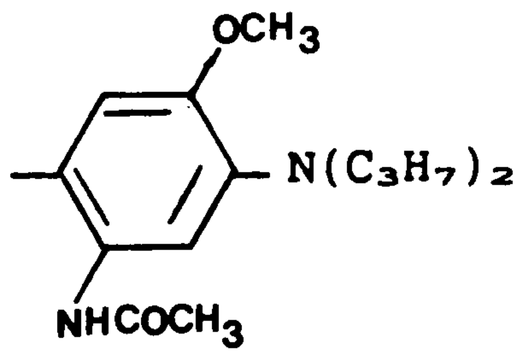	750	82,600

It can be seen from Table 6 that very strong electron donor and acceptor groups suitably positioned within the molecule coupled with extended conjugation and heterocyclic rings are necessary to obtain

near-infrared absorption with just one azo linkage.

A recent patent by Gregory[43] describes the use of disazo dye systems in order to obtain near-infrared absorption. For instance (44) absorbs at 706nm in ethyl ethanoate. As with the previous dyes

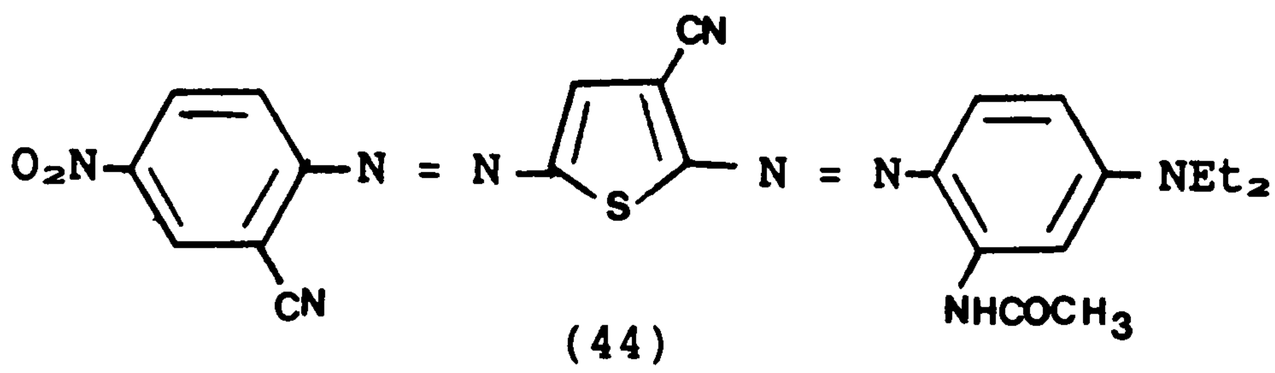

(44)

of type (43), dye (44) utilises the concept of extended conjugation and so requires a multi-step synthesis route. It is interesting to note that a one-step (diazo coupling) synthesis of near-infrared absorbing dyes is not yet available.

1.3.4 "Methine" and Related Dyestuffs

Methine and related dye chromophores constitute another important class of donor-acceptor chromogen, although they are commercially less important than the azo dyes.

In the broadest sense, this class of dye can be likened to the generalised azo structure (38) except the azo linkage is replaced by a carbon equivalent conjugated bridge, ie. $-(C = C)_n-$, $-(C \blacksquare C)_n-$, $-(C = N)_n-$ or aryl. If the bridge is -C = C- the dyes are classed as styryls or stilbenes; if the acceptor group is carbonyl, such dyes may also be classed as merocyanines.

Not surprisingly, the same principles in displacing the absorption maxima of azo dyes to longer wavelength are applicable to the methines. The methines do have the advantage that the conjugated bridge can be more readily extended in order to effect useful bathochromic shifts. This advantage is limited though, because the systems tend to exhibit convergent behaviour, ie. as the number of double bonds increases the bathochromic shift progressively decreases.

In the mid-1970's a series of methine dyes that possessed near-infrared absorption was discovered[44]. Thus bindone (45), (a dimer of

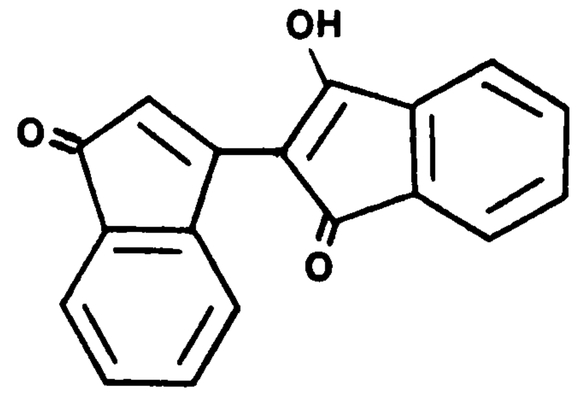

(45)

1,3-indandione) was condensed with a suitably nucleophilic heterocyclic enamine to give, for example (46) and (47). However these infrared dyes, which are merocyanines, suffered from low

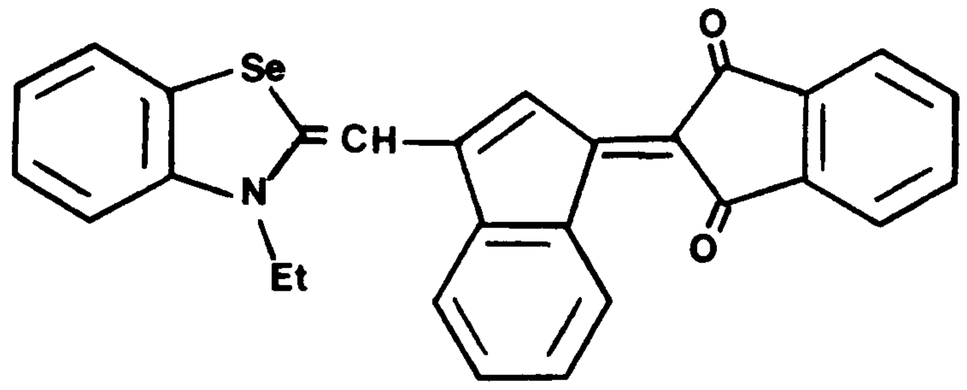

λ_{max}(DMF) = 762nm
700nm
425nm

(46)

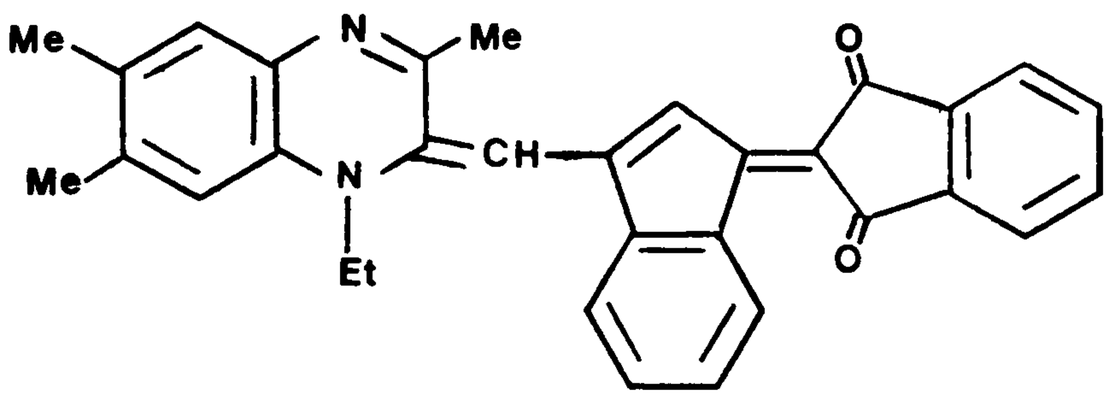

λ_{max}(DMF) = 841nm
782nm
413nm

(47)

solubilities in organic solvents and showed additional multiple peaks in the visible region.

More recently a related series of dyes has been described by Griffiths and co-workers. They showed how the yellow dye (48) could be

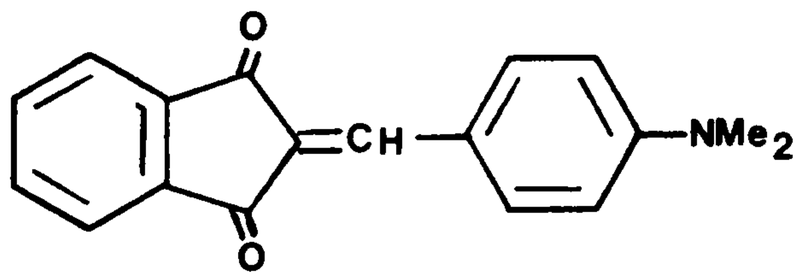

λ_{max} = 481nm (CH_2Cl_2)

(48)

progressively modified in order to obtain infrared absorption (Table 7). The carbon-bridged dyes in Table 7 were prepared by condensing the relevant 1,3-substituted indandione derivative (49) with 4-dimethylaminobenzaldehyde (50) in ethanol or acetic acid to give the desired dye (51) as shown in Scheme 4. The nitrogen bridged

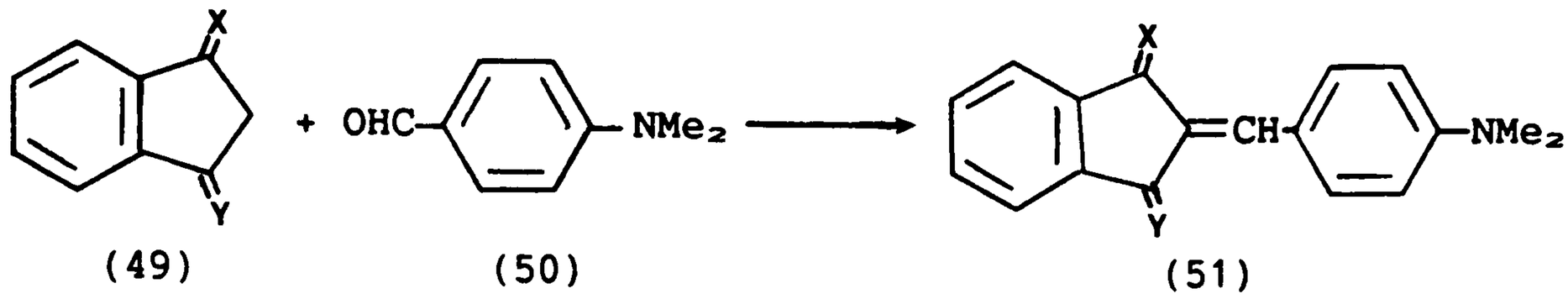

(49) (50) (51)

Scheme 4

(azomethine) analogues (52a) and (52b) were prepared in a similar manner to that shown in Scheme 4 except that 4-nitroso-N,N-dimethylaniline or 4-nitroso-N,N-dimethyl-1-naphthylamine were used respectively in place of the aldehyde (50).

The dyes from Table 7 exhibit typical donor-acceptor characteristics. Thus the replacement of a carbonyl group with the more electronegative dicyanovinyl entity causes a marked red shift, as in (51a) and (51b). As the fundamental chromophore in these dyes can be related to an isoconjugate odd-alternant hydrocarbon, as defined by the perturbational molecular orbital (PMO) theory of Dewar[46], then the central (or bridging) atom will be at an "unstarred" position. The theory predicts that an increase in electronegativity at an unstarred site will cause a bathochromic shift to occur and thus replacement of the central carbon atom with the more electronegative nitrogen atom causes a shift to longer wavelength as shown by comparing (51b) and (52a). Comparison of (52a) and (52b) shows the bathochromic effect of extrachromophoric conjugation.

The azomethine dyes related to (52a), Table 7, have the advantage

Table 7: Methine and related dyestuffs based om dicyanovinyl derivatives of 1,3-indandione[45]

Structure	λ_{max}/nm (CH_2Cl_2)	ε_{max}/$lmol^{-1}cm^{-1}$ (CH_2Cl_2)
(51a) 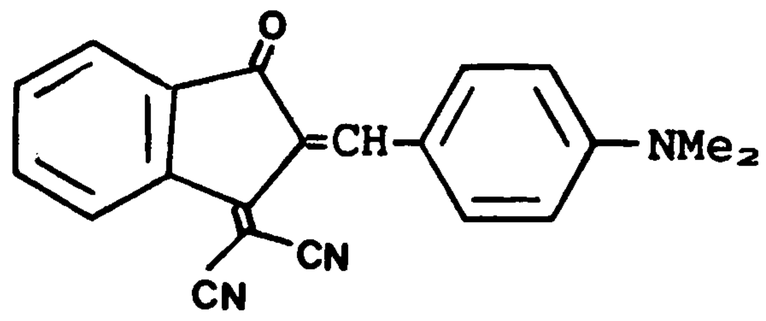	557	55,200
(51b) 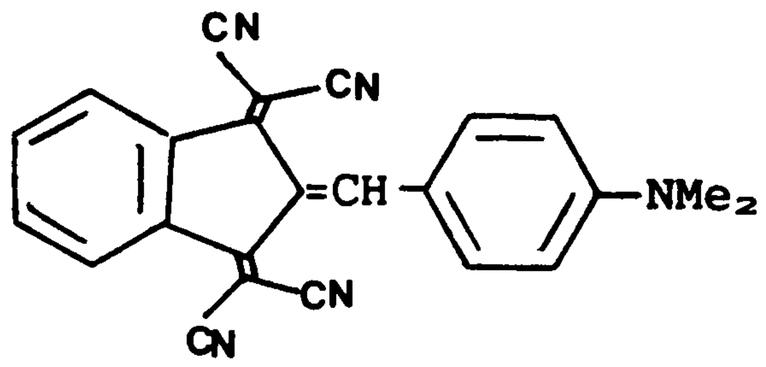	608	33,000
(52a) 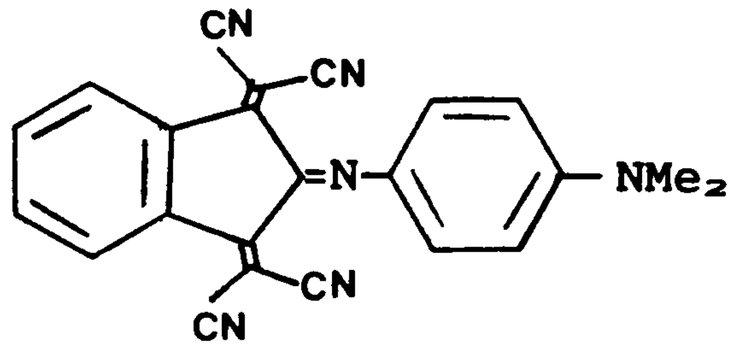	755	25,500
(52b) 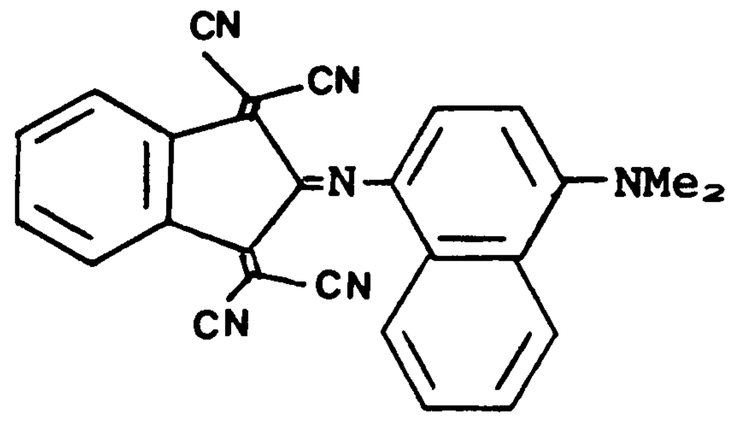	850	Unstable

of low molecular mass which in turn imparts excellent solubility in organic solvents and polymers. In general this is uncommon with the majority of near-infrared absorbing dyes currently available.

1.3.5 Oxocarbon Dyes

1.3.5.1 Squarylium Dyes

Since its accidental discovery in 1959 by Cohen, Lacher, and Park[47,48] squaric acid (53) has become an invaluable intermediate for the preparation of near-infrared absorbing dyes.

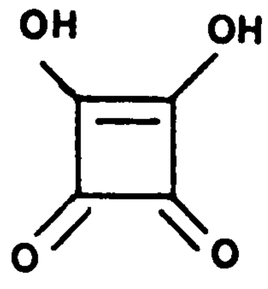

(53)

Squaric acid is a white crystalline dibasic acid which has a pK_2 of 2.2 ($pK_1 \approx 1$) and is therefore almost as strong as sulphuric acid (pK_2 of 1.5). It is a remarkably stable solid due to strong intermolecular hydrogen bonding, and has a decomposition point of about 293°C and an aqueous solubility of ca. 3% by weight at room temperature. Cohen et al interpreted the high acid strength as evidence that the squarate anion was greatly resonance stabilised. This delocalised structure (54) led to the suggestion that the squarate ion was aromatic, and

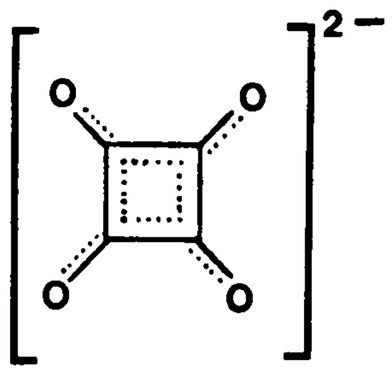

(54)

that the oxocarbon anions may constitute a hitherto unknown aromatic series[49,50]. This is a logical deduction if one of the tautomers, (55), of (54) is considered. Here the cyclobutene ring contains two

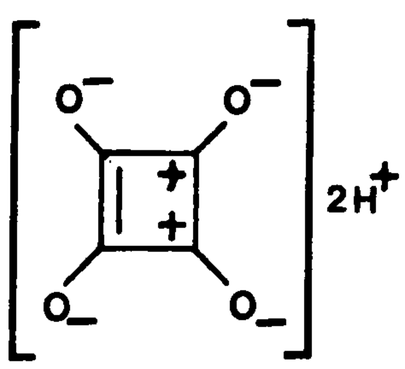

(55)

positive charges and so the ring has two π-electrons, which fits the Hückel (4n+2) rule for an aromatic ring. Evidence from vibrational spectroscopy and x-ray analysis soon confirmed this hypothesis[51-54].

The synthesis of squaric acid has proved difficult although several

routes are available[55]. For instance, Cohen and co-workers prepared squaric acid from chlorofluoromethane (56) by dimerisation and subsequent substitution and hydrolysis as shown in Scheme (5).

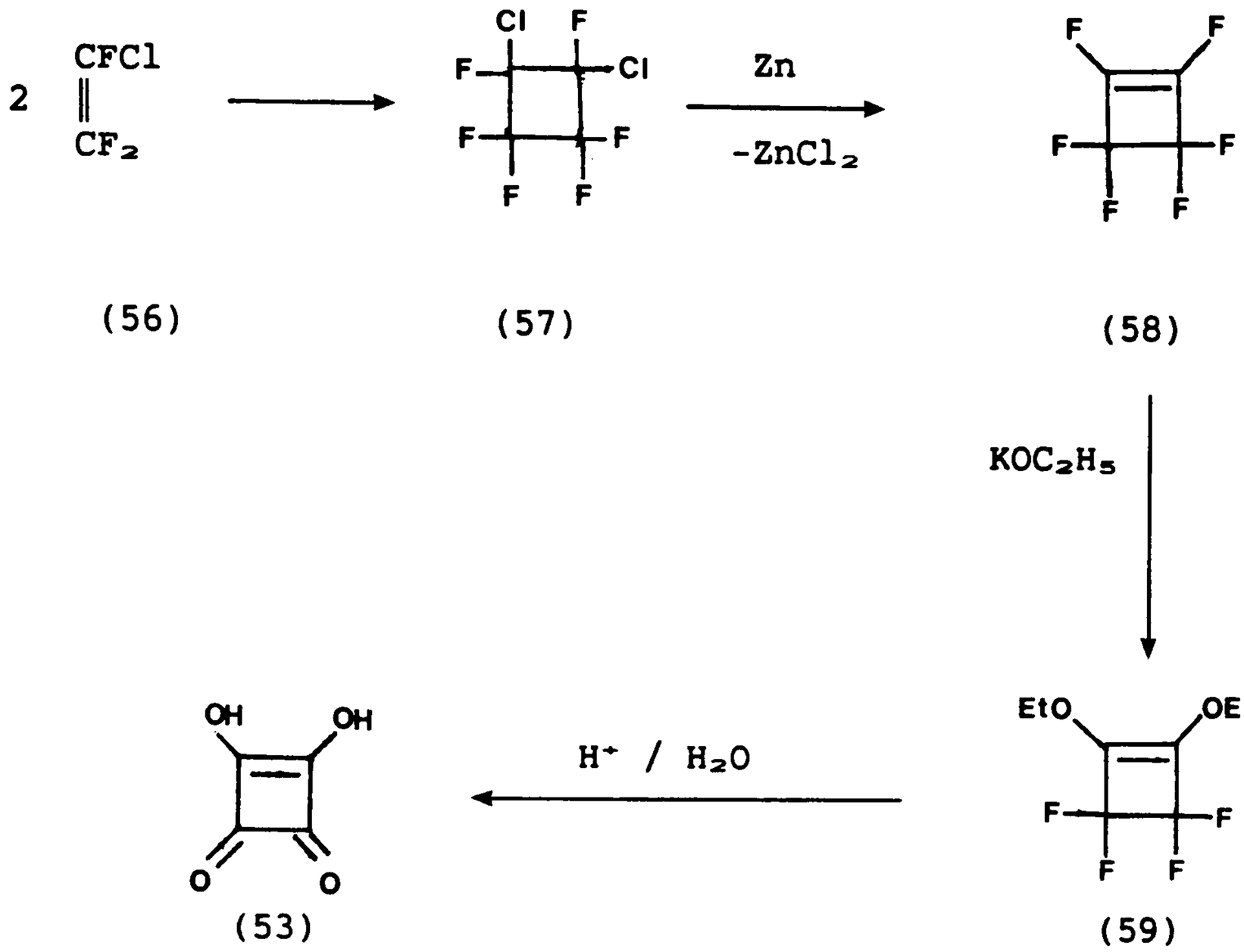

(56) (57) (58) (59) (53)

Scheme 5

Commercially, squaric acid can be obtained from hexachlorobutadiene (60) which is a by-product in the manufacture of perchlorinated hydrocarbons[56]. Thus the diene is heated with 70-96% sulphuric acid for several hours at temperatures between 80 and 150°C to give, on cooling the desired product (Scheme 6)[57]. In the laboratory such reactions are difficult to reproduce efficiently.

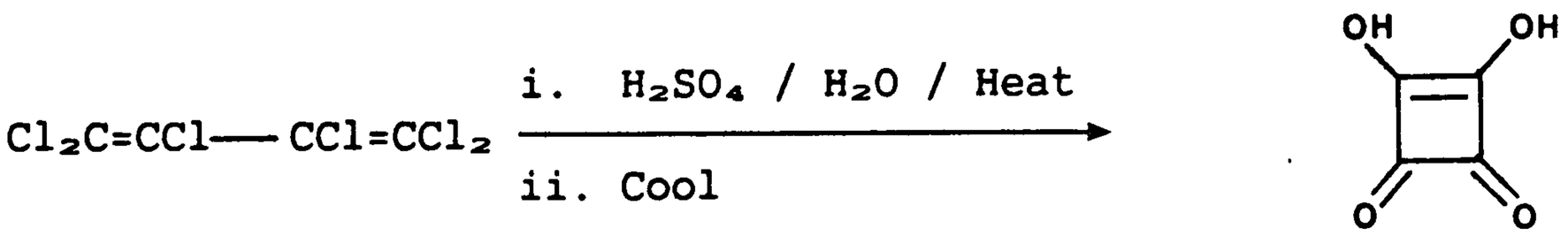

(60) (53)

Scheme 6

In 1965 Treibs and Jacob examined the reaction of pyrroles (61) with squaric acid[58]. The components reacted in a 2:1 molar ratio to give intense red-violet coloured condensation products (62).

Nucleophilic attack took place on opposite carbons in the 4-membered ring and not, as might have been expected, at neighbouring carbon atoms (Scheme 7).

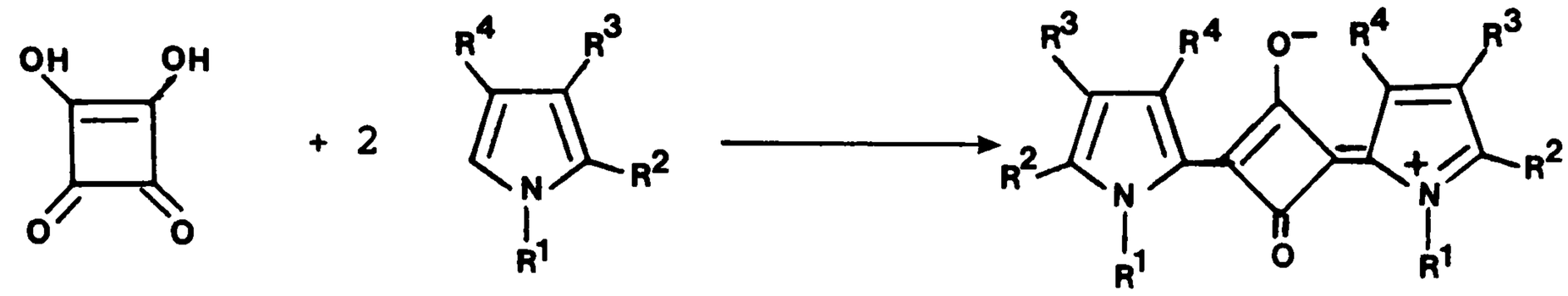

(61) (62)

Scheme 7

These authors also showed that if both the 2- and 5-positions in the pyrrole were occupied then no reaction occurred. However, if both positions were unoccupied then mixtures of dyes with varying colours from green to blue based on structure (63) were obtained.

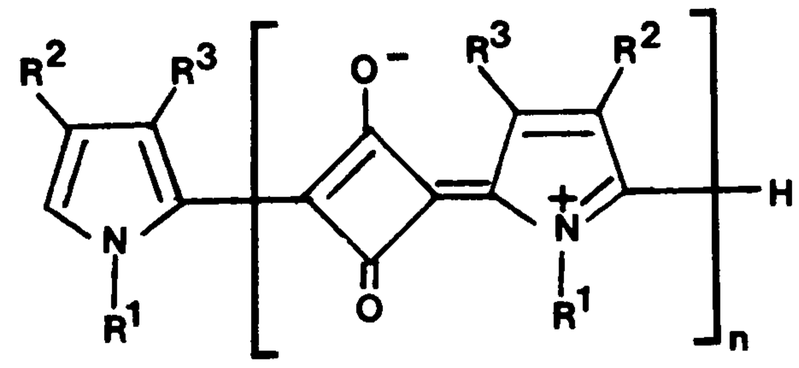

(63)

It is generally recognised that any sufficiently nucleophilic reagent, for example heterocyclic enamines or N,N-dialkylarylamines will react with squaric acid with the formation of a carbon-carbon bond. However, it should be noted that if a primary or secondary arylamine is used, reaction occurs preferentially at the nitrogen atom to form a carbon-nitrogen bond. Such dyes, for example (64)[59] tend to

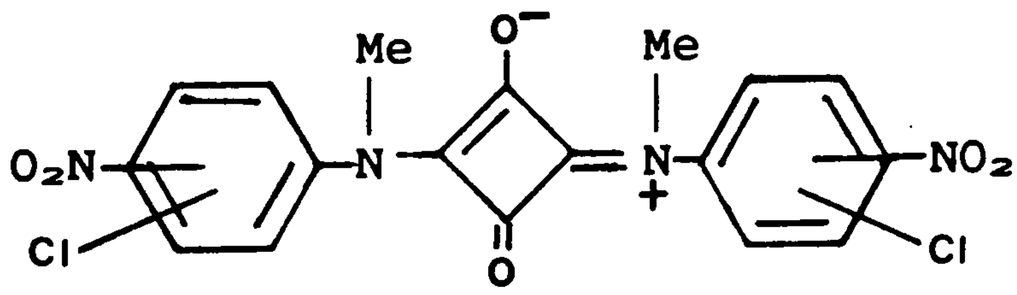

(64)

be yellow in colour and are highly insoluble in organic solvents. If a tertiary amine is used, such as N,N-dimethylaniline reaction occurs at the 4-position of the arylamine, and an intensely coloured dye is formed, eg. (65).

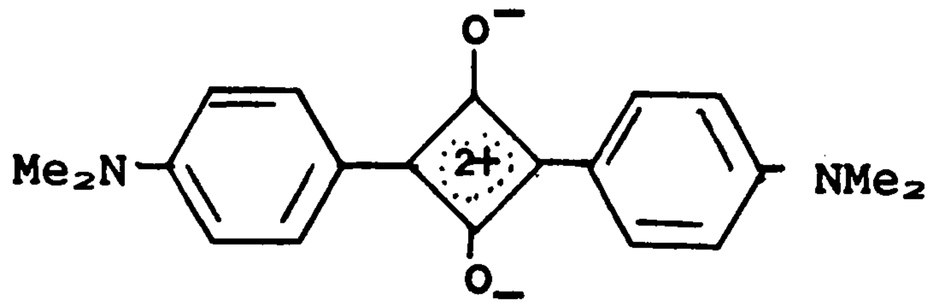

(65)

Dye (65) absorbs at 630nm in dichloromethane which may be compared with the azo dye (66) of similar size which absorbs at 478nm. This

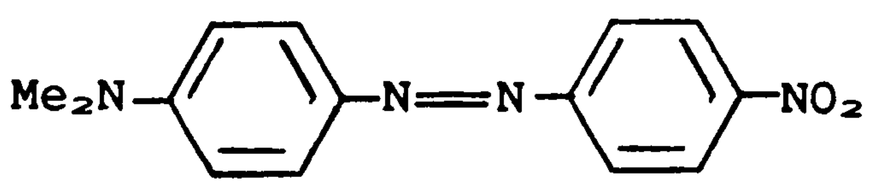

(66)

illustrates how much more bathochromic a simple squarylium dye is when compared to other chromogens.

The bathochromic nature of squarylium dyes can be explained to a large extent by PMO theory. This predicts that if a strong electron donating group is placed at a starred position in a cyanine-type system then a large bathochromic shift should result. An extreme case is (67). Here the overall structure is electronically neutral

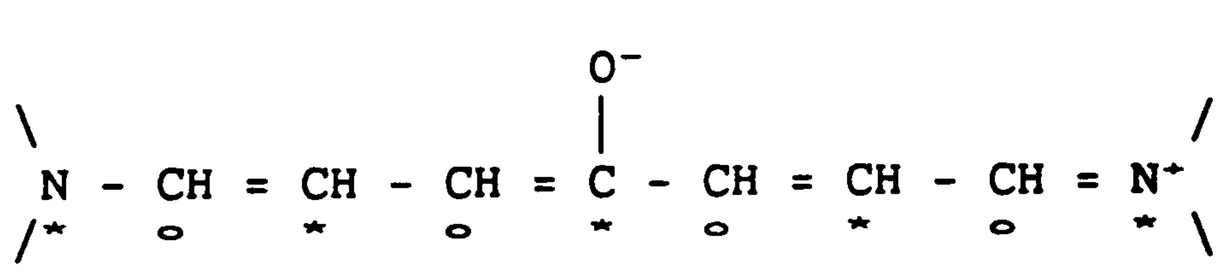

(67)

but a non-polar resonance form cannot be drawn. Squarylium dyes are in fact of this type. Moreover, Dewar's rules also indicate that a further bathochromic shift is obtained if electron withdrawing groups

are positioned at unstarred sites. In the 1,3-squarylium dyes (68) a carbonyl group can be considered to be attached to two such positions.

(68)

Additionally, the dyes are stabilised by the fact that the 4-membered ring dione will readily accept the negative charge and that there is electronic symmetry within the molecule, as proved by single crystal x-ray data[60]. Thus (65) may be considered as a hybrid of the various resonance structures (I) to (IV).

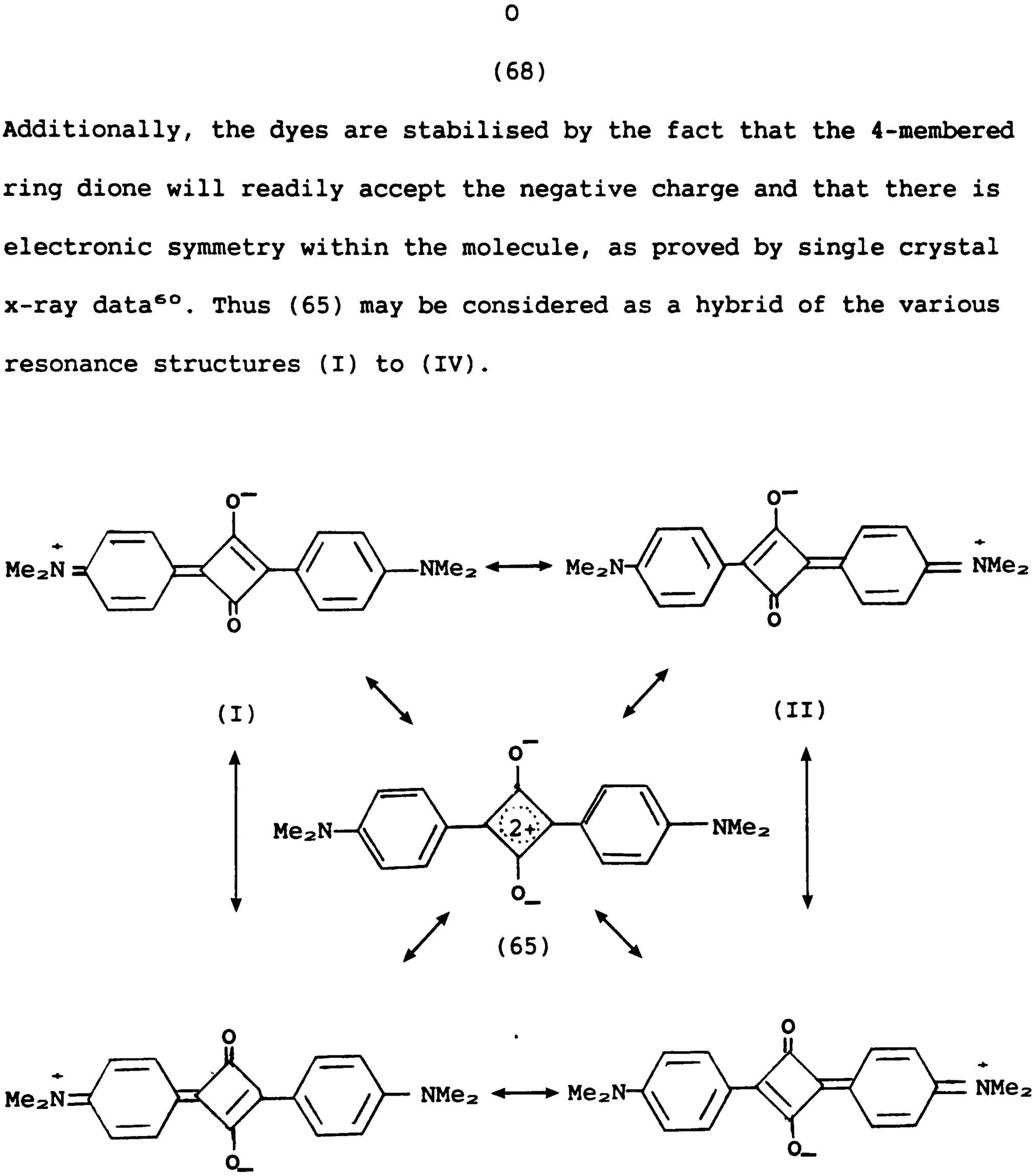

(I) (II) (65) (III) (IV)

Such qualities impart certain characteristics to the squarylium dyes, namely,

a. a large bathochromic shift of the visible absorption band,

b. a narrow band width,

c. a high intensity, and

d. minimal secondary absorption in the visible region.

Squarylium dyes are generally obtained by azeotropically refluxing the chosen nucleophile and squaric acid in a 2:1 mixture of n-butanol and toluene. Law and Bailey[61] demonstrated that the reaction proceeds via the di-n-butylsquarate (70). Having obtained this ester the presence of water or acid in the solvent system is necessary to effect dye synthesis (Scheme 8). These results indicate that the

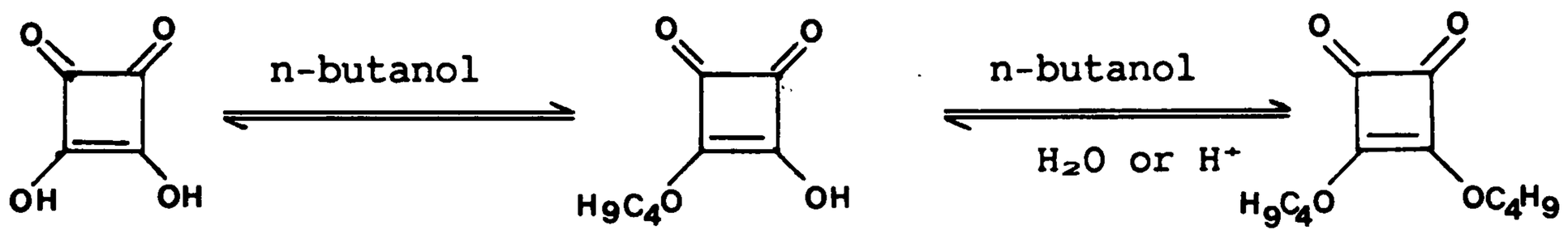

(69) (70)

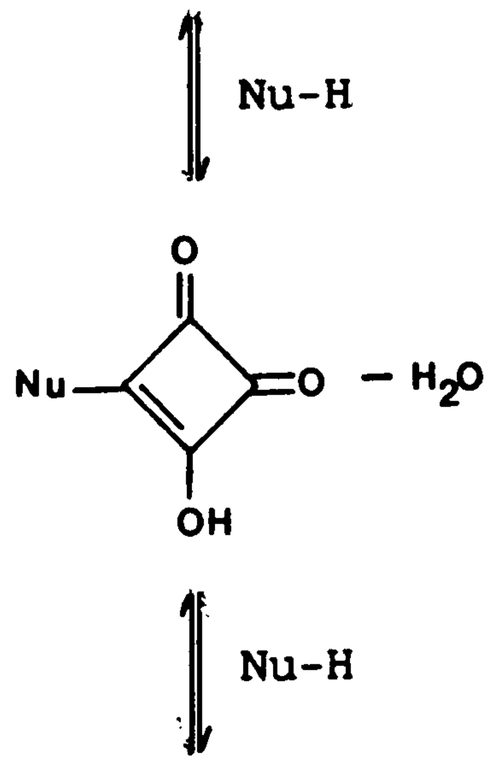

Scheme 8

di-n-butylsquarate is hydrolysed to the monoester (69) and this is the precursor of squarylium synthesis. This was confirmed by Kuramoto et al[62].

Law and Bailey[61] also showed that, with the exception of secondary or tertiary alcohols, other hydroxylic solvents can be successfully substituted for n-butanol and that without such a solvent no reaction occurs.

1,2-Disubstituted squarylium dyes, eg. (71) are also known[63-65].

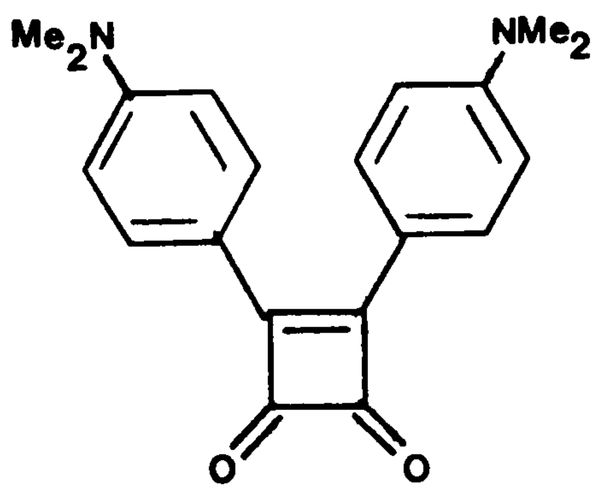

(71)

They are much less bathochromic than the 1,3-squaryliums, and although stable in acid solution tend to ring open and polymerise (Scheme 9) when dissolved in, for example chloroform[61].

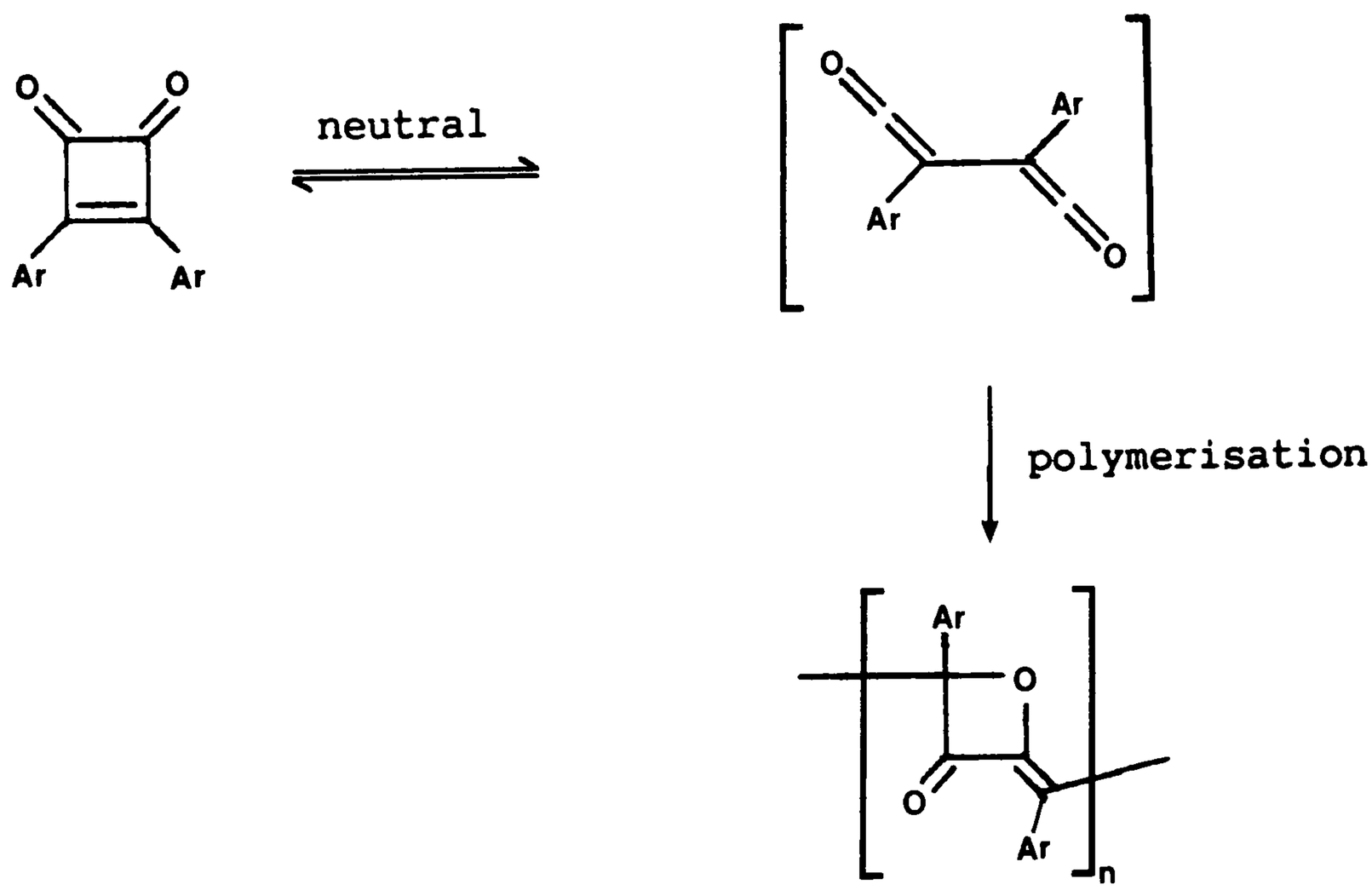

Scheme 9

Unsymmetrical squarylium dyes are also known[66,67]. Table 8 lists some examples, and in spite of their asymmetry they show only one absorption peak in the uv-visible region.

Table 8: Examples of unsymmetrical squarylium dyes[67]

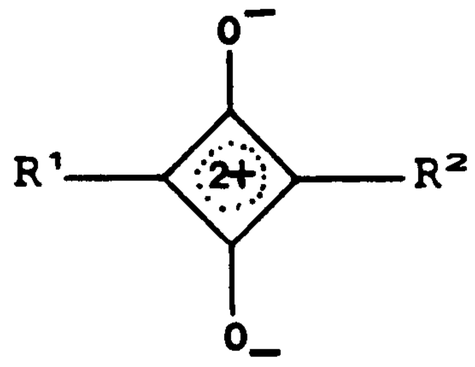

Structure	R^1	R^2	λ_{max}/nm ($CHCl_3$)	ε_{max}/$lmol^{-1}cm^{-1}$ ($CHCl_3$)
(72a)	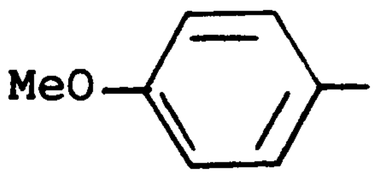	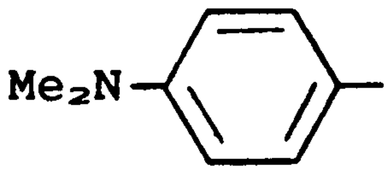	579	53,700
(72b)			590	53,200
(72c)		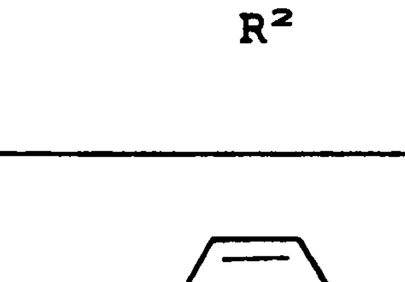	592	53,500

The visible absorption band of squarylium dyes can, with suitable choice of terminal amino residues be displaced into the near-infrared region. Examples of such dyes include the quinolinium derivative (73) and the naphthylamine based system (74)[62,68].

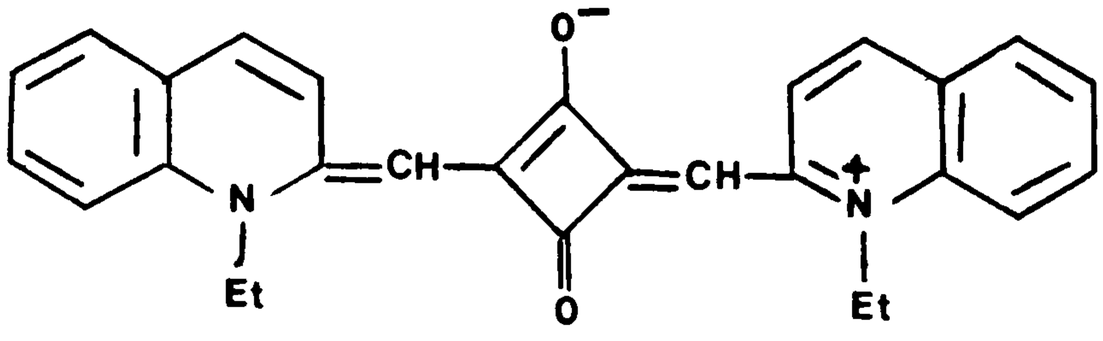

λ_{max} = 732nm (chloroform)

(73)

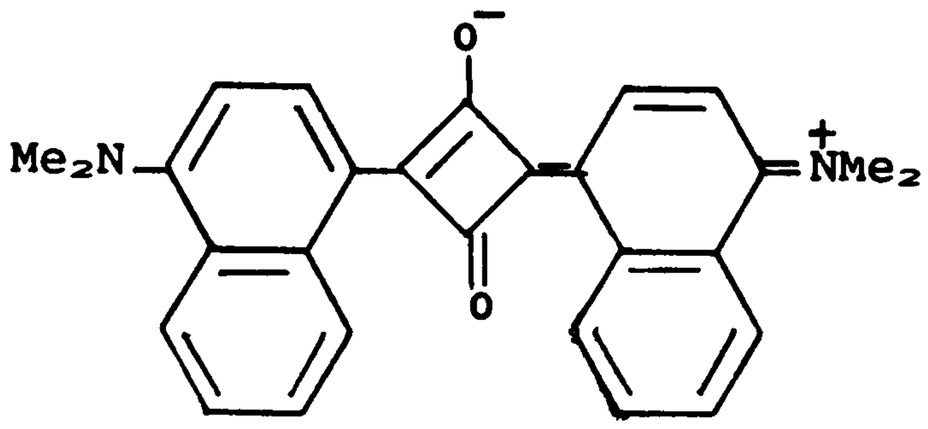

λ_{max} = 716nm (acetone)

(74)

In general, any attempt to shift the absorption band of the squarylium dyes to the infrared is offset by a decrease in dye stability and a general broadening of the maximum absorption band. Such dyes also tend to have low organic solvent solubilities. However, squaryliums have better heat and light stability and are less coloured than cyanine-type dyes. As such, they provide a promising means of obtaining colourless near-infrared absorbing dyes

1.3.5.2 Croconium Dyes

Croconic acid (75) was probably synthesised originally [as the dipotassium salt (76)] by Berzelius, Wöhler and Kindt[69] who, in 1823, it appears were trying to derive a novel industrial preparation of potassium from carbon and potassium hydroxide. Two years later Gmelin isolated the pure dipotassium croconate and croconic acid

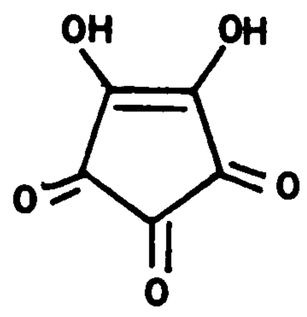

(75)

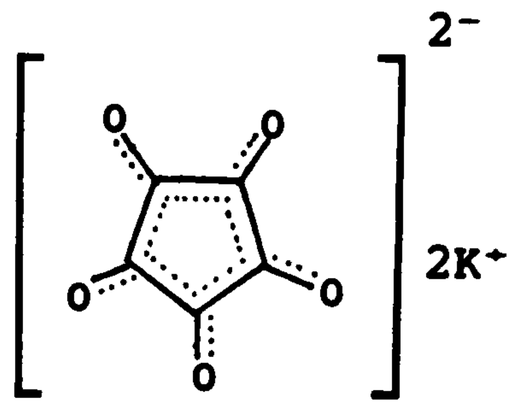

(76)

from this mixture[70]. This date is of historical interest because it was in the same year that Michael Faraday first isolated benzene from illuminating gas oil. Thus the croconate ion and benzene must share the distinction of being the first aromatic compounds to have been isolated. Unlike benzene, whose aromatic properties were soon realised, those of croconic acid were not appreciated for another 133 years. Even then Yamada only mentioned the fact that such a system may be aromatic in passing at the end of a lengthy article and so it was overlooked[71]. It was not until after the discovery of squaric acid in 1959 that the aromatic properties of croconic acid were recognised.

Croconic acid itself is a light-sensitive yellow solid that, unlike squaric acid, is very hygroscopic. Consequently when it is synthesised the initial product is the trihydrate[72]. The anhydrous acid can be obtained by heating the trihydrate at 120°C for 2-4 hours. Croconic acid slowly decomposes when heated above 150°C. It may be characterised as the dimethyl ether which has a melting point of 113°C.

Surprisingly since Gmelin's discovery of croconic acid, an alternative route for its synthesis (Scheme 10)[73] has not been found. Thus the desired hexahydroxybenzene (77) undergoes ring contraction *via* an α-oxo rearrangement, which is related to the benzilic acid rearrangement, to yield the dianion (78), in the form of its metal salt.

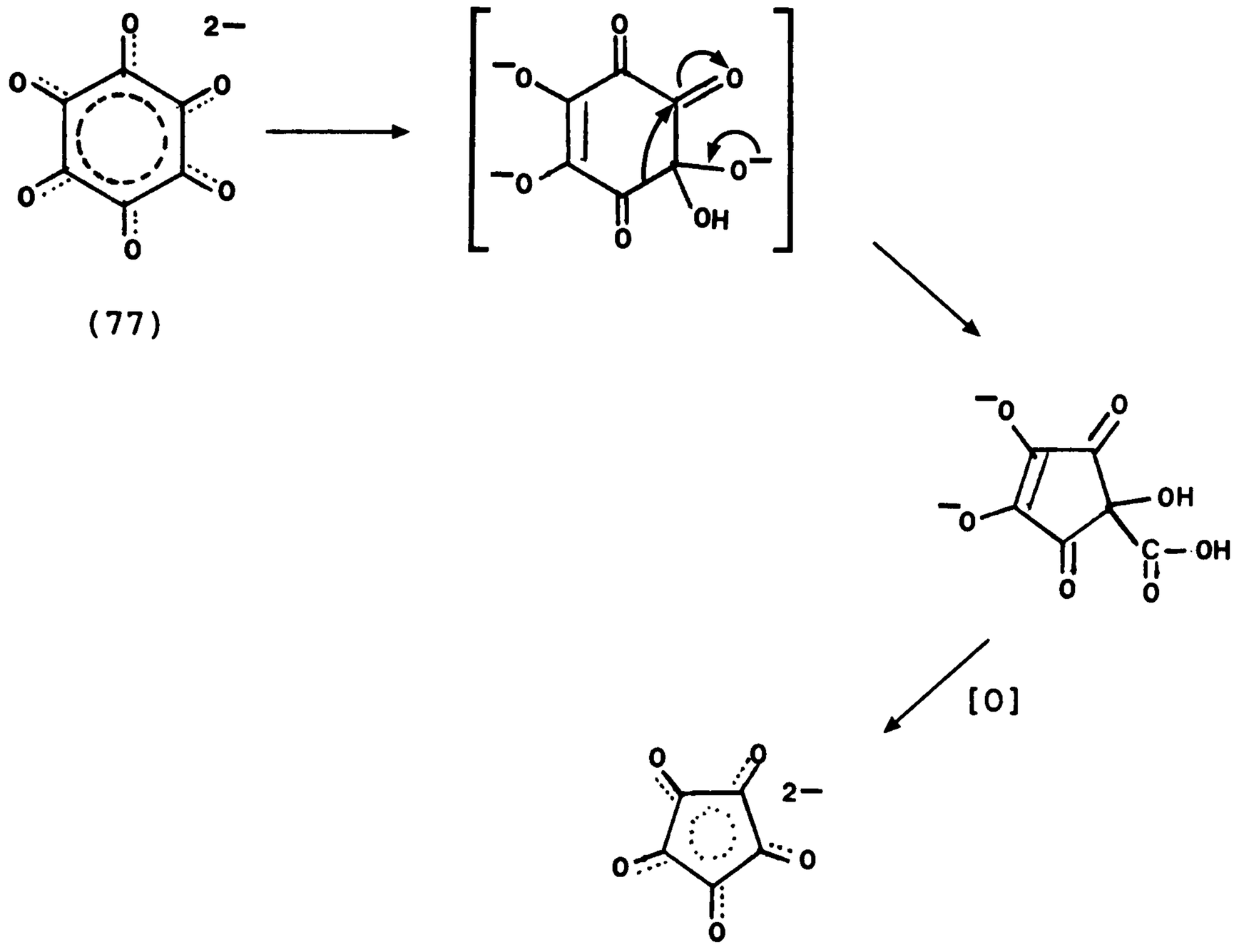

(77) (78)

Scheme 10

The synthesis can be simplified somewhat by using a starting material of a higher oxidation state. Thus croconic acid is efficiently prepared by the oxidation of tetrahydroxy-p-benzoquinone (79)[72] or rhodizonic acid (80)[71] with manganese dioxide followed by

(79) (80)

addition of barium chloride in order to obtain barium croconate. Treatment of this salt with warm dilute mineral acid yields croconic acid trihydrate. Currently croconic acid is not offered commercially.

A far more amazing synthesis of croconic acid has recently been

postulated by Hartley, Wolff and Travis[74], who suggested that trace amounts of croconic acid are created in the cloud top region of Venus from carbon monoxide. As croconic acid is a strong uv-visible absorber this would account for the yellow colour and uv-absorbing cloud features of the planet. Experimental results have been obtained which appear to support this theory.

Croconic acid appears to have a very unusual mobile structure as pointed out by Hirata and co-workers (Scheme 11)[75]. Normally the acid

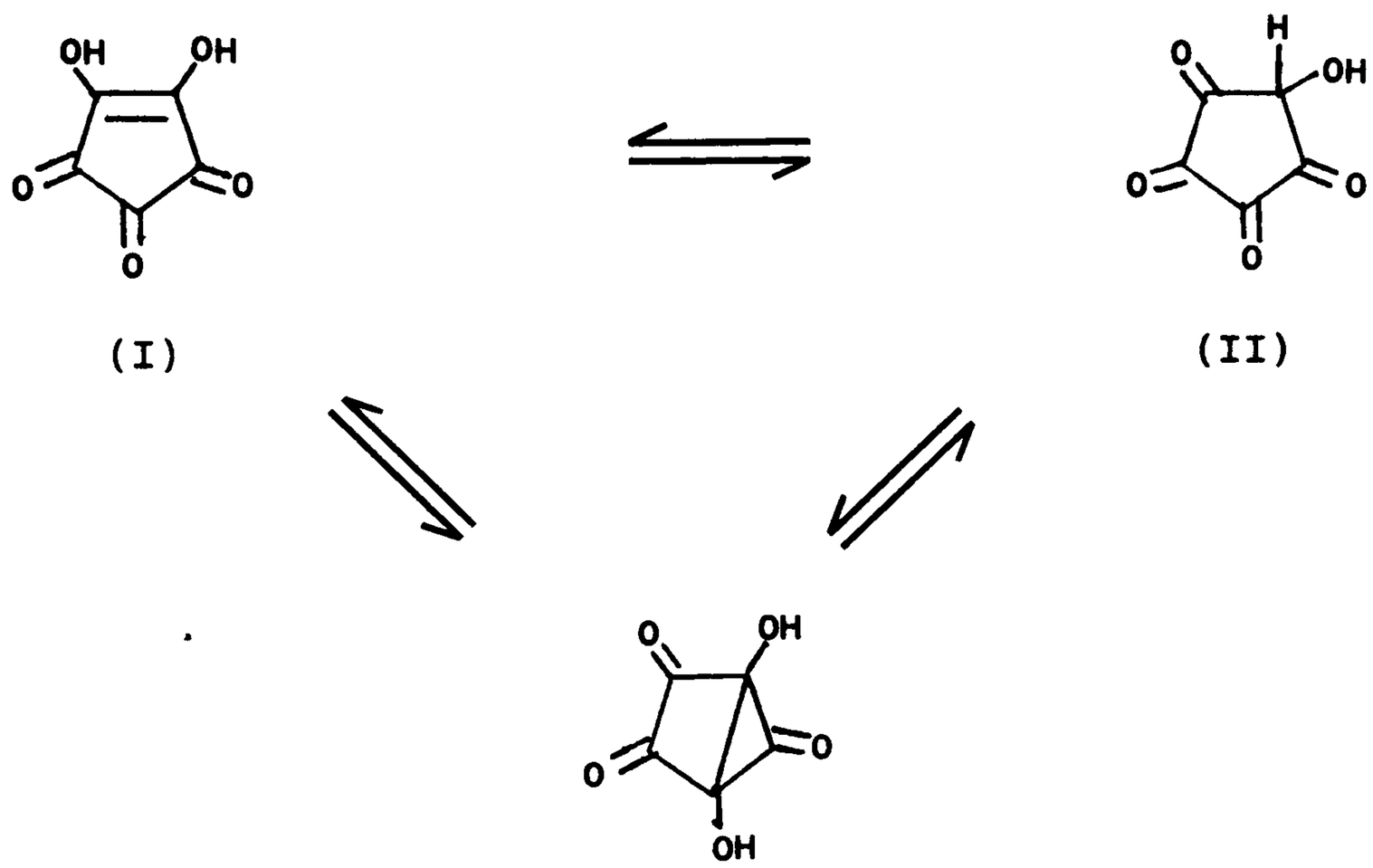

(I) (II) (III)

Scheme 11

is considered to be an equilibrium mixture of (I) - (III). When it reacts as the enediol it possesses structure (I) and when the acid is decolorised by light the equilibrium is shifted to (III).

In 1973, Treibs and Schulze reported the synthesis of several pyrrole based croconium dyes (81)[76]. The dyes were unstable and so

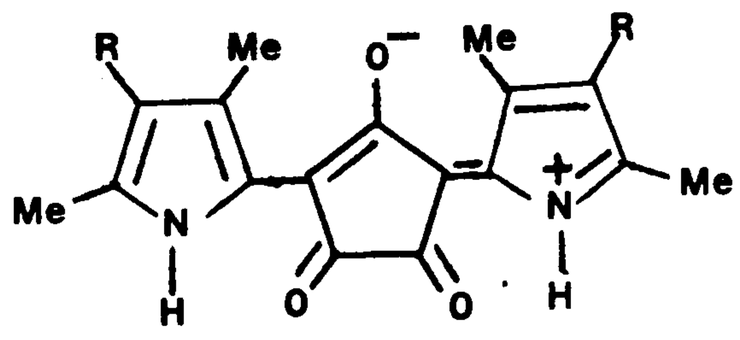

(81)

problems were encountered in their purification. However the dyes were green in colour and thus far more bathochromic than the analogous squarylium pyrroles (62).

In the same paper a series of pyrrole dyes derived from the 6-membered ring oxocarbon rhodizonic acid (80) were prepared. The dyes (82) were violet in hue and therefore more hypsochromic than the

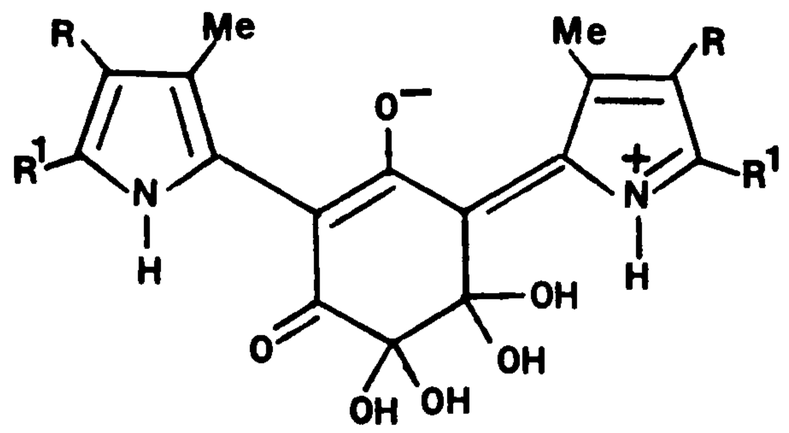

(82)

pyrrole croconiums. Their absorption peaks were also much broader.

In the same year croconic acid was used as a reagent to identify indoles by "complexing" with them to form red-blue products[77].

In the late 1970's Fatiadi successfully condensed malononitrile with croconic acid to obtain "croconate violet"(83) and "croconic acid blue"(84)[78,79]. As the name implies croconate violet is an intense

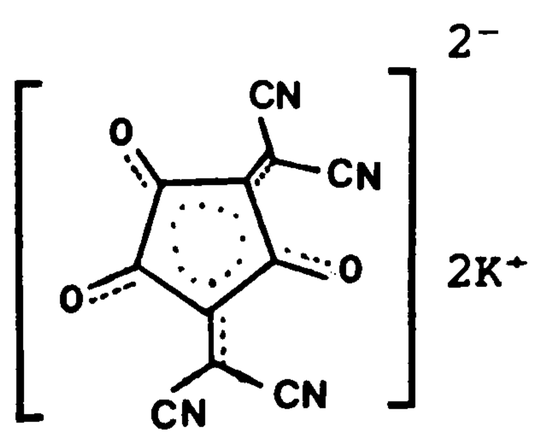

(83)

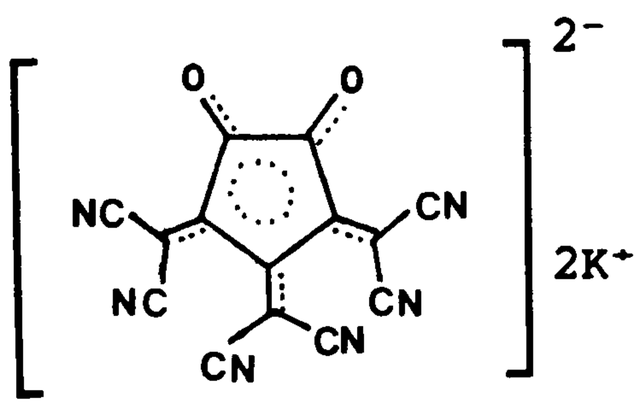

(84)

violet colour absorbing at 533nm (ε_{max}=100,000). It is prepared by heating the dipotassium croconate with the appropriate quantity of malononitrile in aqueous solution. Croconic acid blue absorbs at 600nm (ε_{max}=55,000) in aqueous solution and it is prepared by the

action of malononitrile on croconic acid, again, in a hot aqueous solution but treatment with potassium methoxide in methanol is necessary to obtain the dipotassium salt. Croconic acid blue is very solvatochromic, giving red solutions with λ_{max} at 475-480nm in anhydrous acetone or alcohol.

As mentioned earlier with the pyrrole dyes (81), the croconiums are more bathochromic than the squaryliums. This additional red shift of about 130nm can be explained by PMO theory. The same arguments as previously developed for the squarylium system (68) are applicable to the idealised croconium configuration (85), except that in (85) there

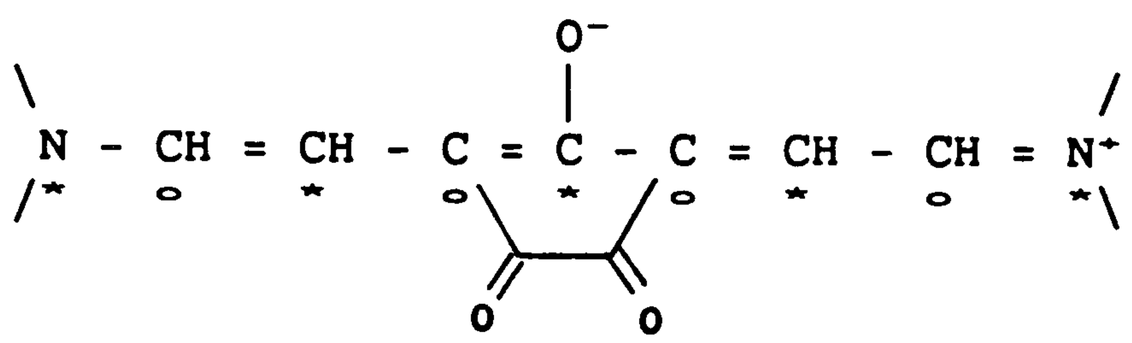

(85)

are two carbonyl groups sharing two unstarred positions instead of just the one in the squarylium system (68). Additionally the negative charge is stabilised by delocalisation over a 5-membered ring trione instead of a 4-membered ring dione. Hence, the croconium dyes are more bathochromic than their squarylium counterparts.

It is rather surprising that it was not until the early 1980's that croconium dye chemistry began to evolve rapidly[80]. This late development must be partly attributable to the fact that croconic acid is apparently rather more selective than squaric acid with regards to the nucleophiles it will react with. For instance, there is currently no method for the condensation of simple N,N-dialkylarylamines with croconic acid, whereas such condensations occur readily with squaric acid. However, if a 3-hydroxy-N,N-dialkyaniline is used the croconic acid readily condenses forming a carbon-carbon bond at the 3-position

of the arylamine. Croconic acid appears also to react readily with enamines, eg. Fischer's base. Apart from these two classes of nucleophile, at present little else appears to react with croconic acid to form suitably bathochromic dyes.

Several croconium dyes were recently reported by Matsuoka et al[81], Table 9, which illustrate the general characteristics of the chromophore. All the dyes were near-infrared absorbing with very high extinction coefficients and narrow band widths. The dyes also exhibited negative solvatochromism due to the fact that the ground state has a more polar structure than the excited state[3]. In addition these dyes have three carbonyl groups that can strongly interact with the polar solvent, thus also aiding the ground state stability.

Table 9: Near-infrared absorbing croconium dyes[81]

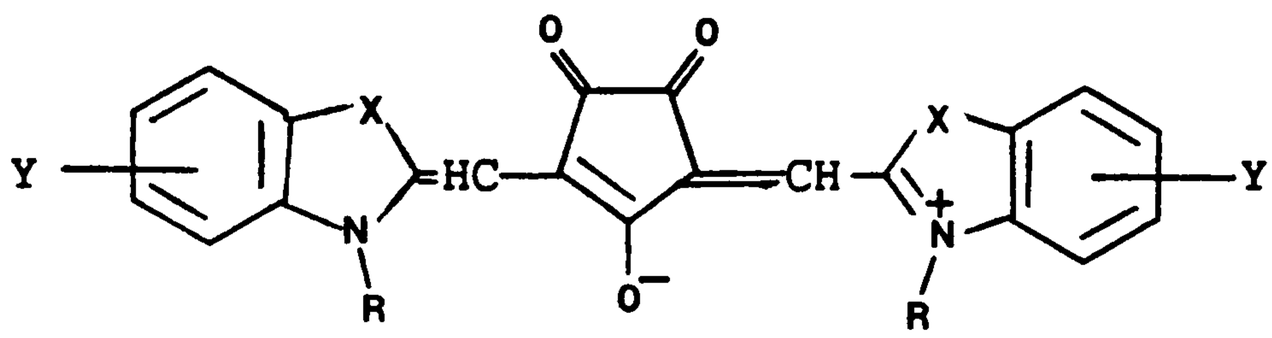

(86)

Structure	X	Y	R	λ_{max}/nm		ε_{max}/$lmol^{-1}cm^{-1}$
				CH_3CN	CH_2Cl_2	CH_3CN
(86a)	CH=CH	H	Et	832	850	222,000
(86b)	CMe_2	Benzo	Me	791	804	108,000
(86c)	Se	H	Et	789	804	200,000
(86d)	S	H	Et	771	784	223,000
(86e)	CMe_2	H	Me	764	775	97,000

1.4 METAL COMPLEX DYES

1.4.1 The Phthalocyanines

In 1928 iron phthalocyanine (87; M=Fe) was synthesised as a by-product in the manufacture of phthalimide. It was soon realised that if the central iron atom was replaced by copper an improved blue pigment was obtained, ie. copper phthalocyanine (87; M=Cu), [λ_{max}=678nm (vapour phase)][82].

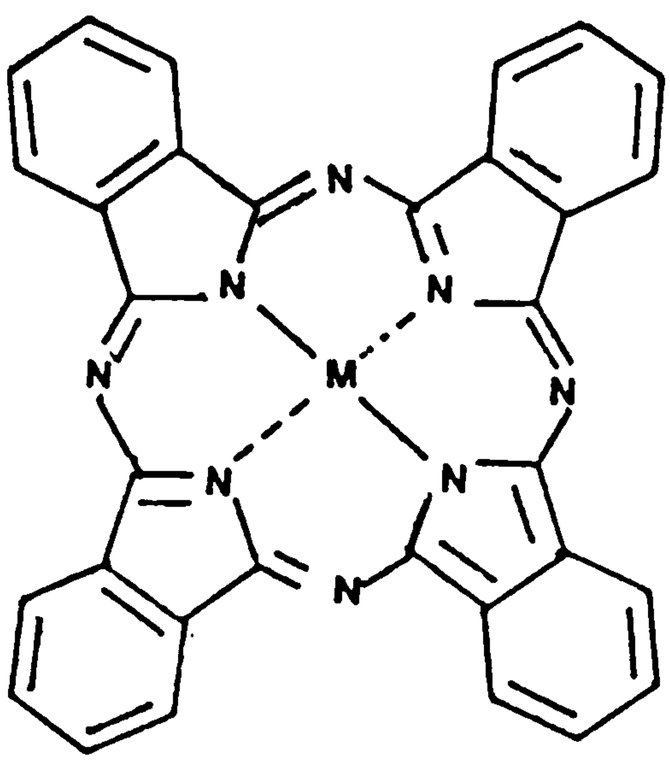

(87)

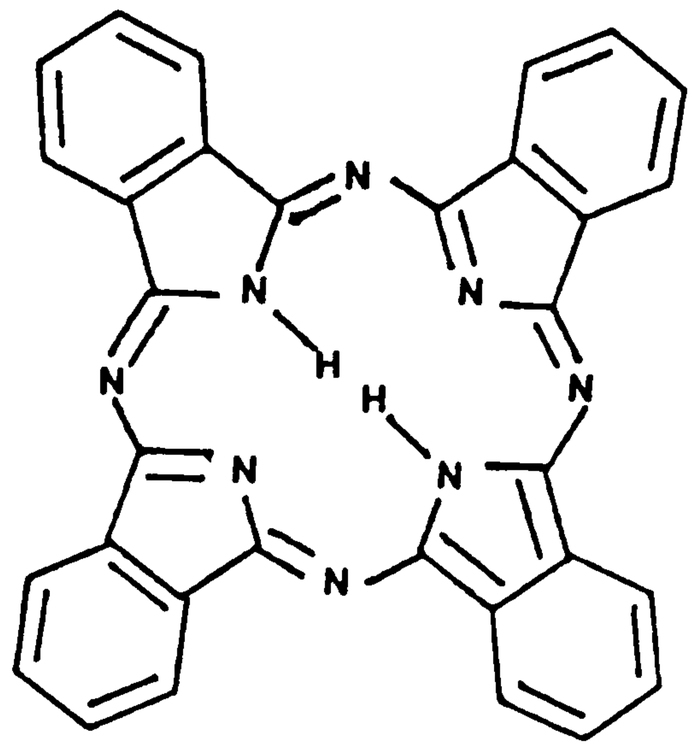

(88)

Phthalocyanines are one of the most stable and tinctorially strong classes of chromogen known. As such, they have received much attention as potential near-infrared absorbers[83].

Bathochromic shifts can be induced into the phthalocyanines by various means, namely,

a. polymorphism in the solid state,

b. the use of different complexing metals,

c. the incorporation of electron donor substituents into the system and,

d. benzannelation.

A number of polymorphic forms of both metallised and metal-free phthalocyanines are known and used commercially. For example, copper phthalocyanine exists in two major polymorphic forms, the blue α-form and the greener, more stable ß-form. The x-form of the metal free

phthalocyanine (88) is particularly interesting from the infrared dye chemist's viewpoint because, besides possessing a peak at ca. 680nm, it absorbs intensely at 800nm.

The use of different central metal atoms can have a profound effect on the spectral properties of the phthalocyanines (Table 10). Thus

Table 10: Phthalocyanines (87) containing different central metal atoms[84-86]

Structure	M	λ_{max}/nm	Structure	M	λ_{max}/nm
(87a)[84]	Mg	675	(87g)[84]	Cu	678
(87b)[84]	AlCl	680	(87h)[84]	Sn	672
(87c)[84]	$SnCl_2$	680	(87i)[85]	$Si(OSi(\underline{n}\text{-}C_6H_{13})_3)_2$	668
(87d)[84]	Fe	658	(87j)[86]	Pb	790
(87e)[84]	Co	672	(87k)[86]	Ti	720
(87f)[84]	Ni	671			

structures (87a) - (87i) all absorb intensely in the red region of the spectrum and so produce blues and greens. Dyes (87j) and (87k) with lead and titanium atoms respectively show absorption maxima in the near-infrared. Many other metals, for example zirconium and molybdenum have been incorporated into the phthalocyanine skeleton in order to obtain highly coloured dyes and pigments[87], but it is the indium chloride and vanadyl based phthalocyanines, such as (89) and (90) respectively, that appear to have attracted greatest interest as infrared absorbers[88,89].

The use of suitably positioned electron donor groups can also induce red-shifts into phthalocyanine systems. For example, if the lead phthalocyanine (91) is considered where X = H then the λ_{max} is 790nm [structure (87j), Table 10]. However if X is N,N-dibutylamino the maximum absorption is displaced to 850nm and if X is morpholino the λ_{max} is 900nm.[90]

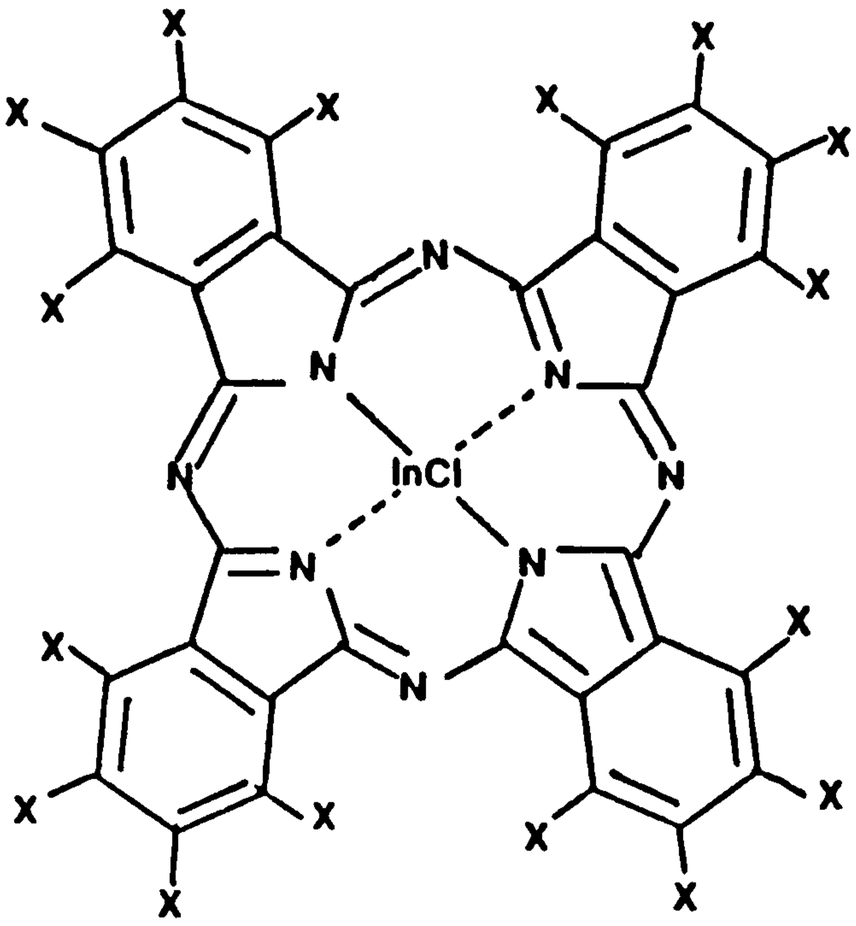

X = EtS

λ_{max} = 830nm

(89)

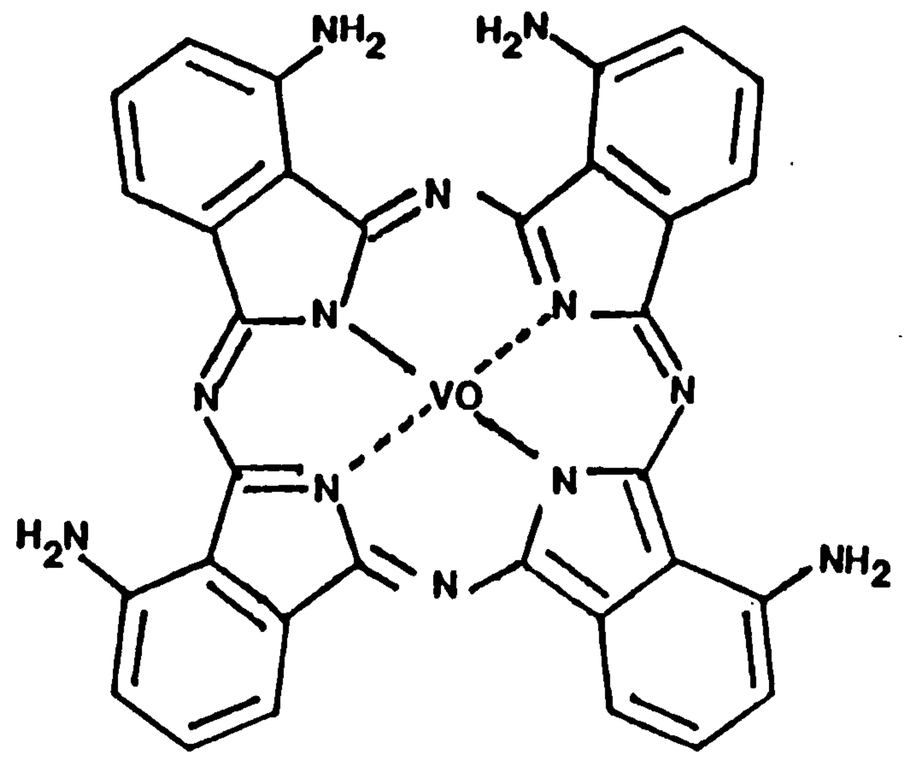

λ_{max} = 762nm

(90)

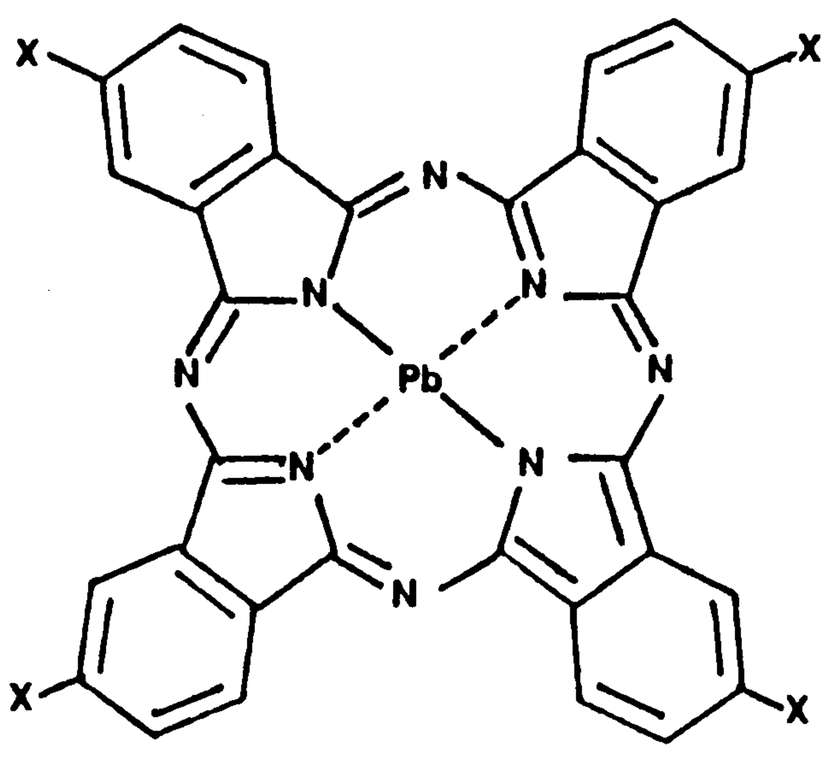

(91)

If the sixteen peripheral positions in copper phthalocyanine are substituted with 4-methylthiophenol then the resulting dye [CuPc-(-S- 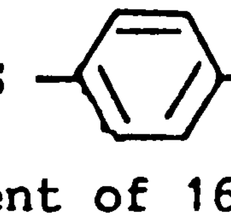 -Me)$_{16}$] absorbs at 770nm with an extinction coefficient of 162,000 in chloroform[91]. Thus, when it is considered that copper phthalocyanine itself is only soluble in sulphuric acid, besides inducing an appreciable shift to longer wavelength into the system, the 4-methylthiophenol groups have also significantly enhanced the dye's solubility.

Extending the conjugation of the phthalocyanines by linear

benzannelation also induces a bathochromic shift. The naphthalocyanine dye (92a) absorbs at 772nm, a red shift of some 104nm[85] relative to the benzene analogue [(87i), Table 10].

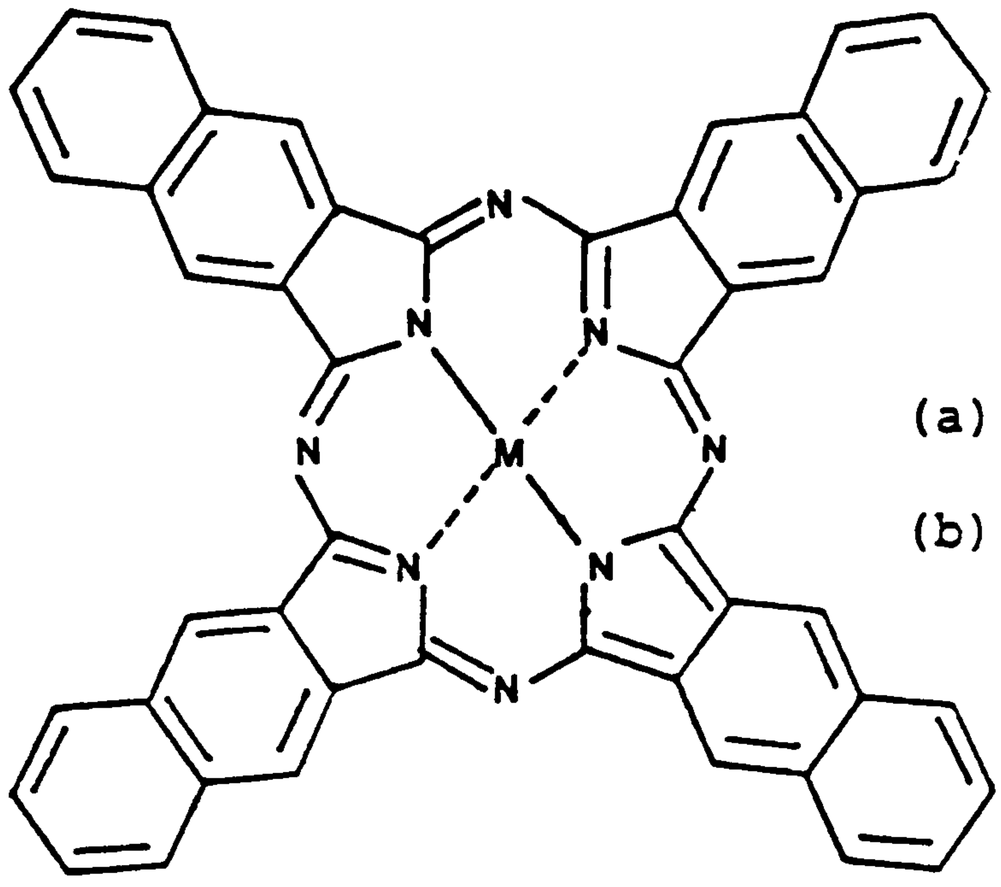

(a) M = $Si(OSi(\underline{n}\text{-}C_6H_{13})_3)_2$

(b) M = Zn

(92)

Non-linear benzannelation also displaces the absorption maxima of these dyes to longer wavelengths, though to a lesser degree. For example, (93) absorbs at 710nm whereas (92b) absorbs at 760nm[92].

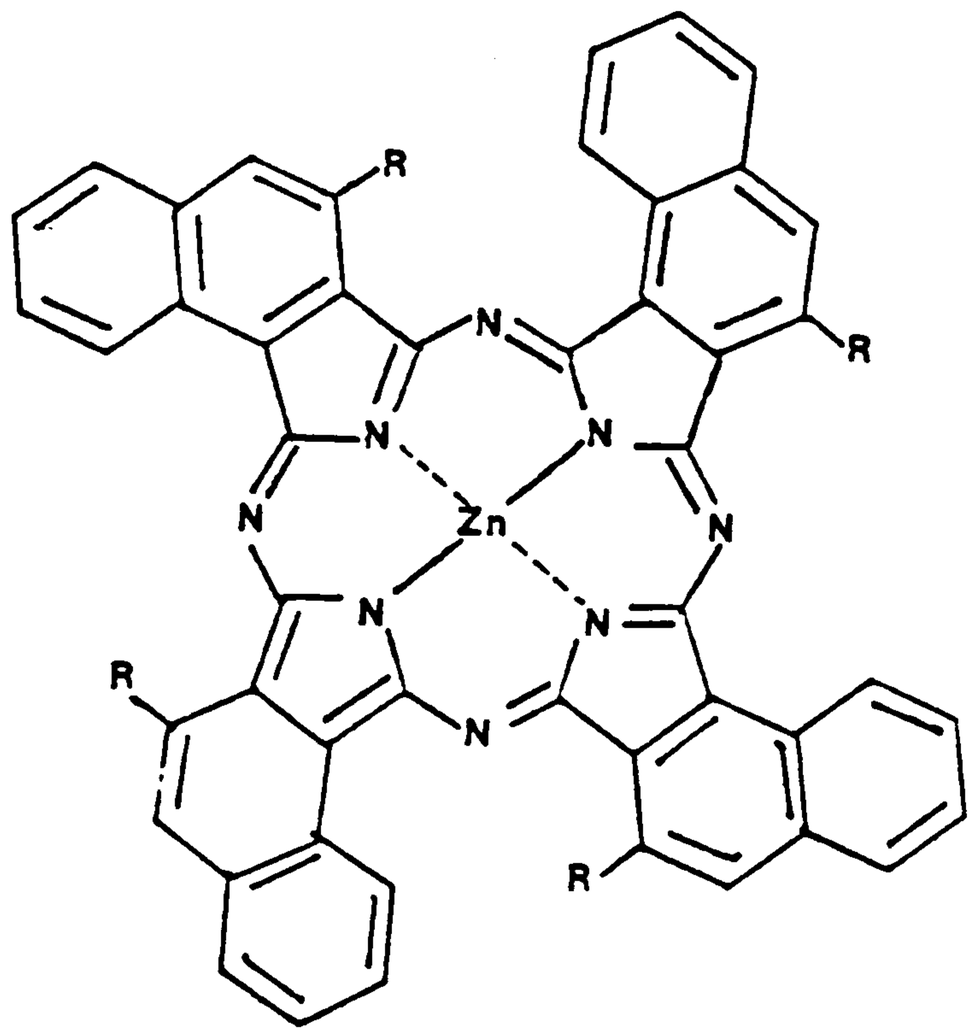

R = $\underline{n}\text{-}C_8H_{17}$

(93)

The phthalocyanine and naphthalocyanine infrared dyes have the best all round stability of the currently known infrared dye classes, and as such are marketed commercially. Their uses include optical data

storage media, security printing and machine readable inks, and charge generation material. Consequently work in this area is currently very active[93].

1.4.2 Metal Complexes of the Dithiolenes and Related Compounds

1,2-Dithoiols or dithiolates, eg. (94), were studied intensively in

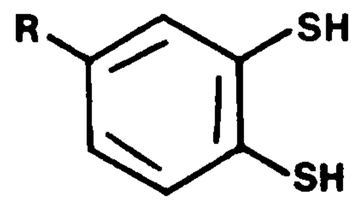

(94)

the mid 1930's as chelating agents[94]. Thus, (94; R=Cl or Me) could be complexed with mercury, zinc, and cadmium cations to give spirocyclic complexes of the type (95).

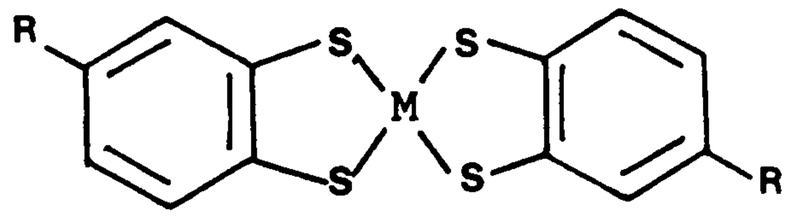

R = Me, Cl
M = Hg, Zn, Cd

(95)

Interest in this type of complex continued and, for example, during the 1940's and early 1950's work on toluene-3,4-diol as an analytical reagent was described[95].

It was only in 1962 that the first infrared absorbing nickel

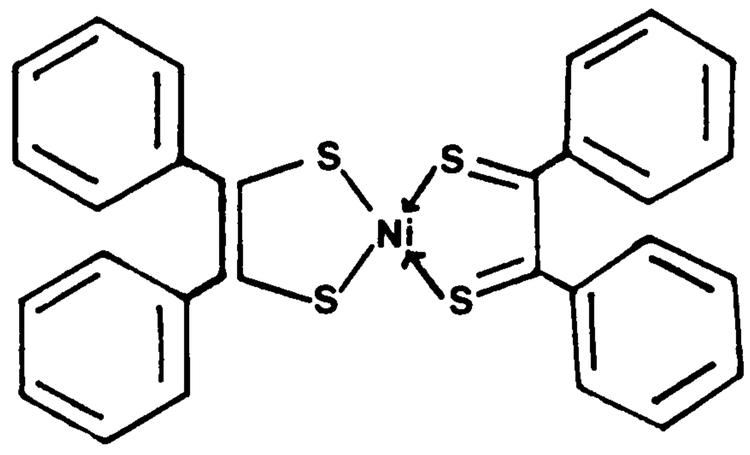

(96)

dithiolene complex was obtained as an unexpected product from the reaction of $Ni(CO)_4$ and sulphur with diphenylacetylene, in an attempt to synthesise thioaromatics using transition metals as catalysts[96]. The complex (96) absorbed at a much longer wavelength than previously known nickel complexes. These complexes could initially only be prepared with some difficulty in low yields by the reaction of alkynes with certain metal sulphides. More recently, complexes of this type have been prepared by refluxing benzoin with P_4S_{10} in dioxane to form the thiophosphoric ester of dithiobenzoin and then adding nickel acetate to form the dithiolene complexes (Scheme 12)[97].

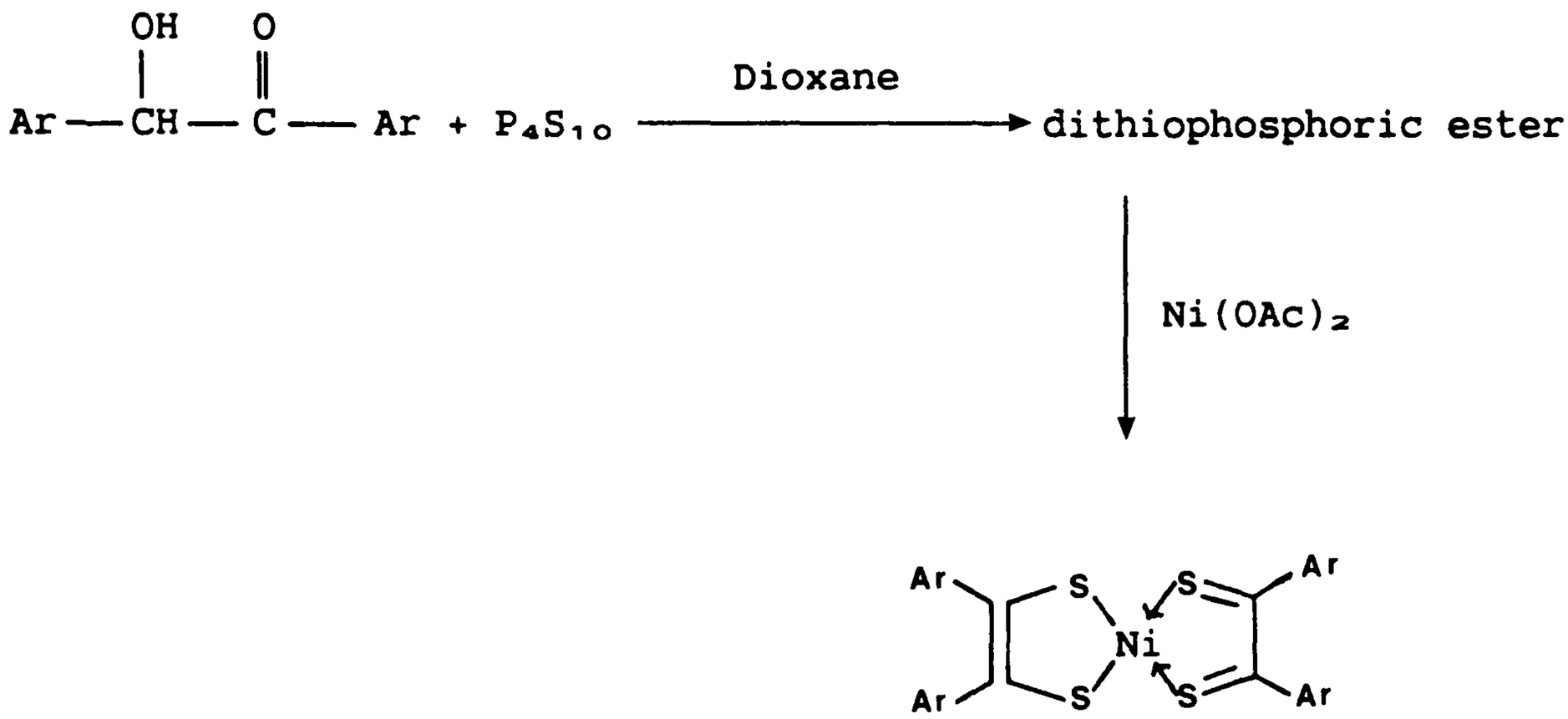

Scheme 12

The complexes are exceptionally air stable and most are stable to non-oxidising acids. All show an intense absorption in the near-infrared region of the spectrum. As this absorption is $\pi \longrightarrow \pi^*$ in nature it is strongly dependent on substituent effects in the ligand. This is exemplified by the spectroscopic data contained in Table (11)[68a]. Evidently phenyl groups extend the conjugation which effects a bathochromic shift and at the same time noticeably increases the extinction coefficient. Electron donor groups have a bathochromic effect and acceptor groups a hypsochromic effect.

Table 11: Spectroscopic data for some typical examples of 1,2-dithiolene complexes[6a]

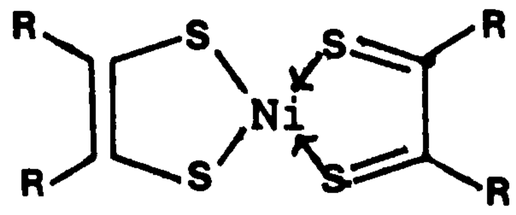

(97)

Structure	R	λ_{max}/nm	ε_{max}/$lmol^{-1}cm^{-1}$ ($x10^{-4}$)
(97a)	$-CH_3$	714[a]	2.82
(97b)	$-CF_3$	714[a]	1.22
(97c)	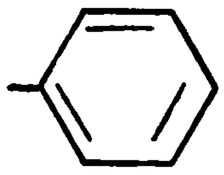	866[a] 855[b]	3.01 3.02
(97d)	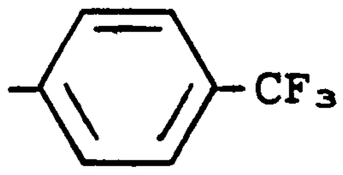	832[b]	2.99
(97e)	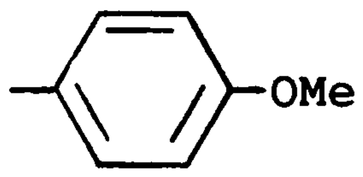	894[b]	2.80

(a) - measured in $CHCl_3$
(b) - measured in CH_2Cl_2

The λ_{max} of such complexes can be influenced not only by the central metal atoms and the substituent groups R (97), but also by the nature of the chelating atoms. For example, nitrogen can be used instead of sulphur as recently demonstrated by Matsuoka et al[9a]. These workers synthesised dyes of the general formula (99) by, firstly, reacting the required phenylenediamine (98) with an ethanolic

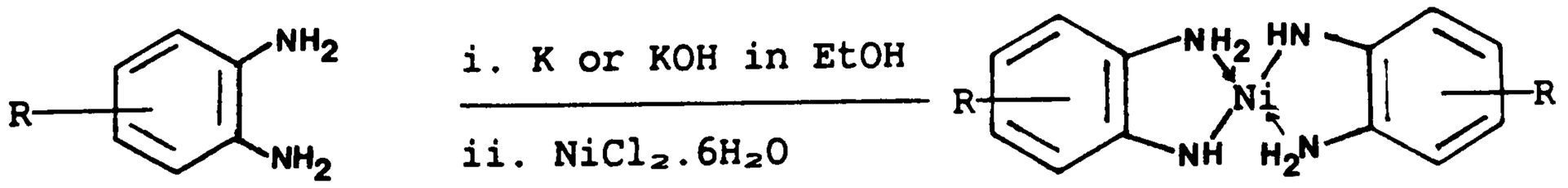

(98) (99)

Scheme 13

solution of potassium ethoxide or potassium hydroxide followed by addition of nickel (II) chloride hexahydrate dissolved in ethanol to effect complex formation (Scheme 13). The dyes of this type are also infrared absorbing.

Nickel dithiolenes are known to be singlet oxygen quenchers and hence inhibit the photofading of dyes[99,100]. Thus, such complexes have been incorporated into cyanine-dye containing optical data storage media, to retard photofading of the cyanine dye which is prone to attack by singlet oxygen[101].

Nickel dithiolenes have also found use as Q-switch dyes, eg. (100a) and (100b) are marketed by Eastman-Kodak for this purpose. 1,2-nickel dithiolenes also find use in laser recording materials, having good

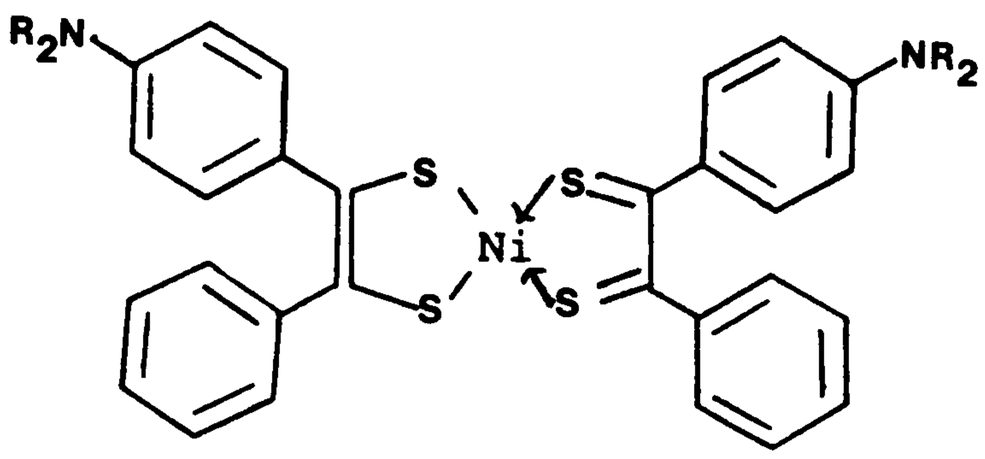

(a) R = Me
(b) R = Et

(100)

sensitivity, high readout signal-to-noise ratio and good degradation resistance. I.C.I. manufacture organic and water soluble (sulphonated) versions for specialised ink applications. Work on these complexes is currently very active[102].

1.4.3 Metal Complex Dyes with Heterocyclic Indophenol-type Ligands

It has been discovered recently that certain indophenol donor-acceptor derivatives complexed to metals at the acceptor group produce dyes that are very bathochromic and show increased extinction coefficients[103]. The dyes generally possess good physical and chemical properties for practical use in laser-diode optical data storage.

One such group of dyes is derived from the indoaniline derivative (103) which may be prepared by coupling 8-hydroxyquinoline (101) with a 4-dialkylaminoaniline hydrochloride (102) in the presence of an

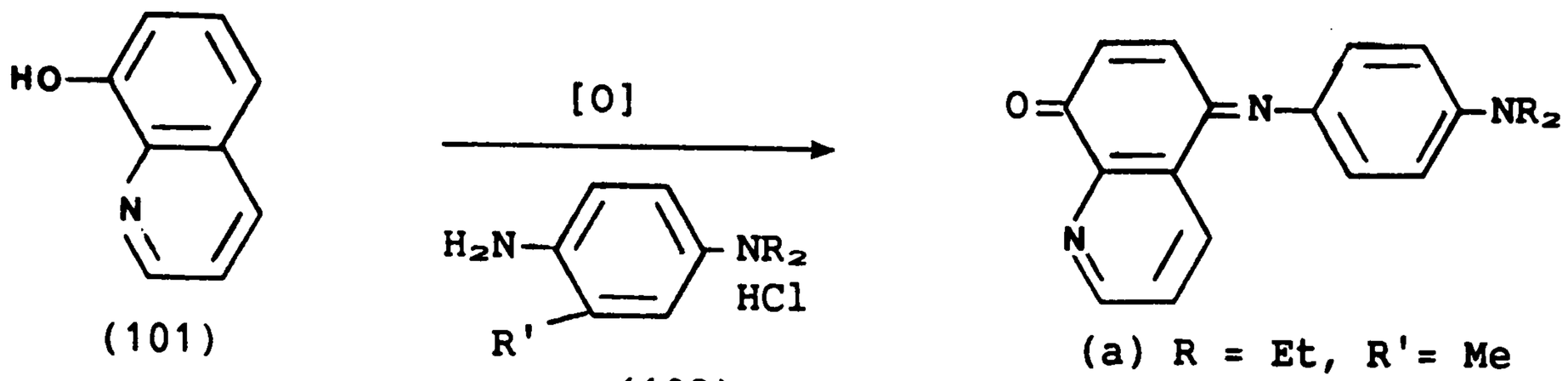

(101) (102) (a) R = Et, R'= Me (b) R = Me, R'= H (103)

Scheme 14

oxidising agent (Scheme 14). When complexed to the appropriate metal, the complexes obtained are of the generalised formula (104). Spectral

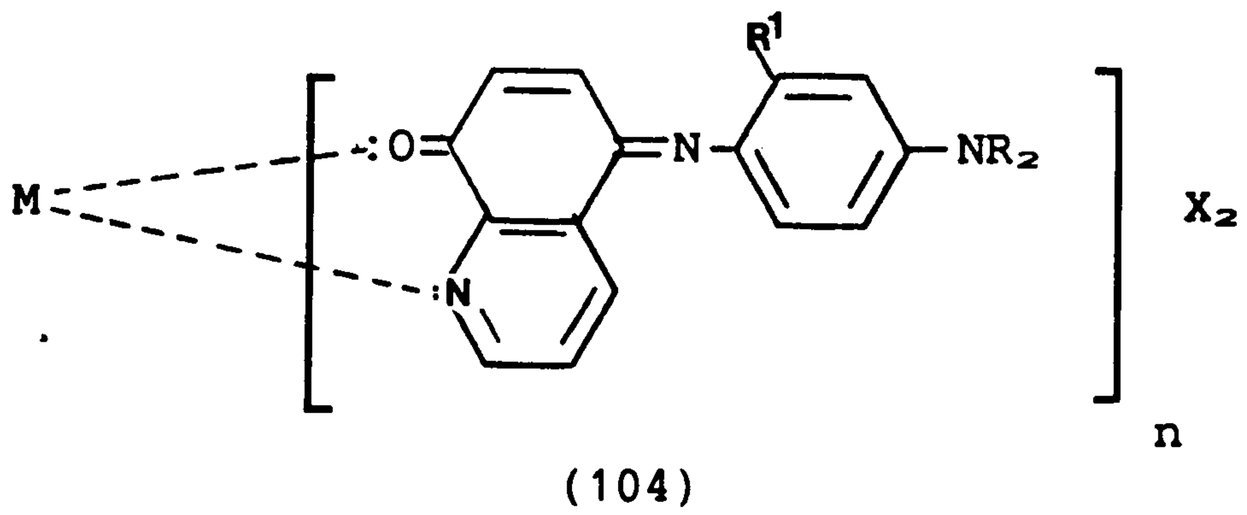

(104)

data for some of these complexes are summarised in Table 12[104]. It

Table 12: Spectral properties of indophenol-type dyes of the general formula (104)[104]

Structure	M	R	R^1	X	n	λ_{max}/nm(EtOH)	ε_{max}/$lmol^{-1}cm^{-1}$ (a)
(104a)	Cu	Et	Me	ClO_4	2	776	144,000
(104b)	Cu	Et	Me	ClO_4	1	721	60,000
(104c)	Ni	Et	Me	ClO_4	2	775	118,000
(104d)	Ni	Et	Me	ClO_4	1	742	72,000
(104e)	Cu	Me	H	ClO_4	2	772	144,000
(104f)	Cu	Me	H	ClO_4	1	722	69,000
(104g)	Ni	Me	H	ClO_4	2	742	75,000
(104h)	Ni	Me	H	ClO_4	1	728	60,000

(a) - measured in ethanol

can be seen that bidentate complexes absorb at longer wavelengths and with higher extinction coefficients than the equivalent monodentate dyes. Additionally the bidentate copper dyes absorb at longer wavelengths than the equivalent nickel dyes but when the monodentate complexes are considered the reverse is true

Ligands of the type (105a) and (105b) have also been complexed to Ni^{2+}, across the atoms marked * and **, to give complex dyes that

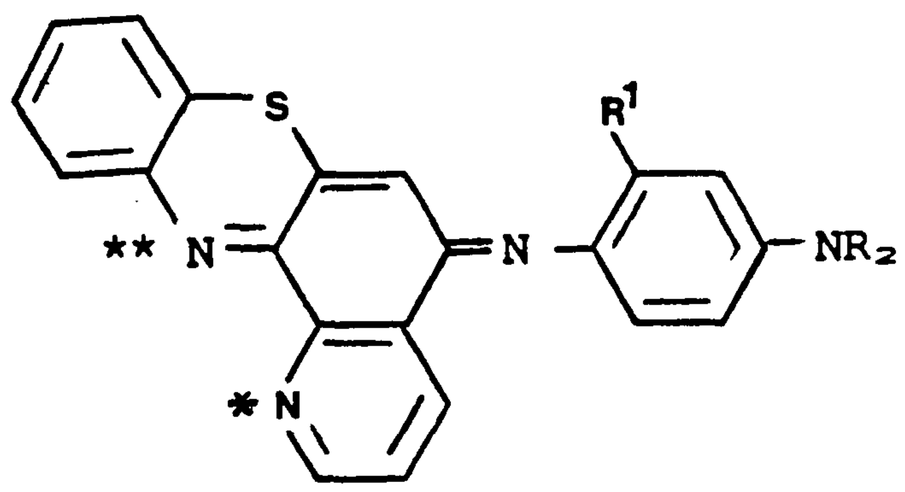

(a) R = Et, R'= Me
(b) R = Me, R'= H

(105)

absorbed at 782 - 838nm[105]. These ligands were prepared, in about 50% yields, according to Scheme 15 by adding (106) and potassium hydroxide to a refluxing ethanolic solution of (103). If the thiol (106) is

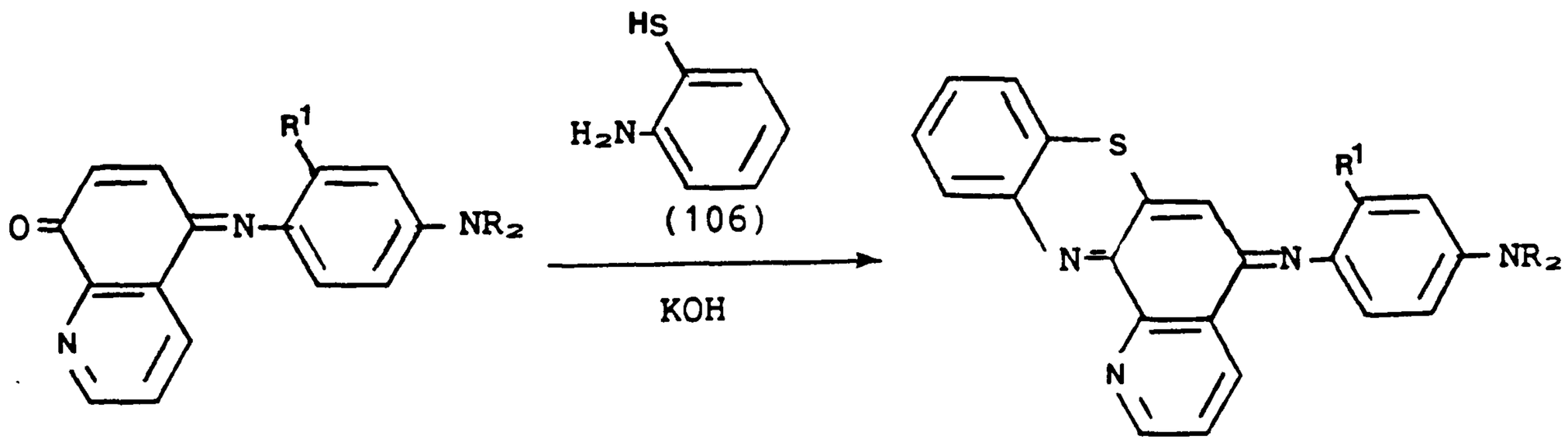

(103) (106) (105)

Scheme 15

replaced by o-aminophenol then ligands of the general formula (107) are afforded. When complexed to Ni^{2+} in ethanol, the complex of (107a) has a λ_{max} of 797nm, with an extinction coefficient of

38,900lmo $l^{-1}cm^{-1}$. Similarly the nickel complex of (107b) absorbed at 746nm in dimethylformamide/chloroform[106].

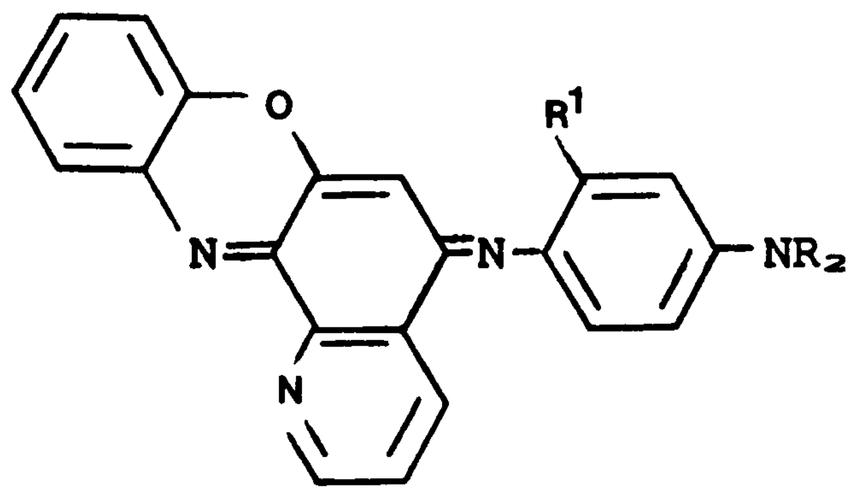

(a) R = Et, R'= Me
(b) R = Me, R'= H

(107)

2. RESULTS AND DISCUSSION

2.1 APPROACHES TO HIGHLY BATHOCHROMIC AZO DYES

As noted in the introduction, (Section 1.3.3) infrared azo dyes are surprisingly few in number, even though azo dyes are the most numerous class in commercial use and have been investigated in great detail over many years. The only infrared examples to date include types (108), (44), and some metal complexes.

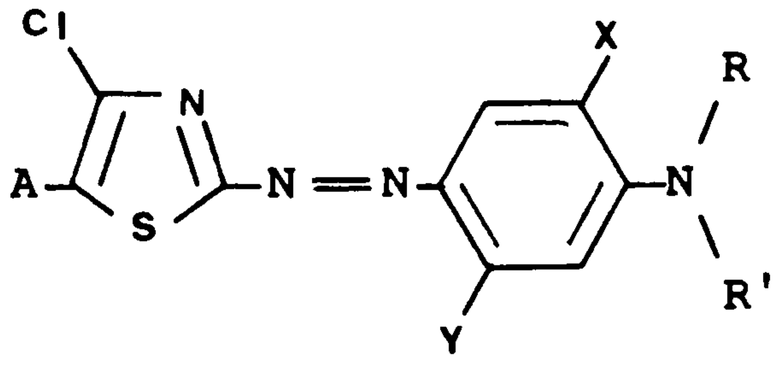

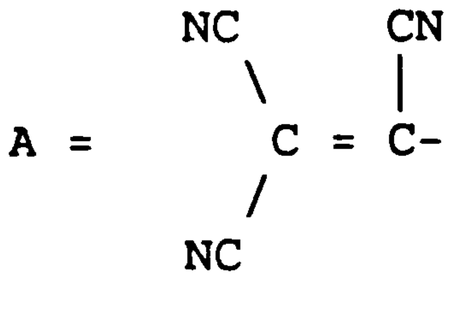

or

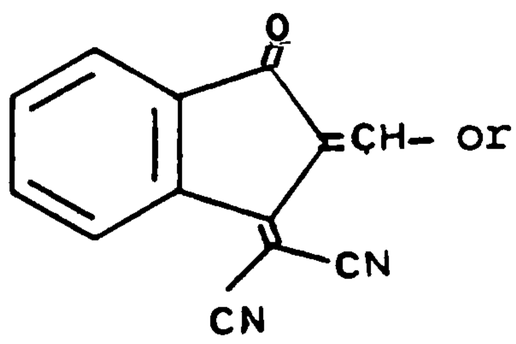

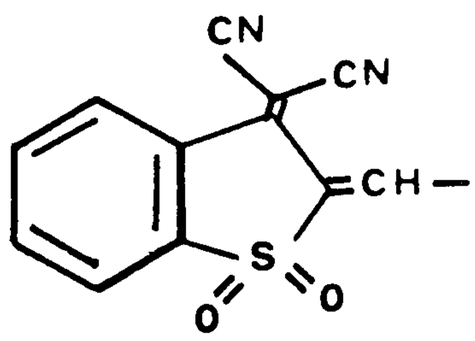

(108)

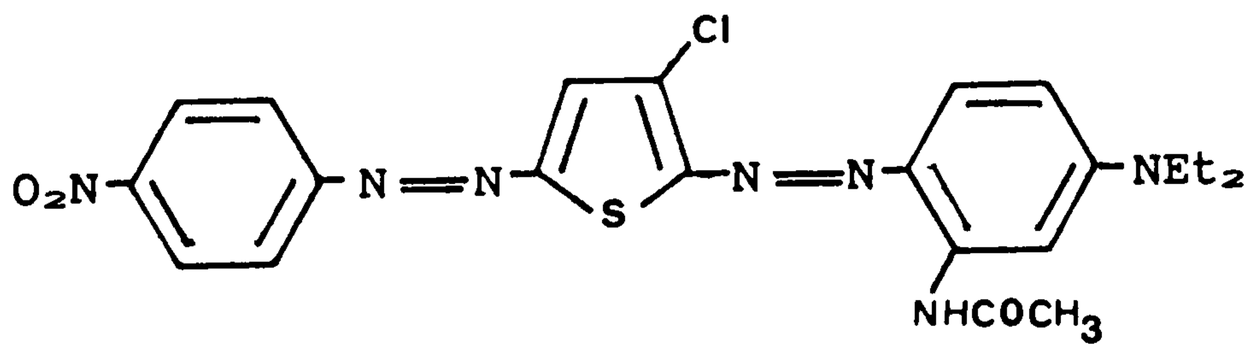

(44)

These dyes have a common donor-acceptor chromophoric system with an extremely powerful donor group, [X = OCH_3, Y = NHAc in (108)] and very powerful acceptor groups [A in (108)]. The thiazole and thiophene rings in (108) and (44) also contribute a useful bathochromic effect because of their readily polarisable π-electron systems.

The effect of donor strength of the absorption maxima of azo dyes can be seen by consideration of the simple series of dyes in Table 13[68]. In particular it can be seen, from Table 13, that an acylamino

Table 13: <u>The effect of electron donor strength on monoazo dyes</u>[68]

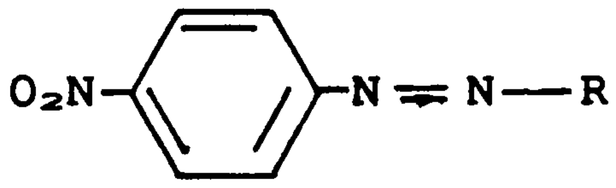

(109)

Strucure	R	λ_{max}/nm(CH_2Cl_2	ε_{max}/$lmol^{-1}cm^{-1}$ (CH_2Cl_2)
(109a)	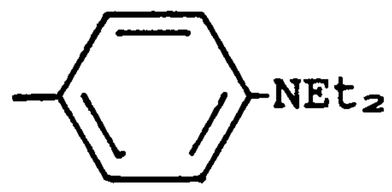	498	35,400
(109b)	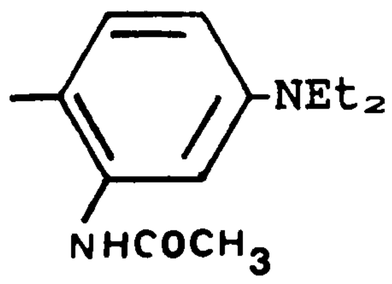	522	48,850
(109c)	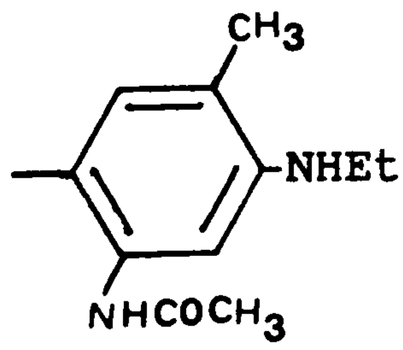	508	37,500
(109d)	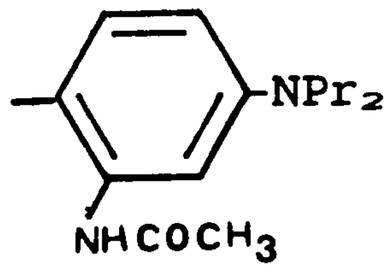	523	53,900
(109e)	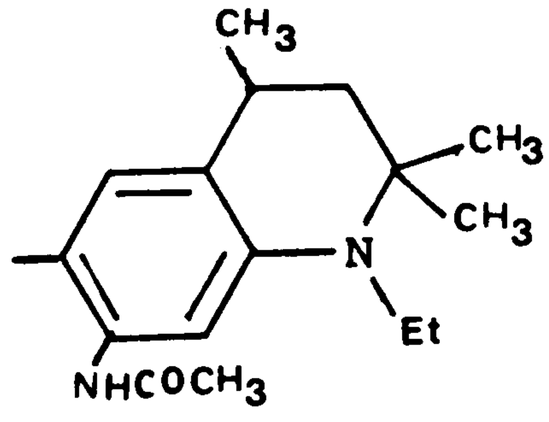	543	48,550

group ortho to the azo linkage in the donor half of the molecule causes a bathochromic shift. This can be explained both in terms of additional +M electron donation and enhanced planarity due to hydrogen bonding. Structure (109e) shows the effect of fusing the electron donor nitrogen atom in a ring system. The lone pair electrons of the nitrogen are held more rigidly in conjugation with the π-electron system and so give a significant bathochromic shift.

As part of the study of new infrared dyes, an examination was made of azo dyes with less common, powerful electron donor groups, in particular the dihydroperimidines (110), perimidines (111), substituted benzindole (112) and Michler's ethylene derivatives (113).

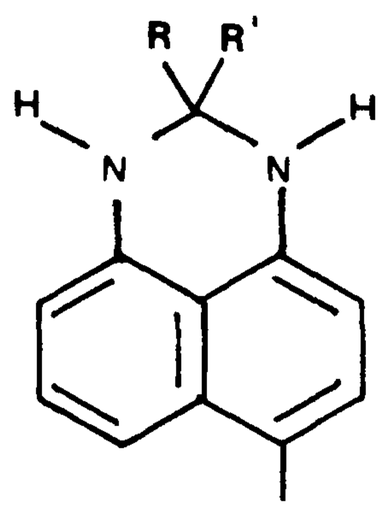

(110)

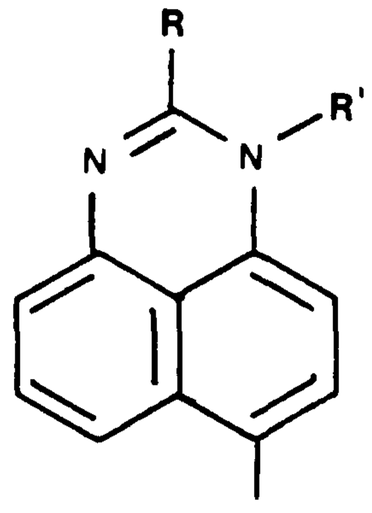

(111)

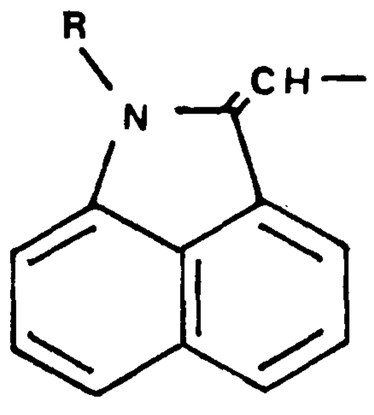

(112)

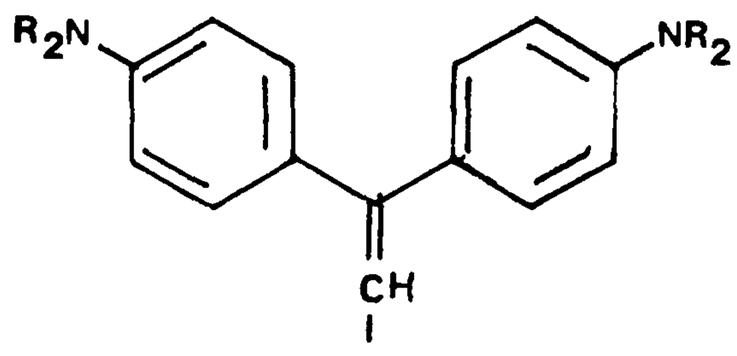

(113)

The spectroscopic influence of these groups was examined as this would facilitate the design of new infrared azo dye systems.

2.1.2 Azo Dyes Based on Perimidine and Dihydroperimidine Electron Donor Systems

The perimidines (114) and dihydroperimidines (115) have the potential to form azo dyes by direct diazo coupling, and they

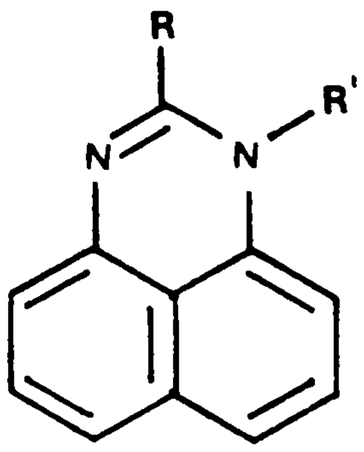

(114)

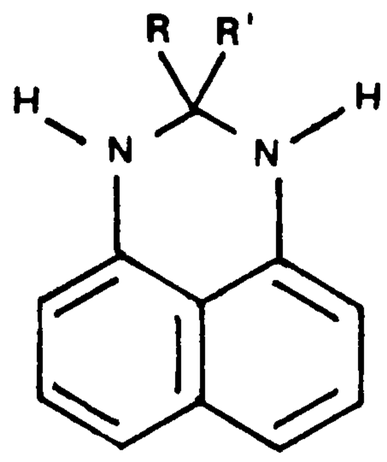

(115)

themselves provide powerful electron donor residues.

Although systems of types (114) and (115) have been well covered in reviews[107,108] reports of dyes based on perimidines and dihydroperimidines appear to be few and far between.

In 1955 Jeffreys acknowledged the electron releasing potential of the perimidine system and synthesised unsymmetrical cyanine-type dyes, for example (116) which is lemon yellow in colour[109].

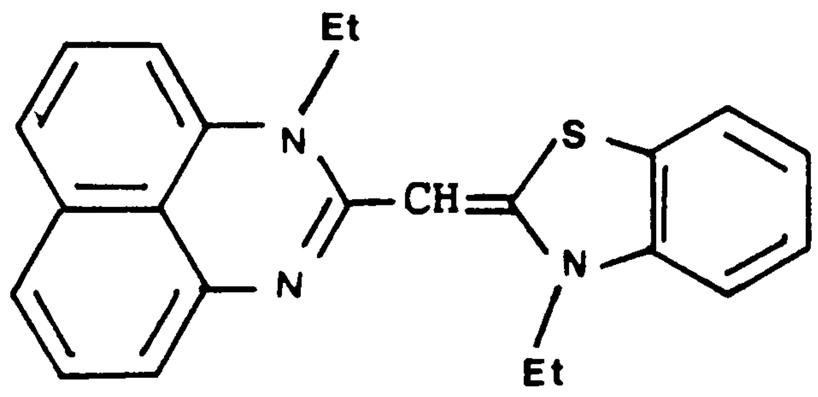

(116)

In the same paper the dihydroperimidine based dyes (117a) and (117b) were described. These red dyes absorbed at ca. 515nm in benzene and exhibited negative solvatochromism, absorbing at about

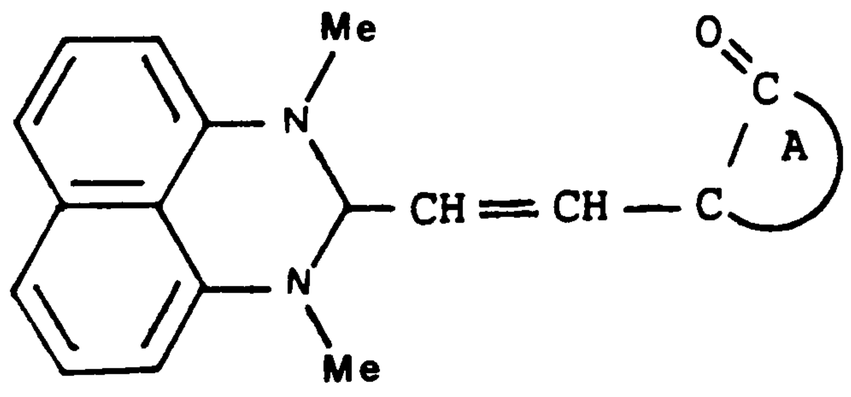

(117a) A = 2-ethylthiothiazol-5-one

(117b) A = 3-methyl-2-thiothiazolid-5-one

508nm in methanol. Negative solvatochromism only occurs in dyes that

have highly polarised ground states. Thus the large +M effect of the dihydroperimidine system is apparent.

In 1972 Allum and Abou-Zeid synthesised several monoazo dyes derived from perimidine itself of the general formula (118)[110]. These

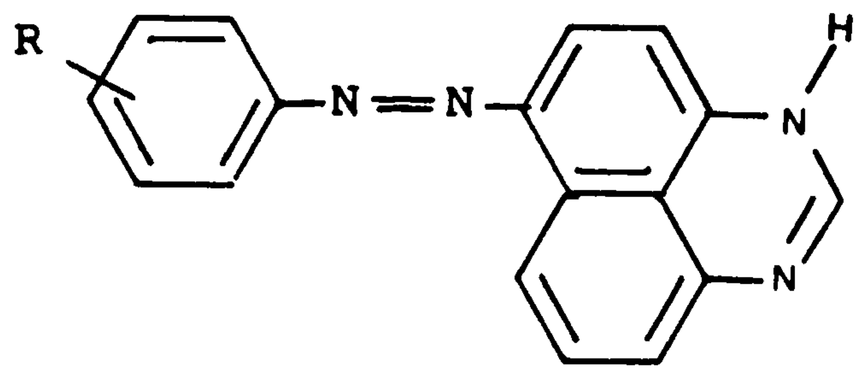

(R = Cl, OH, Me)

(118)

dyes were then dyed on nylon and their lightfastness properties assessed. No reference to structural characterisation of the dyes was made.

In 1977 Pfüller, Franz and Preiss undertook the characterisation of Sudan Black B[111], a commercially available dye derived from 2,2-dihydro-2,2-dimethyl-1H-perimidine that is used in the manufacture of black ball point pen inks[112]. It transpired that the commercial Sudan Black B contained a minimum of 18 fractions and that the two main

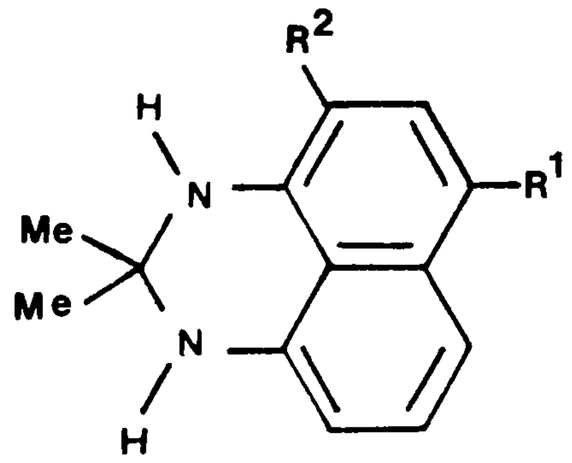

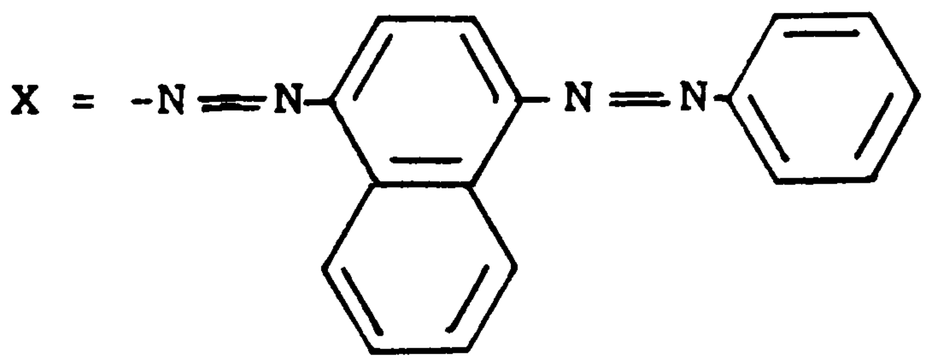

(119a) R^2 = H, R^1 = X

(119b) R^1 = H, R^2 = X

fractions (97.5%) were the para and ortho derivatives (119a) and (119b) respectively, in a ratio of 3:1. As Sudan Black B is a complex disazo dye it is perhaps not surprising that so many fractions were

present.

In the present study, systematic variation of the dihydroperimidine and perimidine systems have been investigated for representative simple monoazo dyes. In this way the colour and constitution characteristics of these electron donor groups could be studied in detail.

2.1.2.1 Synthesis of Intermediates and Dyes

The two perimidines used in this work were (120a) and (120b).

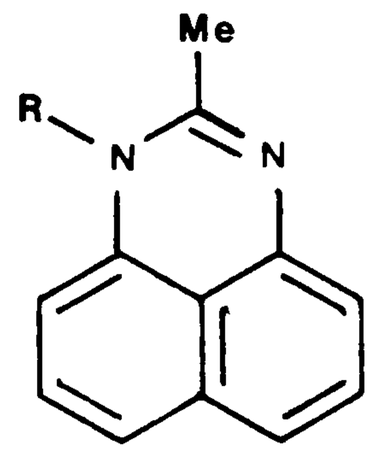

(120a) R = H

(120b) R = Et

These were prepared as shown in Scheme 16. The success of the first

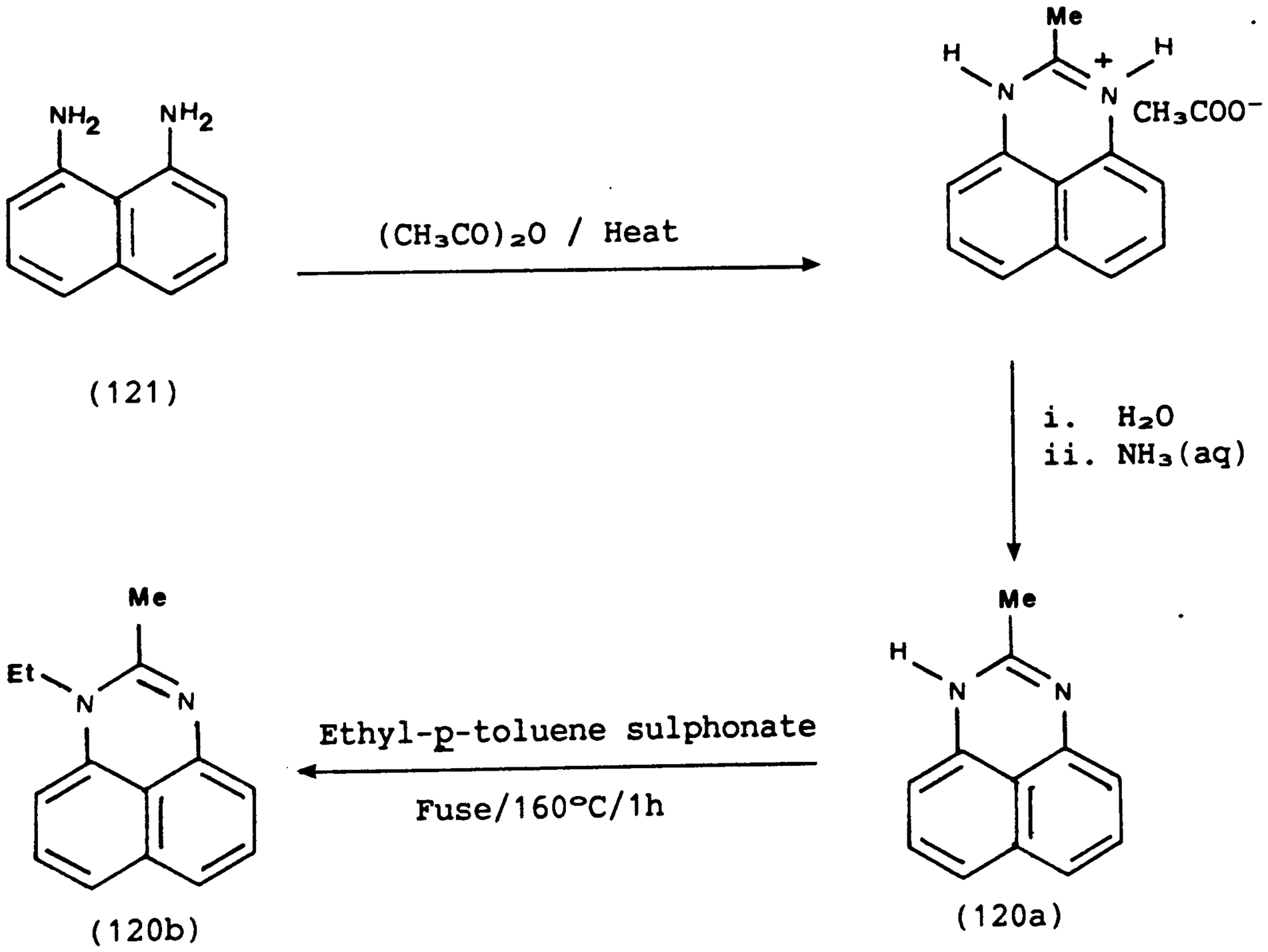

Scheme 16

stage of this sequence was very much dependent on the purity of 1,8-diaminonaphthalene (121). The commercial material was purified by recrystallisation from ligroin (b.p. 100-120°C). Fusion of the acid free perimidine (120a) with ethyl-p-toluene sulphonate and subsequent purification by column chromatography gave the 1-ethyl-2-methylperimidine (120b) as pale yellow crystals. The last stage of this synthesis was the only effective way of N-alkylating (120a), which was surprisingly resistant to alkylation.

It has also been reported in the literature that perimidines can be prepared by the condensation of aldehydes with 1,8-diaminonaphthalene[107,113]. Accordingly the synthesis of (122) was attempted. It was hoped that the n-heptyl chain would aid the organic solvent solubility of any resultant dyes. However, although various

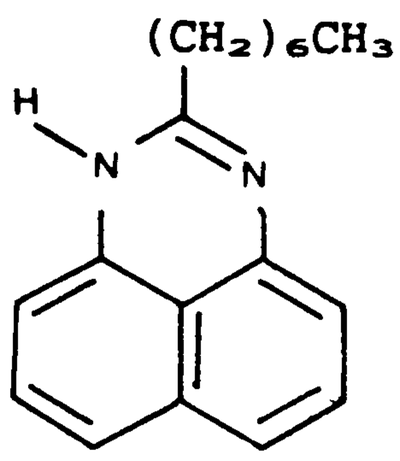

(122)

conditions were employed (including, for example, acid catalysis, the use of a variety of solvents and azeotropic removal of water) the desired product could not be isolated.

The dihydroperimidines, as well as related intermediates (124) and (125) that were prepared are listed in Table 14. The dihydroperimidines were prepared by one of two routes as shown in Schemes 17 and 18. The first method, Scheme 17, was utilised, in most cases, for those ketones that were liquid at room temperature. Thus recrystallised 1,8-diaminonaphthalene was dissolved in water with the minimum amount of ethanol to effect solution and the ketone added. After addition of a catalytic amount of sulphuric acid the solution

Table 14: Dihydroperimidine intermediates prepared in this work for synthesis of monoazo dyes

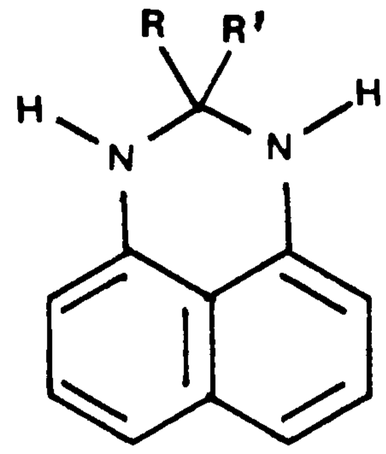

(123)

Structure	R	R'
(123a)	$-CH_3$	$-CH_2CH(CH_3)_2$
(123b)	$-CH_3$	$-CH(CH_3)_2$
(123c)	$-CH_3$	$-(CH_2)_4CH_3$
(123d)	$-CH_2CH_3$	$-(CH_2)_4CH_3$
(123e)	$-CH_2CH_3$	$-CH_2CH_3$
(123f)	$-CH_2CH_3$	$-CH_2CH(CH_3)CH_2CH_3$
(123g)	$-CH_3$	$-CH_2CH_2COO(CH_2)_3CH_3$
(123h)	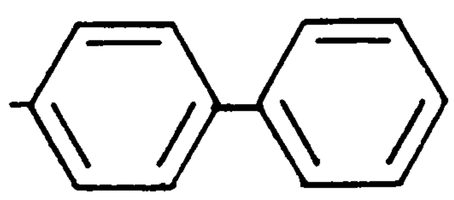	$-CH_3$
(123i)	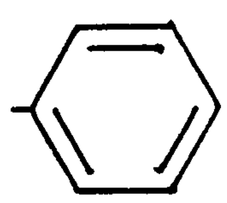	$-CO$ 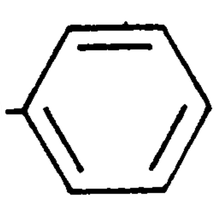

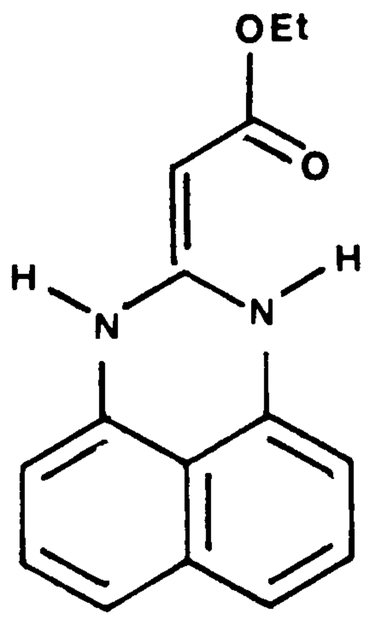

(124)

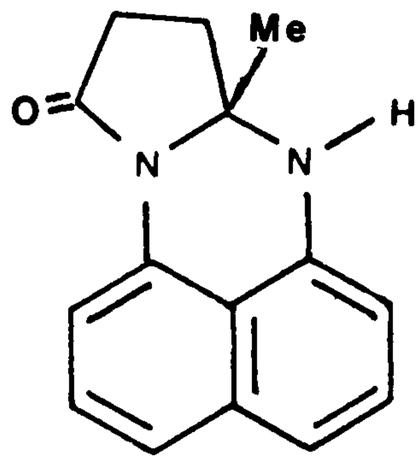

(125)

was heated at 60°C for 30 minutes. Cooling followed by neutralisation with aqueous sodium hydroxide generally afforded a white precipitate

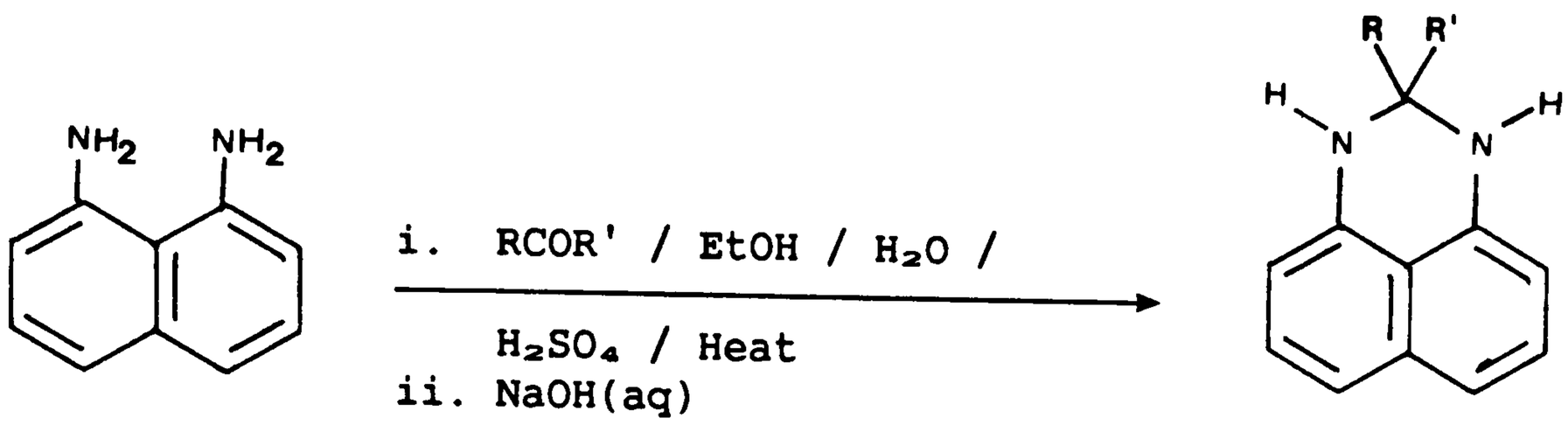

Scheme 17

of the dihydroperimidine. For the solid ketones, for example benzil or acetyl biphenyl Scheme 18 was followed. Water was not present in this case, a catalytic amount of p-toluene-sulphonic acid rather than sulphuric acid was used and higher temperatures and longer reaction

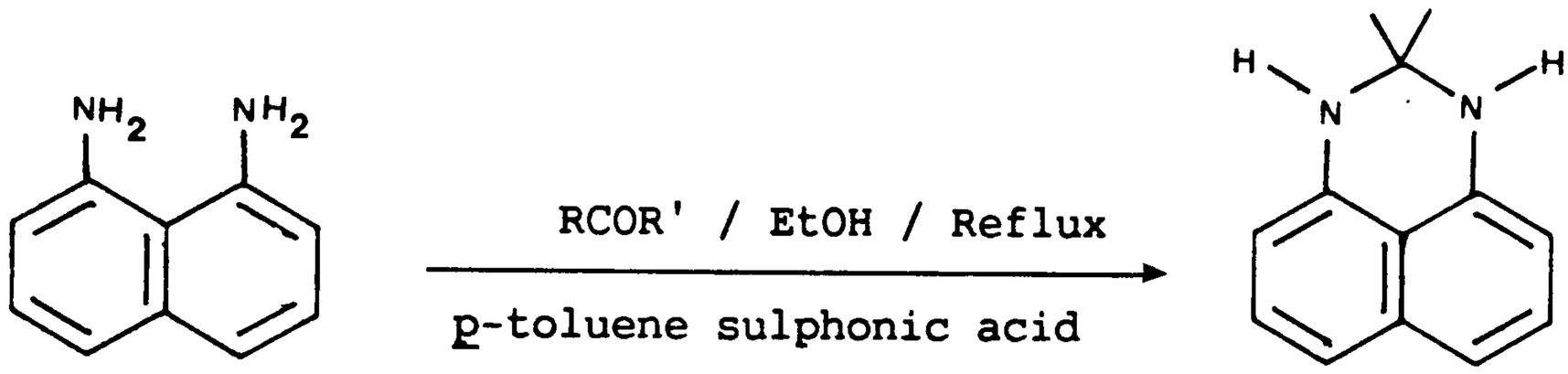

Scheme 18

times were necessary. Where derivatives were made by both methods it was apparent that the method in Scheme 18 leads to purer, more easily isolated products.

The dihydroperimidine (124) was synthesised as in Scheme 19, by heating 1,8-diaminonaphthalene with diethyl malonate at 150°C for 4 hours and was deposited as a pale yellow precipitate on cooling.

The fused ring dihydroperimidine (125) was obtained via the cyclisation of dihydroperimidine (123g), as shown in Scheme 20, by heating (123g) in ethanol with p-toluene-sulphonic acid as catalyst. The structure of (125) was confirmed by microanalysis and by infrared spectroscopy. Whereas the uncyclised derivative (123g) exhibited a

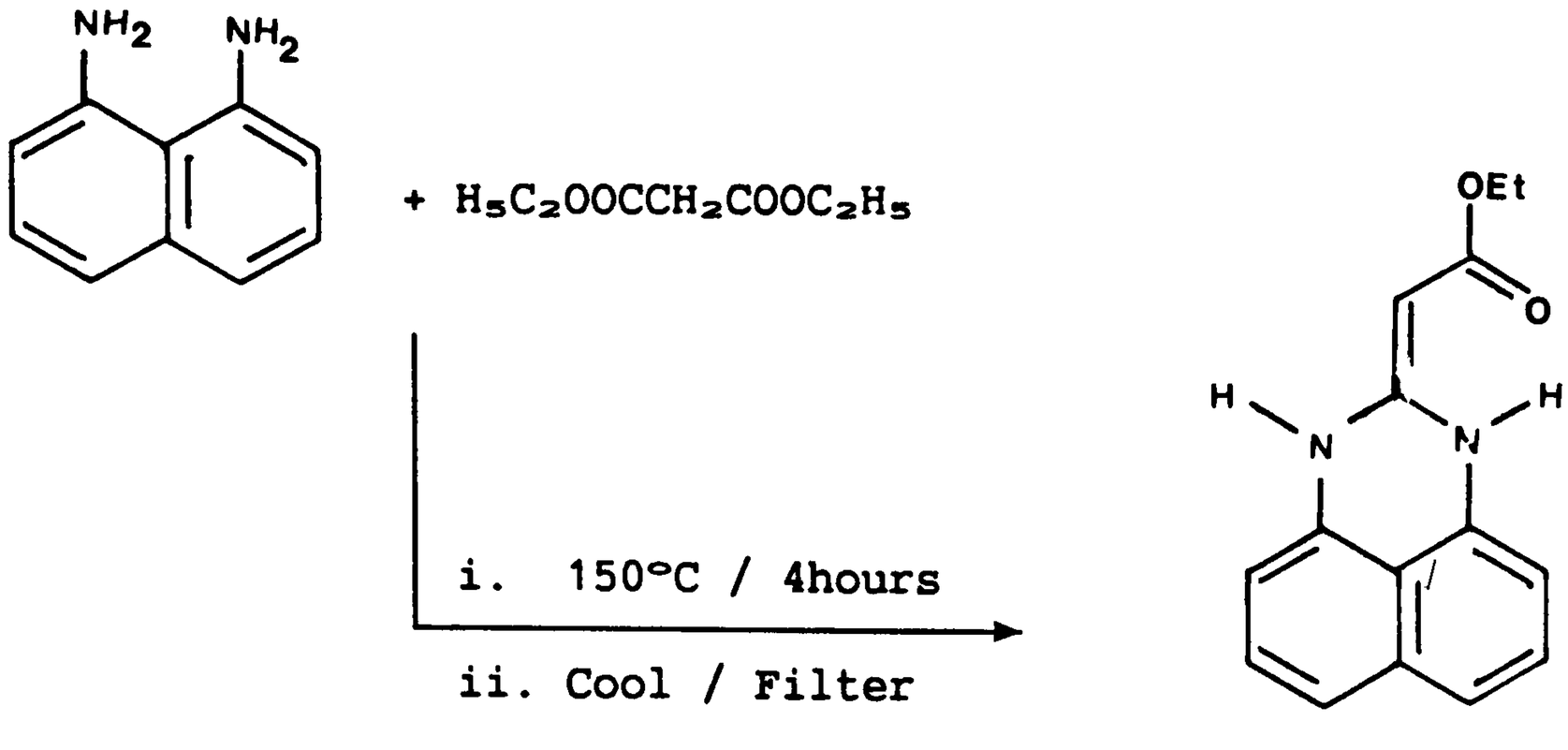

(124)

Scheme 19

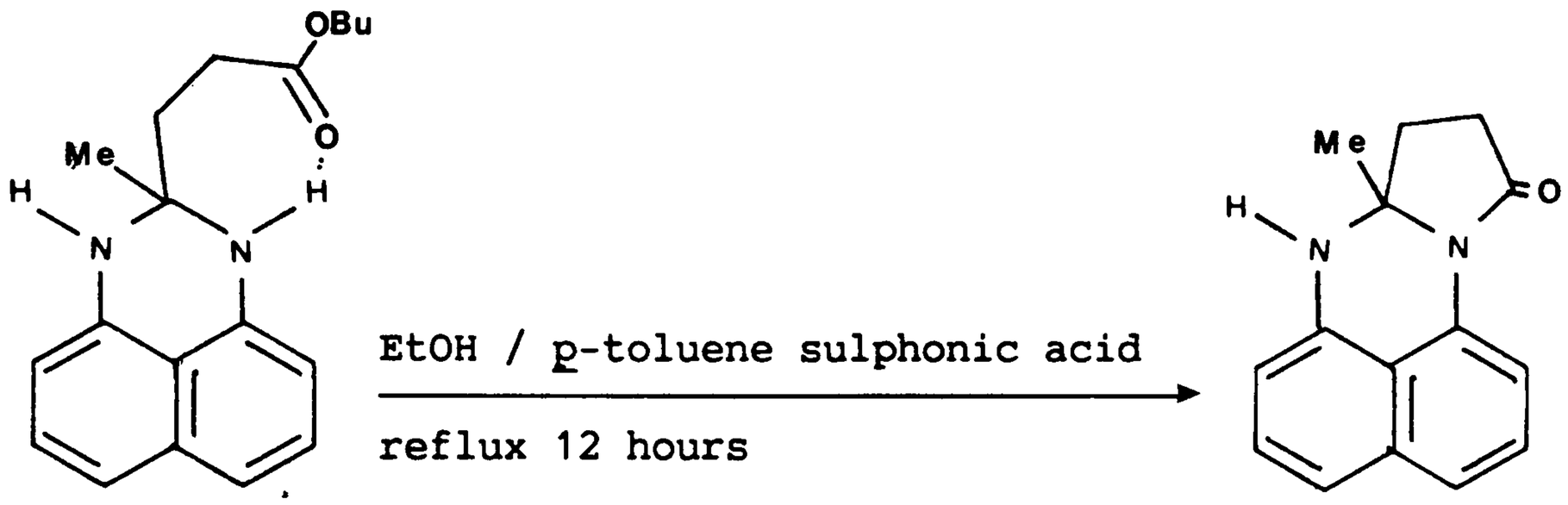

(125)

Scheme 20

carbonyl frequency of 1714cm^{-1} (characteristic of a hydrogen bonded saturated ester) the cyclised derivative (125) showed corresponding absorption at 1689cm^{-1}, typical of a 5-membered ring lactam.

The reaction of benzil with one equivalent of 1,8-diaminonaphthalene to form the dihydroperimidine (123i) is particularly interesting as it is at variance with literature claims.

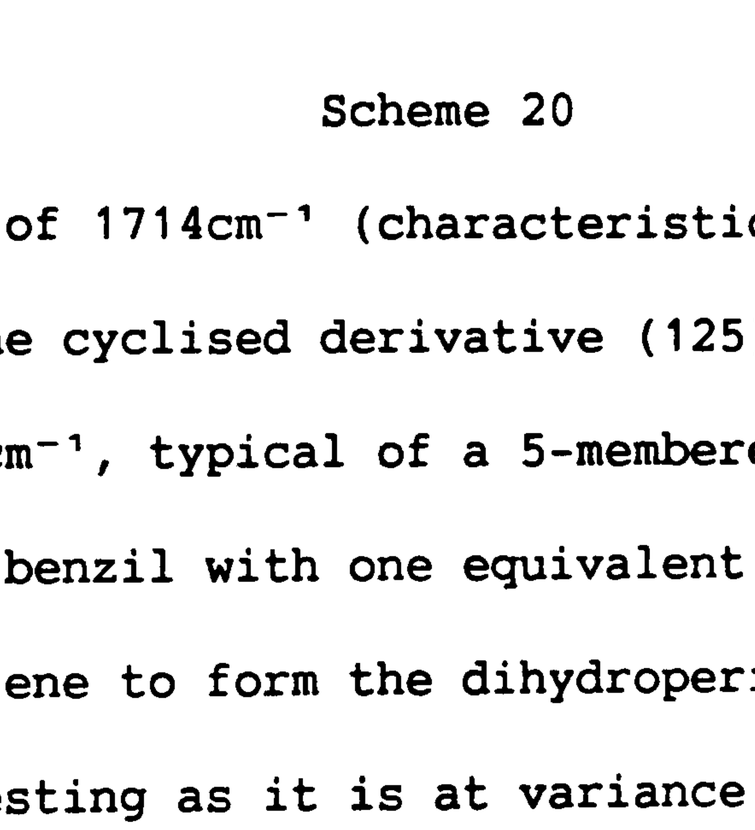

(126)

The compound gave the correct microanalysis for structure (123i) and its i.r. spectrum showed a C=O stretching frequency at 1680cm^{-1}, as expected for a phenyl ketone with some intramolecular hydrogen bonding. In European Patent 0 071 197A1[114] it was claimed that this reaction gave a product of structure (126). That the patent is in error can be deduced from two additional observations. Firstly, in refluxing ethanol (as used in the patent method) even if an excess of 1,8-diaminonaphthalene is used the dihydroperimidine (123i) precipitates from the hot solution. Thus, in ethanol at least, it is not possible to condense two molecules of 1,8-diaminonaphthalene to benzil. Secondly the product (123i) showed identical chemical reactivity to other dihydroperimidines in Table 14.

The two perimidines (120a) and (120b) and the dihydroperimidines (123a) - (123i), (124) and (125) were then examined as coupling components in the synthesis of azo dyes. For convenience the 4-nitrobenzene diazonium ion was used, thus giving ortho and para 4-nitrophenylazo derivatives.

From the work of Pfüller, Franz and Preiss[112] in their evaluation of Sudan Black B it is known that the coupling of diazonium ions to dihydroperimidines can be complex and indeed within this work this also proved to be the case.

Diazotisation of 4-nitroaniline was carried out by the standard suspension method. Thus 4-nitroaniline was heated in an acetic acid : hydrochloric acid mixture until dissolved, and the hot, clear solution was poured into a mixture of ice and sodium nitrite solution to give a solution of 4-nitrobenzenediazonium chloride.

In the preliminary coupling reactions, the dihydroperimidine or perimidine was dissolved in water with the minimum amount of acetic acid to effect solution and to this was added the diazonium solution at 0 - 5°C. However, t.l.c. analysis of the coupling products from

such reactions showed the presence of several products, making isolation and purification of the major components impractical.

A study of the pH dependence of the diazo coupling reaction giving the 2,2-dihydro-2,2-dimethyl-1H-perimidine dyes (127) and (128) was undertaken[115]. It was concluded that, regardless of pH, the coupling

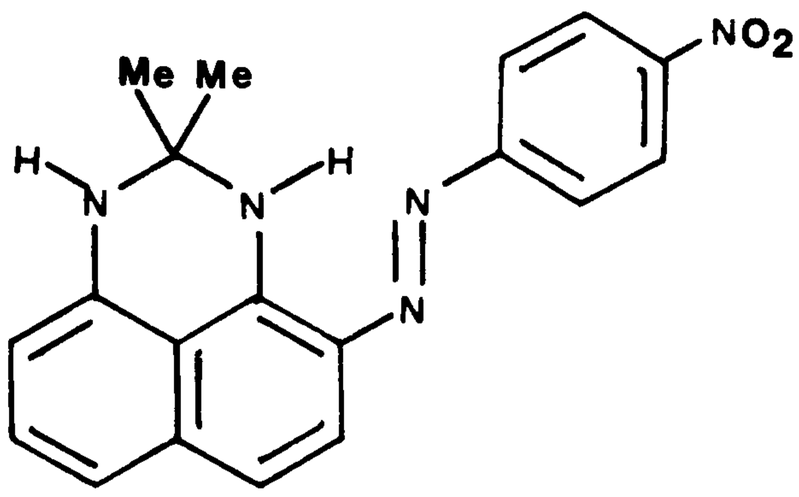

(127)

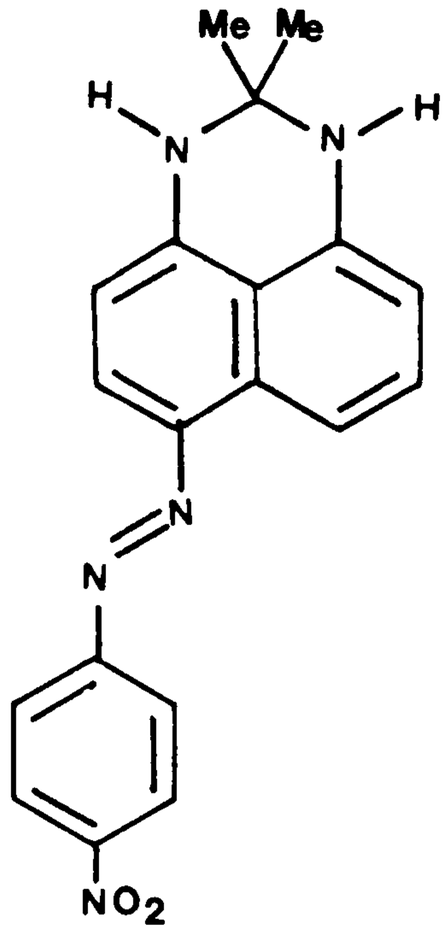

(128)

reaction was always complex, forming at least six different products in all cases. However the cleanest couplings were obtained in the pH range 3-7. It may be that at pH values below 3 and above 7 the dihydroperimidine ring system is hydrolysed back to 1,8-diaminonaphthalene. This will also couple with the diazonium ion leading to other azo dye products. Apart from the desired dyes (127) and (128) and dyes formed from 1,8-diaminonaphthalene another product will be the N-coupled derivative (129).

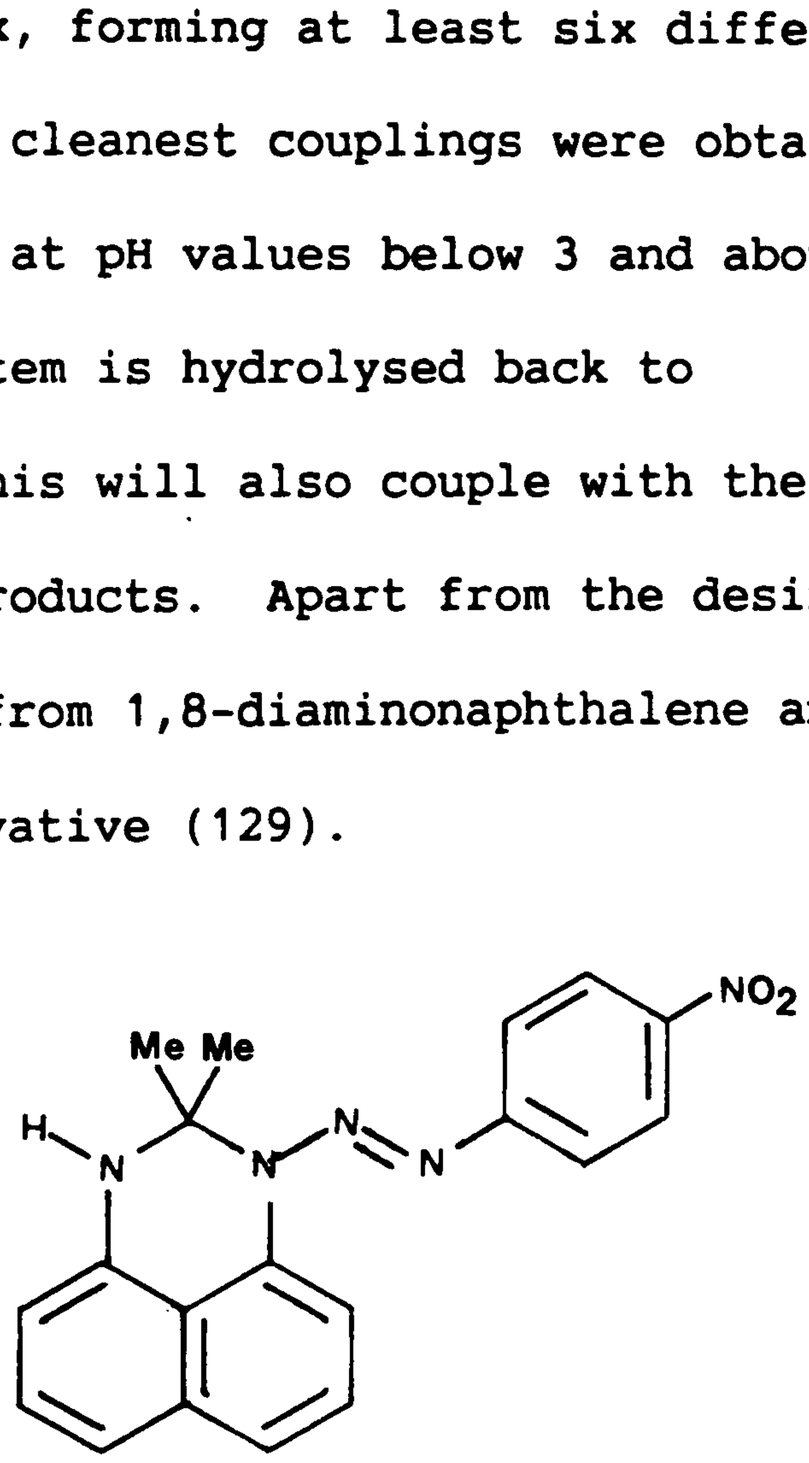

(129)

The influence of solvent on the coupling reaction was then

examined, and this gave promising results. Thus the dihydroperimidine dimethylformamide was treated with a solution of diazotised 4-nitroaniline. In the case of acetone and glacial acetic acid complex mixtures were again obtained. However, in the case of dimethylformamide two major fractions only, presumably the ortho and para derivatives were detectable on t.l.c. It was then possible to separate and isolate each major component, by column chromatography and to characterise them by microanalysis or mass spectrometry. The structures of the azo dyes prepared are summarised in Table 15.

Table 15: Structures of 4-nitrophenylazo dyes (X = $4\text{-}O_2NC_6H_4N_2$) synthesised

Structure		R	R'
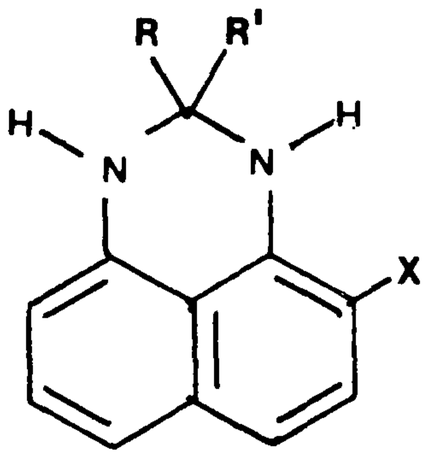 (130)	(a)	$-CH_3$	$-CH_2CH(CH_3)_2$
	(b)	$-CH_3$	$-CH(CH_3)_2$
	(c)	$-CH_3$	$-(CH_2)_4CH_3$
	(d)	$-CH_2CH_3$	$-(CH_2)_4CH_3$
	(e)	$-CH_2CH_3$	$-CH_2CH_3$
	(f)	$-CH_2CH_3$	$-CH_2CH(CH_3)CH_2CH_3$
	(g)	$-CH_3$	$-CH_2CH_2COO(CH_2)_3CH_3$
	(h)	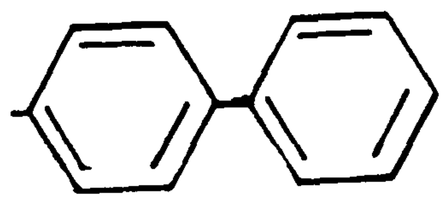	$-CH_3$
	(i)	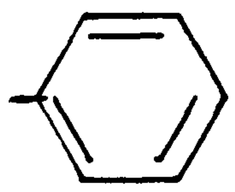	$-CO$ 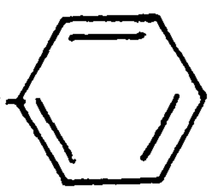
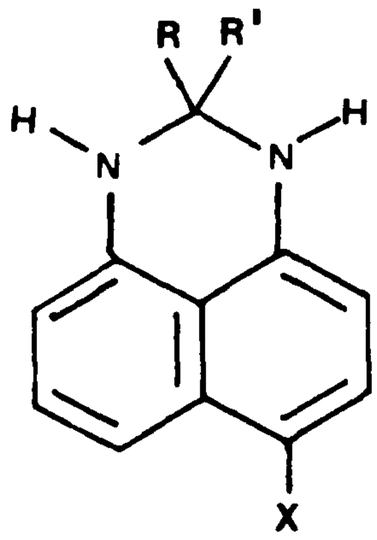 (131)	(a)	$-CH_3$	$-CH_2CH(CH_3)_2$
	(b)	$-CH_3$	$-CH(CH_3)_2$
	(c)	$-CH_3$	$-(CH_2)_4CH_3$
	(d)	$-CH_2CH_3$	$-(CH_2)_4CH_3$
	(e)	$-CH_2CH_3$	$-CH_2CH_3$
	(f)	$-CH_2CH_3$	$-CH_2CH(CH_3)CH_2CH_3$

Table 15: continued

Structure	R	R'
(g)	$-CH_3$	$-CH_2CH_2COO(CH_2)_3CH_3$
(h)	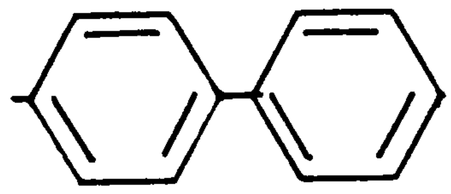	$-CH_3$
(131) (i)	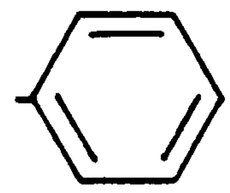	-CO- 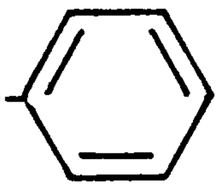
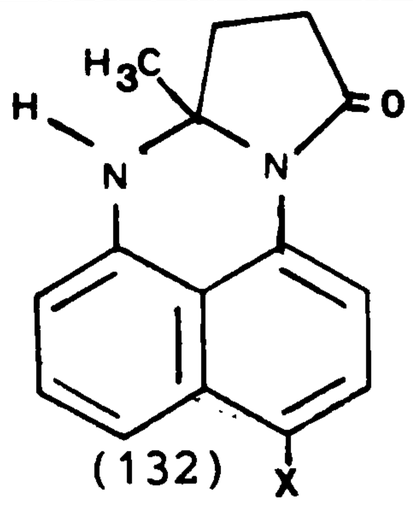 (132)	——	——
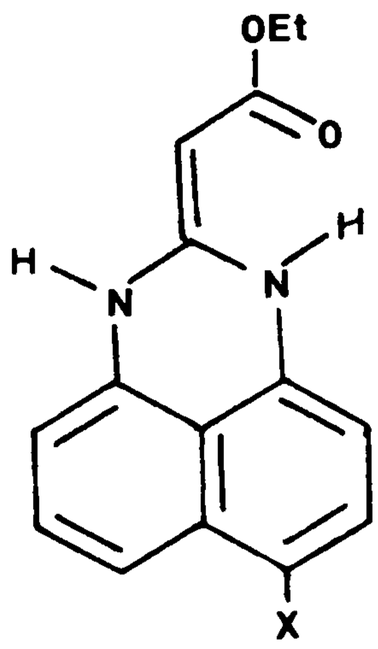 (133)	——	——
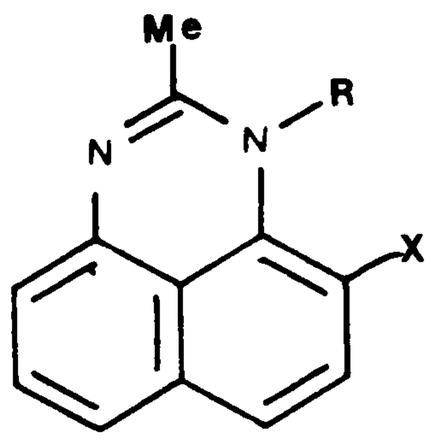 (134) (a)	-H	——
(b)	$-CH_2CH_3$	——
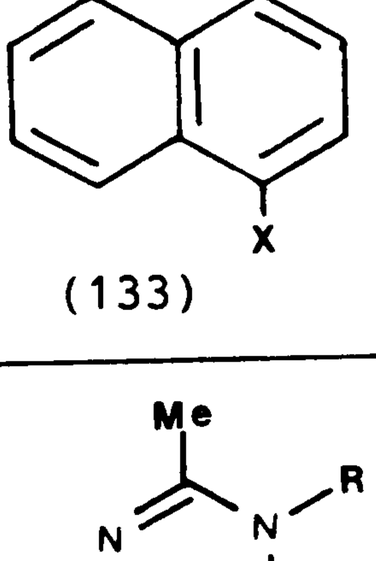 (135) (a)	-H	——
(b)	$-CH_2CH_3$	——

The isomeric dyes (134a) and (135a) derived from the unalkylated perimidine (120a) proved by far the most difficult to synthesis and isolate. It appeared that the non-alkylated NH group is more prone to N-coupling to the diazonium ion than, for example, the -NH groups of the dihydroperimidines (123). This may reflect the greater steric hindrance in (123) to ortho coupling. Thus full characterisation of (134a) and (135a) was not possible.

With the exception of dyes (132) and (133) all the couplers gave both the ortho and para coupled isomeric dyes. It was found that in all cases these could be separated chromatographically, the ortho isomer showing an appreciably higher R_f on silica than the para isomer. This is a well known phenomenon in hydroxy azo dyes and reflects the intramolecular hydrogen bonding in the ortho isomers which reduces their polarity and affinity for the absorbent :cf. (136) and (137).

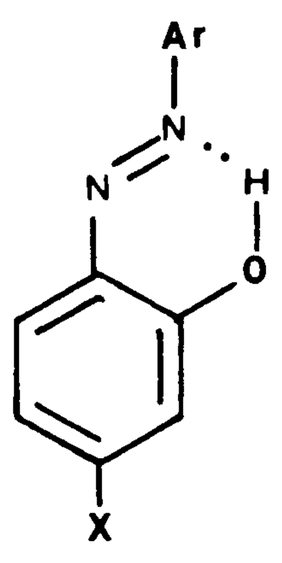

(136)

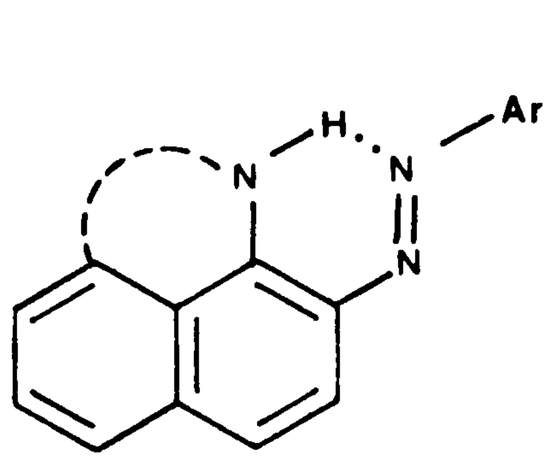

(137)

Confirmation that it was indeed the ortho coupled product that had the higher R_f value was made by ^{1}H-n.m.r. spectroscopy of representative examples [(130h) and (131h)]. Thus the ^{1}H-n.m.r. spectrum of the ortho dye (130h) showed a non-hydrogen bonded NH at δ=5.0 and a broader strongly deshielded proton at δ=11.3 corresponding to the hydrogen bonded NH. For the para derivative (131h) the NH protons were located at δ=4.7 and δ=5.4, the latter corresponding to the NH proton para to the deshielding 4-nitrophenylazo group. For both dyes the position and multiplicities of the aromatic protons

agreed with the assigned structures.

In the case of dyes (132) and (133) only one major product was formed as shown chromatographically and the low R_f values suggested that <u>para</u> coupling had occurred preferentially. The <u>para</u> structures were confirmed again by ^{1}H-n.m.r. spectroscopy. Thus the spectra were consistent with the overall 4-nitrophenylazo structure and the absence of a strongly deshielded NH signal at δ <u>ca.</u> 11, in the case of (132) confirmed that <u>para</u> coupling had occurred.

The spectrum of (133) was much more complex however, in that it did show a strongly intramolecularly hydrogen bonded NH proton at δ=16.6. This could be attributed to hydrogen bonding to the ester carbonyl group as shown in (133a). Interestingly the second NH proton is also

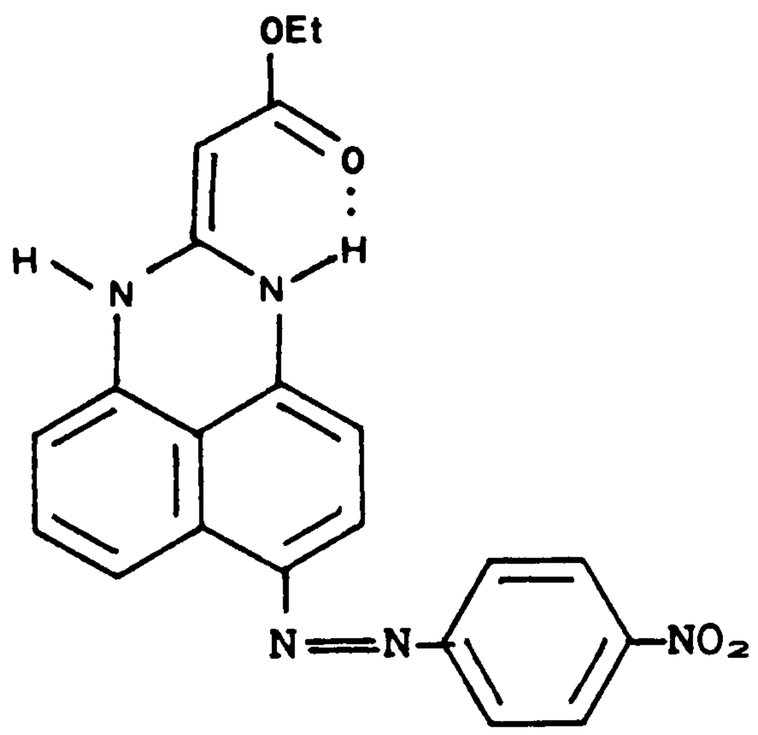

(133a)

at much lower than in other dihydroperimidine systems, at δ=10.8 (rather than 5). This may be attributed to the strong delocalisation of the nitrogen lone pairs into the acrylate ester residue thus deshielding the NH proton , <u>i.e.</u>

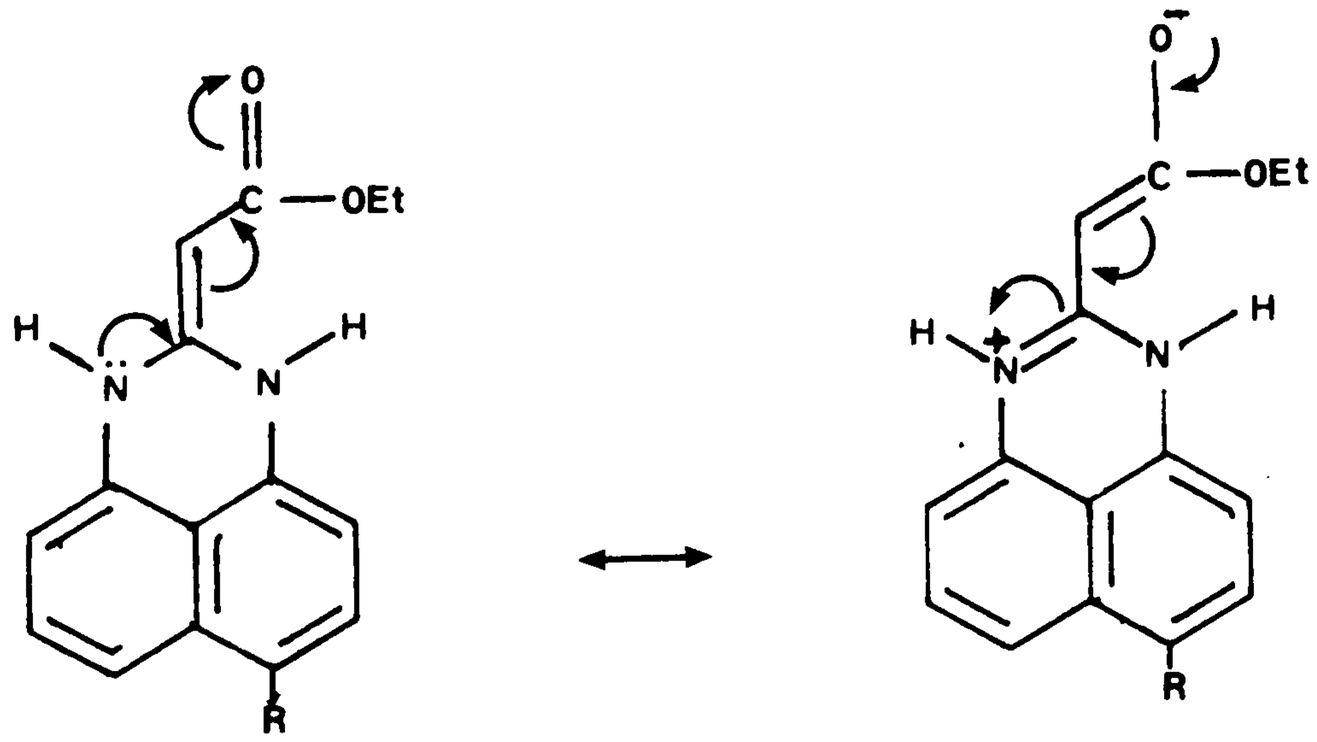

2.1.2.2: Light Absorption Properties of the Arylazo-perimidines and Dihydroperimidines

The visible absorption spectra of the 4-nitrophenylazo dyes (130)-(135) were measured in dichloromethane and toluene, so giving an indication of the influence of solvent polarity on the spectra. Molar absorption coefficients were determined for dichloromethane solutions and were measured only for those compounds fully characterised by microanalysis or mass spectrometry and shown to be pure by t.l.c. The spectral characteristics of the ortho coupled dyes are summarised in Table 16 and those of the para coupled analogues in Table 17.

Table 16: Spectroscopic data for the ortho 4-nitrophenylazo derivatives of dihydroperimidines and perimidines

Dye	λ_{max}/nm (CH_2Cl_2)	(CH_2Cl_2) (Toluene)	ε_{max}/ $1mol^{-1}cm^{-1}$ (CH_2Cl_2)	$\Delta\lambda_{max}$/nm (CH_2Cl_2-Tol)
(130a)	559	558	———	+1
(130b)	559	559	———	0
(130c)	558	558	———	0
(130d)	557	557	———	0
(130e)	557	556	———	+1
(130f)	558	557	15,100	+1
(130g)	556	554	14,300	+2
(130h)	561	562	13.800	-1
(130i)	523	523	10,000	0
(134a)	555	550	———	+5
(134b)	562	558	7,500	+4

From a comparison of the λ_{max} values presented in Table 13 and those summarised in Tables 16 and 17, it can be seen that the dihydroperimidine and perimidine ring systems are powerful electron donating residues. Typically the perimidine residue gives para-substituted dyes with a λ_{max} ca. 590nm which are much more

Table 17: Spectroscopic data for the para 4-nitrophenylazo derivatives of dihydroperimidines and perimidines

Dye	λ_{max}/nm (CH_2Cl_2)	(Toluene)	ε_{max}/ $lmol^{-1}cm^{-1}$ (CH_2Cl_2)	$\Delta\lambda_{max}$/nm (CH_2Cl_2-Tol)
(131a)	545	547	———	-2
(131b)	546	546	———	0
(131c)	547	547	———	0
(131d)	546	546	———	0
(130e)	544	545	———	-1
(131f)	546	545	15,000	+1
(131g)	509	494	15,100	+15
(131h)	547	548	15,300	-1
(131i)	524	523	9,500	+1
(132)	503	505	33,600	-2
(133)	396	395	50,500	+1
(135a)	590	578	———	+12
(135b)	596	580	12,100	+16

bathochromic than any other simple monoazo dye derived from the same diazo species. In fact the dyes (135a) and (135b) are probably the only blue dyes yet synthesised which are monoazo, containing only a nitrophenylazo group and are not thiophene or thiazole based. The ortho-substituted analogues (134a) and (134b) absorb at somewhat shorter wavelengths than the para isomers, and are violet in colour.

The dihydroperimidine dyes are interesting in that they show different behaviour. Thus the ortho derivatives absorb at longer wavelengths (λ_{max} ca. 560nm) than their para isomers (λ_{max} ca. 545nm). It is also apparent that the dihydroperimidine system, whilst still a powerful electron donating residue (cf. Table 13) is not as effective as the perimidine system, with its additional conjugation. The slightly greater bathochromic character of the ortho

dihydroperimidine dyes compared with the <u>para</u> isomers may be explained in terms of intramolecular hydrogen bonding as shown in (138). This

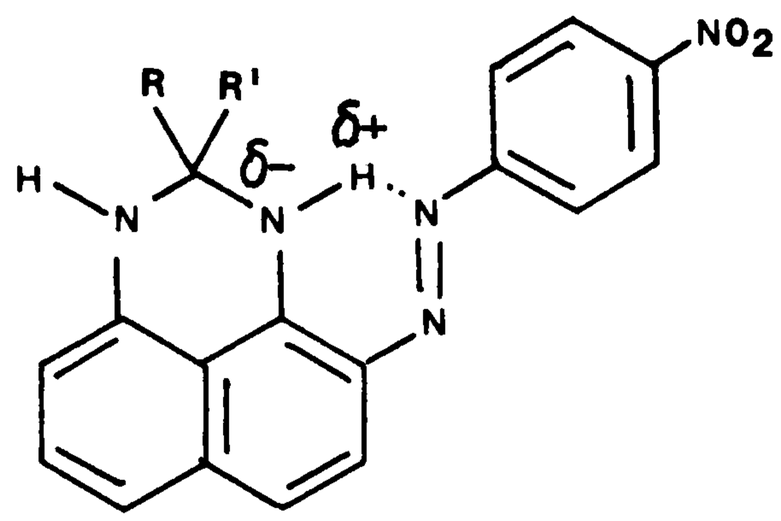

(138)

not only induces greater molecular planarity but also provides a δ^+ on the azo ß-nitrogen atom, and a δ^- charge on the associated NH nitrogen atom. This enhances the general donor-acceptor characteristics of the dye and so leads to a bathochromic shift.

The reverse situation observed for the perimidine dyes is less easily rationalised, but is accounted for by more detailed MO calculations (see later). However, it is worthy of note that PPP-MO calculations do indicate that the site of greatest electron density available for coupling in 1-ethyl-2-methylperimidine is the position shown in (139). The dye formed by coupling at this site exhibits a

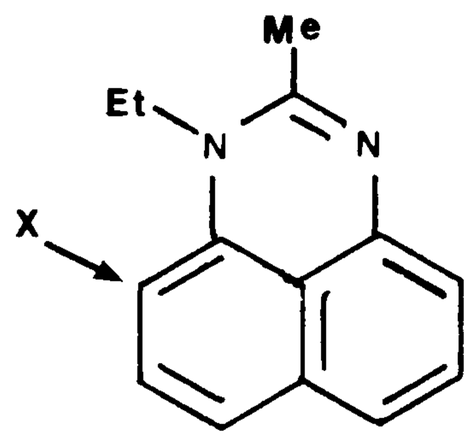

(139)

steric clash between the ethyl group and the phenylazo residue. This inherent non-planarity will contribute to a reduction in the λ_{max} value and also the molar extinction coefficient. Band broadening also occurs, and thus as well as absorbing at a shorter wavelength dye (134b) is also duller than the isomeric (135b).

Dye (133) is particularly interesting and shows exceptional

properties, absorbing at very short wavelengths (λ_{max} ca 395nm). To rationalise such a hypsochromic shift it was initially thought the diazonium ion must have N-coupled to form the the diazoamine derivative (140). If this were the case however, then acid catalysed

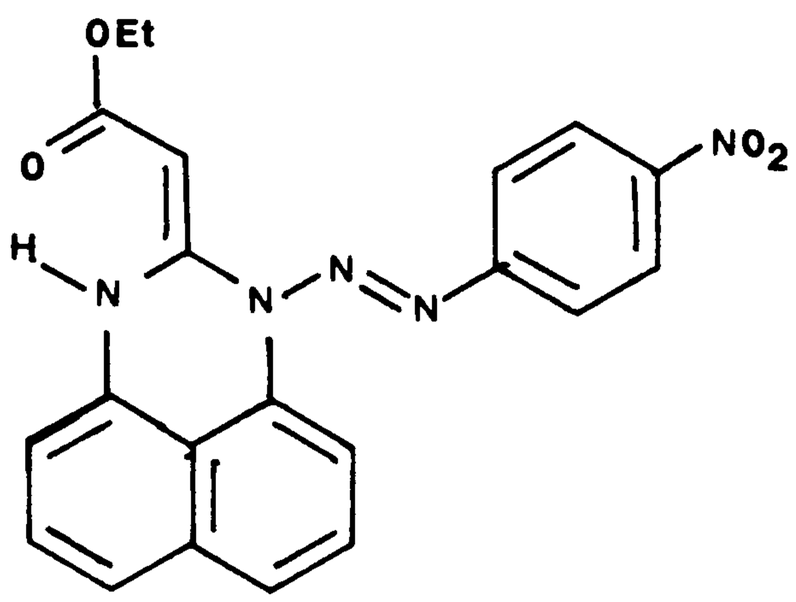

(140)

cleavage of this species should regenerate the 4-nitrobenzenediazonium ion which could be trapped by a suitably powerful nucleophile. To test this, phloroglucinol was used as the nucleophile as this would couple to the diazonium ion to give an intensely coloured dye. However no coupling to this species could be detected, and it was concluded that (133) was the correct structure for the product. As noted previously the structure (133) was confirmed by ^{1}H-n.m.r. spectroscopy.

Dye (132) absorbs about 60nm to shorter wavelengths than the uncyclised analogue (131g). Evidently the -M effect of the

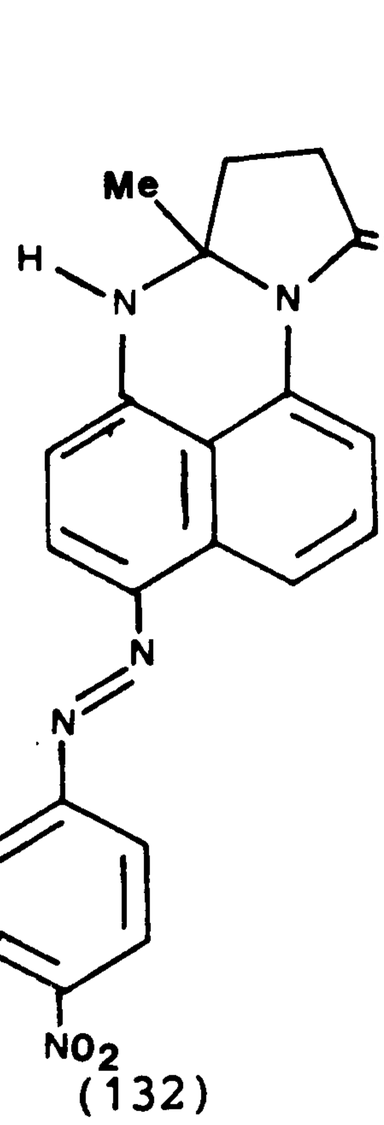

(132)

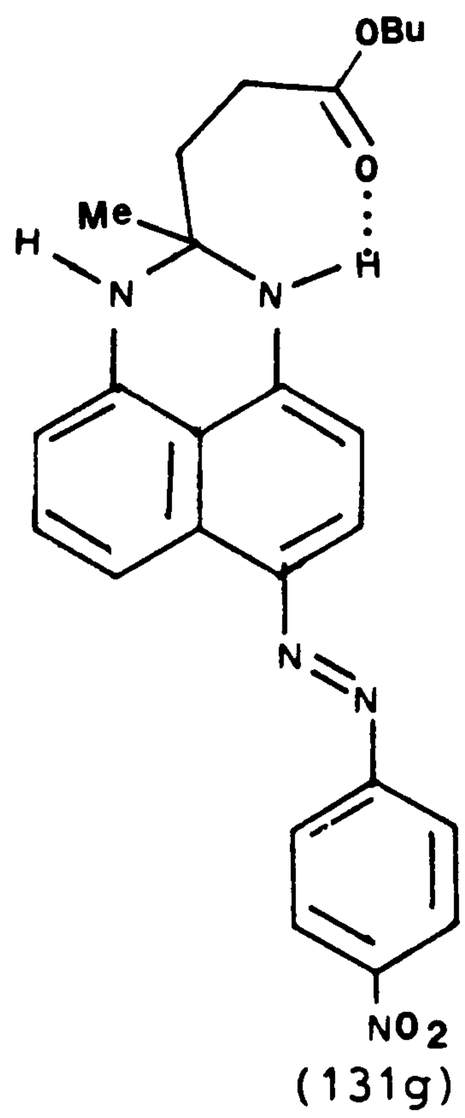

(131g)

carbonyl group bonded to the dihydroperimidine nitrogen significantly reduces the electron donating capacity of the dihydroperimidine residue, which in turn shifts the λ_{max} to shorter wavelengths. Interestingly the ε_{max} value for (132) was much greater than for analogue (131g), suggesting that in (132) the additional annelation enforces greater overlap of the NH lone pair electrons with the rest of the π-electron system of the chromophore [cf. Table 13 dye (109e)].

The two isomeric dyes (130i) and (131i) which are derived from the 2-benzoyl-substituted dihydroperimidine (123i) also exhibit a

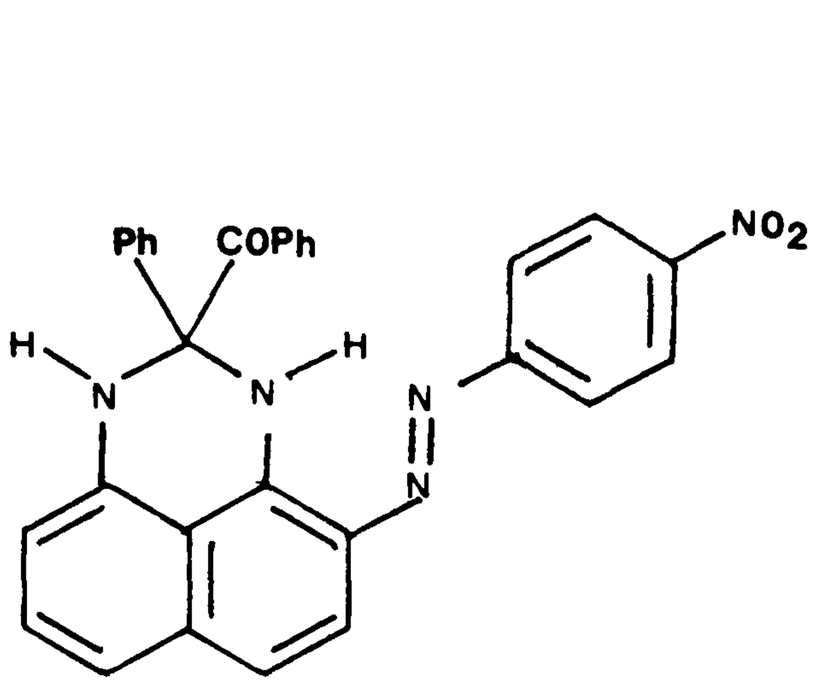

(130i)

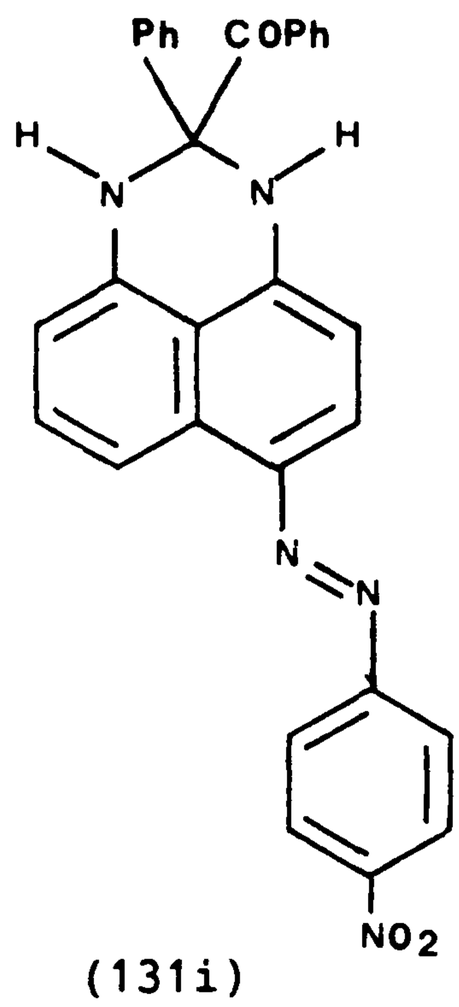

(131i)

significant hypsochromic shift and reduction in intensity when compared to those dyes derived from 2,2-disubstituted dihydroperimidines. The presence of the 2-carbonyl group in (130i) and (131i) evidently reduces the electron donating strength of the dihydroperimidine moiety. The hypsochromic and intensity lowering effects of electron withdrawing groups attached to the α-carbon atom of an N,N-dialkylaminobenzene are well known[116]. An example is provided by comparison of dyes (141) and (142). Thus a hypsochromic shift of 56nm occurs when a cyano group is introduced into the α-position of (140). A reduction of the molar extinction coefficient is also observed.

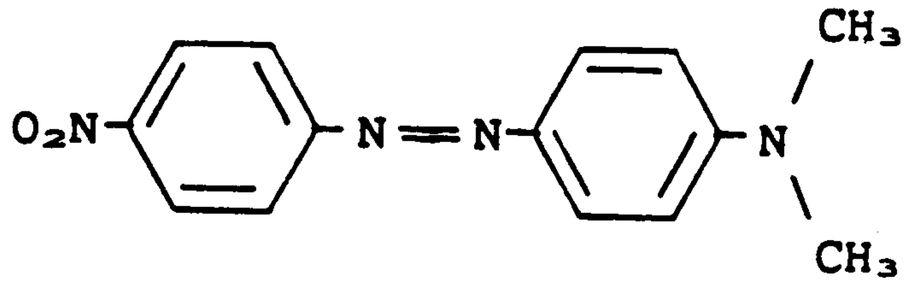

λ_{max}(EtOH) = 478nm ε_{max} = 33,100 $lmol^{-1}cm^{-1}$

(141)

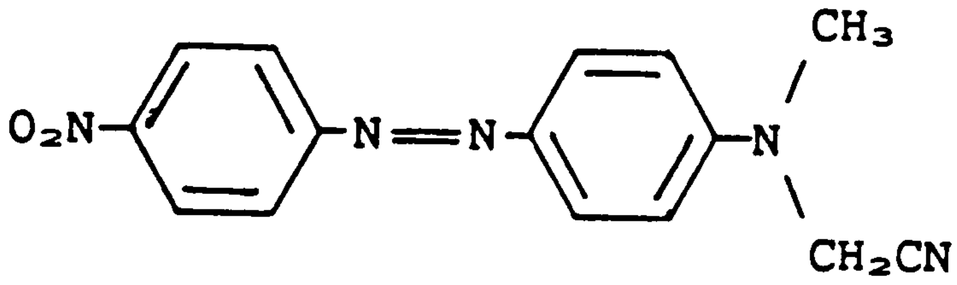

λ_{max}(EtOH) = 422nm ε_{max} = 26,000 $lmol^{-1}cm^{-1}$

(142)

For the majority of dyes listed in Tables 16 and 17 the extinction coefficients were relatively low compared to most aminoazo dyes (ε_{max} ca. 30,000$lmol^{-1}cm^{-1}$). In addition the dyes showed broad absorption bands, of half-band widths ca. 125nm, eg. Fig.4. Most aminoazobenzene

Fig. 4: UV-visible spectrum of dye (130g) in dichloromethane

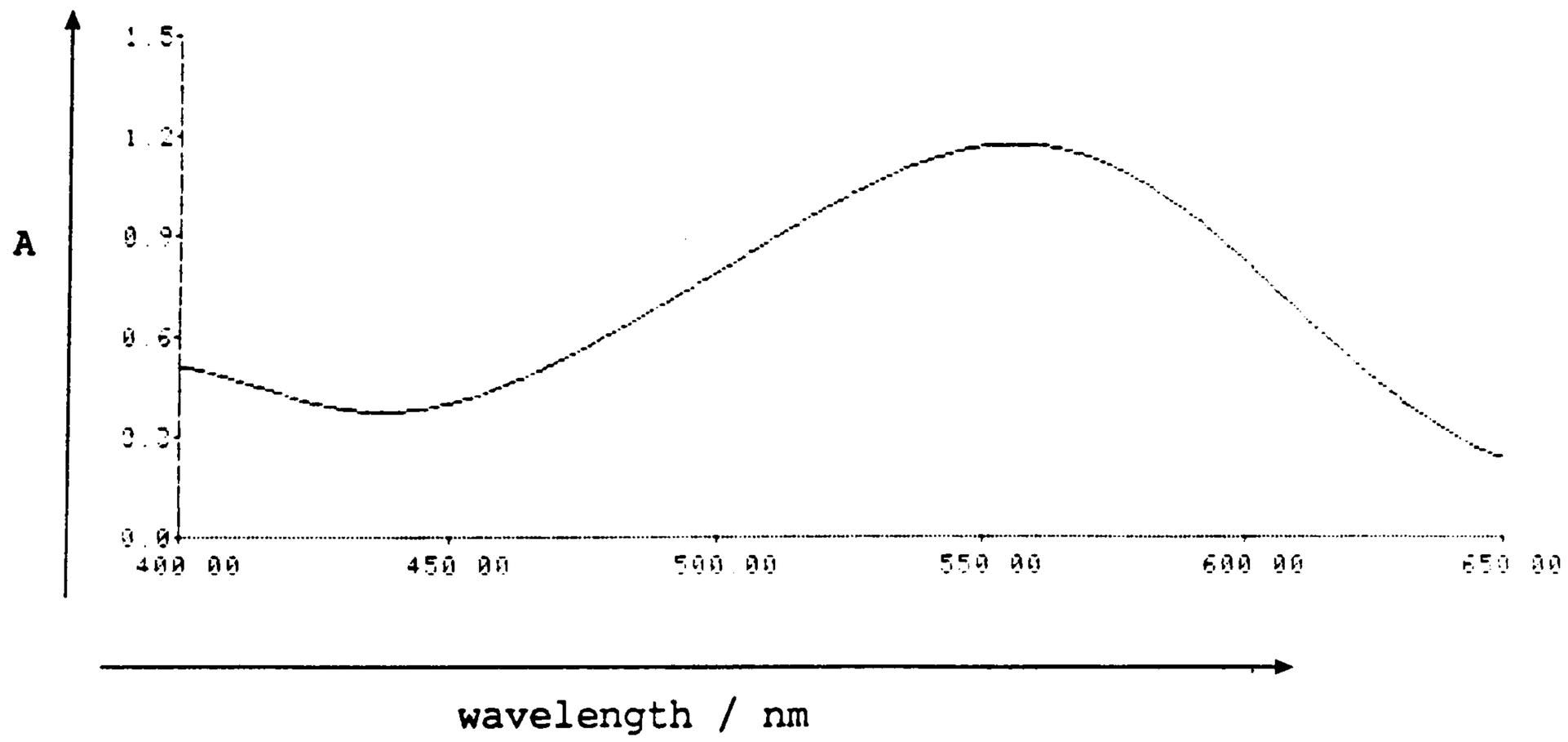

A - absorbance

dyes have half-band widths of ca. 95nm. The low extinction coefficient may be attributed to this band broadening as it is band area that is a true measure of absorption intensity.

The light absorption properties of the dyes were next examined

theoretically by carrying out PPP-MO calculations on representative examples.

As the nitrogen atoms in the dihydroperimidine and perimidine ring systems are held rigidly in conjugation with the rest of the π-system, their π-electrons are more readily donated than, for example, in the case of simple aminoazo dyes. Therefore, previously available PPP-MO nitrogen parameters derived for simple arylamines failed to give satisfactory results when used in these calculations. For example when, for dye (131h), each dihydroperimidine nitrogen was given the

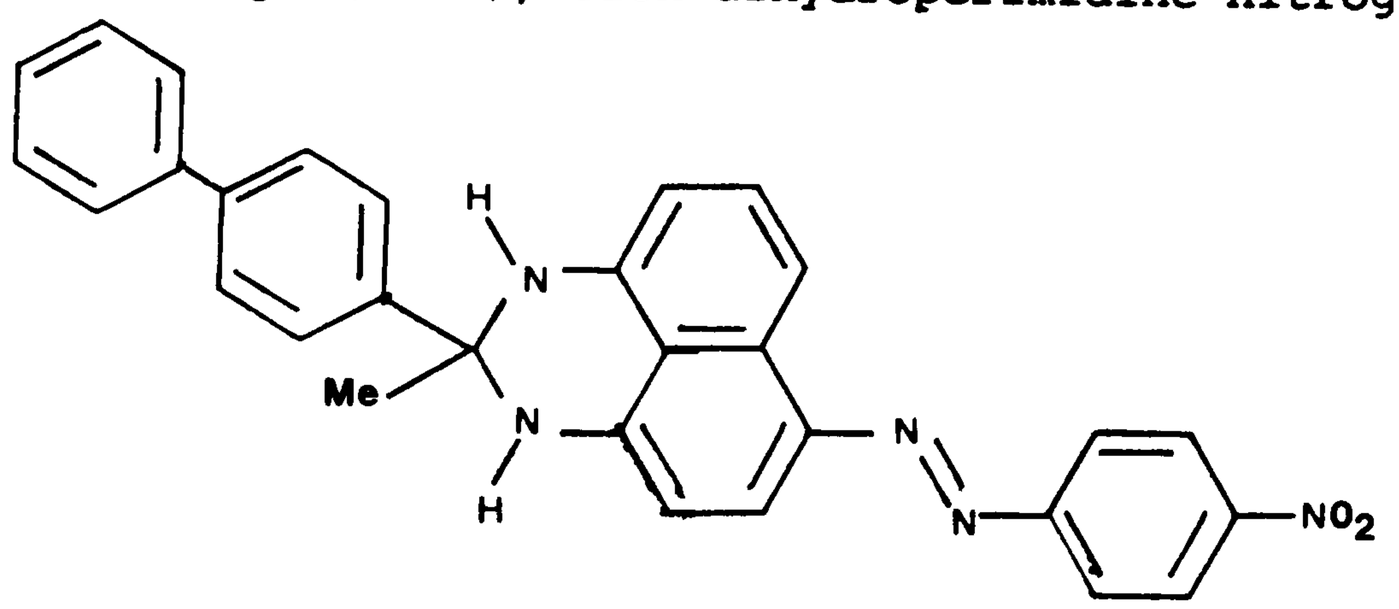

(131h)

VSIP value of 18.0eV and an electron affinity of 8.0eV (these values being those for the nitrogen atom of the dimethylamino group), the calculated λ_{max} was 489nm, a shortfall of some 58nm from the observed value. New VSIP and electron affinity values were therefore evaluated to allow for the enhanced +M effect exhibited by dihydroperimidine and perimidine ring nitrogen atoms. If (131h) is again considered, then lowering the VSIP value to 14.8eV and the electron affinity to 4.0eV (both of new these values showing the increased electron donating strength of the nitrogen atoms) results in a calculated λ_{max} value of 543nm, a deviation of only 5nm from the observed value. The two values were, in fact, found to give the best overall results for non-alkylated, non-hydrogen bonded perimidine/dihydroperimidine ring nitrogen atoms.

The N-ethyl nitrogen in dyes (134b) and (135b) has additional electron releasing strength due to the +I contribution from the alkyl

substituent. Accordingly, the VSIP value was further reduced to 13.8eV and the electron affinity to 3.0eV. For these two dyes standard π-equivalent ring nitrogen values of VSIP = 12.0eV and electron affinity = 0.5eV were employed for the remaining ring nitrogens.

For reasons previously discussed, dyes (130i) and (131i) absorbed at shorter wavelengths than the other 2,2-disubstituted dihydroperimidine dyes. Therefore, in the PPP-MO calculations the VSIP and electron affinity values for the dihydroperimidine nitrogen atoms were raised from 14.8eV to 15.8eV and from 4.0eV to 5.2eV respectively to allow for the -I effect of the α-carbonyl group. These new values then gave calculated λ_{max} values in good agreement with experiment.

The hydrogen bonded dihydroperimidine nitrogen atoms in the ortho coupled dyes again required new VSIP and electron affinity values. When calculating absorbance values for these dyes the presence of hydrogen bonding could be compensated for by retaining the previously mentioned VSIP value of 14.8eV for nitrogen, but increasing the electron affinity to 6.0eV.

Apart from these modifications to the nitrogen donor atom parameters, all other atom and bond parameters for the dyes were those described elsewhere for general applicability. Calculated and experimental λ_{max} values for representative dyes are presented in Tables 18 and 19. It can be seen that there was generally good agreement between theory and experiment. Dye (133) is exceptional in that its observed λ_{max} value differs markedly from the calculated value. In agreement with the ε_{max} values listed in Table 17, the oscillator strengths of (132) and (133) were higher than those for the other para-coupled dyes.

Having obtained a reasonable correlation between the calculated and experimental λ_{max} values of the azo dyes, it was then of interest to

Table 18: PPP-MO calculated λ_{max} values for representative ortho 4-nitrophenylazo dihydroperimidines and perimidines

Dye	λ_{max}/nm (Calc)	λ_{max}/nm (Toluene)	$\Delta\lambda_{max}$/nm (Tol - Calc)	Oscillator stength (f) (Calc)
(130h)*	557	562	+5	0.52
(130i)	532	523	-9	0.81
(134a)	556	550	-6	1.70
(134b)	569	558	-11	1.63

* - any dihydroperimidine dye (130a)-(130g) may be substituted here

Table 19: PPP-MO calculated λ_{max} values for representative para 4-nitrophenylazo dihydroperimidines and perimidines

Dye	λ_{max}/nm (Calc)	λ_{max}/nm (Toluene)	$\Delta\lambda_{max}$/nm (Tol - Calc)	Oscillator stength (f) (Calc)
(131h)*	543	548	+5	1.09
(131i)	520	523	+3	0.82
(132)	480	505	+25	1.84
(133)	505	395	-110	1.34
(135a)	577	578	+1	1.23
(135b)	592	580	-12	1.26

* - any dihydroperimidine dye (131a)-(131g) may be substituted here

examine the ground state charge densities and π-electron density changes for the visible transitions of the dyes, in order to obtain a better understanding of the relationships between their colour and molecular structure. The relevant values for dyes (130h), (131h), (134b) and (135b) are summarised in Figures 5, 6, 7, and 8 respectively. These can be regarded as representative of the ortho and para dihydroperimidine and perimidine dyes.

It should be noted that in Figs. 5(a) - 8(a), the charges refer to electrical charge, i.e. a positive sign means positive charge, a

negative sign a negative charge. In Figs. 5(b) - 8(b) a positive sign means a gain in electron density (negative charge) and a negative sign a decrease in electron density at a particular atom.

Fig. 5: (a) Ground state charge densities and (b) π-electron density changes for the first absorption band of (130h)

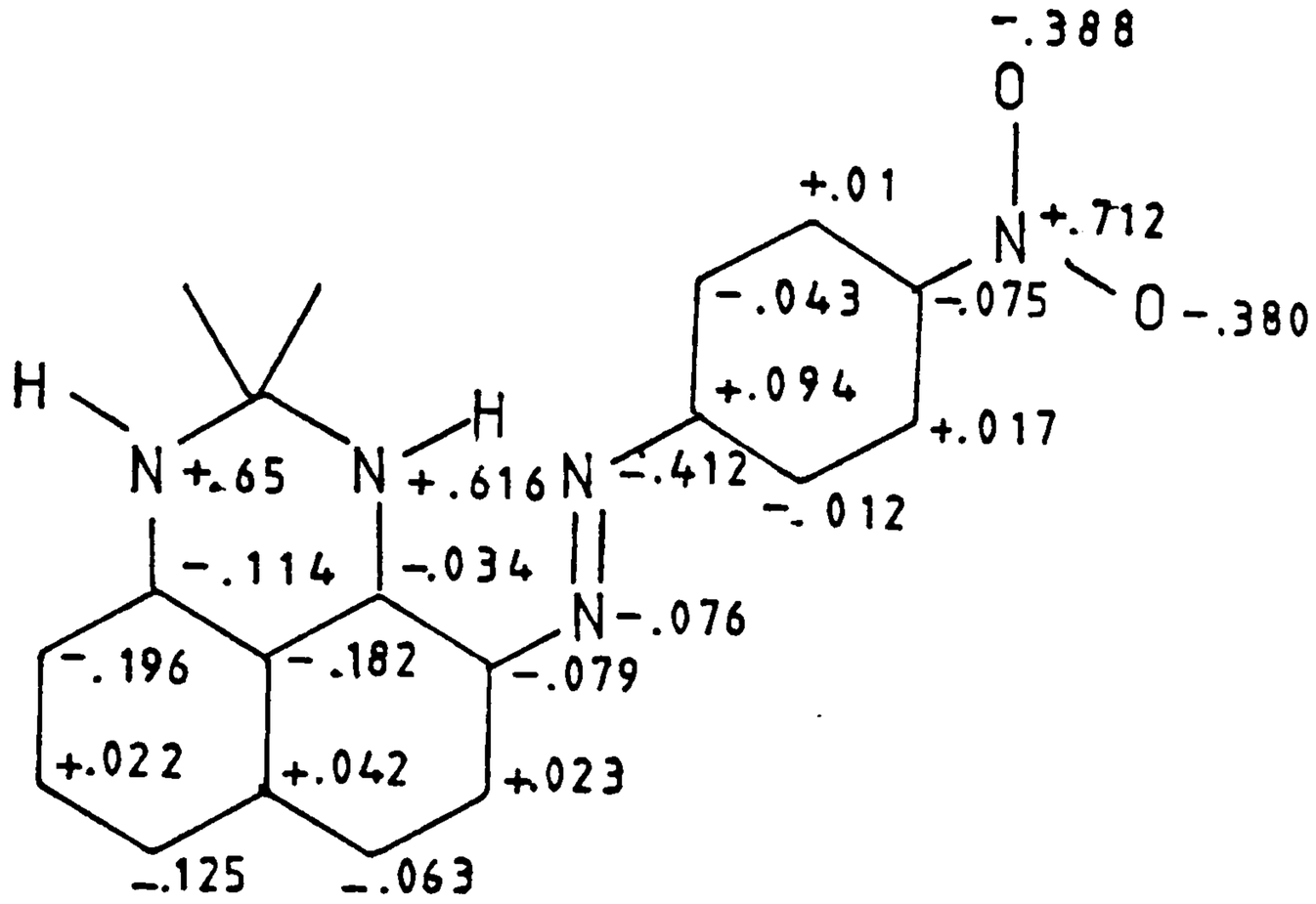

(a)

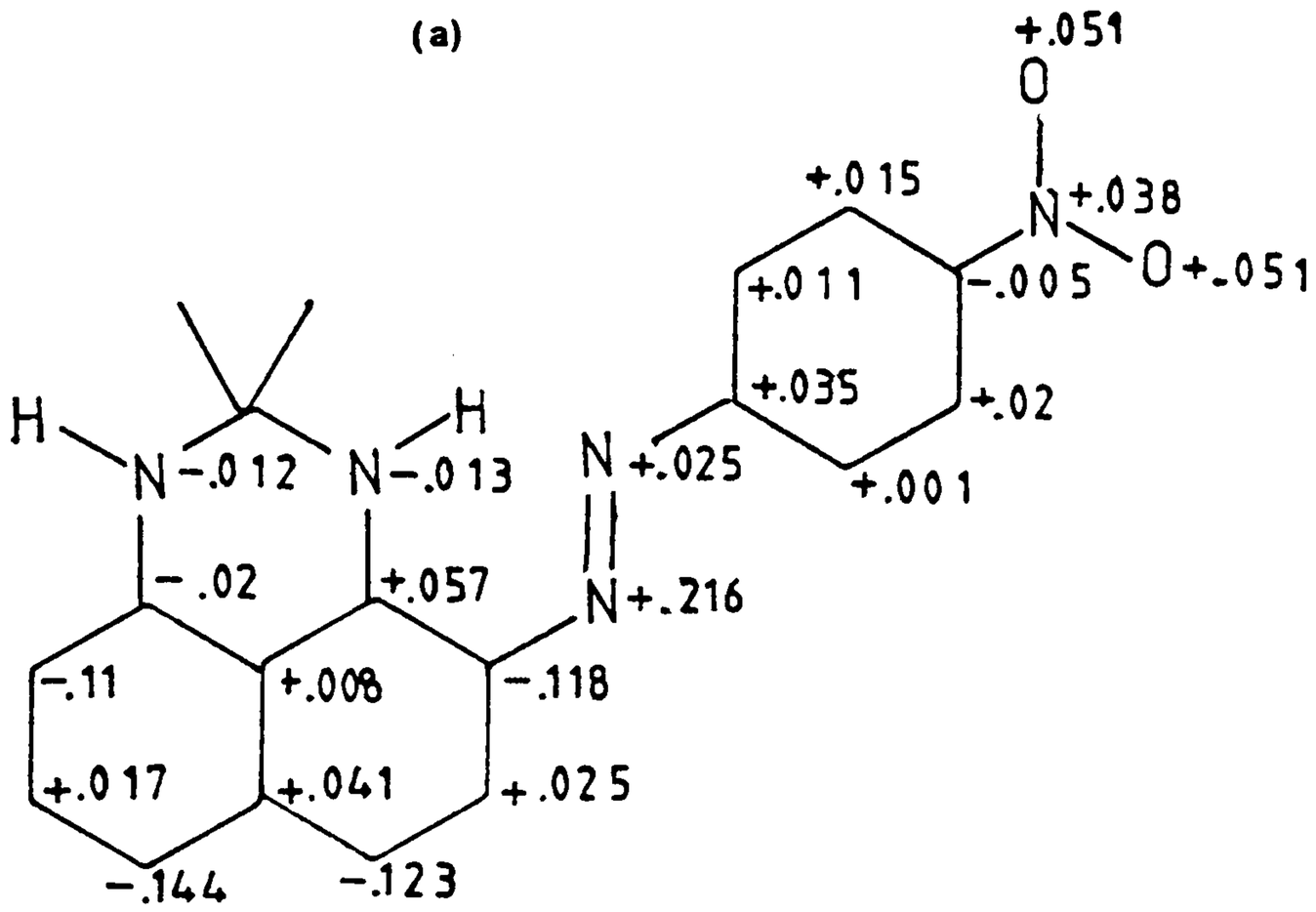

(b) λ_{max} (calc) = 557nm

λ_{max} (toluene) = 562nm

It can be seen from Figs. (5a) and (6a) that for both the ortho and para dyes the π-electron system in the ground state shows the typical migration of electron density from both donor dihydroperimidine nitrogen atoms principally to the acceptor azo- and nitro-groups. In

the case of (130h), rather surprisingly, the nitrogen not directly conjugated to the azo group shows a greater donation of electron

Fig 6: (a) Ground state charge densities and (b) π-electron density changes for the first absorption band of (131h)

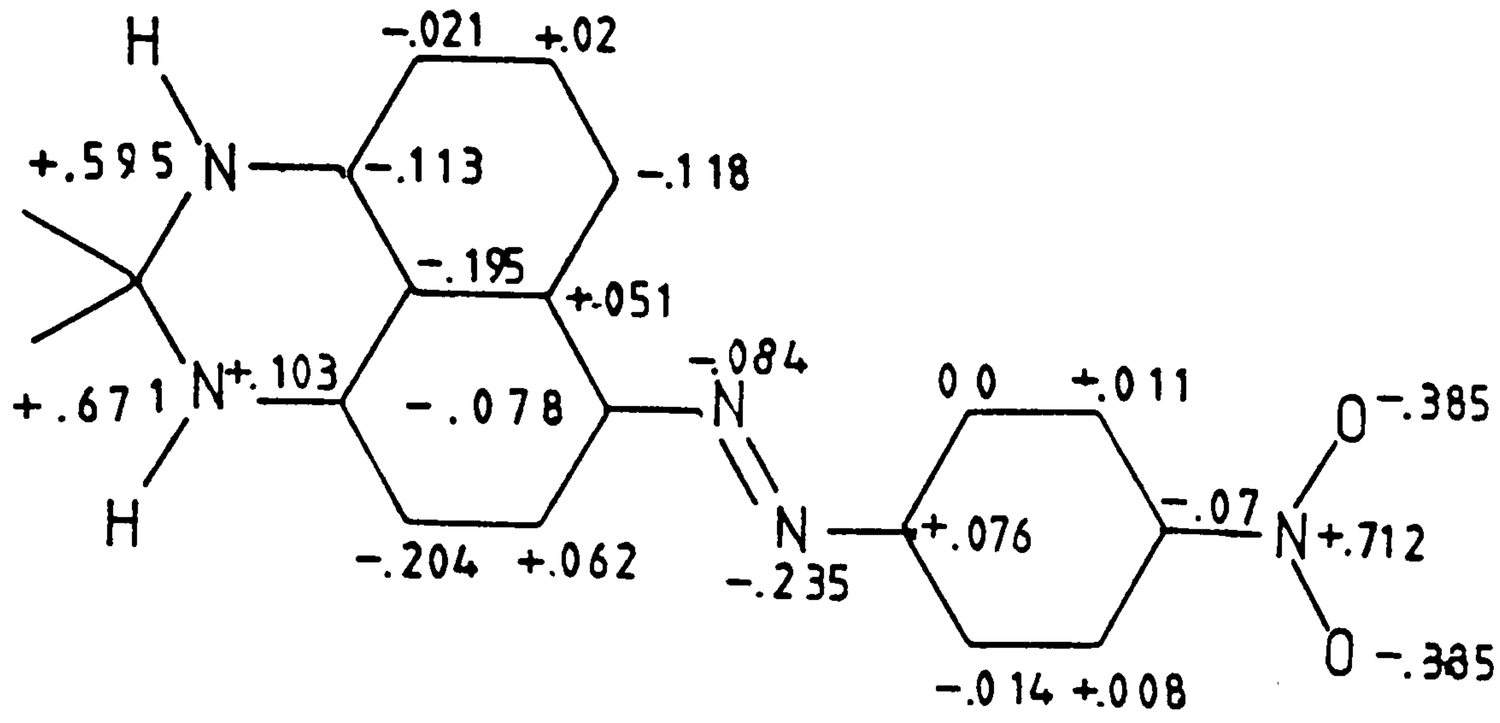

(a)

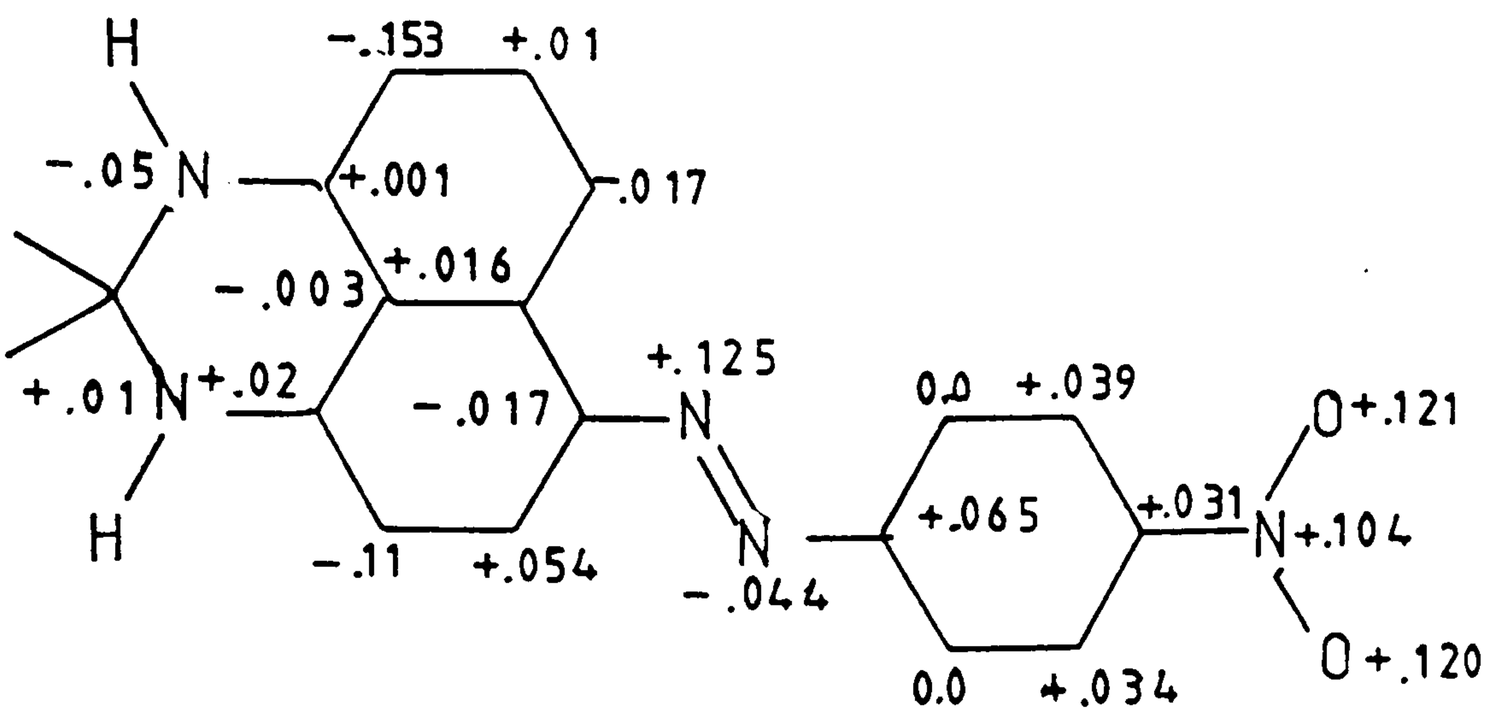

(b)

λ_{max} (calc) = 543nm

λ_{max} (toluene) = 548nm

density than the nitrogen atom that is directly conjugated. The reverse is true for the para dye (131h). There is also a build up of electron density at the ß-azo nitrogen in the ground state in both dyes. Clearly the ground states of both molecules are strongly polarised. Consideration of Figs 5(b)-8(b) shows the changes occurring in the π-electron system accompanying light absorption. Again typical donor-acceptor characteristics are shown. The excited state electron density change for the para dye (131h) shows a small migration of electron density from the nitrogen atom para to the azo

Fig 7: (a) Ground state charge densities and (b) π-electron density changes for the first absorption band of (134b)

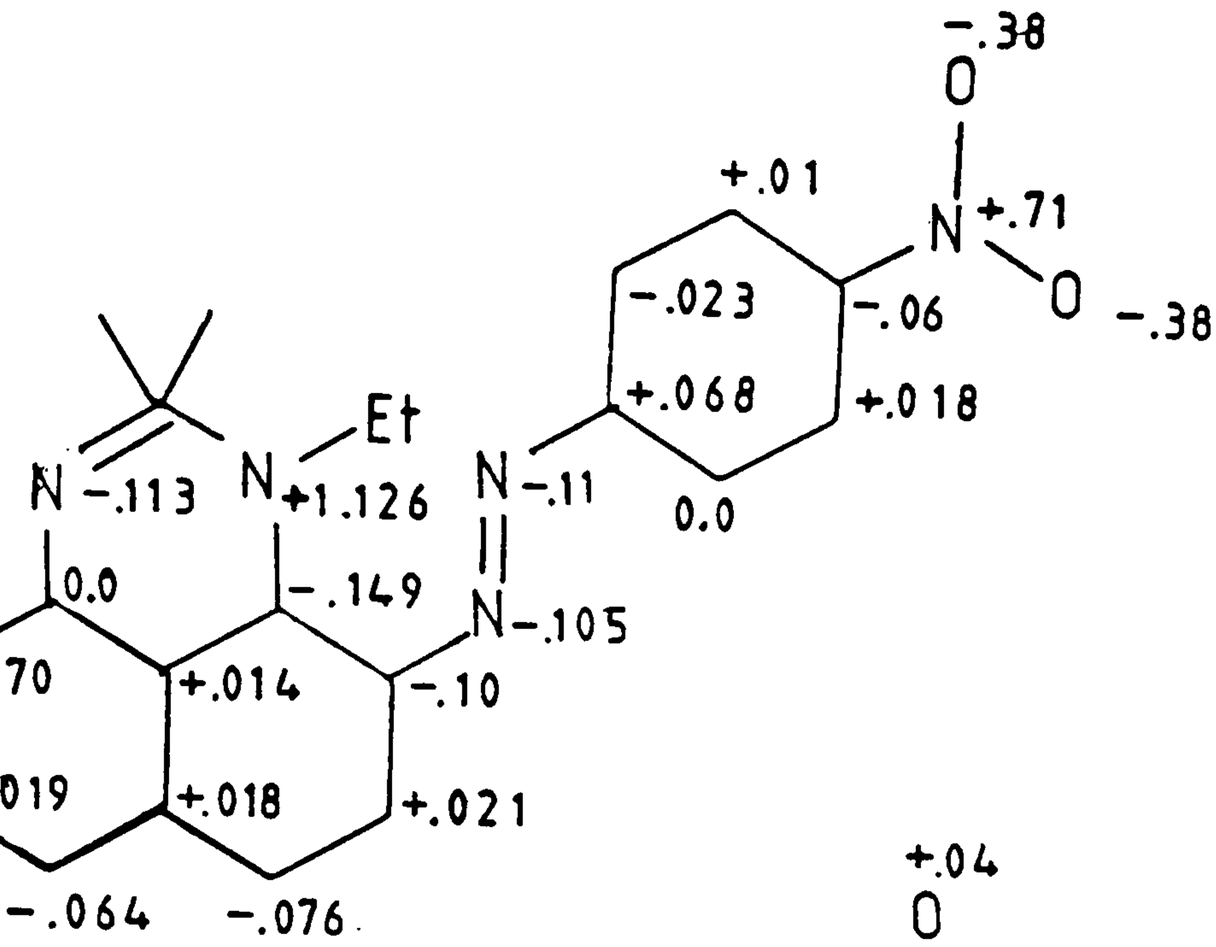

λ_{max} (calc) = 560nm

λ_{max} (toluene) = 558nm

group largely onto the α-azo nitrogen atom and the nitro group. This is typical of other aminoazo dyes[3]. Also, in (130h) the 2,4,6, and 8 positions of the dihydroperimidine ring system (i.e. positions ortho and para to the donor nitrogen atoms) show a strong decrease in electron density in the exited state. This indicates that electron donating groups attached to these positions would contribute a significant additional bathochromic shift. Electron density changes show a similar pattern with the para dye.

The perimidine dyes (134b) and (135b) are included in Figs. 7 and 8 to illustrate the fact that their π-electron behaviour is similar to that of the dihydroperimidine dyes (130h) and (131h).

Fig 8: (a) Ground state charge densities and (b) π-electron density changes for the first absorption band of (135b)

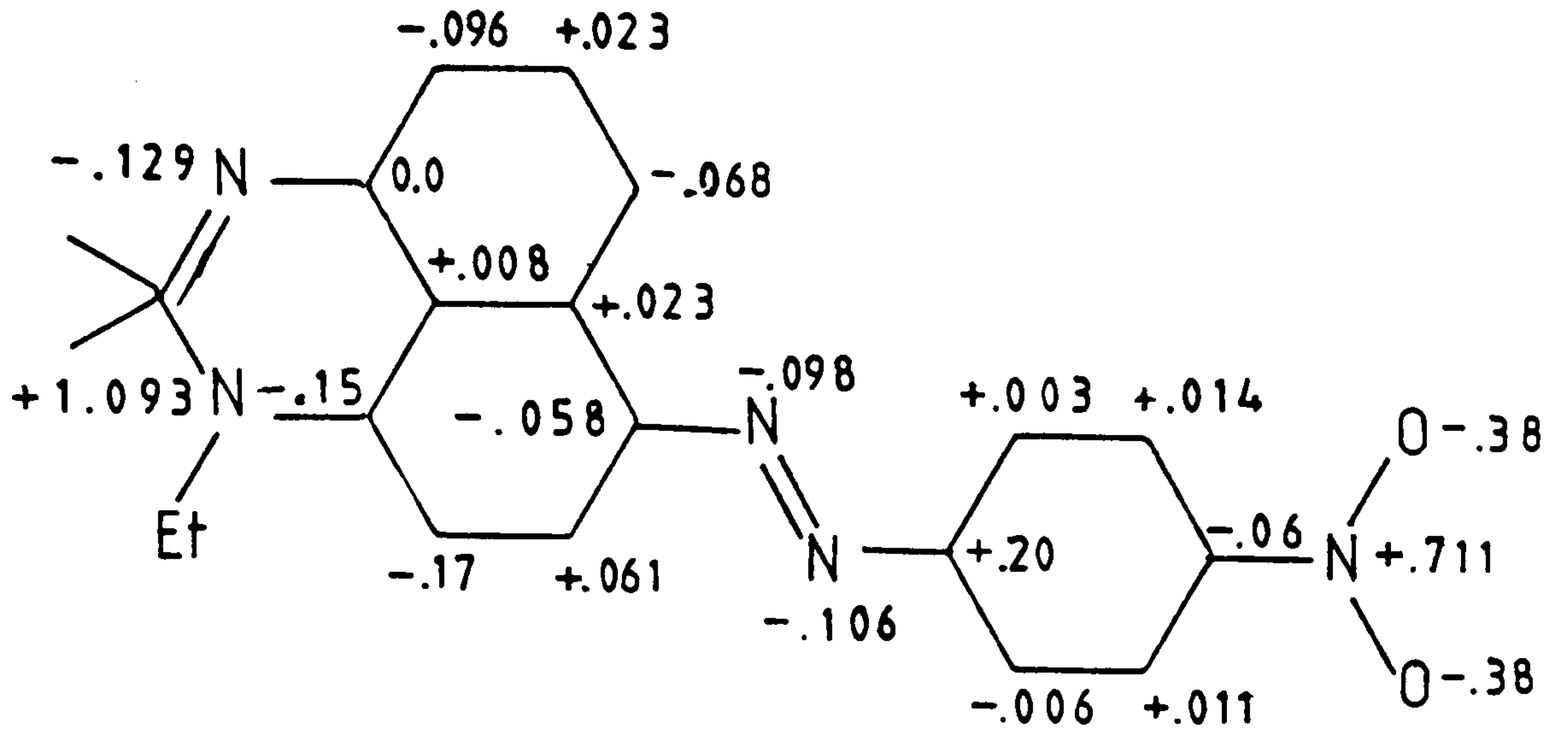

(a)

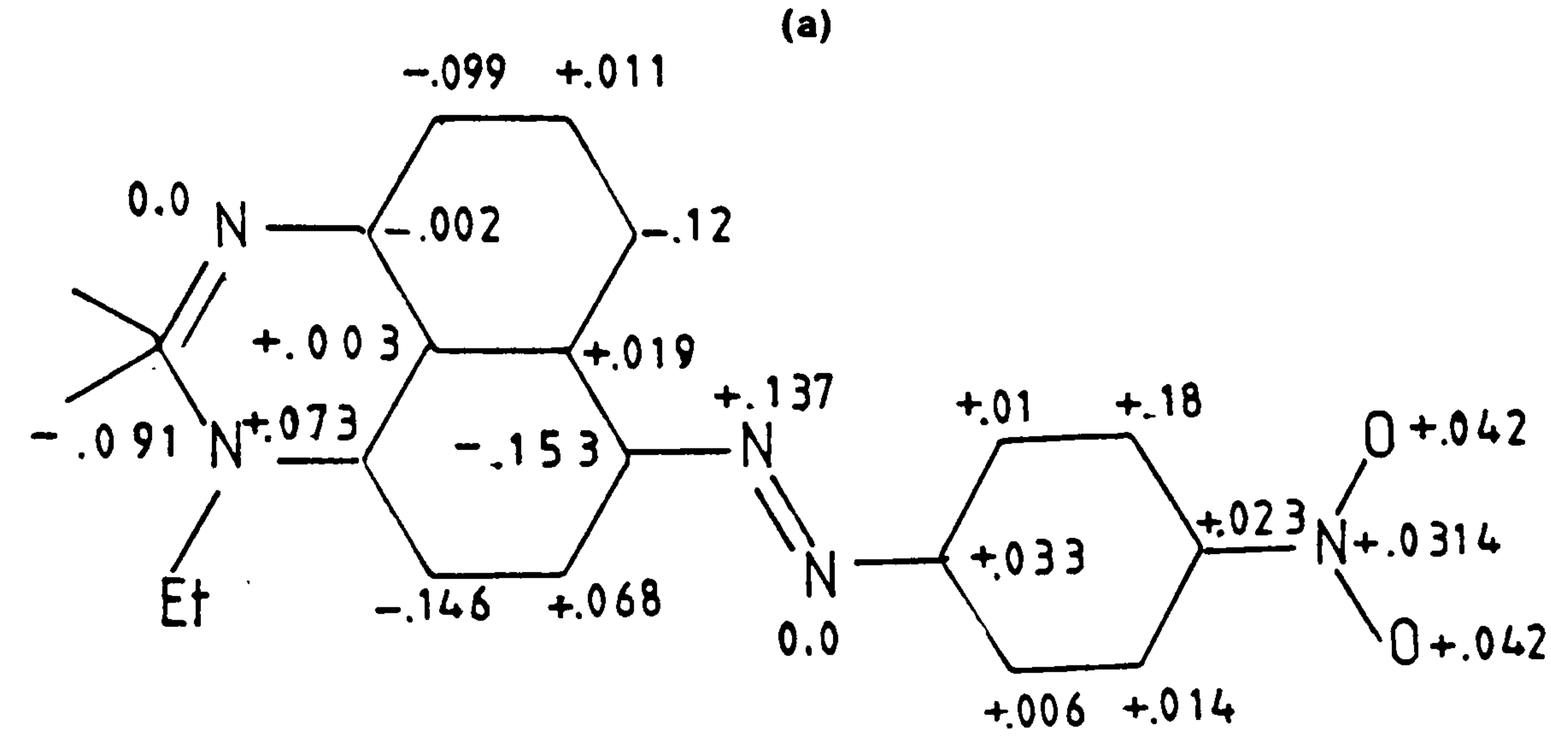

(b)

λ_{max} (calc) = 592nm

λ_{max} (toluene) = 580nm

2.1.2.3 Halochromism of the Azo Dyes

The 4-aminoazo dyes undergo the various protonation equilibria shown in Scheme 21[117-124].

The azonium ion (145) is generally formed predominantly, and differs in colour from the neutral dye (143). This acid induced colour change is called halochromism.

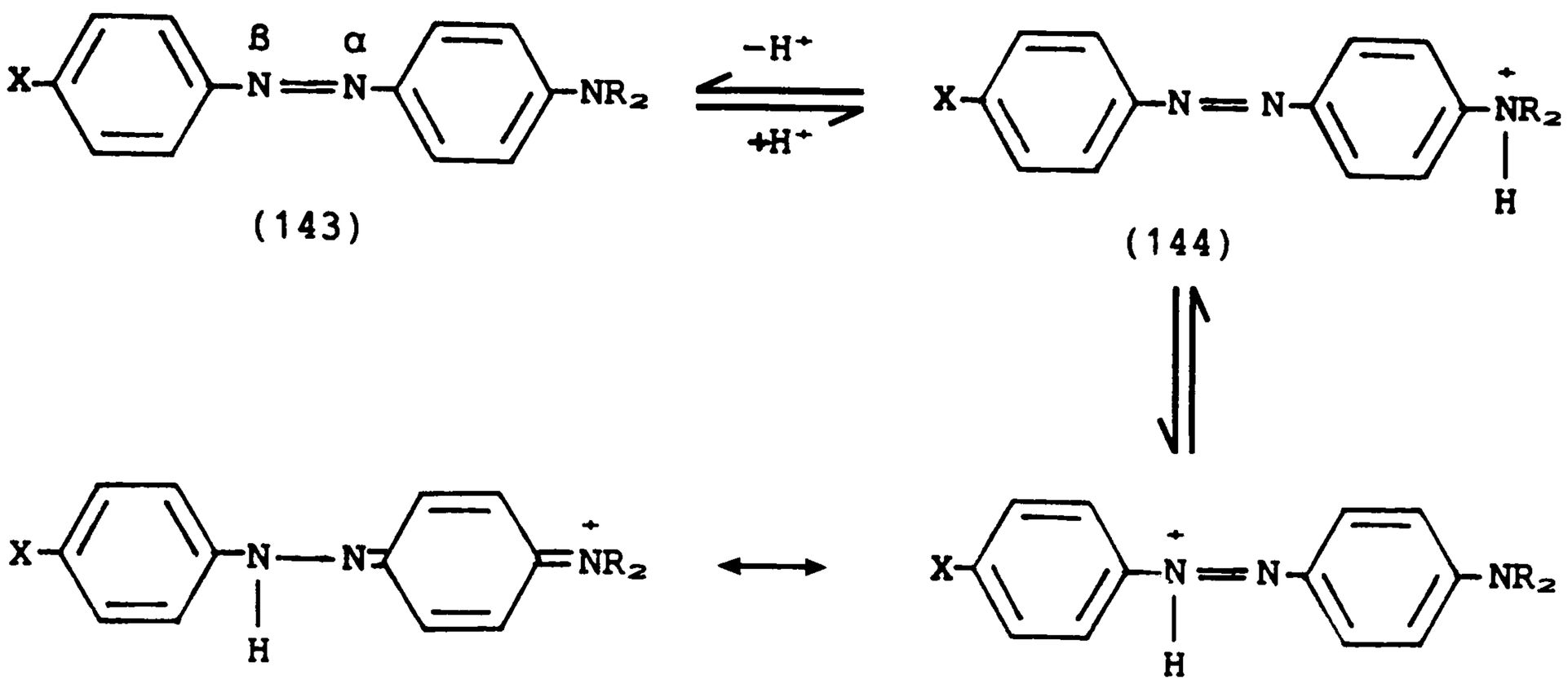

Scheme 21

The azonium ion is usually more bathochromic than the unprotonated dye and the dye is then said to exhibit positive halochromism. The bathochromic shift is due to the nearly equal contributions of the structures (145a)⟷(145b), neither of which involves charge separation. The magnitude of the bathochromic shift on going from neutral to acid solution decreases with increasing electron withdrawing strength of X, or with the introduction of more powerful electron releasing groups in the amino-substituted ring. If the strength of the electron donating groups and/or the electron acceptors is sufficiently high then zero or even negative halochromism may be observed.

The halochromism of representative dihydroperimidine and perimidine azo dyes were determined in pure acetone solution (the solvent was fractionally distilled and dried over a zeolite molecular sieve). Shifts of the absorption maxima on acidification of the solutions with hydrochloric acid are summarised in Table 20. In all cases after recording the spectra, solutions were carefully neutralised with sodium bicarbonate to verify that the original spectra could be completely restored, thus showing that the observed spectral changes

Table 20: Halochromism of representative 4-nitrophenylazo dihydroperimidine and perimidine dyes

Dye	λ_{max}/nm (acetone) Neutral	+HCl	$\Delta\lambda_{max}$/nm = (acidic-neutral)
(130h)*	570	603	+33
(131h)*	555	581	+26
(132)	515	550	+35
(133)	391	378	-14
(134b)	571	477	-94
(135b)	594	494	-100

* - similar observations were found for other 2,2-disubstituted dihydroperimidine dyes

are not due to irreversible decomposition processes.

The results in Table 20 show that the ortho and para 4-nitrophenylazo dihydroperimidine dyes, as well as dye (132), exhibit positive solvatochromism on acidification.

In contrast dye (133) exhibits negative solvatochromism on acidification. This is almost certainly due to the fact that this dye does not form an azonium cation but instead protonates on the 3-nitrogen atom in the dihydroperimidine ring, giving (146). This

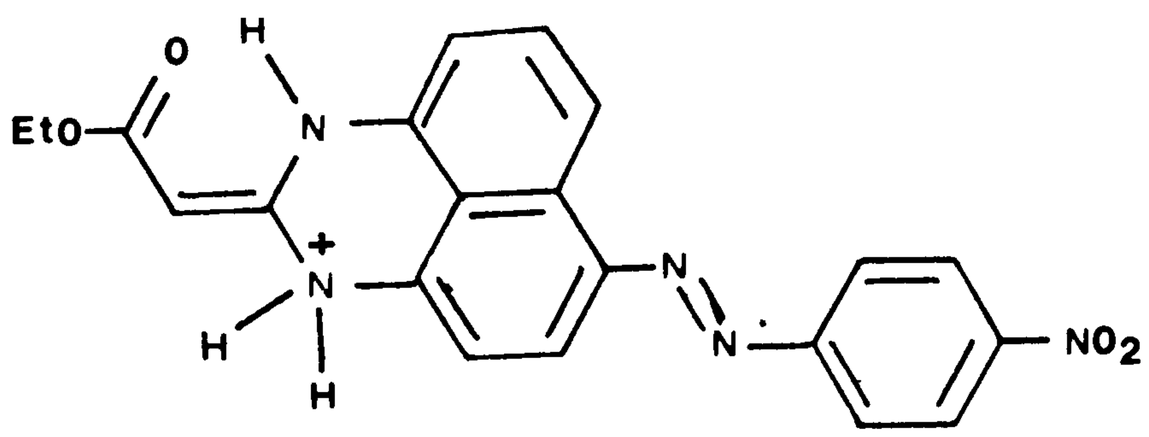

(146)

would give a hypsochromic shift. The failure to protonate on the azo group is an indication of the very weak donation of electrons from the donor nitrogen atoms to the azo group in the neutral dye.

The isomeric perimidine based dyes (134b) and (135b) exhibit marked

negative halochromism. The size of this shift (ca. 100nm) is much larger than might be anticipated for formation of an azonium cation. As with (133), a possible explanation is that protonation on the 3-nitrogen atom of the perimidine ring occurs, as shown in Scheme 22.

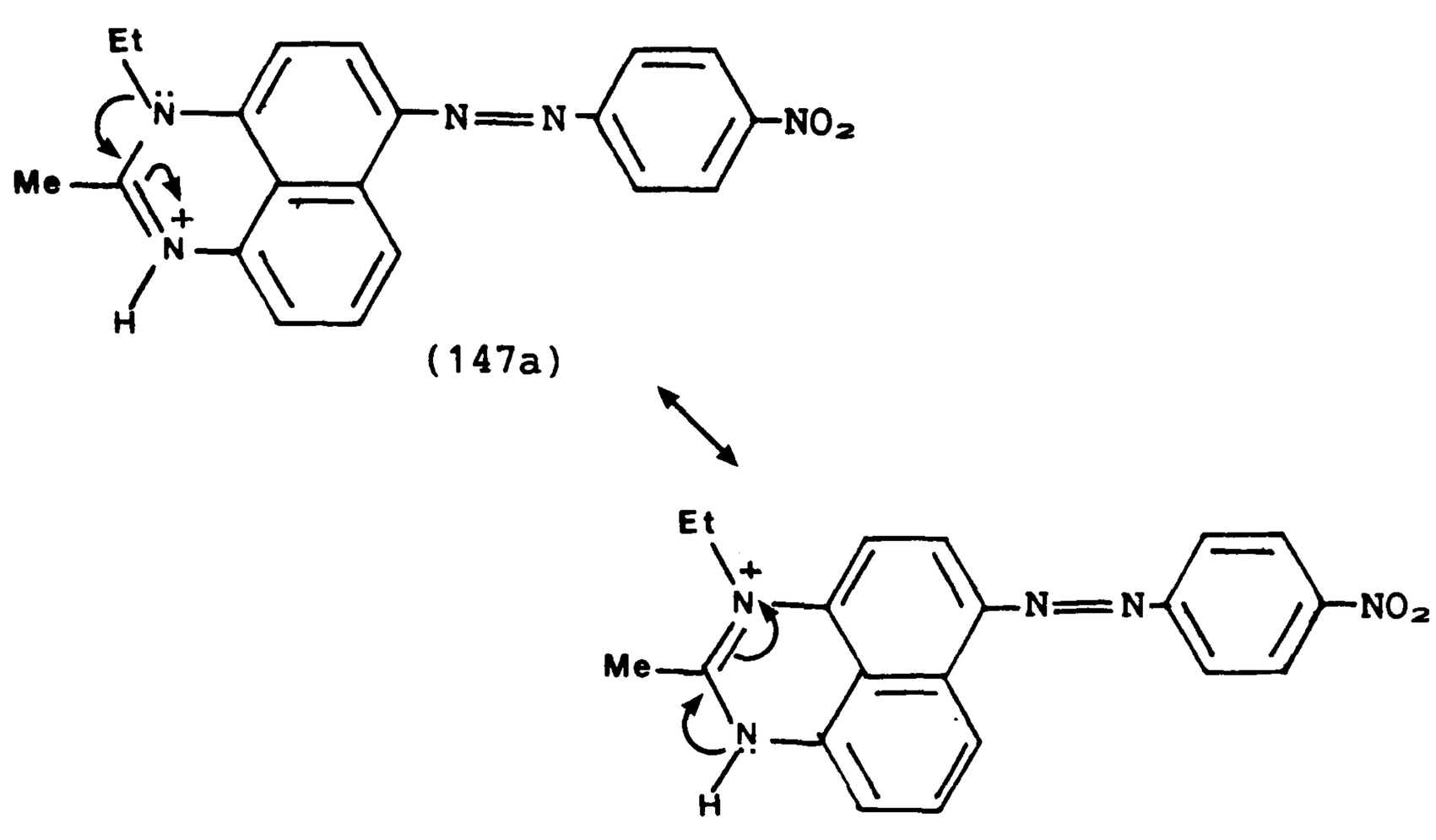

(147a)

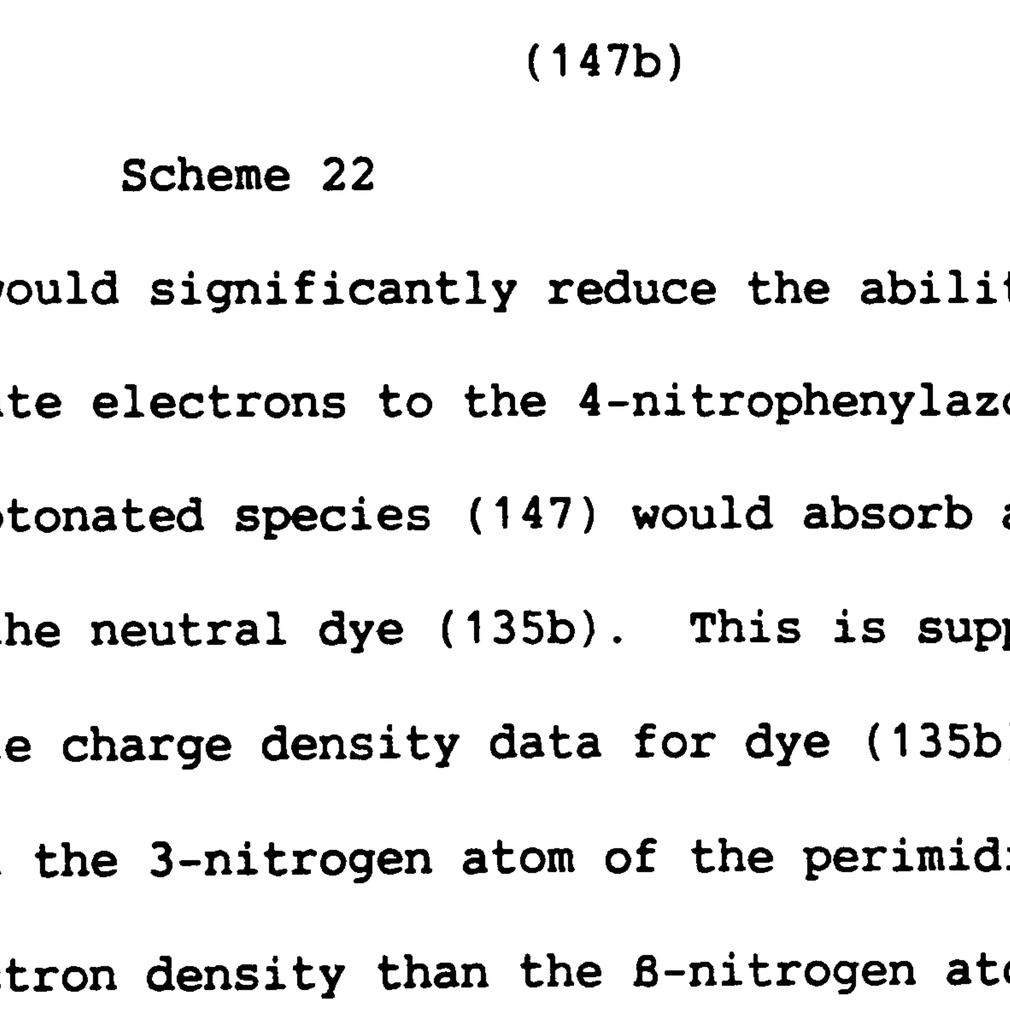

(147b)

Scheme 22

Protonation at this site would significantly reduce the ability of the perimidine residue to donate electrons to the 4-nitrophenylazo residue, therefore the protonated species (147) would absorb at much shorter wavelengths than the neutral dye (135b). This is supported by the calculated ground state charge density data for dye (135b),[Fig. 8(a)] which indicates that the 3-nitrogen atom of the perimidine residue has a greater electron density than the ß-nitrogen atom of the azo-linkage. Hence protonation should occur preferentially at the 3-nitrogen atom of the perimidine ring. The same situation exists for the ortho-analogue in Fig. 7a.

2.1.2.4 Stability Properties Of Dyes (135) - (140)

The stability properties of the highly bathochromic simple monoazo dyes (130) - (135) are of practical relevance if they are to be used

technically. The dyes were considered largely for their potential application in opto-electronic systems, such as laser light absorbers in optical data storage media or as dyes for use in machine-readable inks. Accordingly both the thermal and photochemical properties were assessed.

The method adopted was to cast films of cellulose acetate containing the dye in a fully dissolved state. Such films could then be subjected to heat or photochemical treatment and the degradation of the dye assessed directly by visible absorption spectroscopy. For comparison purposes, a standard dye was required which had reasonable but not exceptional stability as far as textile applications were concerned. The blue thiazole azo dye (148) was elected as standard, and this was readily soluble in cellulose acetate.

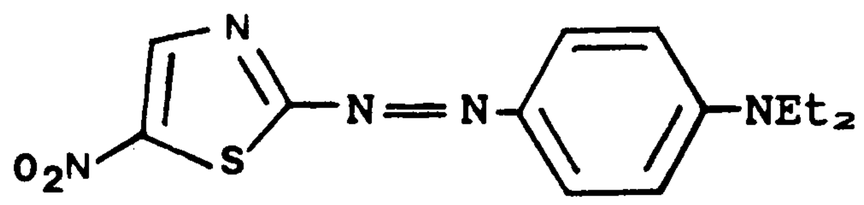

(148)

For photostability evaluation, each film was cut into small pieces and mounted on a slide frame. The films, together with the standard film made up with dye (148) were irradiated for 72 hours using a Microscal Fadometer. The optical densities of the films were measured before and after irradiation and the percentage degradation determined.

In order to assess the thermal stability of the dyes, pieces of the dyed films were sandwiched between a polyester (Melinex) clear film, sealed in an aluminium foil envelope, and heated between the plates of a transfer printing press at 190°C for 1 hour. From the optical density of the films before and after heating, the percentage loss of dye could be calculated. The Melinex film was employed to trap any dye subliming from the acetate film and to permit detection of this

dye. In this way dye degradation in the acetate film could be separated from dye loss by sublimation. However, due to opacification of the Melinex only a qualitative visual assessment of the degree of sublimation could be made. For those dyes which showed no transfer under these conditions the calculated percentage loss of dye in each case represents the true thermal degradation of the dye.

The results for representative ortho coupled dyes are summarised in Table 21 and those for the para dyes in Table 22. The standard dye

Table 21: Thermal and photochemical stabilities of representative ortho coupled 4-nitrophenylazo dihydroperimidine and perimidine dyes

Dye	Photo stability (% loss)	Thermal stability (% loss)
Standard (148)	8	5
(130f)	20	3(a)
(130g)	15	16(a)
(130h)	17	3(a)
(130i)	32	2(a)
(134b)	17	7(a)

(a) - some dye sublimation

showed a 5% loss on exposure to u.v. radiation and an 8% dye loss on thermal treatment.

It can be seen from Tables 21 and 22 that the new dyes generally showed inferior lightfastness but superior heat fastness relative to the standard (148). The thermal stability values quoted are not strictly quantitative, as, in all cases, varying degrees of dye sublimation was evident, but they do give a general guide as to the relative stability. It is interesting to note that the ortho derivatives appeared to sublime more readily than their para

Table 22: Thermal and photochemical stabilities of representative para coupled 4-nitrophenylazo dihydroperimidine and perimidine dyes

Dye	Photo stability (% loss)	Thermal stability (% loss)
Standard (148)	8	5
(131f)	42	3[a]
(131g)	45	2[a]
(131h)	43	2[a]
(131i)	41	Total Decomposition[b]
(132)	58	14[a]
(133)	45	2[a]
(135b)	28	3

(a) - some dye sublimation
(b) - sublimation of the decomposition products or the dye followed by subsequent decomposition was apparent due to brown staining on the Melinex film

analogues. This can be explained by the fact that the intramolecular hydrogen bonding within the ortho derivatives leads to dyes of reduced polarity and higher volatility.

The dyes all exhibited poor lightfastness properties however with, again, the para analogues showing lower stability than the ortho isomers. Presumably intramolecular hydrogen bonding in the ortho dyes contributes to the greater stability.

Those dyes which contained carbonyl groups, namely (130i), (131i) and (132), [but not the ester of (133)], exhibited generally poorer photochemical and thermal stabilities than the other dyes. For example dye (131i) was totally destroyed under the thermal conditions employed, and (132) showed the worst photostability of all the dyes assessed. It would seem that the presence of the carbonyl group accelerates degradation of these dyes.

In conclusion, it can be said that the thermal stabilities of the dyes are satisfactory for most applications, and compare closely with the stability of textile azo dyes. Thus such materials could be used in plastics, coatings etc. which employ moderate processing temperatures. However, the main drawback to the dihydroperimidine and perimidine systems is their generally poor photochemical stability which would severely limit their practical applications in many areas.

2.1.3 Highly Bathochromic Monoazo Dyes Based on Other Novel Coupling Components

In addition to dihydroperimidine and perimidine electron donor groups other apparently very powerful nucleophiles in coupling components for azo dyes are known. Two such systems examined were the bis-(4-dimethylaminophenyl)-ethene (Michler's ethylene) (149) and 1-decyl-2(1H)-methylene-benz[c,d]indole (150).

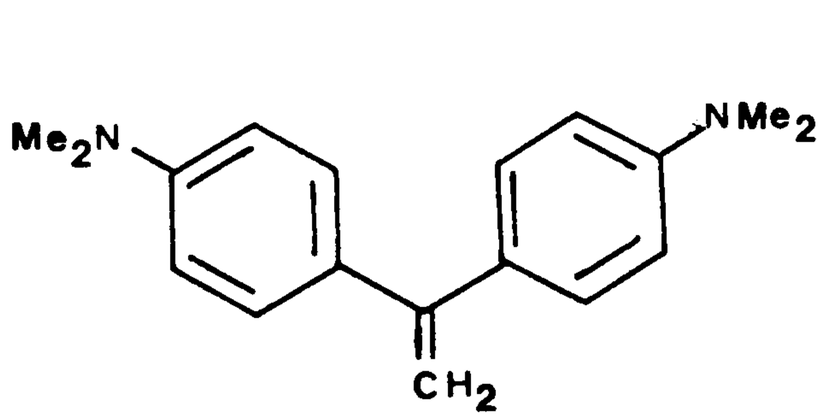

(149)

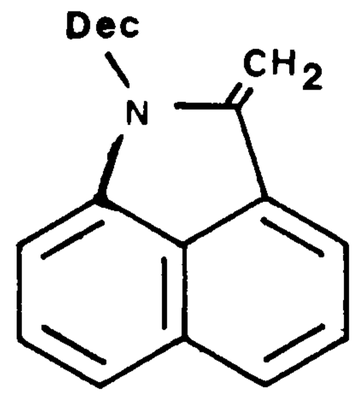

(150)

Non-azo dyes derived from these two systems have been reported in the literature and demonstrate the extremely bathochromic nature of

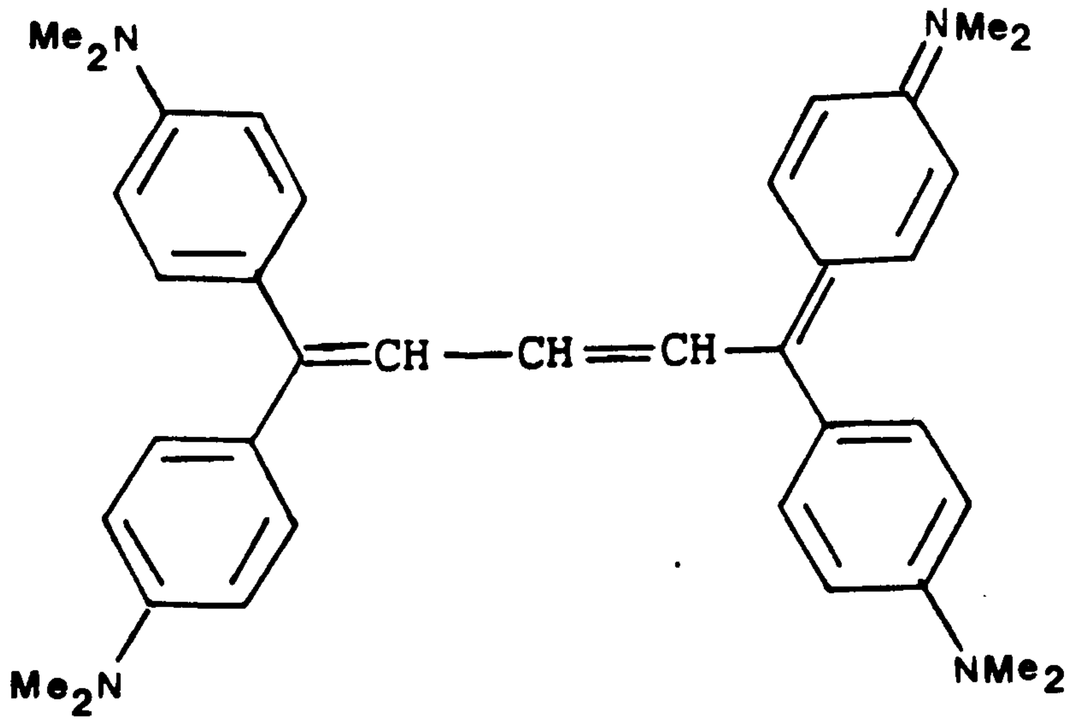

(151)

these electron donating residues[125]. For example the cyanine dye (151), derived from (149) absorbs at 810 and 663nm[126]. Evidently, for the Michler's ethylene, the effect of two 4-dimethylaminophenyl electron releasing species conjugated to the ethene residue results in a powerful nucleophilic species, and in effect a reactive active methylene group.

The highly bathochromic contribution of the benzindole residue (150) can be seen by considering dye (152), which is blue-green in colour[127]. The corresponding system (153) is only red in colour even

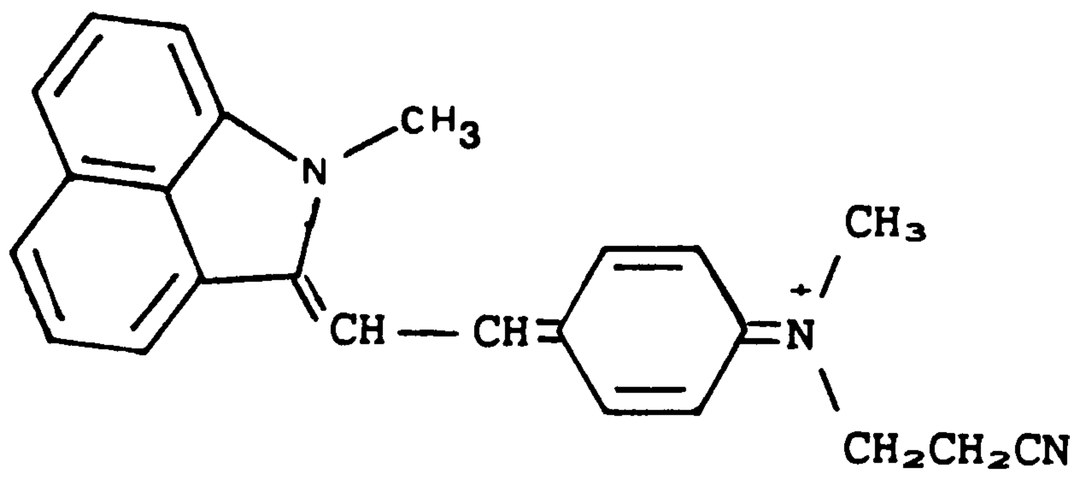

(152)

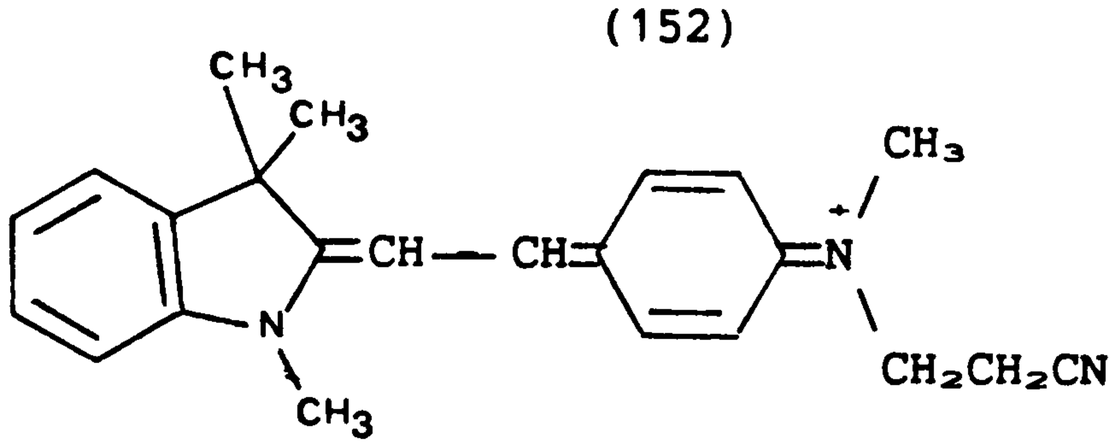

(153)

though it contains a donor -NMe group in a 5-membered ring and has the same conjugation path length between the nitrogen atoms. Clearly the 1.8-linkage of the naphthalene residue in the benzindole species contributes special bathochromic light absorption properties. These cannot be explained by conventional resonance theory arguments but are accounted for readily by the PPP-MO method.

2.1.3.1 Synthesis of Dyes and Intermediates

Michler's ethylene (149) was obtained as a pale green (white when pure) solid via the route shown in Scheme 23[128]. Thus Michler's ketone (154) could be made to react with methyl magnesium iodide in dry ether, but the reaction was slow, and it was necessary to exclude

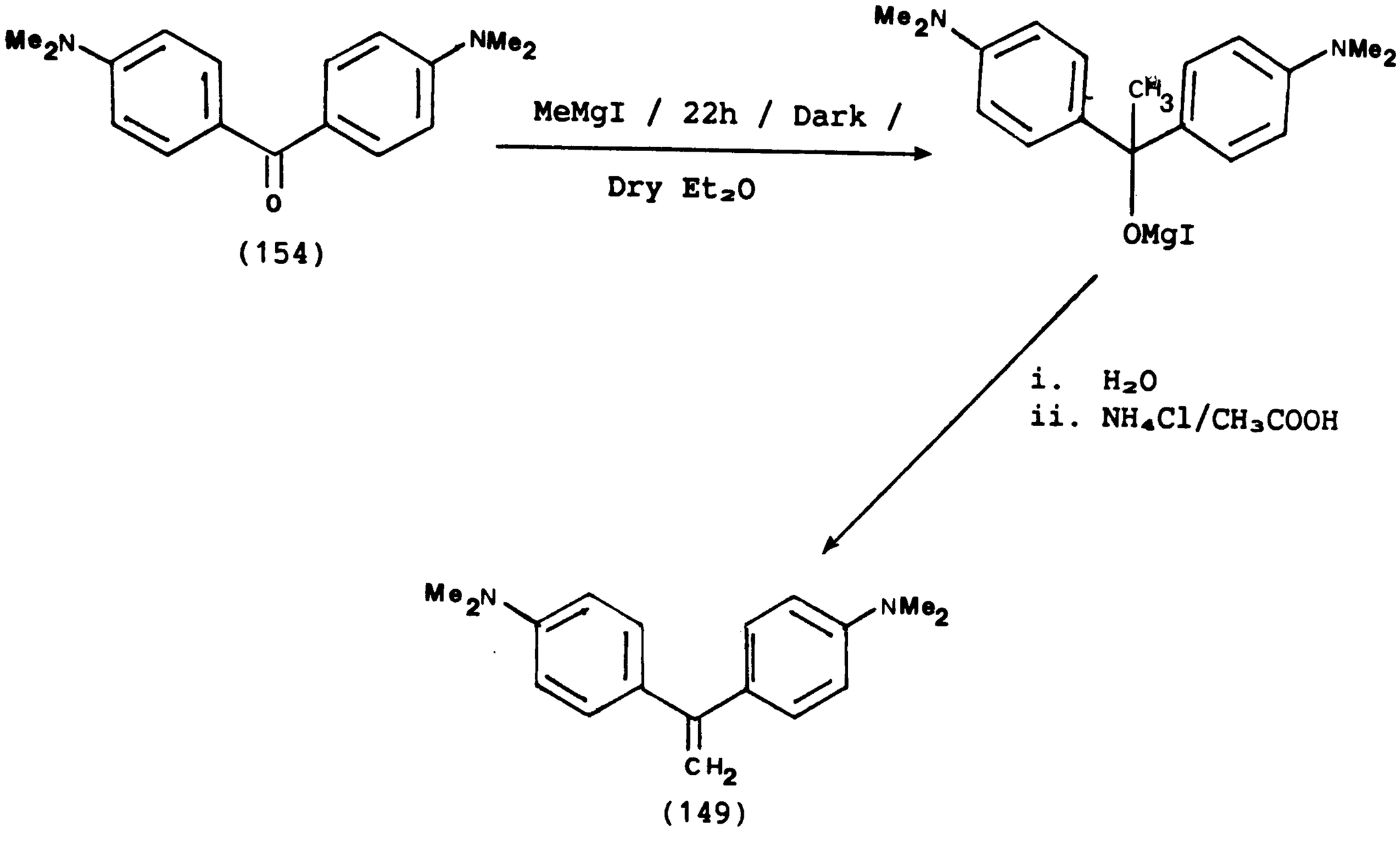

Scheme 23

light during the reaction. Work up with dilute acetic acid gave (144) in low yields (ca. 28%).

The synthesis of 1-decyl-2(1H)-methylene-benz[c,d]indole (150) posed several problems, and the chosen route to (150) is shown in Scheme 24[129-133]. It should be noted that the product was actually isolated as the iodide salt (158). Thus 1-naphthylisocyanate (155) was converted to benz[c,d]indol-2(1H)-one (156). For N-alkylation, n-decylbromide was used, as it was felt that the resultant n-decyl dyes would have good organic solvent solubilities. The N-alkylation was effected under phase transfer conditions with concentrated aqueous sodium hydroxide solution using 18-crown-6. Thus the 18-crown-6 transported the naked hydroxide anion into the organic phase, where deprotonation of (156) occurred. N-Alkylation by n-decyl bromide then occurred in the organic phase, giving (157). Grignard reaction with methyl magnesium iodide in dry ether followed by treatment with dilute hydrochloric acid gave crystals of 1-decyl-2(1H)-methyl-

benz[c,d]indolium iodide (158).

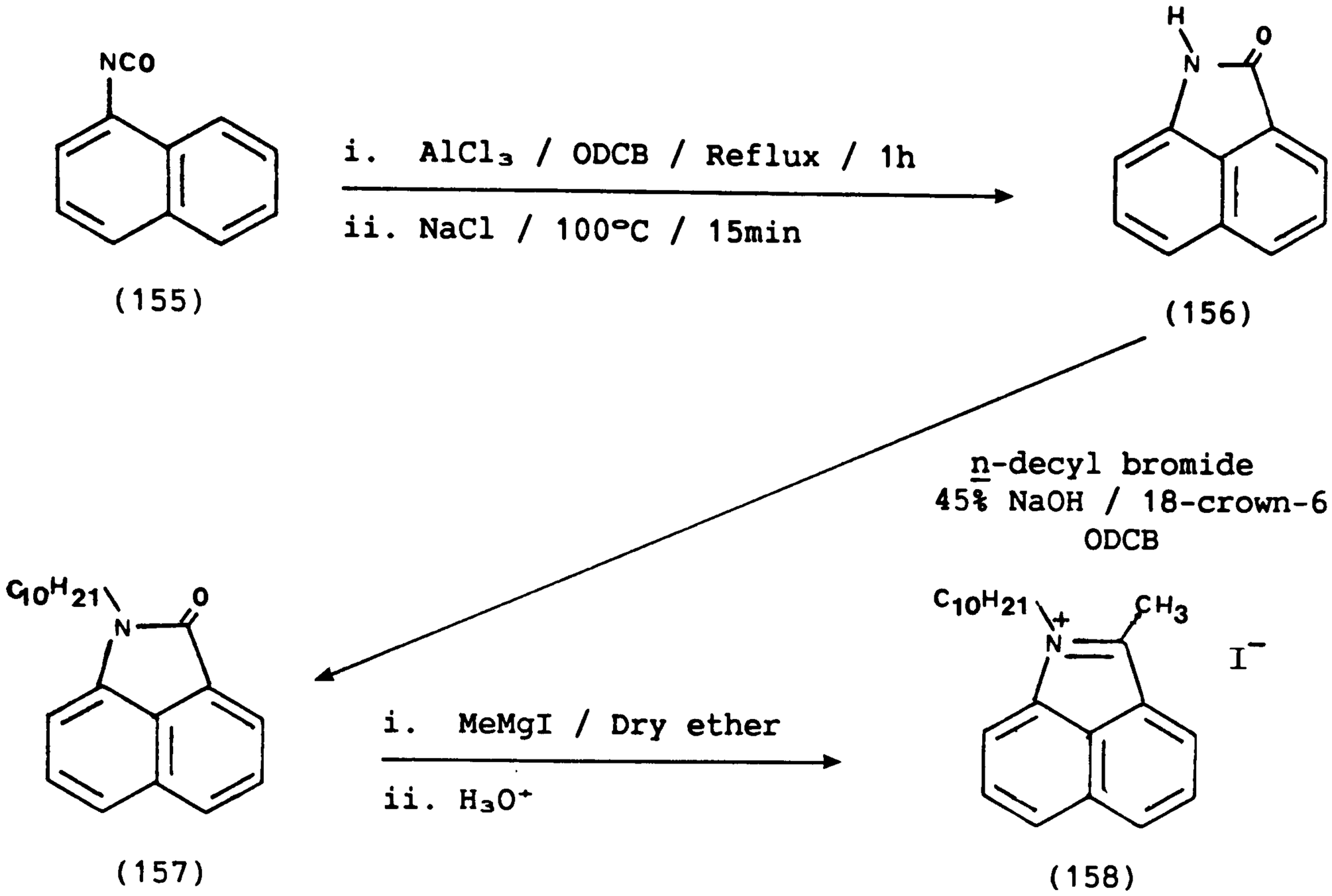

(155) (156) (157) (158)

Scheme 24

The structure of (158) was proved by mass spectrometry which clearly showed a molecular ion m/e at 308, equivalent to the salt minus the iodine atom. It is also of interest that the mass spectrum also showed an intense peak at m/e=168, presumably corresponding to the species (159).

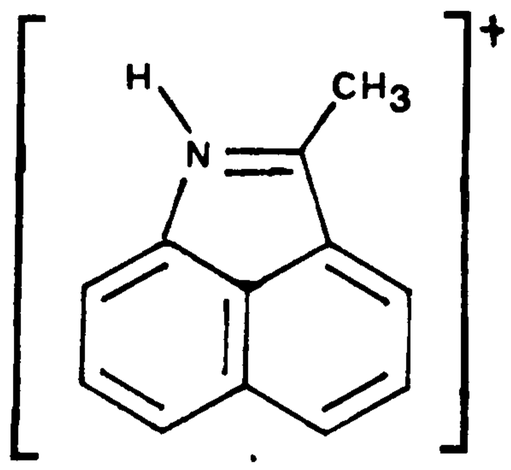

(159)

The severe alkylating conditions used to prepare (158) were essential, and attempts to ethylate the benzindole (156) using diethyl sulphate under typical conditions used for the N-alkylation of primary amides gave no reaction. It would therefore seem that deprotonation

of the amide NH in (156) is more difficult than for simple amides.

Diazo coupling of intermediates (149) and (158) proved surprisingly difficult to achieve. For example, when the Michler's ethylene (149) dissolved in ethanol with a sodium acetate buffer was coupled to diazotised 4-nitroaniline an intense blue product that absorbed at 612nm was observed. Initially this was thought to be the desired product but simple tests showed that acid alone would generate the same blue compound. Even a sodium acetate buffer gave the same result. This product, whose spectrum is shown in Fig. 9, is the

Fig. 9: <u>UV-visible spectrum of protonated Michler's ethylene in dichloromethane</u>

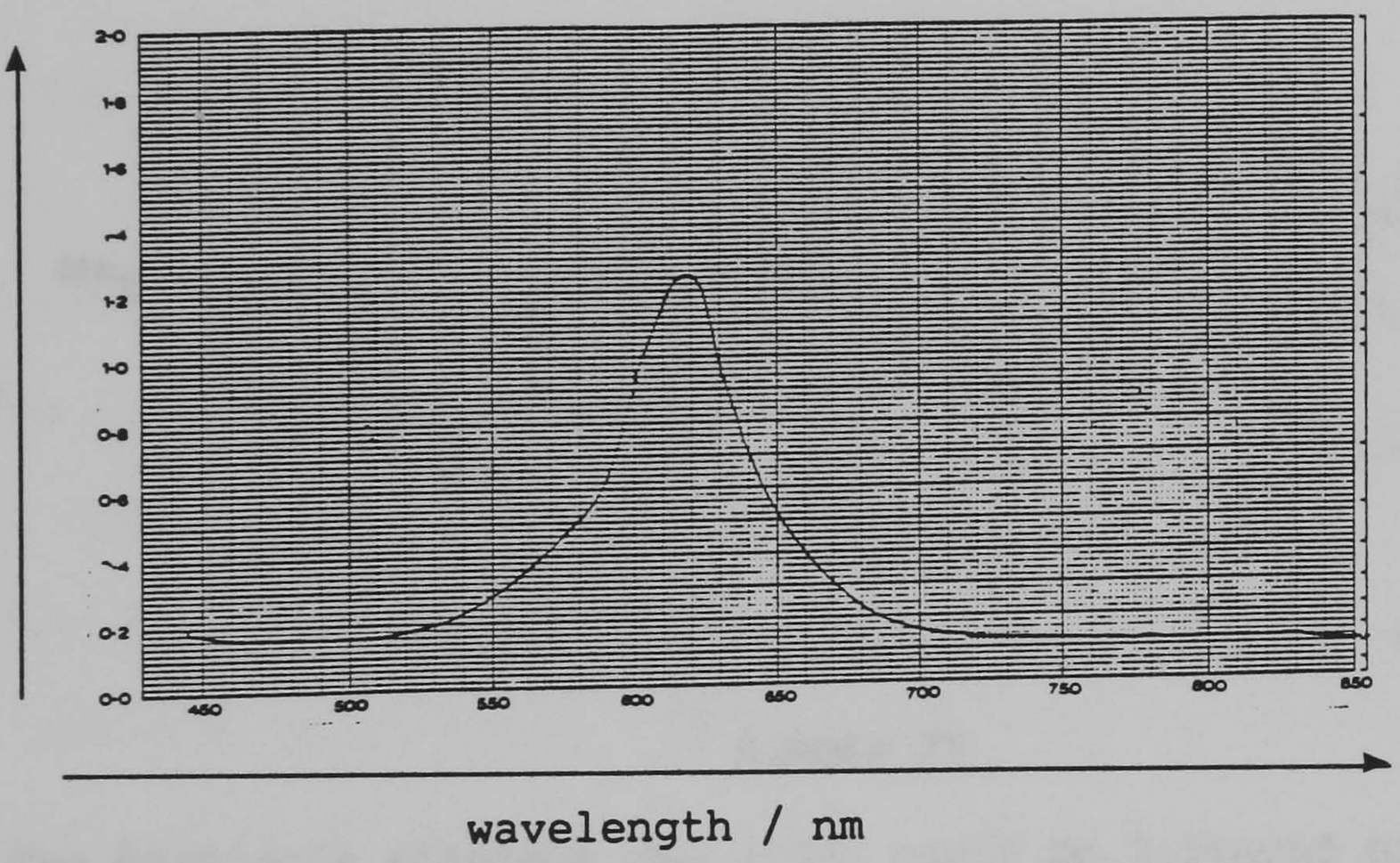

A - absorbance

methyl-substituted Michler's Hydrol Blue cation (160), formed by protonation of the ethene residue. Attempts to couple the benzindole

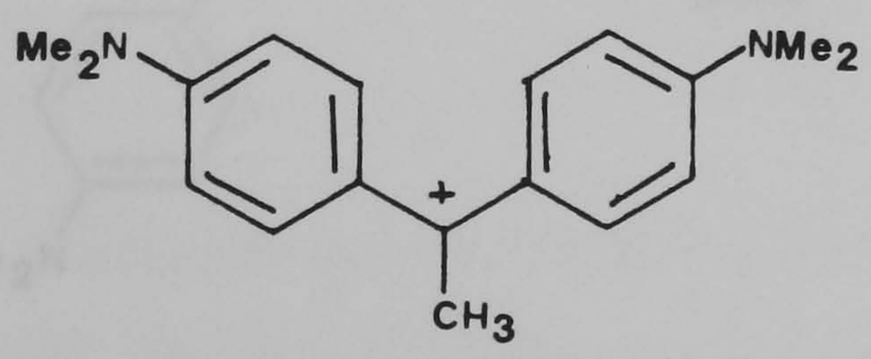

(160)

derivative (158) with 4-nitrobenzenediazonium chloride were also unsuccessful and gave complex mixtures of products.

It was eventually found that the desired coupling reactions could best be effected with the diazonium tetrafluoroborate salt of 4-nitroaniline (161) by dissolving it in ethanol, and adding it to an ethanolic solution of the requisite active methylene compound (Scheme 25).

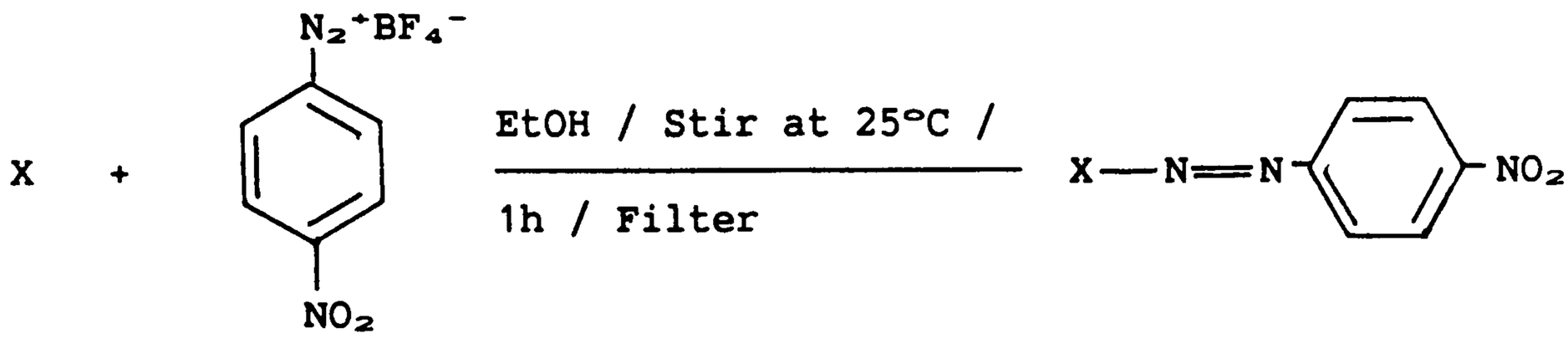

(161)

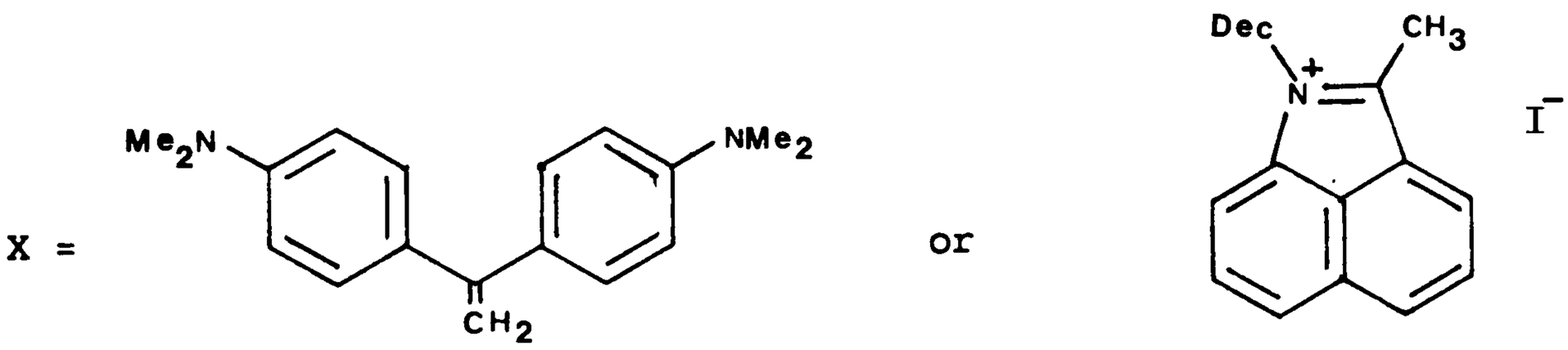

(149) (150)

Scheme 25

The Michler's ethylene dye (162) could be filtered off and recrystallised from ethanol. The structure was confirmed by mass

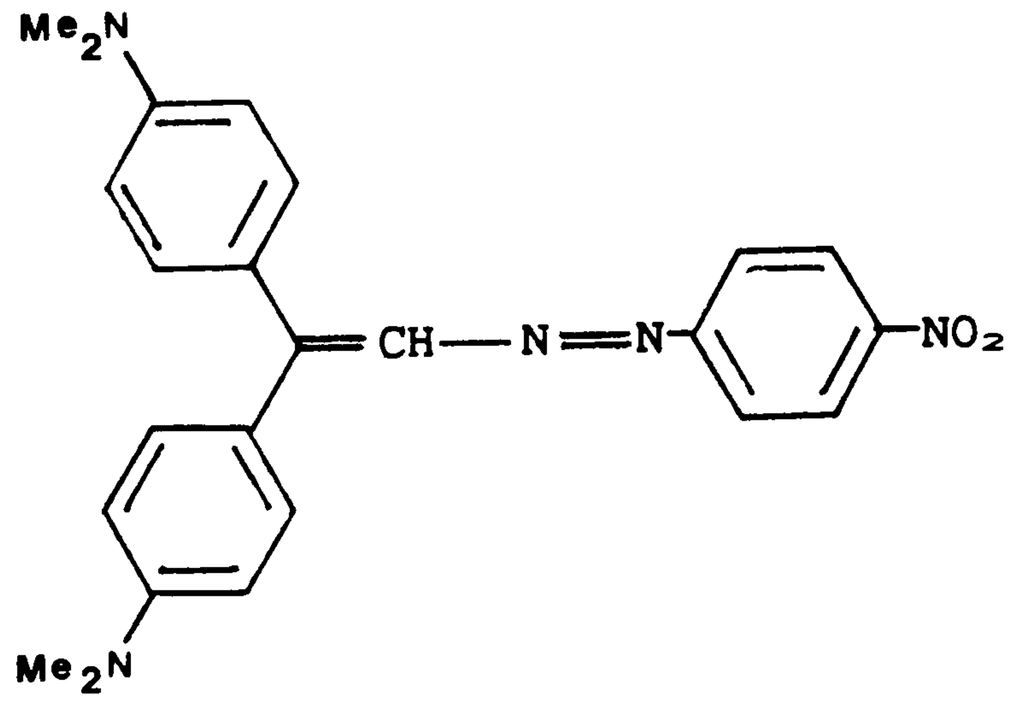

(162)

spectrometry. The benzindole dye (163) was purified by preparative scale t.l.c. and the structure also confirmed by mass spectrometry.

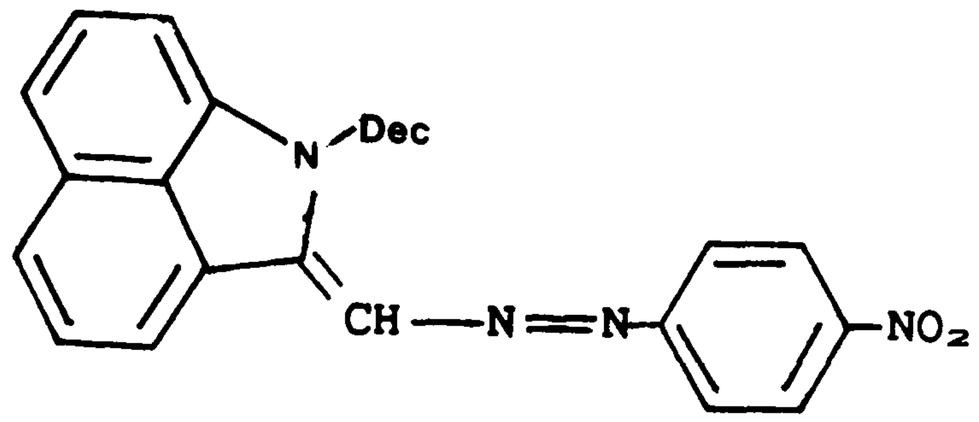

(163)

Unfortunately it was not possible to synthesise any analogues of these dyes using more powerful diazonium salts, since the relevant anhydrous tetrafluoroborate salts could not be isolated.

2.1.3.2 Light Absorption Properties

The absorption spectra of analytically pure samples of dyes (162) and (163) were measured in dichloromethane and toluene. For comparison with molecular orbital calculations the values in toluene were used. Molar absorption coefficients were calculated for dichloromethane solutions. The spectroscopic results are summarised in Table 23 and the PPP-MO calculated values for the dyes are summarised in Table 24.

Table 23: Spectroscopic data for 4-nitrophenylazo dyes (162) and (163)

Dye	λ_{max}/nm (CH_2Cl_2)	(Toluene)	ε_{max}/$lmol^{-1}cm^{-1}$ (CH_2Cl_2)	$\Delta\lambda_{max}$/nm (CH_2Cl_2-Tol)
(162)	681	554	41,500	—
	583		54,500	
(163)	584	575	13,500	-11

The solvatochromic effects exhibited by (162) are particularly interesting as this dye shows characteristics of allopolar isomerism[3]. That is, in dichloromethane the dye exists in two distinct isomeric

forms, namely (162a) and (162b). In (162a) one of the N,N-dimethylaminophenyl rings is twisted out of the plane of the nitrophenylazo residue. This "meropolar" isomer is responsible for

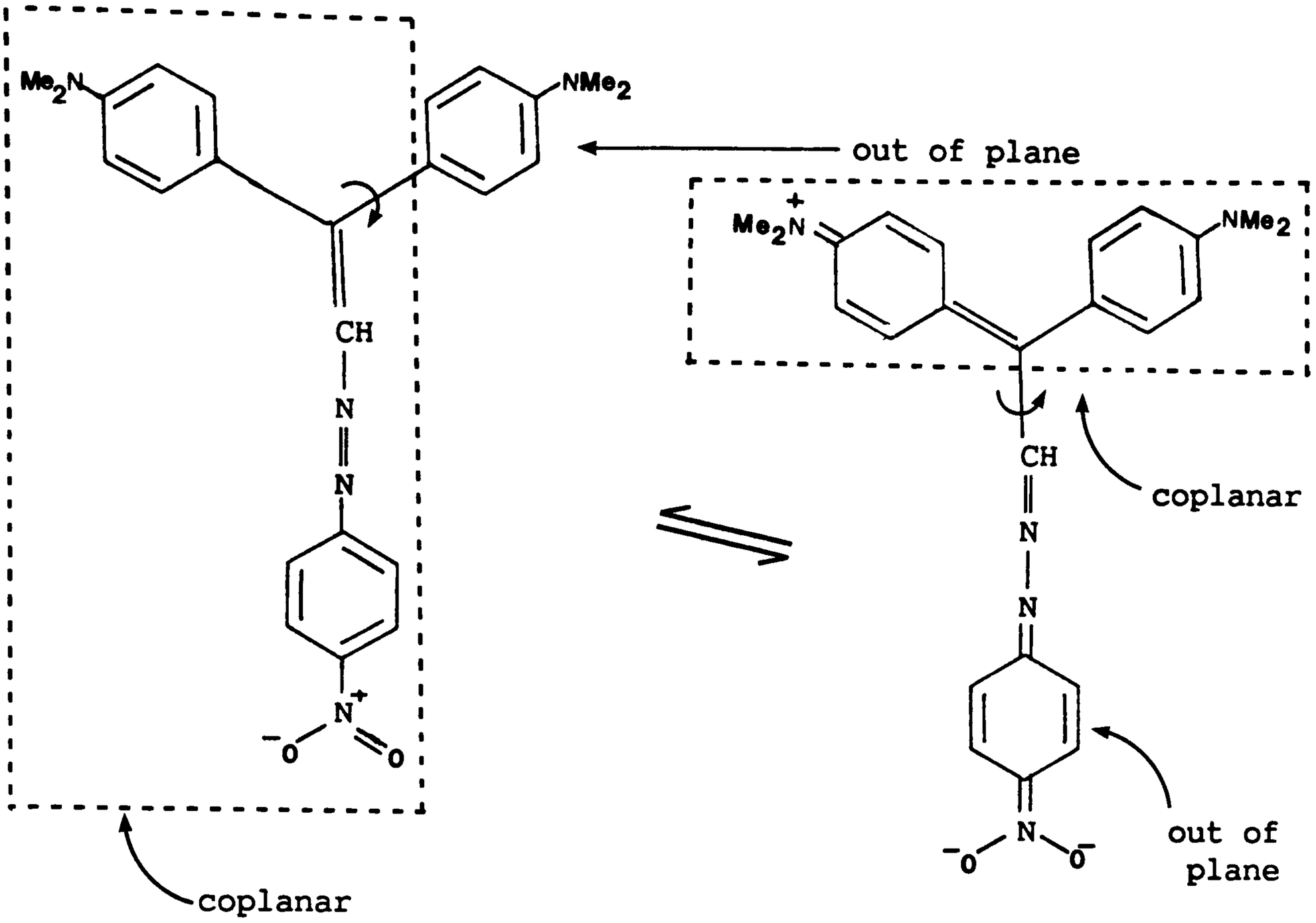

(162a)

(162b)

the peak at 583nm. The second isomer, (162b), termed the "holopolar" form, contains the negatively charged 4-nitrophenylazo residue in a plane perpendicular to the positively charged cyanine-type chromogen containing both N,N-dimethylaminophenyl residues. The cyanine-type residue is analogous to Michler's Hydrol Blue and is thus responsible for the peak at 681nm. It is known that the more polar the solvent the more the holopolar form is stabilised[134]. Therefore in the relatively non-polar solvent toluene the holopolar form is not stabilised and has a very low concentration. Thus the single absorption peak observed at 554nm is due to the meropolar form only. Considering the meropolar peak only, the dye exhibits positive solvatochromism. In acetone the

high polarity results in increase in the concentration of the holopolar form (162b), the two peaks occurring at 568 and 677nm.

The relatively high extinction coefficients for (162) show that, even though planar geometry is not present within the isomers, the dye absorbs strongly.

As with dye (162), the benzindole dye (163) also exhibits positive solvatochromism but, in contrast to (162), the extinction coefficient of this dye is relatively low for an azo dye (usually about 30,000$l mol^{-1} cm^{-1}$), and this is presumably an intrinsic feature of the benzindole electron donor residue.

The PPP-MO calculations for (162) presented problems. The VSIP and electron affinity values used were those for a standard N,N-dimethylamino group nitrogen atom. However the calculated λ_{max} value using such values fell short of the observed value by some 45nm. Evidently the unusual spectroscopic properties of this particular dye cannot be handled satisfactorily by the PPP method if a simple planar geometry is assumed.

Table 24: PPP-MO calculated λ_{max} values for dyes (162) and (163)

Dye	λ_{max}/nm (Calc)	λ_{max}/nm (Toluene)	$\Delta\lambda_{max}$/nm (Tol-Calc)	Oscillator strength (f)(Calc)
(162)	509	554	+45	1.23
(163)	573	575	+2	1.01

For dye (163) it was necessary to find new VSIP and electron affinity values for the ring benzindole nitrogen in order to calculate satisfactory λ_{max} values. Semi-empirical values of 17.75eV and 7.75eV for the VSIP and electron affinity respectively for the nitrogen atom gave a satisfactory result. The values reflect the enhanced electron releasing capacity of the nitrogen atom in a

5-membered ring compared with a normal N-alkyl nitrogen atom. The calculated oscillator strength for (163) is relatively low, consistent with the low ε_{max} value.

The ground state charge densities and π-electron density changes for the visible transition of dye (163) are shown in Fig. 10.

Fig. 10: (a) Ground state charge densities and (b) π-electron density changes for the visible transition of dye (163)

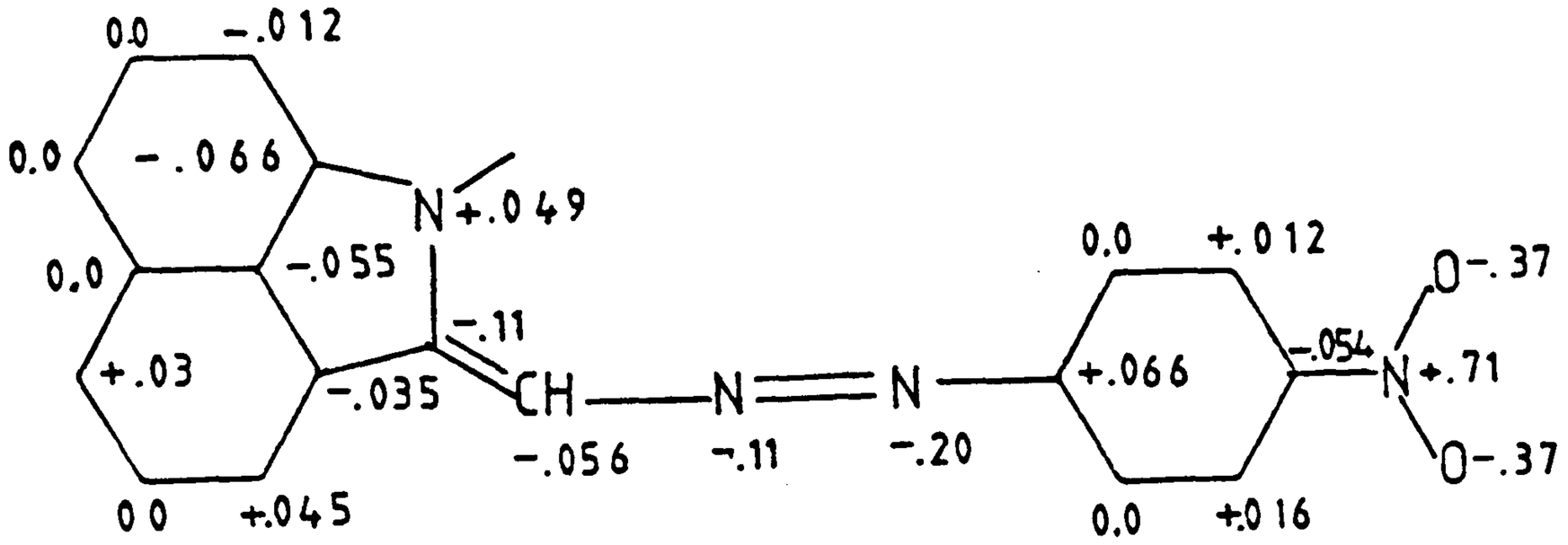

(a)

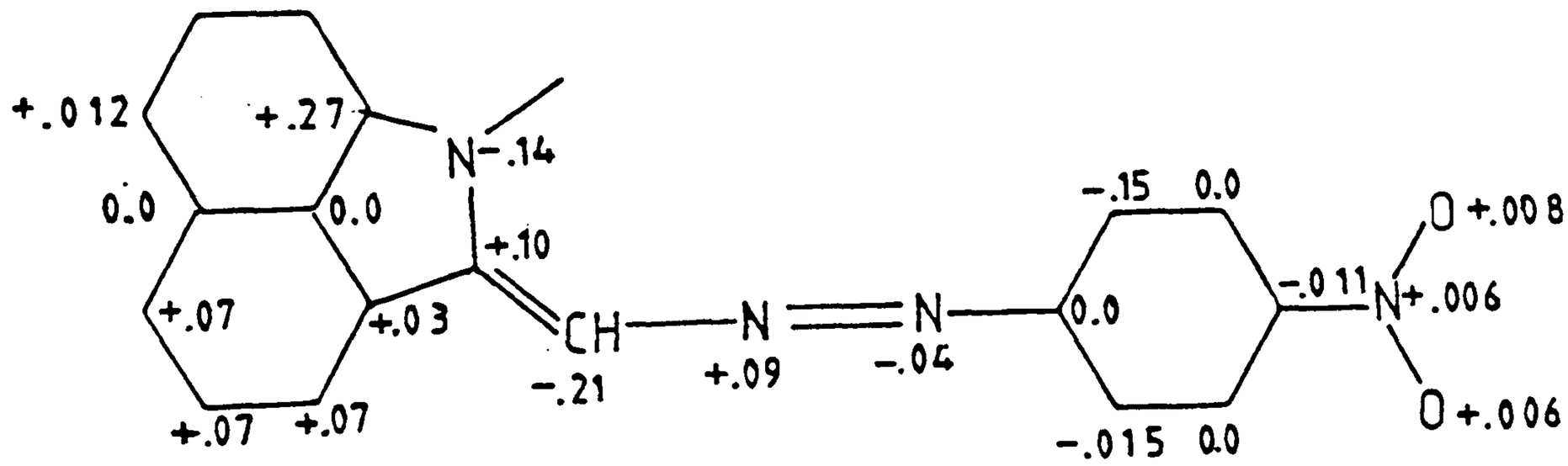

(b)

λ_{max} (calc) = 573nm

λ_{max} (toluene) = 575nm

From Fig. 10(a) it is evident that there is a deficiency of π-electrons at the benzindole nitrogen and an excess of electrons on the nitro group. Thus the molecule shows typical donor-acceptor characteristics, and has a highly polarised ground state.

On excitation, the π-electron system polarises further with a small migration of electron density from the benzindole ring to the azo and nitro groups. The fact that the overall migration is small suggests that charge separation in the ground state is maximal, i.e. the ground

state shows a high degree of bond uniformity [in effect, this implies that forms (163a) and (163b) make an equal contribution to the ground state]. In such cases the excited state will show only a small degree

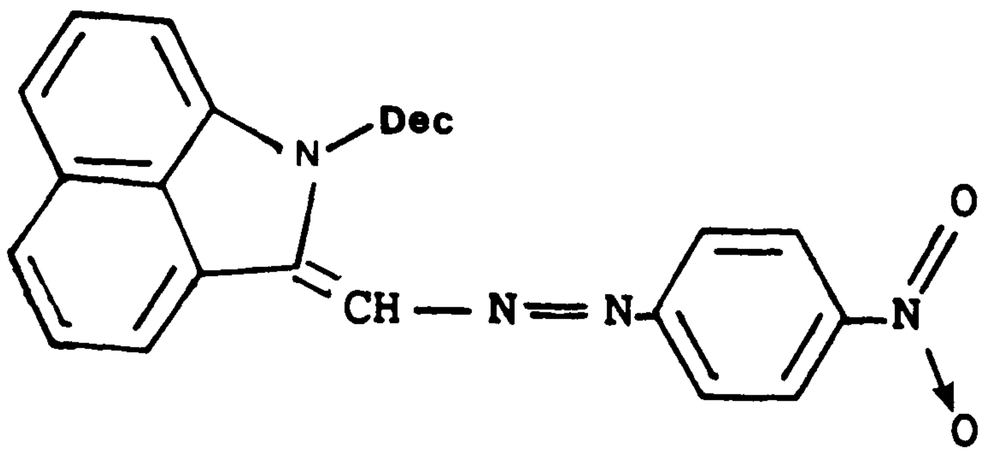

(163a)

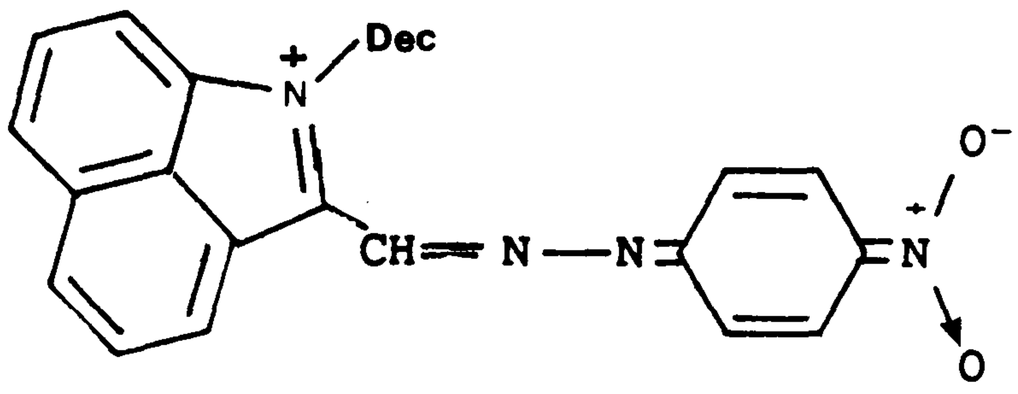

(163b)

of charge migration. Other consequences of this are that the chromophore shows maximum bathochromicity and is also weakly solvatochromic.

As previously discussed, protonation of 4-aminophenylazo dyes occurs almost exclusively at the ß-azo nitrogen to form the azonium ion tautomer, and the shift in λ_{max} is called the halochromism of the dye. The effects of acid on the spectra of (162) and (163) were examined, and the shifts in absorption maxima are shown in Table 25.

Table 25: Absorption spectra of azo dyes (162) and (163) in neutral and acidic solutions

Dye	λ_{max}/nm (acetone) Neutral	+HCl	$\Delta\lambda_{max}$/nm (acidic - neutral)
(162)	568	581	+13
	677	645(a)	-32
(163)	558	559	+1

(a) - point of inflexion

In all cases the protonated solutions were carefully neutralised with a weak sodium bicarbonate solution to ensure that the original spectra could be completely restored.

In the case of dye (162), which exhibits allopolar isomerism, the only true azo peak is that of the meropolar form at 568nm. On protonation this peak shifts to longer wavelength, a positive halochromic shift. However, this result is ambiguous since a positive halochromism could be produced in two different ways. In (164) the normal azonium species is formed, which would be bathochromic. In (165) protonation of one of the amino groups occurs. This in effect

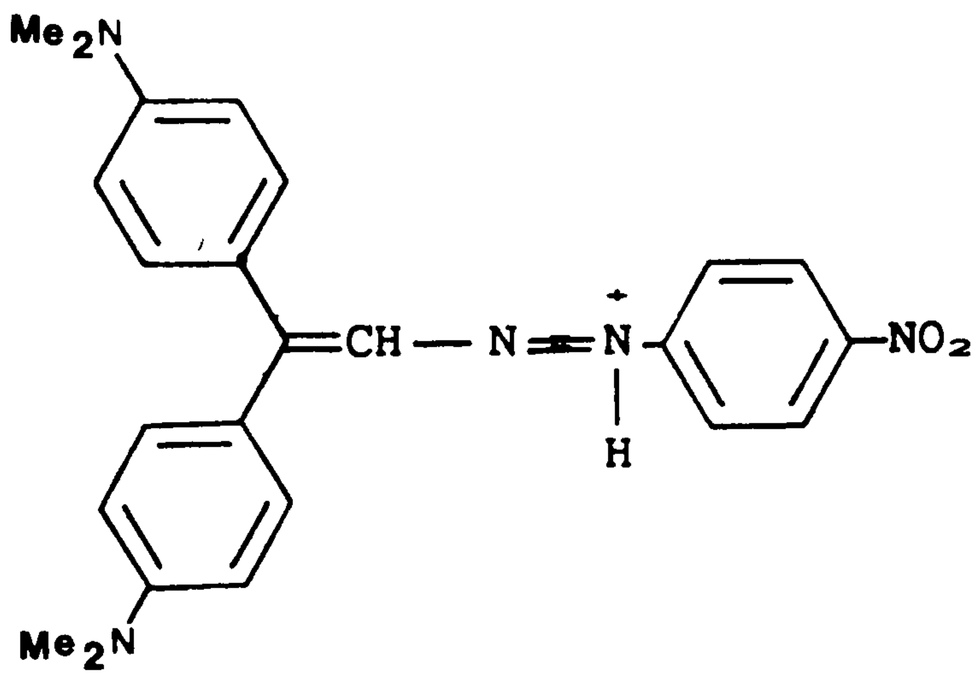

(164)

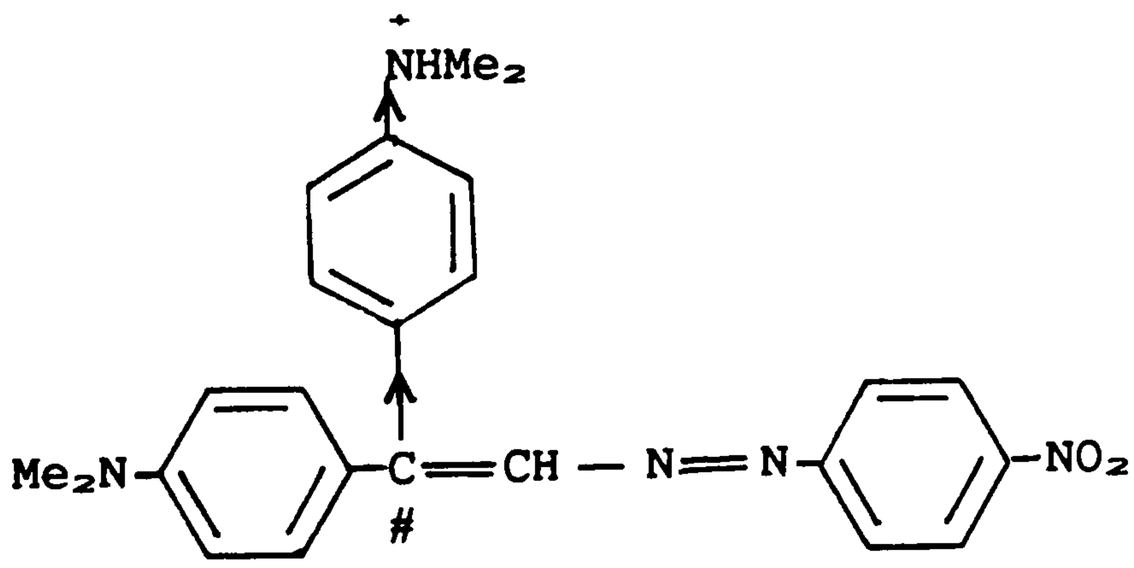

(165)

produces a -I aryl substituent at position # as shown. Since this is an 'unstarred' position within the concepts of PMO theory, then a bathochromic shift is also predicted. On the presently available

evidence it is not possible to decide between (164) and (165).

Dye (163) is interesting because, on protonation, the observed shift in λ_{max} is negligible. The only means of distinguishing between the two spectra is that the protonated form absorbs more intensely with a narrower band width. This is typical of azonium cations, and is conclusive evidence that protonation of the ß-azo nitrogen atom is occurring.

2.1.3.3 Stability Properties of Dyes (162) and (163)

The thermal and photochemical stability properties of these dyes were assessed using the procedures described in Section 2.1.2.4 and the results are summarised in Table 26.

Table 26: Thermal and photochemical stabilities of dyes (162) and (163)

Dye	Photo stability (% loss)	Thermal stability (% loss)
Standard (148)	8	5
(162)	58	Total Decomposition
(163)	76	69

Both dyes appeared to lack light stability with more than half of the dye being destroyed in each case.

Total decomposition of dye (162) occurred during the thermal stability test. Dye (163) also exhibited poor thermal stability.

Thus it can be concluded that, at least as far as azo dyes are concerned, the complex electron donor residues in (162) and (163) result in poor thermal and photochemical stability. Thus dyes of this type have little practical potential.

2.2 Methine and Azomethine Dyes Derived from N-Alkyl-3-cyano-6-hydroxy-4-methyl-2-pyridones

The N-alkyl-3-cyano-6-hydroxy-4-methyl-2-pyridones (166) are of commercial interest as components of textile dyes, and more recently

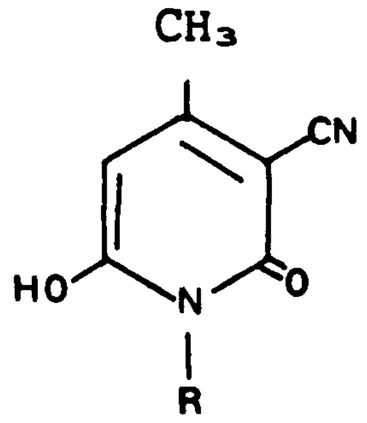

(R = H, alkyl)

(166)

in connection with dyes for high technology applications. For example, yellow dyes of type (167) have been patented for use in

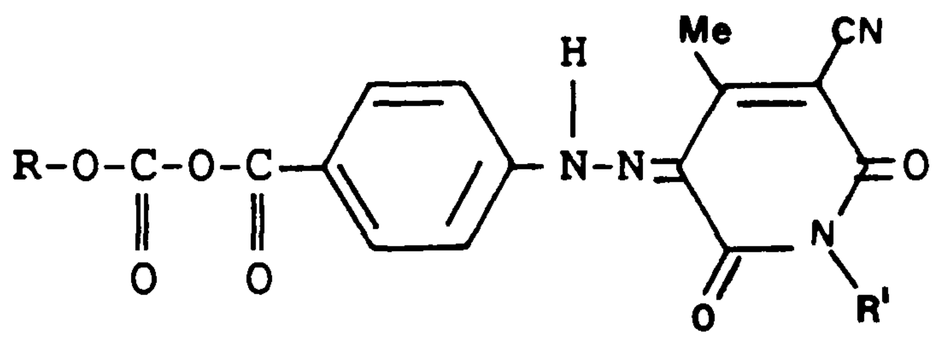

R,R' = alkyl

(167)

thermal transfer in the D2T2 process of electronic photography[135].

The pyridone system (166) behaves like an active methylene compound and will condense with aldehydes and nitroso compounds to give dyes of types (168) and (169). The pyridone residue then acts as a powerful

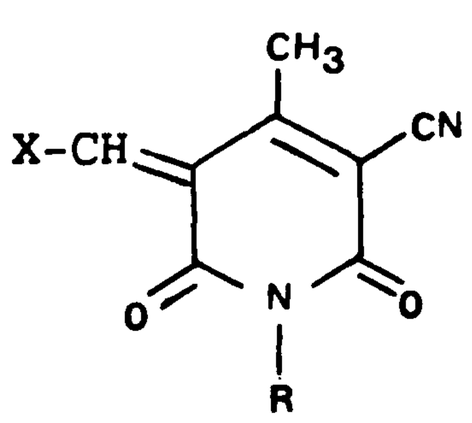

(168)

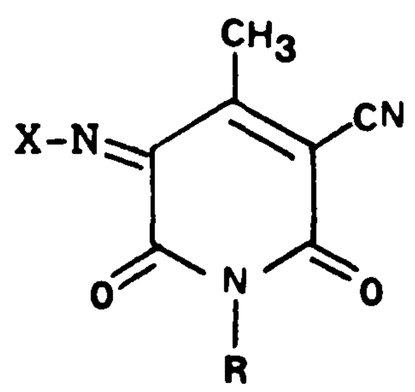

(169)

electron acceptor, as it possesses a cyano and two carbonyl groups. Bello has shown such dyes to be red to blue in colour[68].

A synthetic variant is to formylate or nitrosate the pyridone at the active 5-position to give (170) and (171) respectively. These

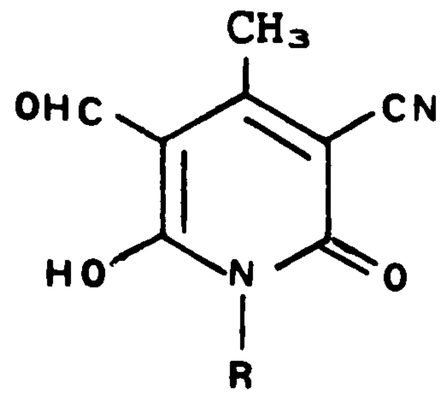

(170)

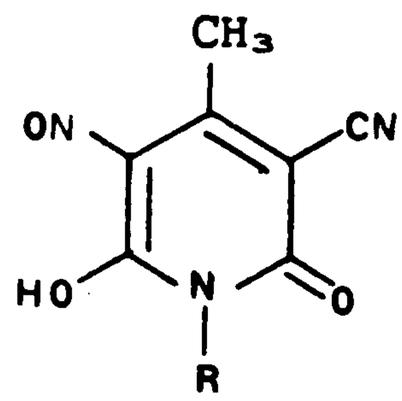

(171)

species can also be condensed with other active methylene compounds to give dyes of the general formula (172) and (173). Such dyes would

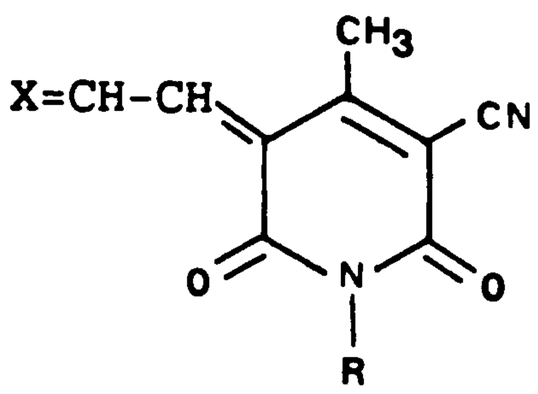

(172)

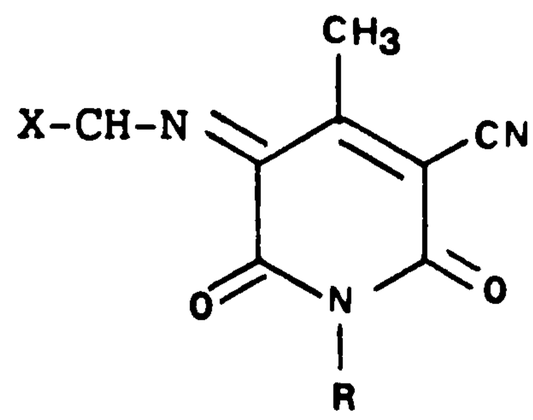

(173)

possess a longer conjugated bridge in comparison with types (168) and (169). This additional conjugation should have a significant bathochromic effect on λ_{max}, and such dyes were investigated for infrared absorption.

2.2.1 Synthesis of Dyes and Intermediates

The active methylenes (enamines) used in this work were Michler's ethylene (149) and 1-decyl-2(1H)-methyl-benz[c,d]indolium iodide (158) described in Section 2.1.3.1. The pyridone (166; R=H) was prepared as shown in Scheme 26. Thus ethyl cyanoacetate (174) was stirred for 12 hours with ammonia to form the amide (175). After addition of ethyl acetoacetate the mixture was heated in an autoclave for 6 hours to give the crude pyridone (166; R=H). Other pyridones with N-alkyl groups were prepared analogously.

Formylation of the pyridones could be readily effected by the

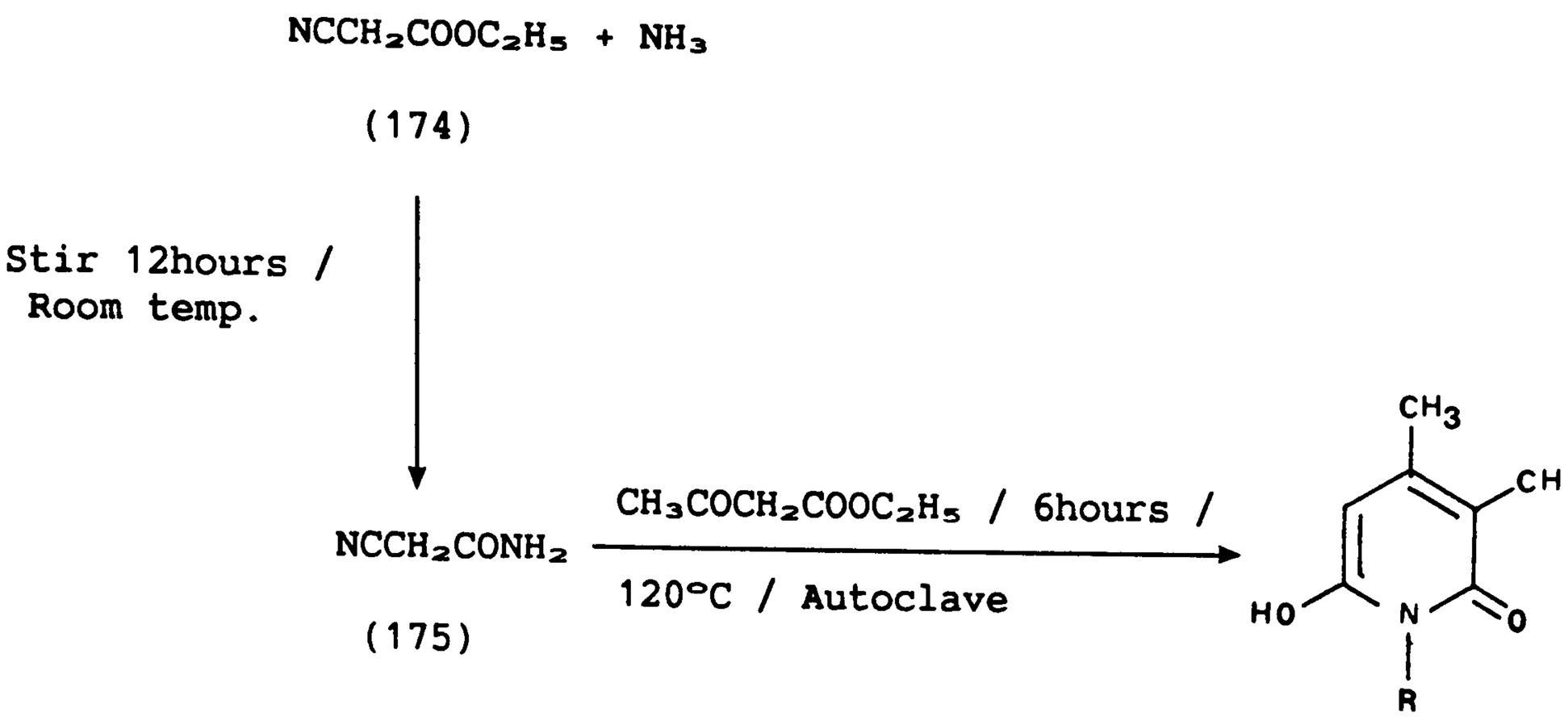

Scheme 26

Vilsmeier reaction ($POCl_3$/DMF), giving (176). Nitrosation of the pyridones was carried out with nitrous acid to give (177).

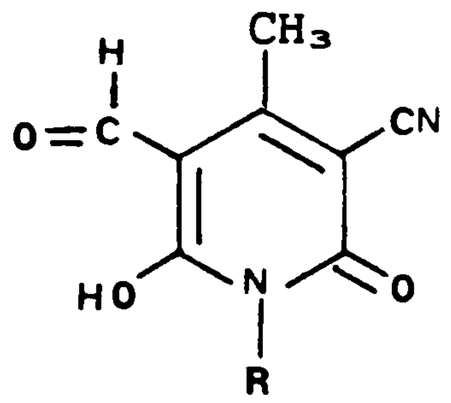

(176)

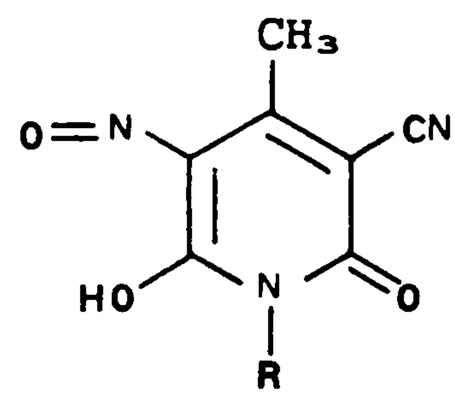

(177)

Condensation of the formylated pyridones with the active methylene compounds (149) and (158) was effected in refluxing ethanol. The resultant dyes (178) and (179) were recrystallised from ethanol or were column chromatographed over silica gel to give analytically pure products.

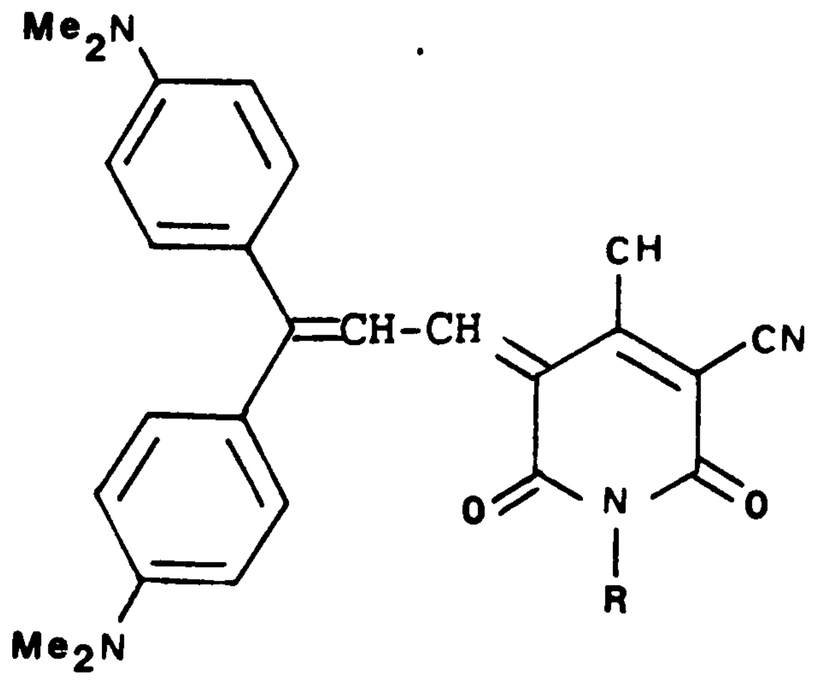

(178)

(179)

The azomethine analogues of (178) and (179) were formed more readily and, for example, reaction of the nitroso pyridone (177; R=H) and the active methylene compound could be effected at room temperature in ethanol. After filtering off the precipitated product, analytically pure samples of (180) and (181) could be obtained by recrystallisation from ethanol or by chromatography over silica gel.

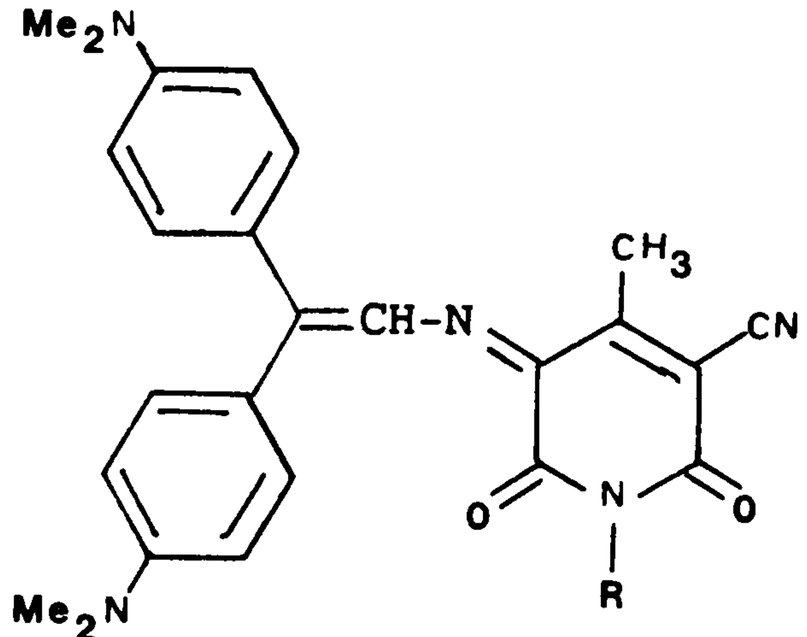

(180)

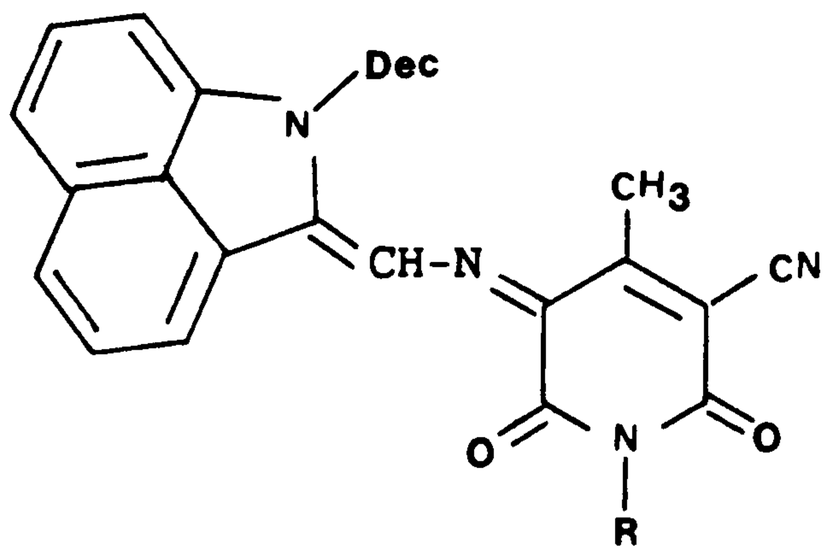

(181)

2.2.2 Light Absorption Properties of Dyes (178) - (181)

The absorption spectra of dyes (178) - (181) were measured in dichloromethane and toluene, and molar absorption coefficients were determined in dichloromethane only. The results are summarised in

Table 27. The structures of these dyes were confirmed by either microanalysis or mass spectrometry.

Table 27: Spectroscopic data for dyes (178a) - (181c)

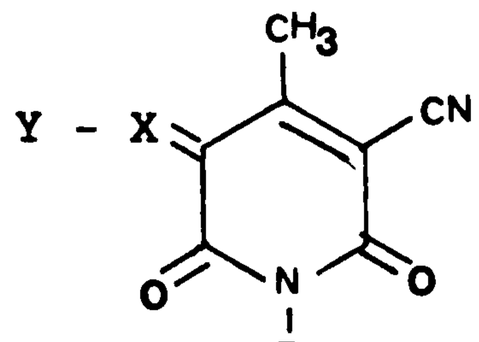

Dye	Y	X	R	λ_{max}/nm CH_2Cl_2	Tol.	ε_{max} (a) (x10^{-4})	$\Delta\lambda_{max}$ (b) /nm
(178a)	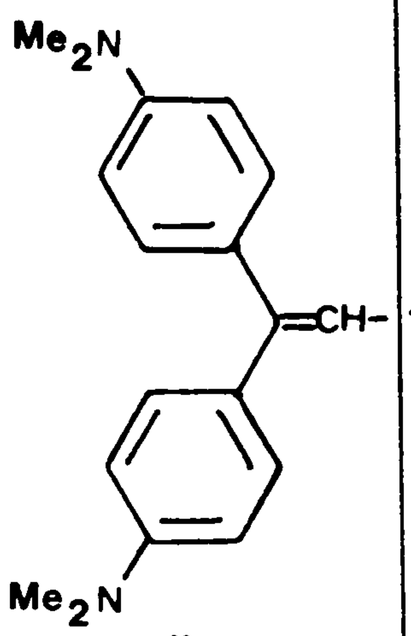	-CH-	-H	635	607	10.2	+28
(180a)	"	-N-	-H	713	680	9.35	+33
(178b)	"	-CH-	-Et	631	603	8.50	+28
(180b)	"	-N-	-Et	712	678	8.05	+34
(178c)	"	-CH-	$(CH_2)_2NMe_2$	635	607	4.52	+28
(180c)	"	-N-	$(CH_2)_2NMe_2$	718	704	3.95	+14
(179a)	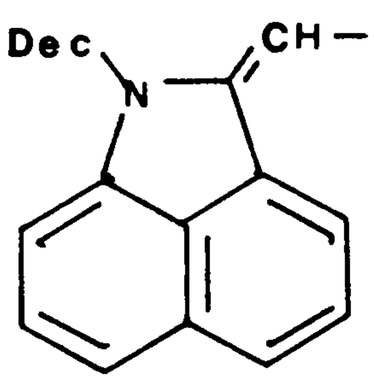	-CH-	-H	639 590	659 611	9.56 7.20	-20 -21
(181a)	"	-N-	-H	698 646	701 649	6.50 5.54	-3 -3
(179b)	"	-CH-	-Et	655 606	658 609	9.05 7.05	-3 -3
(181b)	"	-N-	-Et	694 645	694 646	7.10 6.25	0 -1

Table 27: continued

Dye	Y	X	R	λ_{max}/nm CH_2Cl_2	Tol.	ε_{max} (a) (x10^{-4})	$\Delta\lambda_{max}$ (b) /nm
(179c)	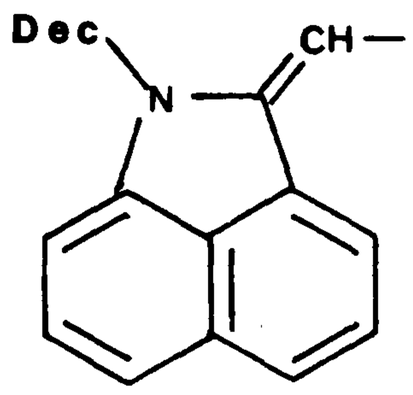	-CH-	$-(CH_2)_2NMe_2$	650	654	3.81 (c)	-4
(181c)	"	-N-	$-(CH_2)_2NMe_2$	689	704	2.55 (c)	-15

(a) - units = $1mol^{-1}cm^{-1}$
(b) - $\Delta\lambda_{max} = \lambda_{max}(CH_2Cl_2) - \lambda_{max}(toluene)$
(c) - These dyes exhibited only one peak. The second, more hypsochromic peak was reduced to a shoulder

From Table 27 it can be seen that dyes (180a), (180b) and (180c) show near-infrared absorption in dichloromethane, but the solutions were intense green because of the broadness of the absorption bands. Clearly the Michler's ethylene residue is a more powerful electron donor than the benzindole residue, and the more bathochromic dyes are those derived from the nitroso pyridones. The latter observation can be readily explained by the PMO theory, since in the nitroso derived dyes the carbon bridging atom at an unstarred position has been replaced by a more electronegative nitrogen atom.

These experimental observations are substantiated by more quantitative PPP-MO calculations, and results for representative dyes are summarised in Table 28.

The pyridone dyes (179) and (181) derived from the benzindole active methylene (158) exhibit negative solvatochromism, indicating that the ground state of the dye chromophore is more polarised than the excited state. Therefore, with dyes (181a) and (181c) λ_{max} values beyond 700nm are observed only in toluene and not in the more polar dichloromethane. This phenomenon is often indicative of highly

Table 28: Comparison of PPP-MO calculated and representative λ_{max} values of representative dyes of type (178) - (181)

Dye	λ_{max}/nm (Calc)	λ_{max}/nm (Toluene)	$\Delta\lambda_{max}$/nm (Tol - Calc)	Oscillator stength (f) (Calc)
(178a)	589	607	+18	1.51
(180a)	664	680	+17	1.53
(179a)	643	659 611	—	1.67
(181a)	705	701 649	—	1.68

bathochromic systems. The dyes derived from Michler's ethylene (149) exhibit positive solvatochromism and, for these dyes therefore the ground state is less polar than the excited state.

The dyes in Table 27 show that although more bathochromic dyes are obtained from aza analogues, such dyes show a general reduction in intensity. Even so, the azomethine dyes still have high extinction coefficients and so give bright blues or greens in solution. N-Alkylation of the pyridone residue also appears to reduce the intensity of the dyes and, with the exception of dye (181a), the longer the chain the lower the extinction coefficient. The introduction of such alkyl groups has little effect on the λ_{max} value however. This indicates that the nitrogen atom of the pyridone ring is only indirectly involved in the electronic excitation process.

The "double peaks" observed in the pyridone dyes (179a), (181a) (179b) and (181b) are not accounted for by the PPP-MO calculations (see Table 28). However these calculations assume planar geometry, whereas the presence of the n-decyl group within the ring may prevent planarity. The 'double peaks' may therefore be the result of a twisting of the dye structure. It should be noted that with dyes (179c) and (181c) the reduction of the second peak to a shoulder was

accompanied by a marked increase in the relative intensity of the longer wavelength peak.

For the PPP-MO calculations in Table 28 all the carbon atoms in the dye molecule (with the exception of the cyano carbon) were given a resonance integral, ß, of -2.4eV, which assumes maximum overlap of the p-orbitals, i.e. a planar structure. The nitrogen atom of the pyridone ring was given a VSIP of 22.5eV and an electron affinity of 10.8eV (these values being those for a nitrogen of a primary amine attached directly to a quinone 2,3-double bond). The standard cyano values gave more satisfactory results than other modified values that have been reported[136]. For the Michler's ethylene-derived dyes standard molecular parameters were available. For the benzindole system the previously ascribed values of VSIP = 17.75eV and electron affinity = 7.75eV were used for the ring nitrogen (see Section 2.1.3.2).

The calculated λ_{max} values for dyes (178a) and (180a) are in reasonable agreement with the observed values in toluene. Thus the suitability of the ring parameters was demonstrated. Agreement between theory and experiment was also satisfactory with the benzindole dyes (179a) and (181a), confirming the adequacy of the previously derived VSIP and electron affinity values for the benzindole.

To examine the relative roles of the various atoms in representative pyridone dye systems in the light absorption process, PPP-calculated ground state charge distributions and π-electron density changes for the visible absorption bands were calculated. Relevant values for dyes (178a) and (179a) are summarised in Figs. 11 and 12. Figs. 11a and 12a show the typical donor-acceptor characteristics of the pyridone dyes. Thus, in the ground state the donor nitrogen atoms carry a net positive charge and the pyridone

Fig. 11: (a) Ground state charge densities and (b) π-electron density changes for the visible transition of dye (178a)

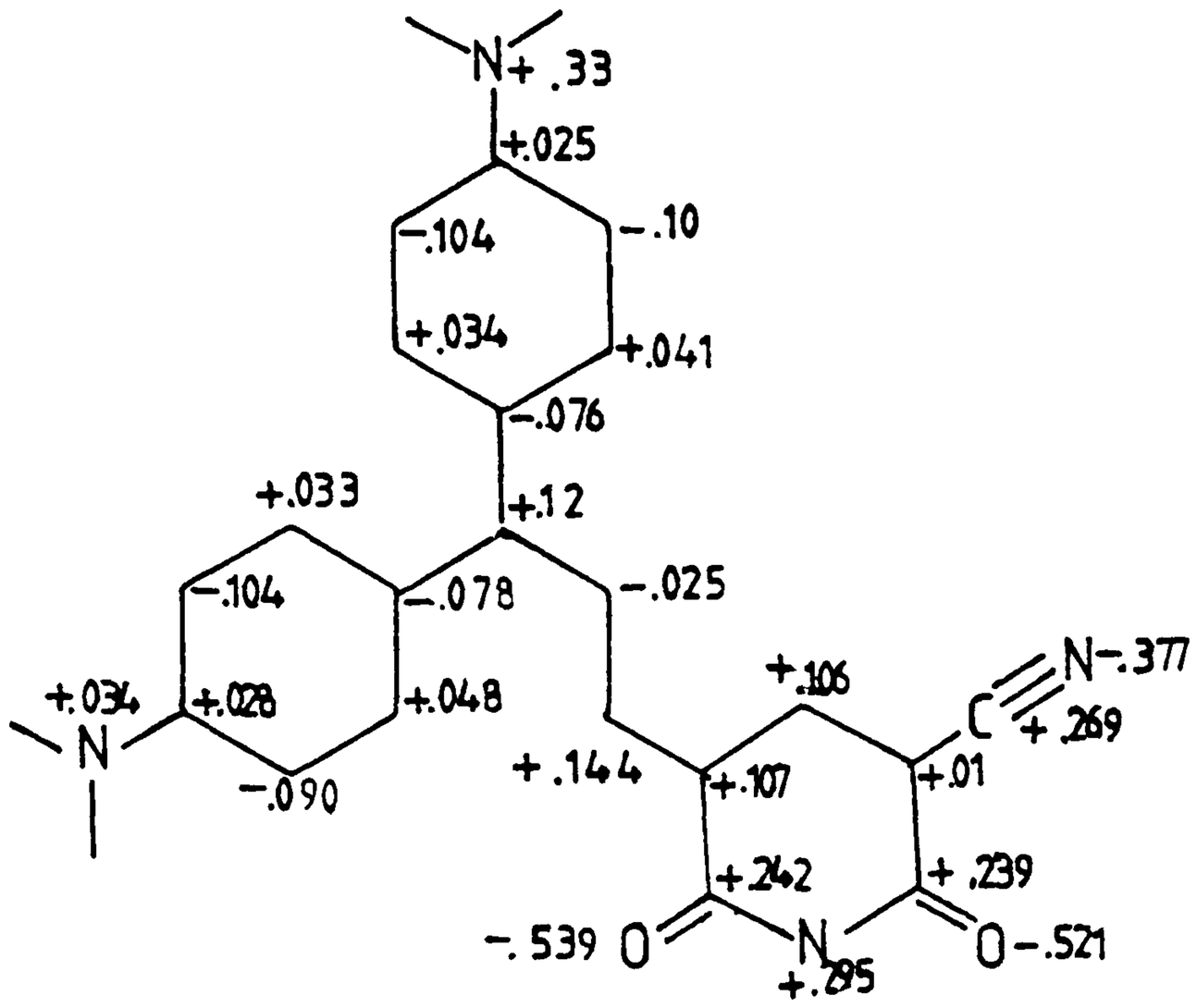

(a)

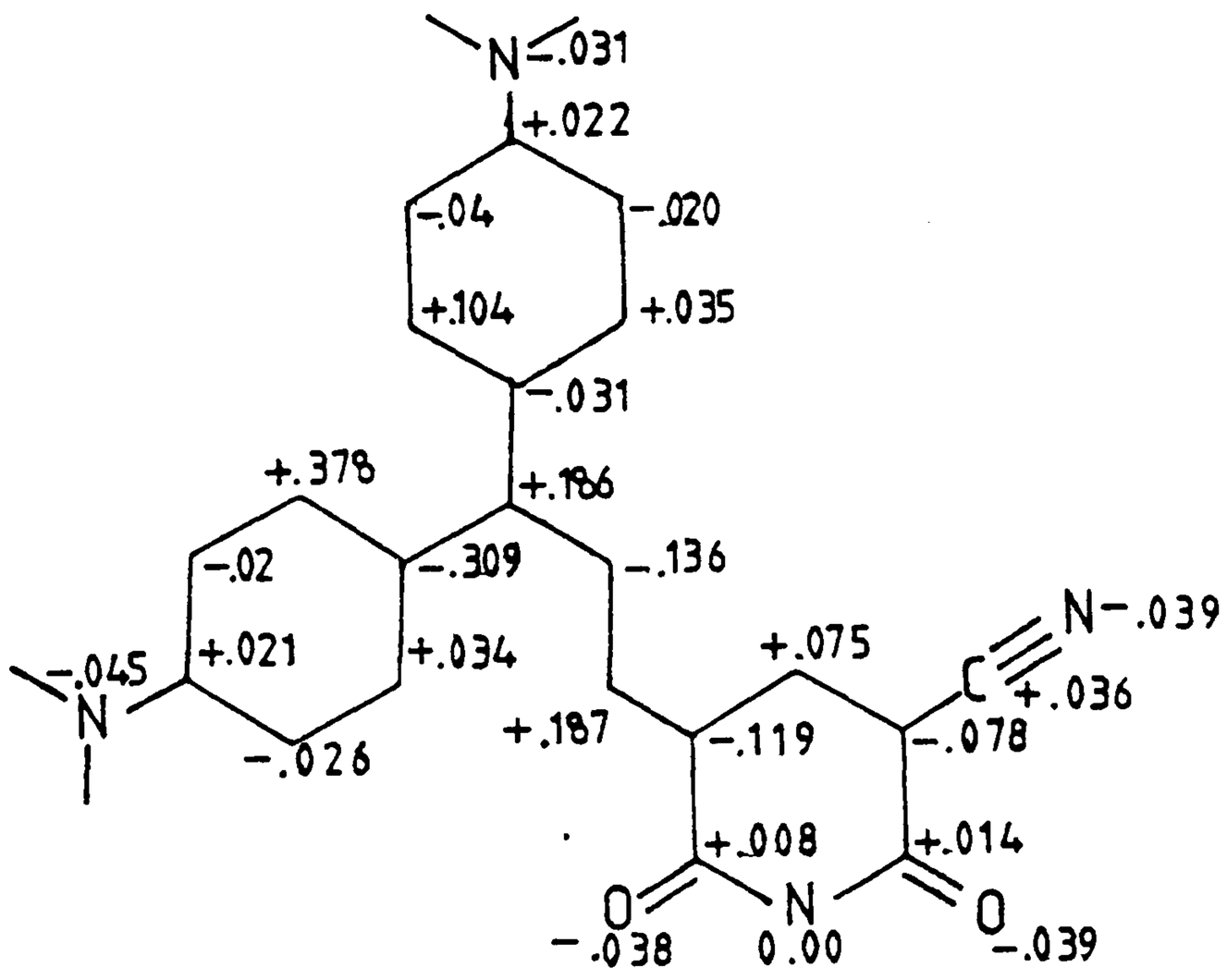

(b)

λ_{max} (calc) = 589nm

λ_{max} (toluene) = 607nm

Fig. 12: (a) Ground state charge densities and (b) π-electron density changes for the visible transition of dye (179a)

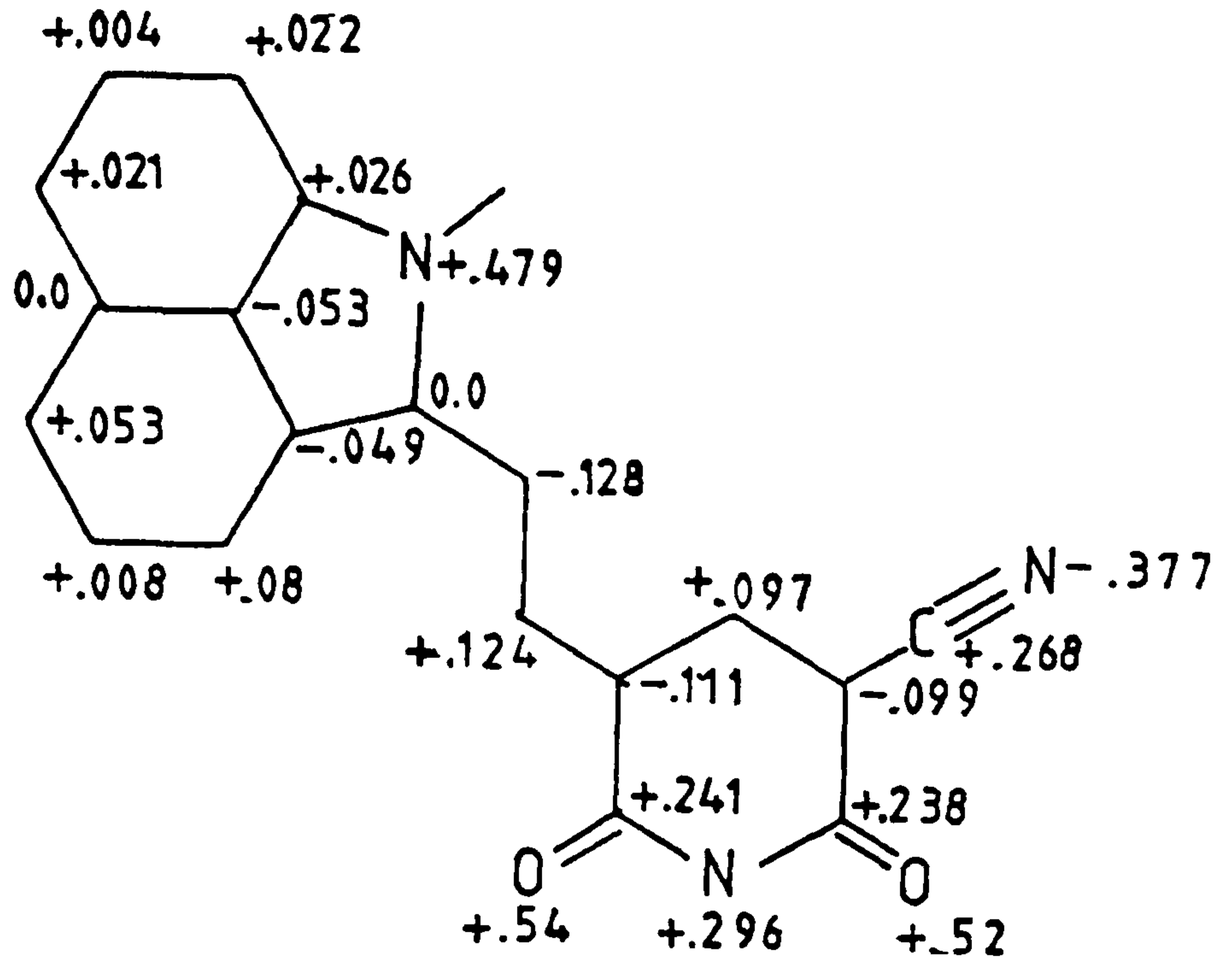

(a)

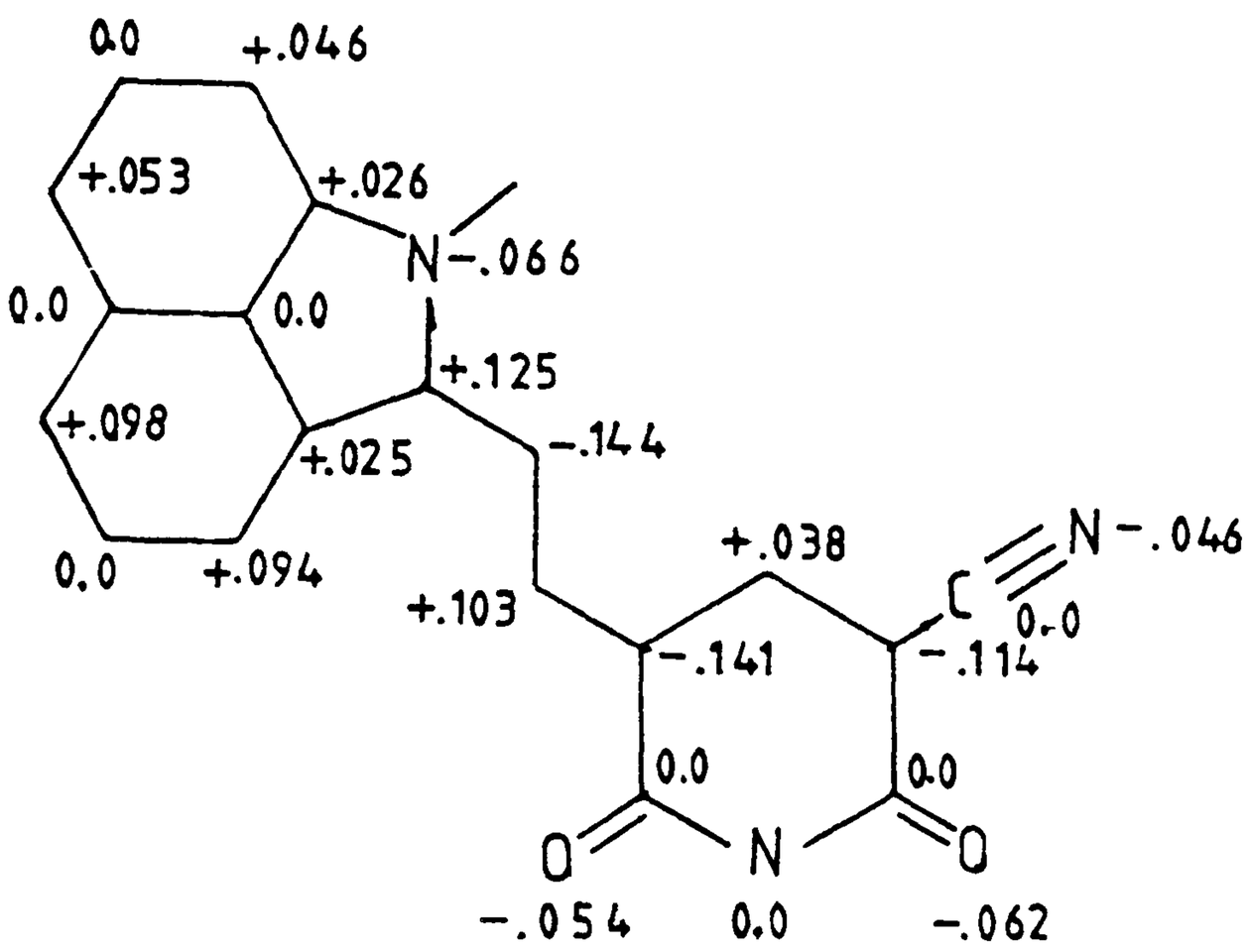

(b)

λ_{max} (calc) = 643nm

λ_{max} (toluene) = 659nm

carbonyl and cyano groups have a net negative charge. However the π-electron density charges for the longest wavelength electronic transition [Figs. 11(b) and 12(b)] show that, rather than the electron

density being lost from the donor residues and gained at the acceptor sites the electron density is built up predominantly at the bridging atoms between the two extremities of the dyes, and a relatively small amount of electron density is lost from both the donor and acceptor heteroatoms. This explains the major importance of the nitrogen bridge in inducing a large bathochromic shift, as it is at that position that the MO calculations predict the largest build up of electron density in the excited state.

The calculations also reveal the minimal involvement of the pyridone ring nitrogen in the light absorption process and its lack of influence on the λ_{max} of the resultant dyes.

2.2.3 Stability Properties of Dyes (178) - (181)

The stability properties of the methine and azomethine dyes (178) - (181) were assessed using the procedure described in Section 2.2.1.4 and the results are summarised in Table 29.

It is evident that the dyes show generally poor stability properties. Dyes (178a), (178b) and (178c) appear to be slightly more lightfast than the analogous dyes (180a), (180b) and (180c) suggesting that the incorporation of a nitrogen bridge into the dye molecule is detrimental to the photochemical stability of the dye. Moreover, the nitrogen bridge causes a marked decrease in thermal stability and total decomposition of (180a), (180b) and (180c) is observed under the test conditions.

With the benzindole dyes of types (179) and (181) the carbon bridged dyes are photochemically less stable than their aza analogues, the opposite to that observed with dyes (178) and (180). The thermal stability tests indicate that for the carbon bridged dyes (179a), (179b) and (179c) the longer the N-substituted chain is on the

Table 29: Stability properties of dyes (178a) - (181c)

Dye	Photo stability (% loss)	Thermal stability (% loss)
Standard (148)	8	5
(178a)	38	63
(180a)	39	Total Decomposition
(178b)	43	46
(180b)	44	Total Decomposition
(178c)	57	65
(180c)	58	Total Decomposition
(179a)	Total Decomposition	27(a) 9(b)
(181a)	58(a) 51(b)	43(a) 14(b)
(179b)	46(a) 47(b)	Total Decomposition(c)
(181b)	36(a) 33(b)	40(a) 11(b)
(179c)	40	Total Decomposition
(181c)	35	38

(a) - values for the more bathochromic of the two absorption peaks exhibited by the dye

(b) - values for the more hypsochromic of the two absorption peaks exhibited by the dye

(c) - total decomposition was accompanied by carbonisation of the dye and the cellulose acetate film

pyridone then the less likely the dye is to be heat stable. For the azomethine analogues (181a), (181b) and (181c) the reverse situation is true.

2.3 OXOCARBON DYES

2.3.1.1 Squarylium Dyes as Potential Near-Infrared Absorbers

Squaric acid (53) behaves as an electrophilic species and, like carboxylic acids, will undergo nucleophilic addition-elimination to give substitution products. Such condensation reactions have been reported with, for example, pyrroles[58], azulenes[137] and tertiary aromatic amines[138]. In all cases a 1,3-disubstituted product is formed, and, for example, pyrroles give (62), N,N-dialkylarylamines give (182) and primary and secondary amines give (183).

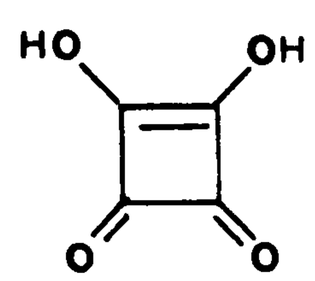

(53)

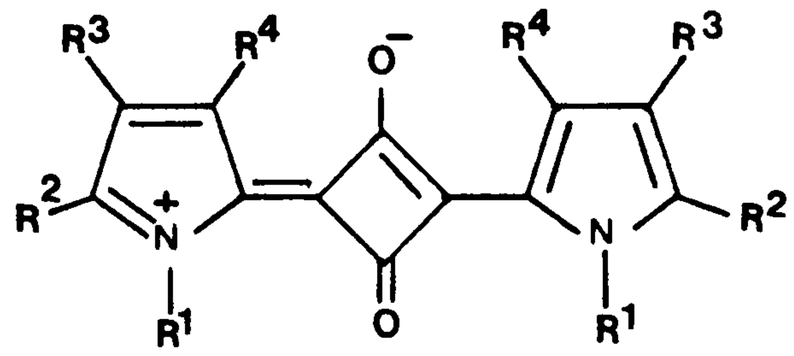

(62)

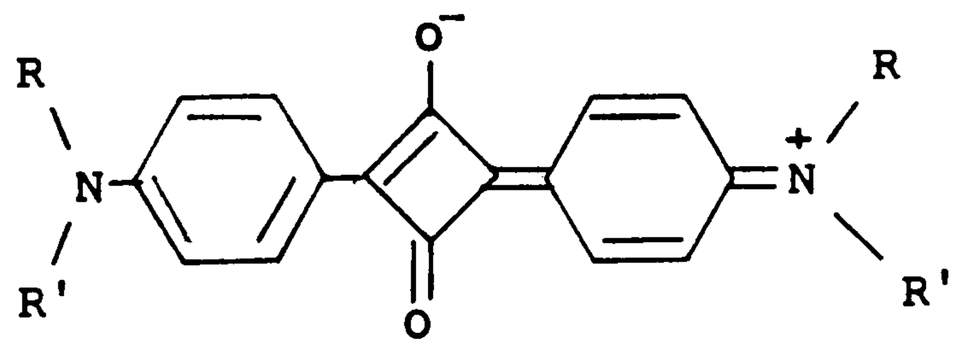

(182)

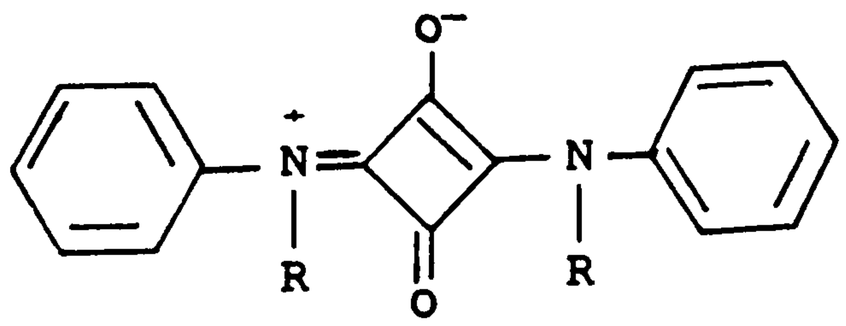

(183)

According to Dewar's rules based on PMO theory a strong electron donor substituted at a starred site in an odd-alternant hydrocarbon will cause a pronounced bathochromic shift of the first absorption band. Further bathochromic shifts are also obtained if electron

withdrawing residues are placed at <u>unstarred</u> sites. As can be seen from (184) squarylium dyes are isoconjugate with an odd-alternant

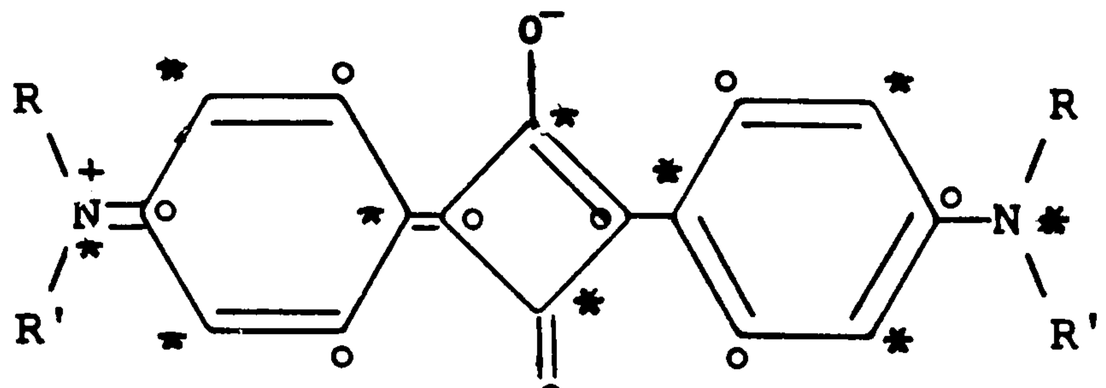

(184)

hydrocarbon system, and thus Dewar's rules can be applied. The central $-O^-$ at a starred position and the central C=O at two unstarred positions accounts for the highly bathochromic character of these dyes, which are generally blue (λ_{max} <u>ca.</u> 650nm).

It is possible to displace the visible absorption band into the near-infrared region of the spectrum by modifying the electron donor termini of the system. For example the pyrylium and thiopyrylium

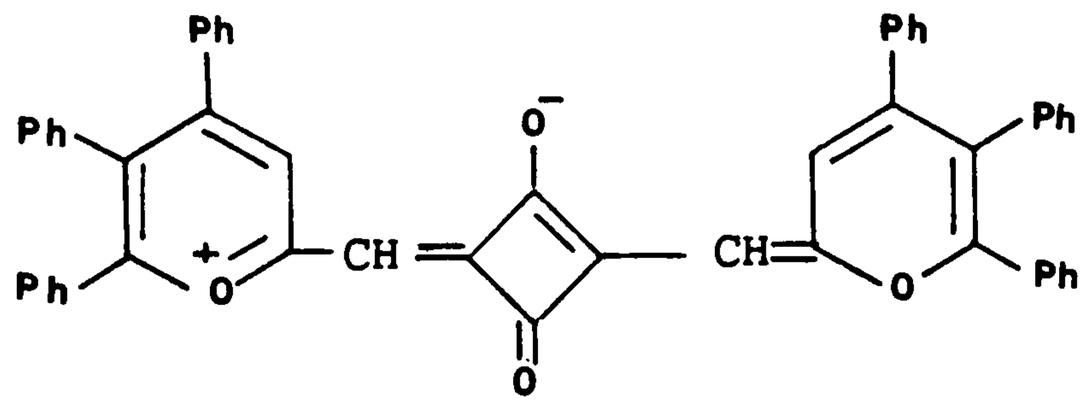

(185)

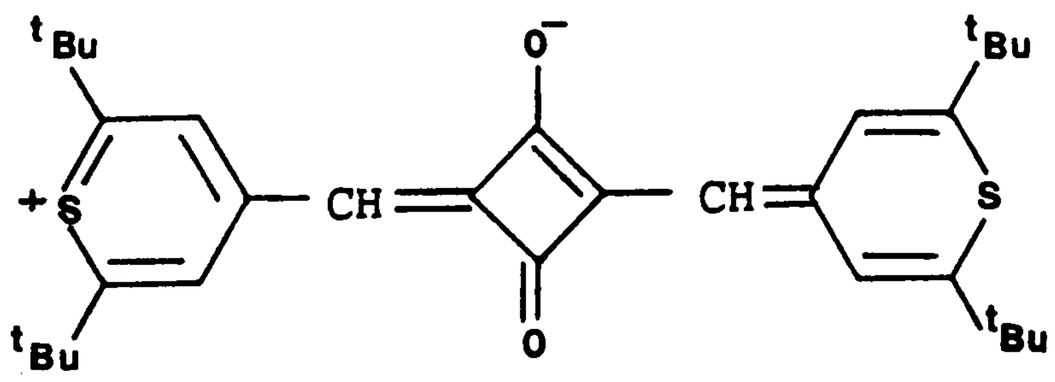

(186)

systems (185) and (186) absorb at 810 and 920nm respectively. Such dyes tend to have lower stability than the arylamine types (182), and thus it was of interest to examine modification of the arylamine residue in (182) to see if dyes beyond 700nm could be prepared.

2.3.1.2 Synthesis of Dyes and Intermediates

Previous unpublished work by Griffiths and Bello had demonstrated that the arylamine system 2,2-dihydro-2,2-dimethyl-1H-perimidine (187) could be condensed to squaric acid to give the dye (188), which was infrared absorbing. This dye absorbed intensely at 800nm in

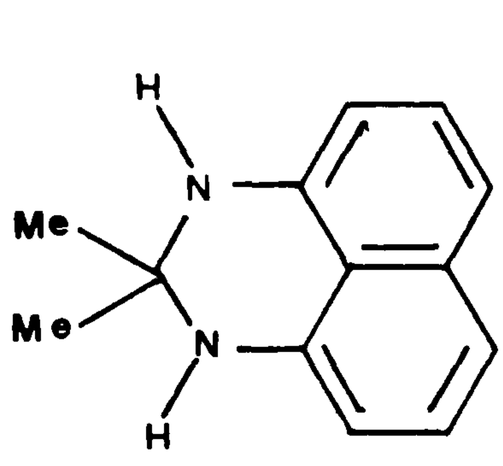

(187)

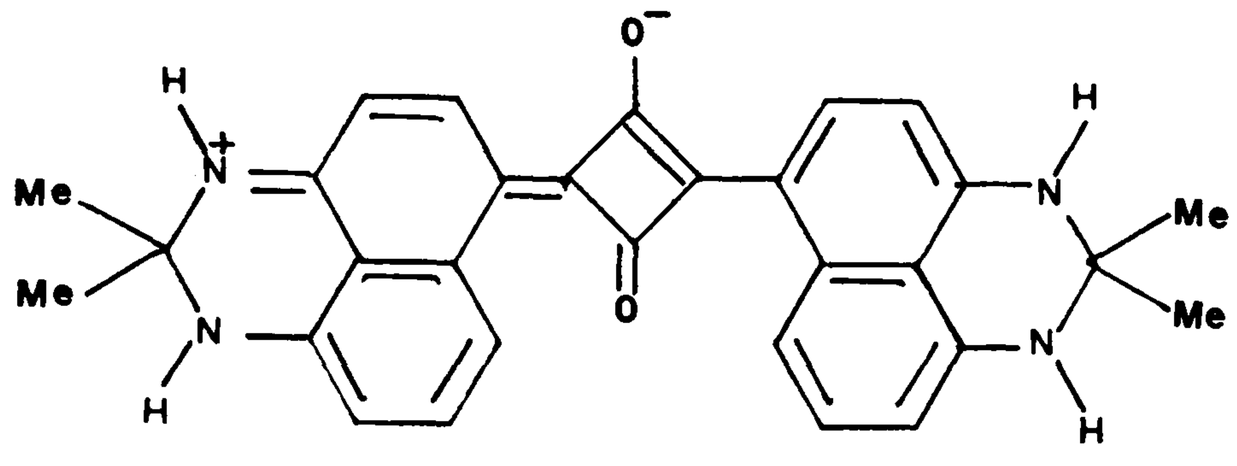

(188)

dichloromethane, and exhibited a narrow absorption band width. However, these advantageous properties were of little practical value because of the highly insoluble nature of the dye. As this work was of a preliminary nature, further derivatives of (188) were not investigated. The synthesis of other derivatives was therefore examined to try to enhance the solubility of the dyes, and to establish the relationships between absorption wavelength, stability, and chemical structure.

The condensation of squaric acid with dihydroperimidines was easily effected in boiling n-butanol/toluene mixtures under conditions of azeotropic removal of water. The dihydroperimidines used were (123a), (123e) - (123i) (Table 14, Section 1.2.1.2). The resultant dyes are listed in Table 30.

It was found that the dyes of type (189) which possessed shorter R

Table 30: Near-infrared absorbing dihydroperimidine based squarylium dyes

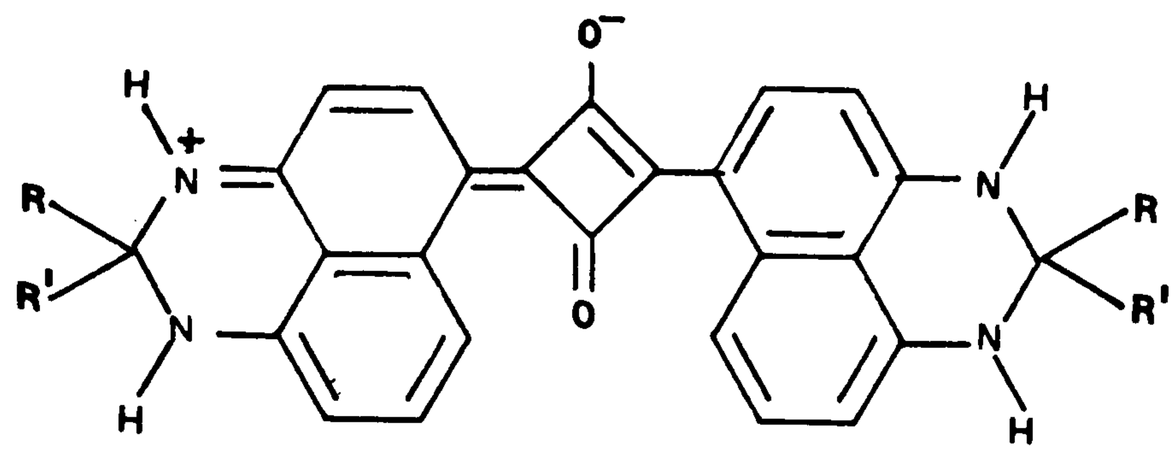

(189)

Structure	R	R'
(189a)	-Et	-Et
(189b)	-Me	$-CH_2CH(CH_3)_2$
(189c)	-Et	$-CH_2CH(CH_3)CH_2CH_3$
(189d)	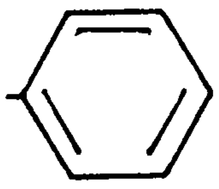	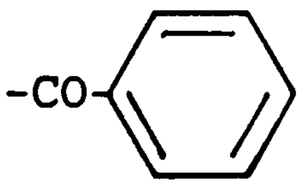
(189e)	-Me	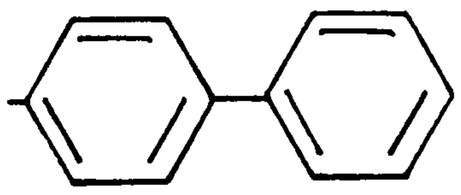
(189f)	-Me	$-C_2H_5COOC_4H_9$

and R' chains, namely (189a) and (189b) did not exhibit significantly enhanced solubility when compared to (188). Dyes (189c) and (189f) were considerably more soluble on organic solvents than (189a) and (189b), undoubtedly due to the longer chain substituents. However (189c) and (189f) still lacked appreciable solubility in more non-polar solvents such as toluene. It was found that incorporation of aromatic residues into dihydroperimidines at the 2-position, to give dyes (189d) and (189e), gave a greatly enhanced solubility in non-polar solvents, even in ligroin. Of the dyes listed in Table 30, (189e) was the most universally soluble. With the more soluble dyes, i.e. (189c) - (189f) their isolation was more difficult as they did

not precipitate from the reaction solution. Solvent removal, even under vacuum, led to some dye decomposition. However, it was found that by using n-propanol instead of n-butanol the synthesis proceeded as well, but the alcohol could be removed by washing with water (n-butanol is not totally water miscible). After washing, the toluene layer could be dried and passed directly down a silica gel 60 column to obtain the pure dye. This procedure was followed for all the other squarylium dyes, except where stated otherwise.

Not surprisingly, all the dyes (189a) - (189f) showed very similar light absorption properties. More pronounced structural variations were then examined in an attempt to vary the position of the absorption band further.

The dihydroperimidines (124) and (125), described in Section 2.1.2.1 were thus examined. The expected dyes have the structures (190) and (191) respectively. Reaction of (124) with squaric acid

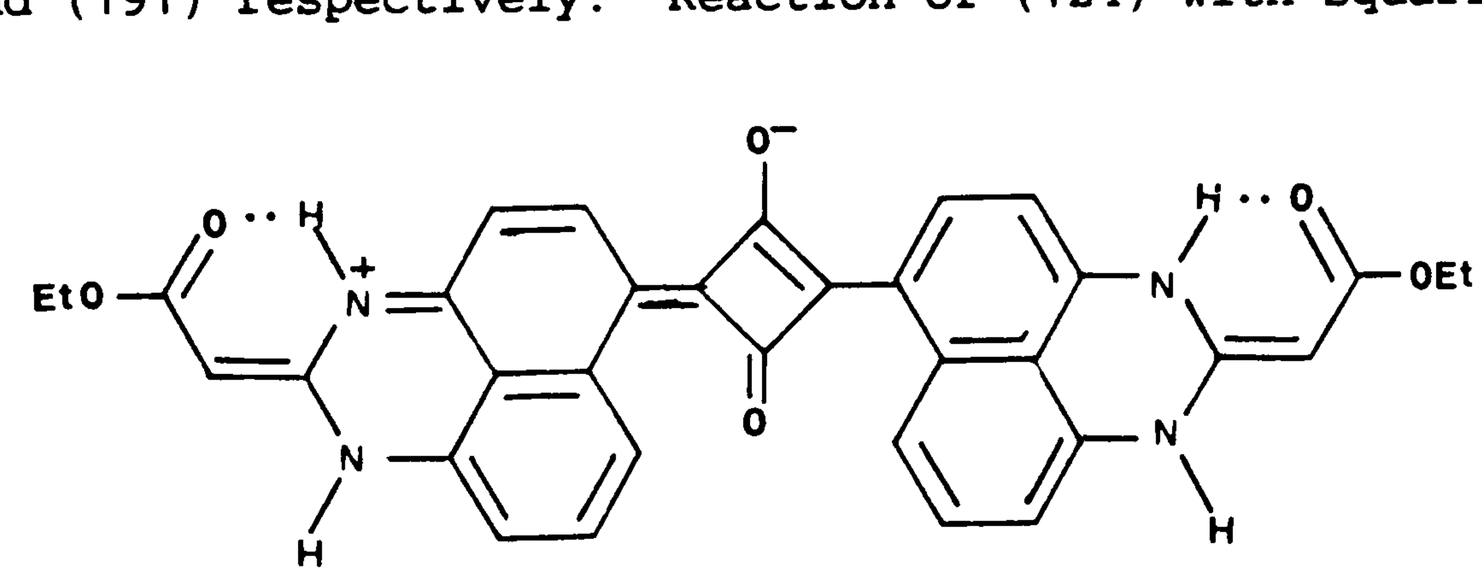

(190)

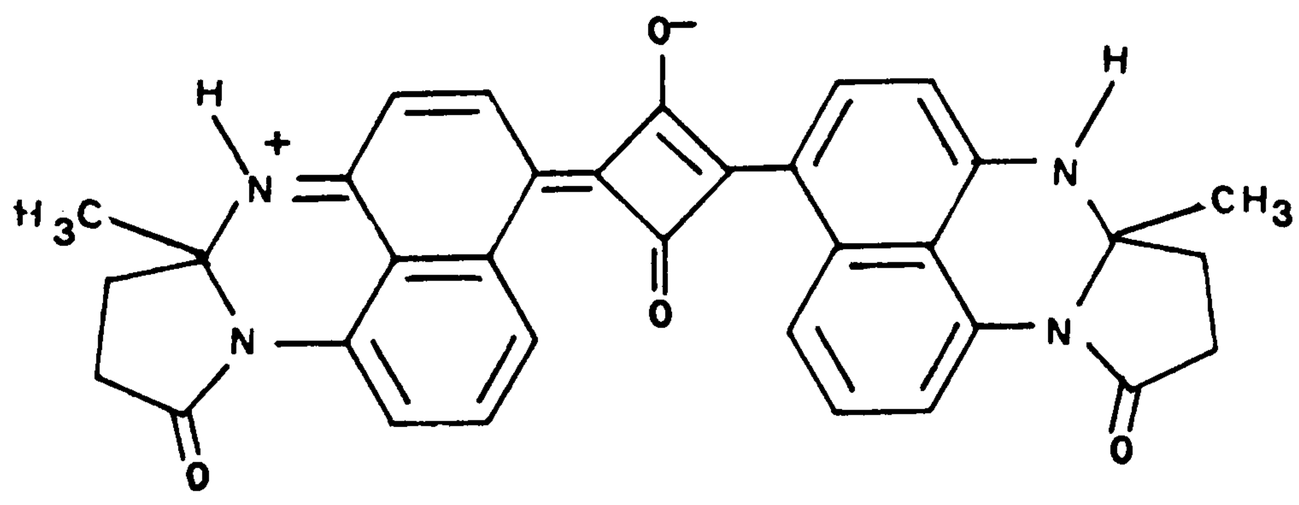

(191)

gave a dull red crystalline solid on cooling the reaction mixture, the crude product having λ_{max} = 541nm in hot dimethylformamide. Unfortunately the dye proved highly insoluble, more closely resembling a pigment than a dye. This lack of solubility may be due to the

presence of intra- as well as inter-molecular hydrogen bonding within the dye crystal matrix. It was thus not possible to isolate the dye in a pure state for characterisation purposes. Even fast atom bombardment spectrometry failed to give a detectable molecular ion peak, and thus the assigned structure (190) must remain tentative. Reaction between the tetracyclic dihydroperimidine (125) and squaric acid proved relatively complex, although infrared absorbing products were formed. On cooling the reaction mixture no product separated and thus, after removal of the n-propanol, column chromatographic separation was carried out. This afforded two major green fractions, the first eluted component having λ_{max} = 788nm in dichloromethane and the more strongly retained component having λ_{max} = 753nm in the same solvent. Unfortunately microanalysis and fast atom bombardment mass spectrometry on both fractions failed to confirm the structure of the dye as (191).

In addition to the dihydroperimidine squarylium dyes, other types of squarylium dyes were synthesised. Thus, the squarylium dye (192) was obtained as metallic green crystals from the relatively slow reaction of 1-ethyl-2-methylperimidine (120b) with squaric acid in a boiling n-butanol/toluene mixture under conditions of azeotropic removal of water. It was characterised by microanalysis. The dye absorbed at surprisingly short wavelength [$\lambda_{max}(CH_2Cl_2)$ = 595nm] compared to the dyes of type (189), and was bright blue in colour.

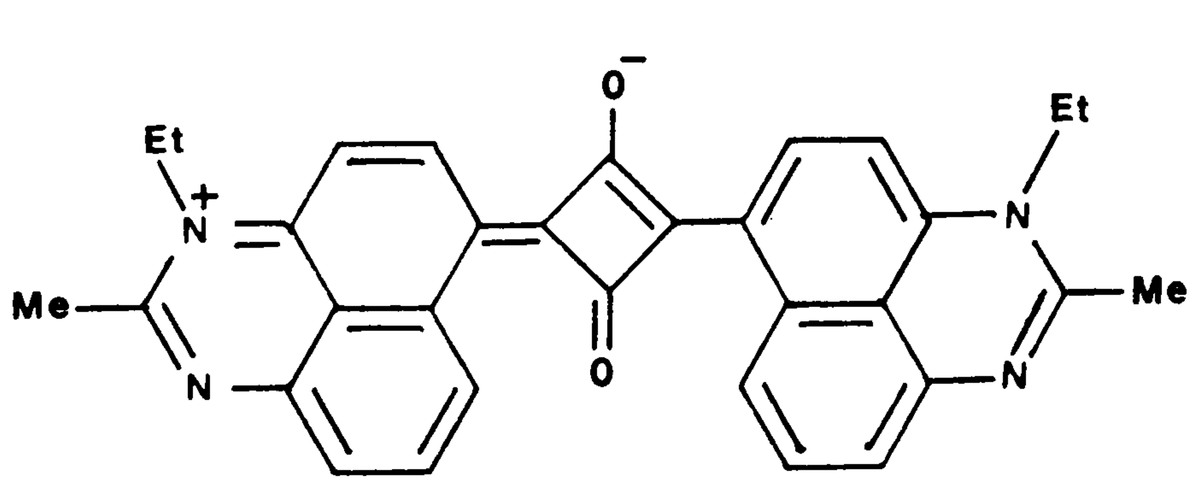

(192)

Two additional novel near-infrared absorbing squarylium dyes (193) and (194) were obtained successfully by condensing Michler's ethylene and 1-decyl-2(1H)-methyl-benz[c,d]indolium iodide (158) with squaric acid respectively. Problems were encountered in achieving efficient

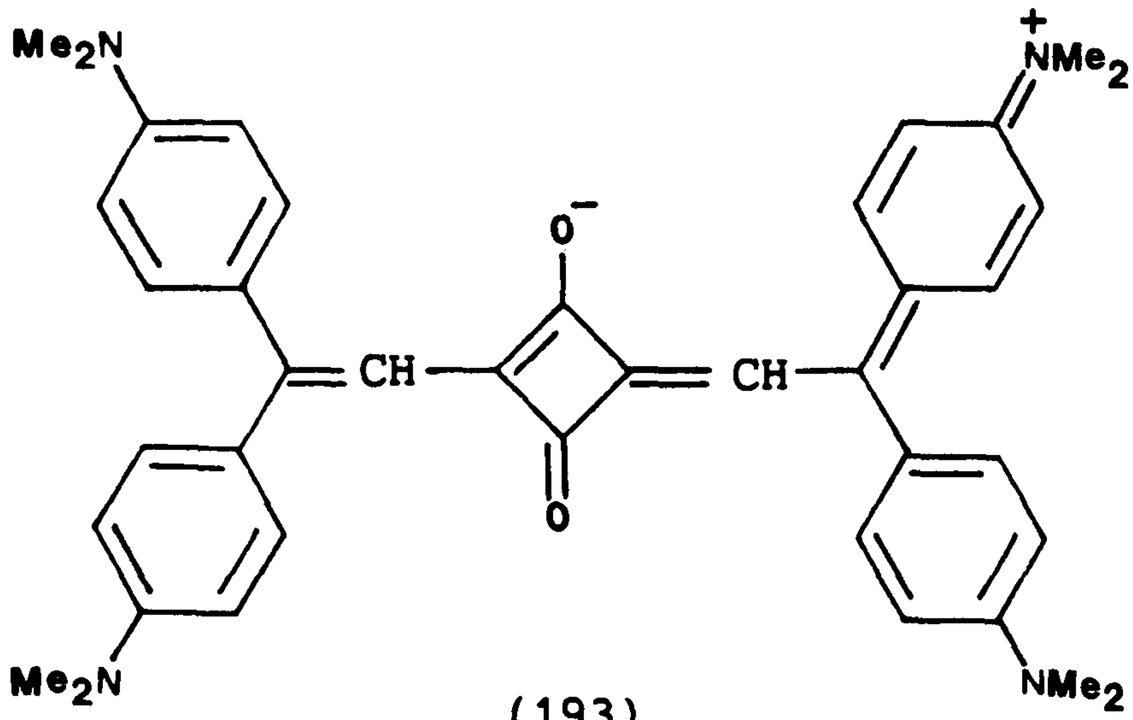

(193)

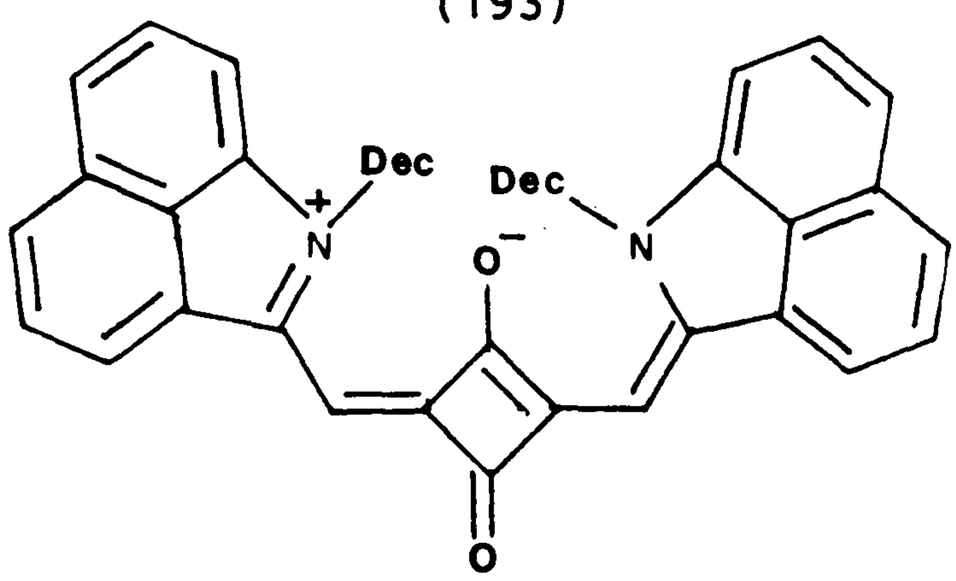

(194)

formation of (193), apparently due to the various acid-mediated side reactions of the Michler's ethylene, squaric acid itself providing a proton source (see Section 2.1.3.1). Consequently the dye could only by isolated in very small amounts, just sufficient for characterisation by mass spectrometry, and for spectroscopic and stability measurements.

Dye (194) was highly soluble in a wide range of solvents and was the most bathochromic of the squarylium dyes synthesised in this work. Thus it had a λ_{max} = 900nm in toluene. It was therefore disappointing to find, several months after synthesis of this dye that a West German Patent had recently been granted covering the preparation of this dye[139].

2.3.1.3 Light Absorption Properties of the Squarylium Dyes

The light absorption properties of the squarylium dyes were measured in dichloromethane and toluene, and the results are summarised in Tables 31 and 32. Molar extinction coefficients were recorded in dichloromethane. For comparison with molecular orbital calculations toluene was taken as the non-polar solvent.

Table 31: Spectroscopic data for new squarylium dyes

Dye	λ_{max}/nm (CH_2Cl_2)	(CH_2Cl_2) (Toluene)	ε_{max}/$lmol^{-1}cm^{-1}$ (CH_2Cl_2)	$\Delta\lambda_{max}$/nm (CH_2Cl_2-Tol)
(189a)	805	808	155,000	-3
(189b)	803	807	136,000	-4
(189c)	806	807	128,000	-1
(189d)	809	817	135,000	-8
(189e)	805	813	148,000	-8
(189f)	800	807	189,000	-7
(192)	595	603	151,000(a)	-8
(193)	809	809	169,500	0
(194)	884	900	161,500	-16

(a) - may be slightly low value due to low solubility of the dye in dicloromethane

From Table 31 it is evident that, as would be expected, varying the substituents on the 2-position of the dihydroperimidine systems has little effect on the λ_{max} values of the dyes. Thus (189a) - (189c) and (189e) and (189f) show very similar properties. The benzoyl dye (189d) does absorb at slightly longer wavelengths than the other dihydroperimidine dyes in toluene, and this may be due to intramolecular hydrogen bonding of the NH proton to the carbonyl group.

The dihydroperimidine dyes show only small solvatochromic effects, which is to be expected for symmetrical squarylium dyes. Thus neither

the ground state or the excited state has a permanent dipole moment, as shown by PPP-MO calculations. The perimidine dye (192), Michler's ethylene dye (193) and benzindole dye (194) similarly exhibited only small solvatochromic effects.

Dye (192) absorbs at a notably shorter wavelength than the analogous dihydroperimidine dyes giving an intense blue in dichloromethane. This is somewhat surprising when the simple azo dyes discussed in Section 2.1.2 are considered, as in these chromophores the perimidine based dyes absorbed at <u>longer wavelengths</u> than the dihydroperimidine analogues. The PPP-MO method was applied to the problem (see Table 32) and this in fact predicted that (192) should be significantly <u>more bathochromic</u> than analogous dihydroperimidine dyes, at variance with experiment. This raises doubts about the assigned structure (192), and attempts to confirm the structure of (192) by ^{1}H-n.m.r. were hampered by the low solubility of the dye in organic solvents. However if the visible absorption curve obtained for (192) is compared with that of dye (189d), as shown in Fig. 13, the

Fig. 13: <u>Absorptiom spectra of dyes (192) and (189d) in dichloromethane</u>

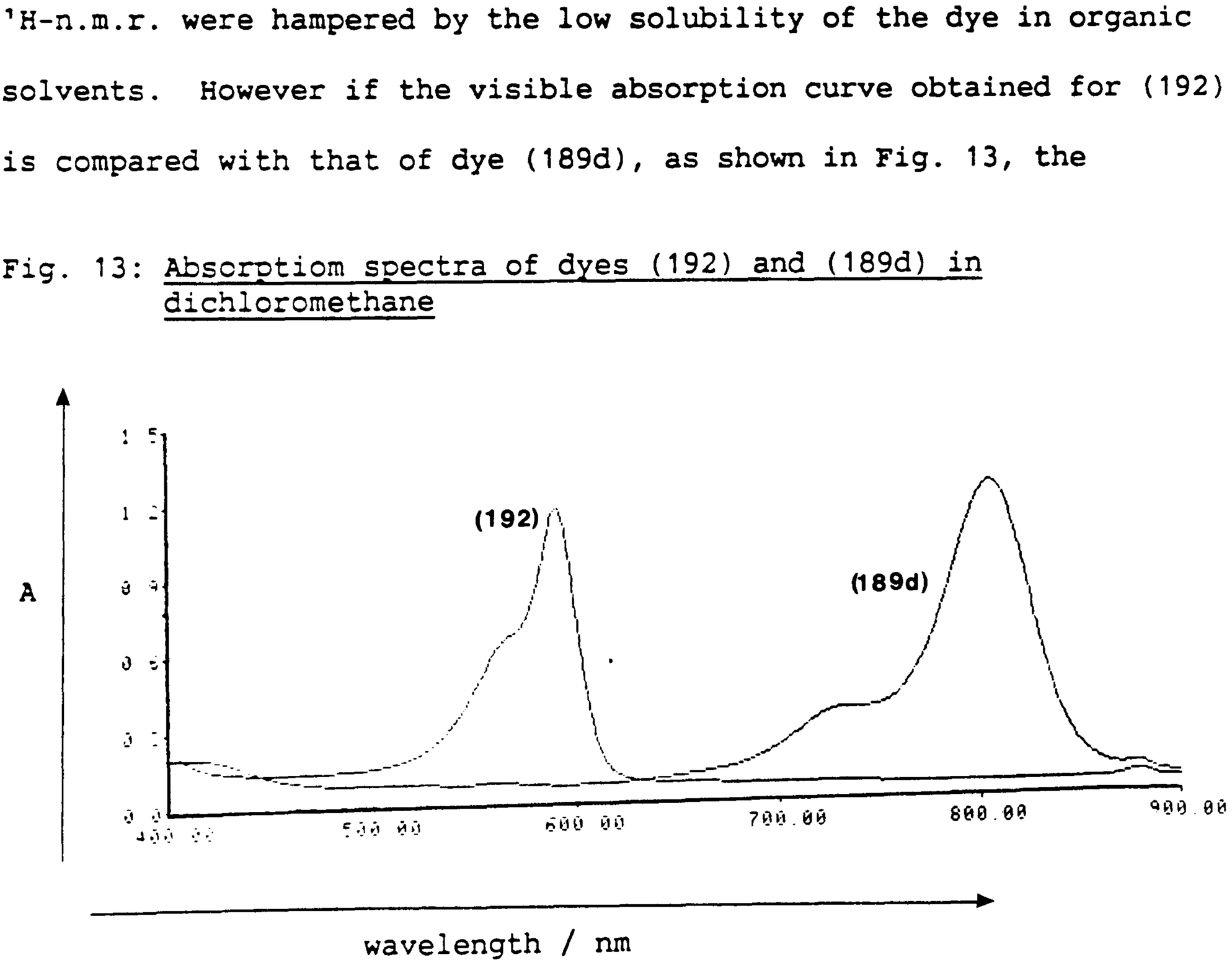

A - absorbance

similarities in shape between the two are apparent, strongly suggesting that (192) does at least contain the fundamental squarylium chromophore.

The spectrum of (189d) is typical of the squarylium dyes, which generally exhibit an intense sharp peak in the visible/near-infrared region of the spectrum accompanied by a weak shorter wavelength tail. The band width of the main peak increases as the absorption maximum moves to longer wavelengths. This type of absorption curve typifies systems that have a high degree of electronic symmetry.

As can be seen from Table 31 the Michler's ethylene and benzindole dyes (193) and (194) respectively are particularly effective as infrared absorbers, and the latter dye is one of the most bathochromic squarylium dyes yet synthesised.

An attractive feature of the spectra of the infrared absorbing squarylium dyes, as can be seen from Fig. 13 is the very low absorption in the visible region. Thus, the dyes in Table 31, except (192), were colourless to the human eye in solutions giving an absorbance value of ca. 1 at λ_{max}.

Furthermore, with the exception of (192) and (194) all the dyes absorb in the region of the gallium-aluminium-arsenide laser emission, and are thus of practical potential.

The absorption spectrum of representative squarylium dyes were calculated by the PPP-MO method, and the results are summarised in Table 32. The VSIP and electron affinity values used for the dihydroperimidines and perimidines were those developed for the monoazo dyes in Section 2.1.2.2 and the VSIP and electron affinity values used for the benzindole residue were those described in Section 2.1.3.2.

In general the calculated results agreed well with experiment, dye (192) being a notable exception. The slight overestimation of the

Table 32: Comparison of PPP-MO calculated and experimental absorption maxima of representative squarylium dyes

Dye	λ_{max}/nm (Calc)	λ_{max}/nm (Toluene)	$\Delta\lambda_{max}$/nm (Tol-Calc)	Oscillator strength (f)(Calc)
(189a)	769	808	+39	1.97
(189d)	774	817	+43	2.00
(192)	936	603	-333	1.84
(193)	834	809	-25	1.50
(194)	958	900	-58	2.60

absorption maxima of dyes (193) and (194) may be partly attributed to the fact that the PPP-MO method assumes a planar geometry, which is certainly not the case with these dyes, as shown by molecular models.

It is of interest that the calculated λ_{max} value for the uncharacterised dye (191) was 739nm. Thus this predicted value is less than that calculated for typical 2,2-disubstituted analogues.

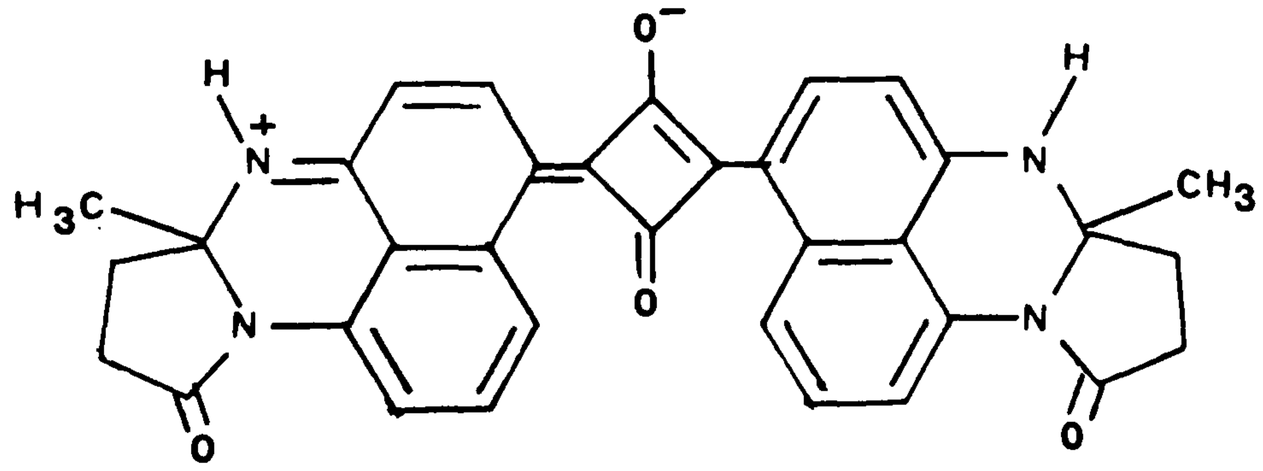

(191)

Thus the MO-calculations support the argument that one of the two blue-shifted fractions obtained from the reaction mixture via column chromatography may be the desired product (191).

Calculated ground state charge densities and the π-electron density changes for the visible absorption bands for dyes (189a) and (194) are presented in Figs. 14 and 15 as typical data for infrared squarylium systems.

From Figs. 14 and 15 the high polarity of each half of the molecule

Fig. 14: (a) Ground state charge densities and (b) π-electron density changes for the first absorption band of dye (189a)

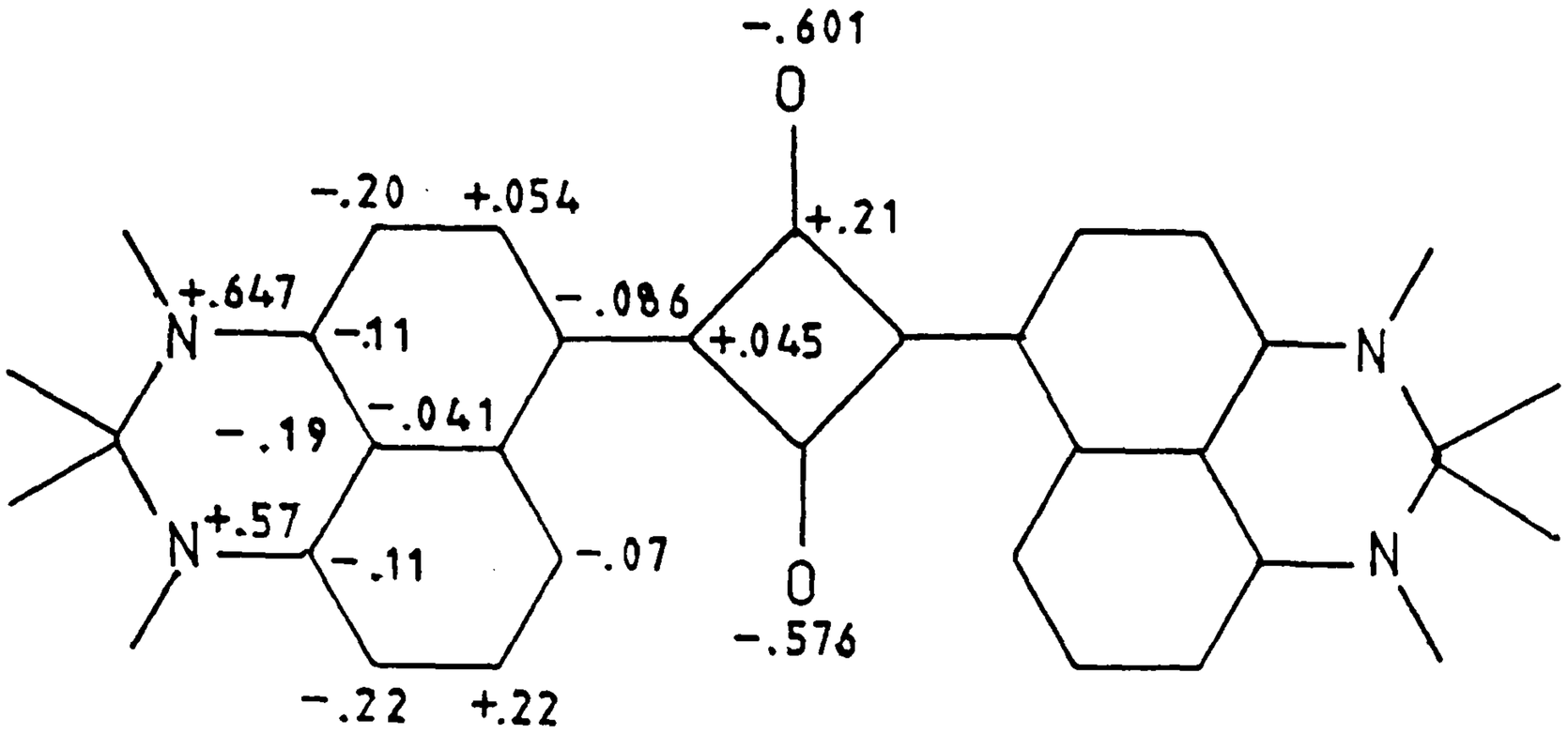

(a)

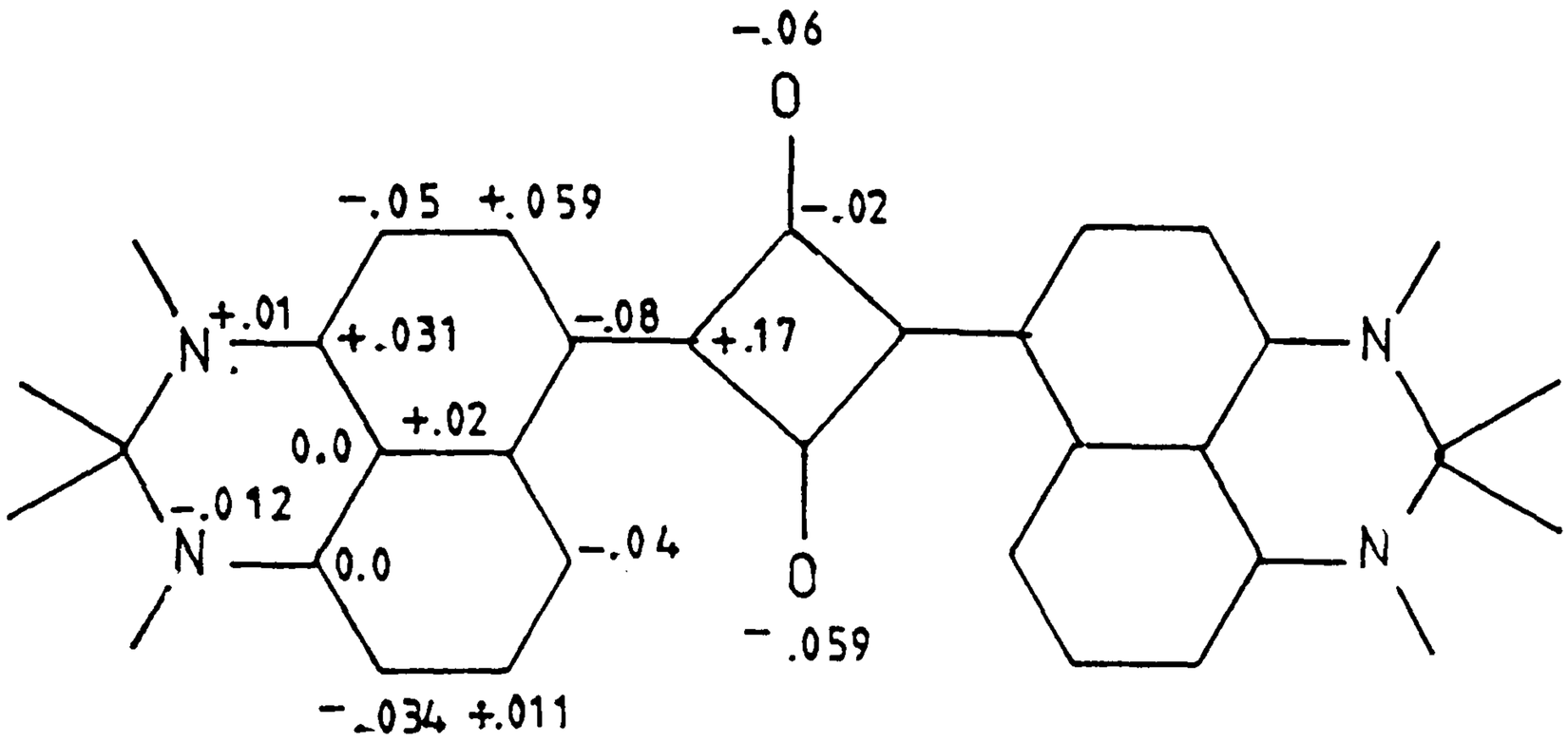

(b)

λ_{max} (calc) = 768nm

λ_{max} (toluene) = 808nm

in the ground state is apparent, with electron density being removed from the donor nitrogen groups. The overall dipole moment of the molecule is zero however, as would be expected.

The electron density changes for the dihydroperimidine dye (189a) in Figure 14(b) is particularly intriguing because the nitrogen atoms that are in direct conjugation with the squarylium ring appear to gain electron density on excitation, whereas the nitrogen atoms attached to the other rings lose electron density.

Fig. 15: (a) Ground state charge densities and (b) π-electron density changes for the first absorption band of dye (194)

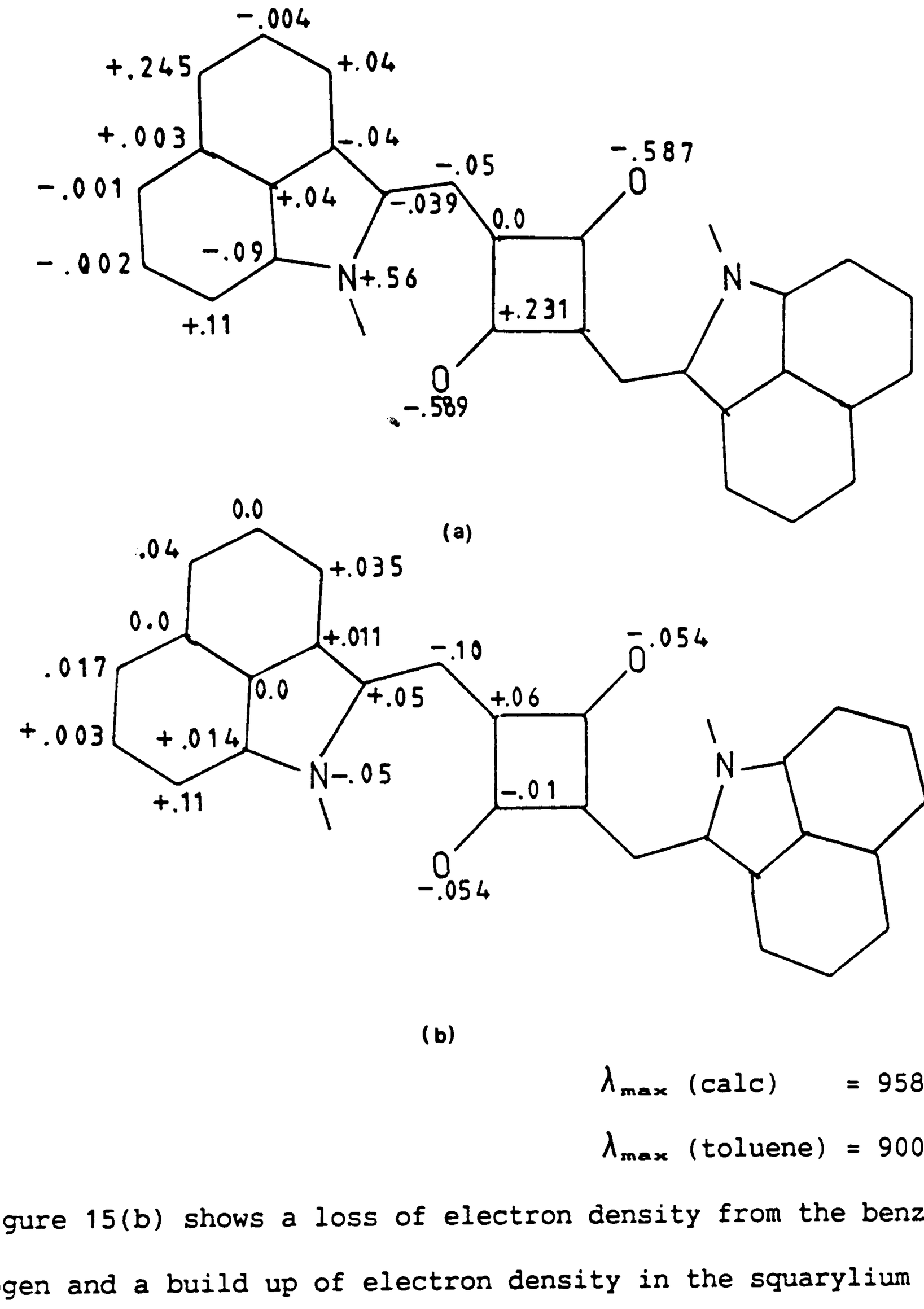

λ_{max} (calc) = 958nm

λ_{max} (toluene) = 900nm

Figure 15(b) shows a loss of electron density from the benzindole nitrogen and a build up of electron density in the squarylium and benzindole aromatic rings.

2.3.1.4 Stability Properties of Squarylium Dyes

The stability properties of the squarylium dyes were assessed using the procedures described previously in Section 2.1.2.4 and the results are summarised in Table 33. The thiazole dye (148) was taken as the standard.

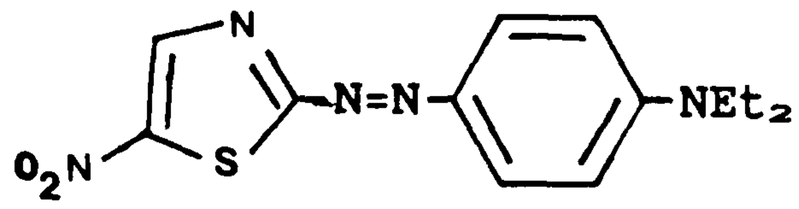

(148)

Table 33: Stability properties of the squarylium dyes

Dye	Photo stability (% loss)	Thermal stability (% loss)
Standard (148)	8	5
(189a)	62	47
(189b)	91	60
(189c)	92	62
(189d)	85	38
(189e)	73	17
(189f)	83	55
(192)	9	8
(193)	54	59
(194)	14	22

Relative to the standard, the dihydroperimidine squarylium dyes exhibited particularly poor photochemical and thermal stabilities. The diethyl substituted dye (189a) appeared to be the most stable of the alkyl substituted dihydroperimidines, and these tended to show a general decrease in stability with increasing alkyl chain length.

The aryl substituted dihydroperimidine squarylium dyes (189d) and (189e) exhibited significantly better thermal stabilities than the other dihydroperimidine dyes, and better lightfastness than dyes (189b) and (189c). Thus (189d) and (189e) would appear to possess the best overall properties for practical application purposes.

Dye (192) is markedly more stable than the other dyes in Table 33.

This is not surprising as, in most cases the more hypsochromic the squarylium dye system, the less susceptible it becomes to chemical attack. This statement does not however hold true for dye (194), which is the most bathochromic in the series. Thus (194) exhibits the best lightfastness, and, with the exception of (189e), the best thermal stability of the infrared absorbing dyes listed in Table 33.

In the thermal stability tests, all the dyes in Table 33 showed a yellowing of the cellulose acetate films after 1 hour at 190°C indicating the presence of decomposition products.

2.3.2.1 The Croconium Dyes

Croconic acid (75) has recently been of interest as a source of i.r. dyes because when it is reacted with certain heterocyclic enamines highly bathochromic dyes of the general formula (195) are produced[81].

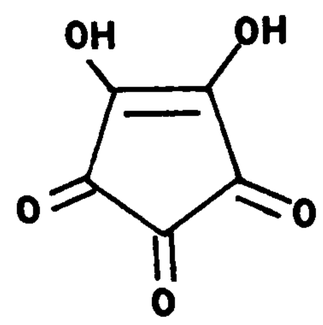

(75)

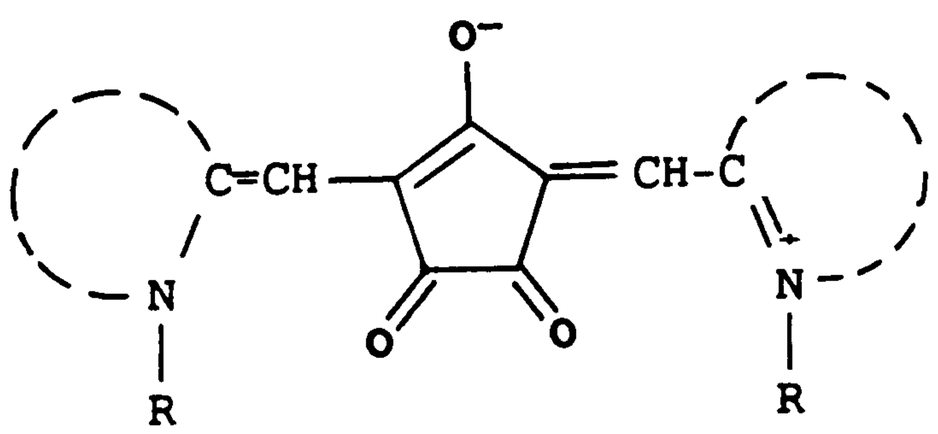

(195)

As with the squarylium system, the highly bathochromic nature of the croconiums can be explained in terms of Dewar's rules, (i.e. PMO theory). Thus if (196) is considered then it is evident that, in the 5-membered ring there is a strong electron donor ($-O^-$) at a starred site and two electron accepting carbonyl groups at two unstarred positions. Dewar's rules then predict a bathochromic shift for both

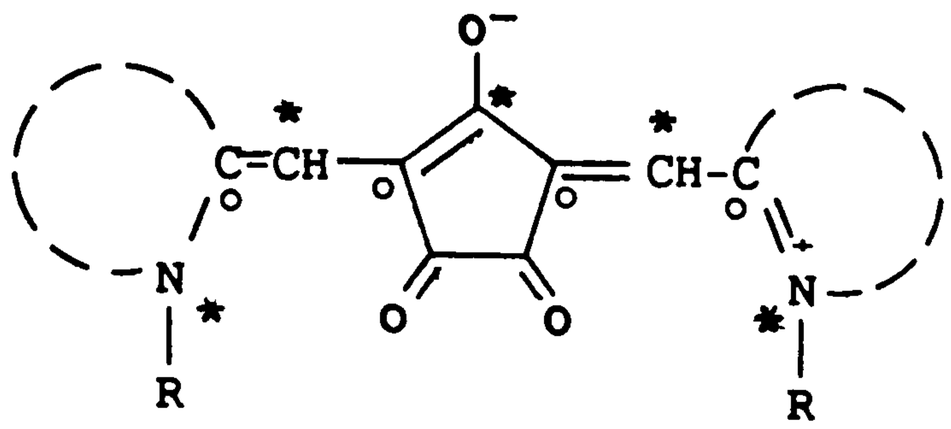

(196)

types of perturbation, and these effects reinforce to result in the exceptionally large bathochromic shift observed in practice.

Although croconium dyes have often been cited in various Japanese patents dealing with optical recording media, very little is known about the spectral characteristics, and synthesis of these dyes. In fact, to date only one paper has appeared in the open literature[81], and this gave no experimental details for the synthesis of the dyes.

Thus the preparation of a range of croconium dyes was undertaken, both to define the spectroscopic properties of the system in comparison with the squarylium dyes, and to define the limitations of the synthetic procedure.

2.3.2.2 Synthesis of Dyes and Intermediates

Croconic acid was obtained in the anhydrous state as a pale yellow hygroscopic powder in a 5-step synthesis starting from chloranil, as shown in Scheme 27[72,140]. Thus chloranil (197) was heated with sodium methoxide to give tetramethoxy-p-benzoquinone, (198). Treatment of this with acetic acid-hydrobromic acid resulted in demethylation to give (199) as deep red crystals. The tetrahydroxy-p-benzoquinone (199) was then oxidised with active manganese dioxide in alkaline solution and addition of barium chloride gave the barium salt of croconic acid as an insoluble yellow crystalline solid (200). Treatment of the salt with warm dilute sulphuric acid for

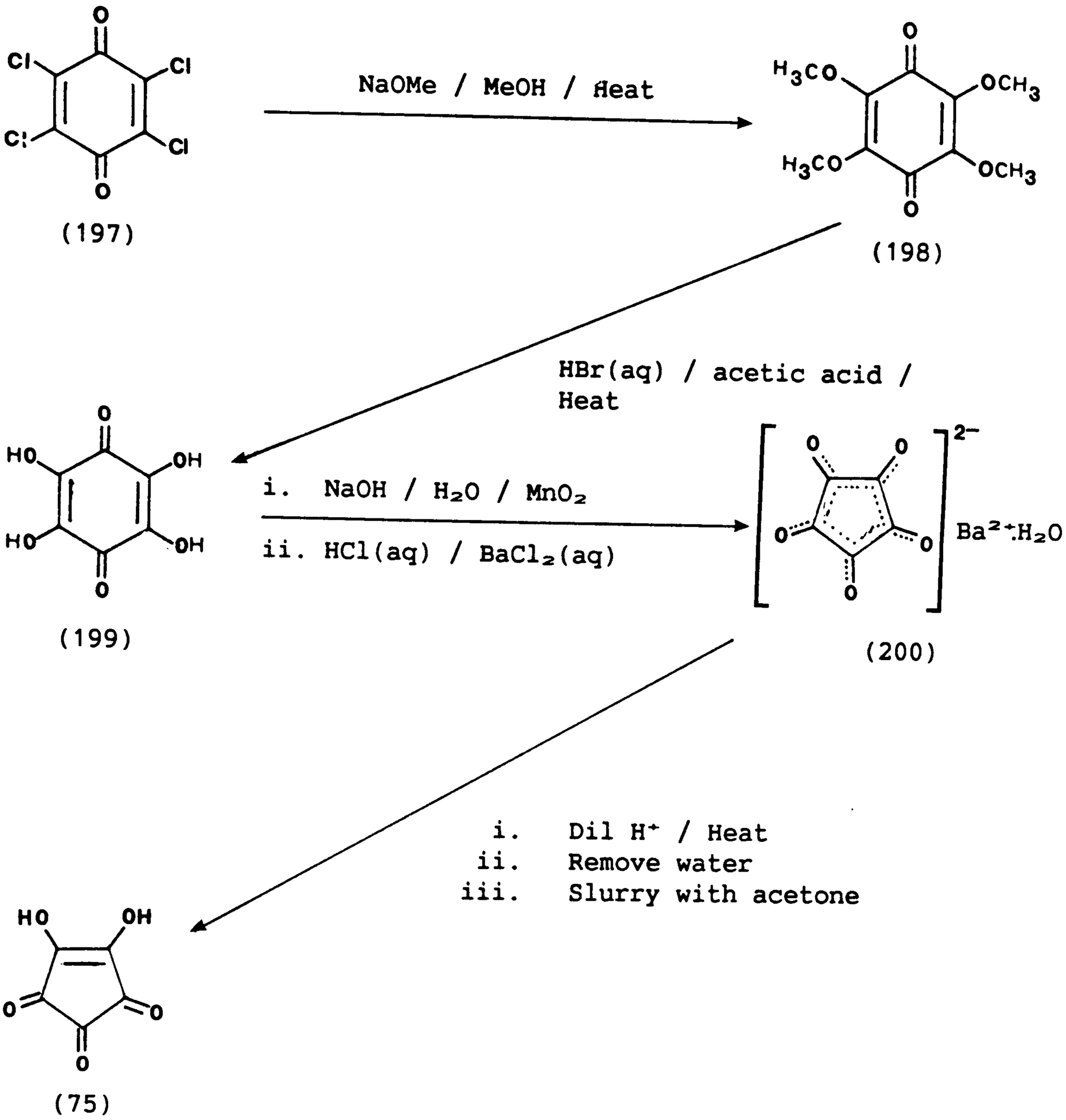

Scheme 27

35-40 minutes followed by removal of barium sulphate gave a solution of free croconic acid. Water removal by rotary evaporation gave the hydrated croconic acid as a yellow/brown tar. The literature method for purifying this was both tedious and inefficient, whereas it was discovered that triturating the tar with acetone rapidly gave anhydrous croconic acid as pale yellow crystals, in high yields. The anhydrous nature of the product was confirmed by ^{13}C-n.m.r. (Fig. 16) which clearly showed only one peak at 178ppm corresponding to the equivalent carbon atoms of croconic acid (the peak at 40ppm is due to

Fig. 16: ^{13}C-n.m.r of anhydrous croconic acid

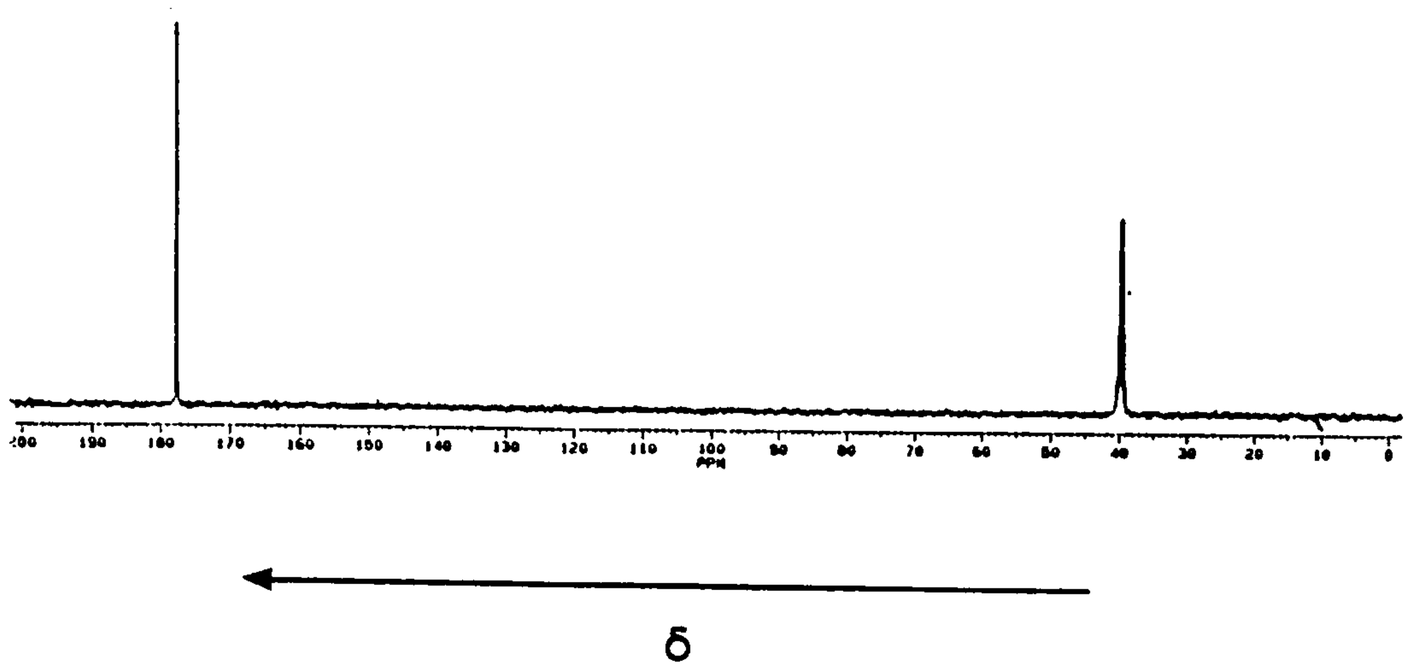

DMSO). The result was rather surprising as the literature methods all produce croconic acid as the trihydrate (201).

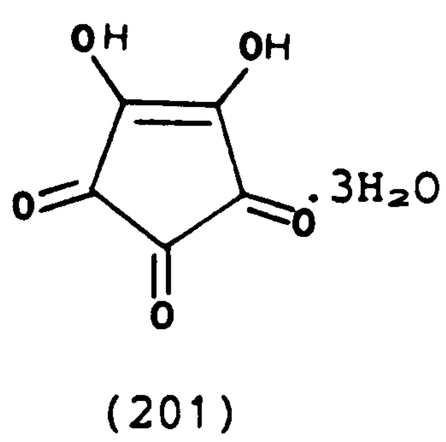

(201)

The reactions of croconic acid with the various types of nucleophile used successfully with squaric acid, Section 2.3.1.2 were examined using similar reaction conditions (i.e. refluxing in n-propanol/toluene with azeotropic removal of water). It was noted that croconic acid was less reactive than squaric acid, and no reaction occurred with simple N,N-dialkylarylamines or their substituted derivatives, that is with the exception of their 3-hydroxy derivatives (202).

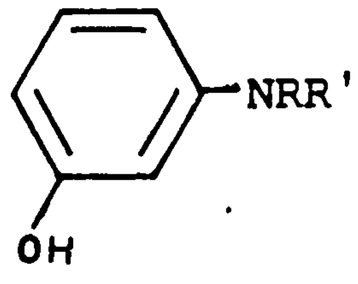

(202)

The first croconium dye to be synthesised was thus the dye (203), prepared from 3-hydroxy-N,N-diethylaniline. The product was purified

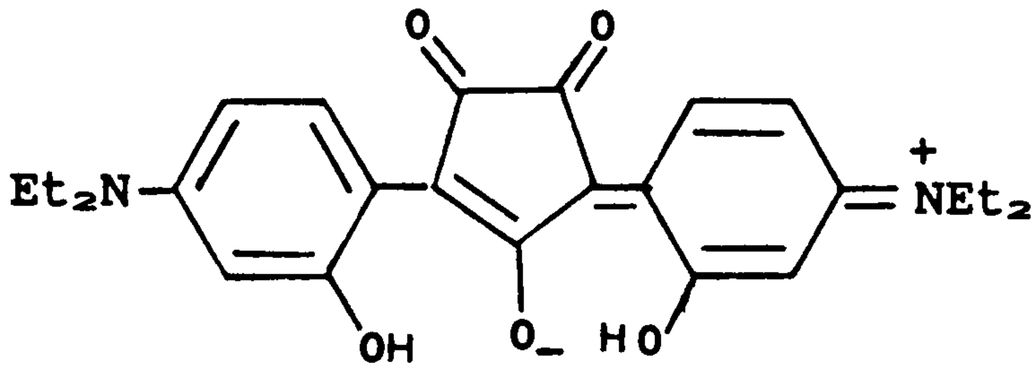

(203)

by column chromatography (silica gel 60; as aluminium oxide tended to decompose the dye) and was characterised by microanalysis. It formed dark brown crystals, and absorbed at particularly long wavelengths (λ_{max} = 822nm in dichloromethane).

Dye (204) was obtained readily in a similar manner from 8-hydroxyjulolidine and was characterised by microanalysis. As would be expected, due to the enhanced planarity of the chromophore this dye

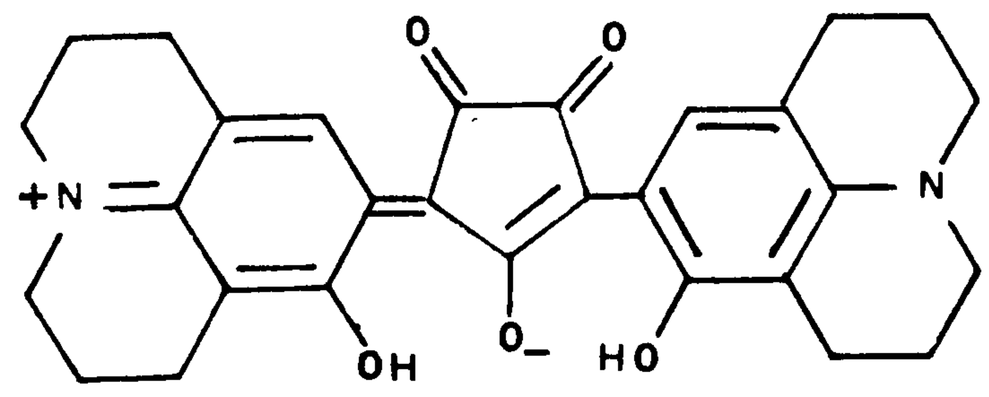

(204)

absorbed at even longer wavelengths than (203) (λ_{max} = 854nm in CH_2Cl_2). This reaction was of particular interest as it occurred readily at room temperature, and was thus particularly suited to a kinetic study to determine the characteristics of the croconic acid condensation process. Such a study is discussed later in Section 2.3.2.5.

Dye (205) was obtained inefficiently as pale yellow-brown crystals from the reaction of N-(-3-hydroxyphenyl)morpholine with croconic acid. It proved highly insoluble in common organic solvents (even in hot dimethylformamide) and thus satisfactory purification could not be

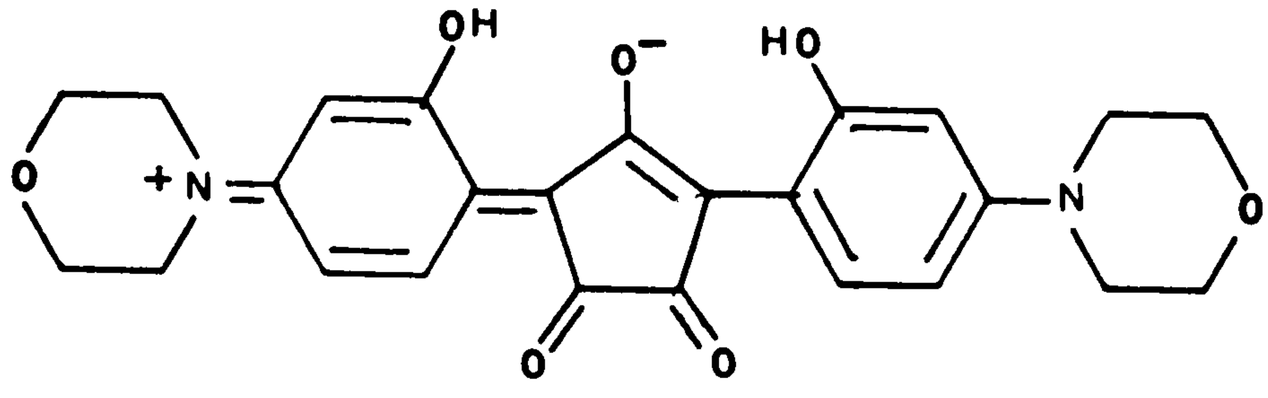

(205)

achieved. The dye gave the expected M+1 ion peak by FAB-mass spectrometry.

The synthesis of croconium dyes from 3-acylamino-N,N-dialkylanilines has not been reported in the literature and thus this was investigated. The synthesis of dye (206) was attempted from 3-acetylamino-N,N-diethylaniline. Although the reaction solution

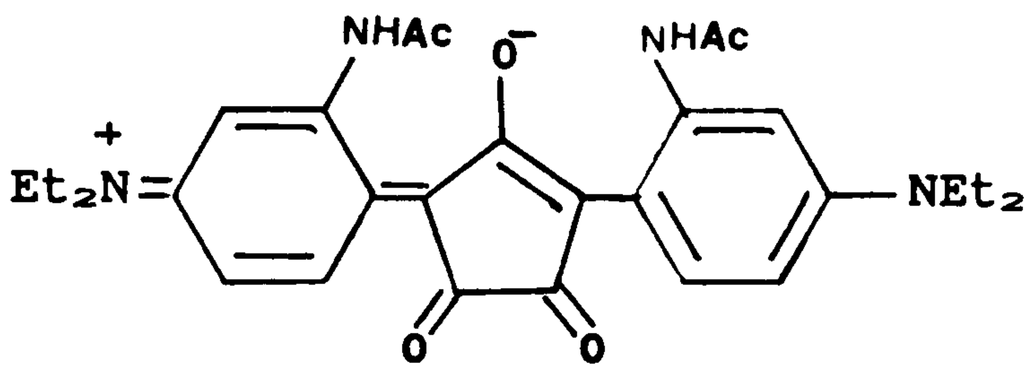

(206)

showed an absorption peak at 845nm (in acetone), the dye was formed in only low yield and could not be isolated. Prolonged heating of the reaction mixture resulted in decomposition of the product. However, in the case of N-ethyl-7-propionamido-2,2,4-trimethyltetrahydroquinoline, which has enhanced nucleophilic reactivity because of the enforced overlap of the amino nitrogen lone pair electrons with the benzene ring, isolation of the croconium dye (207) was possible using column

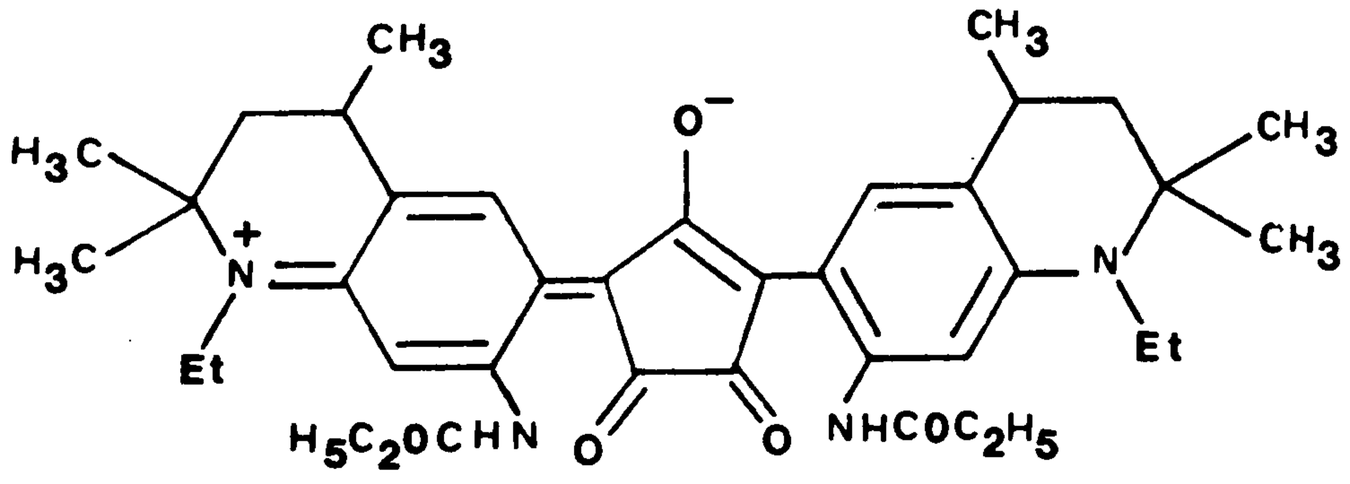

(207)

purification with silica gel 60. This dye was exceptionally bathochromic with an absorption maximum at 900nm in toluene.

As mentioned earlier, croconic acid will react with heterocyclic enamines. Thus the highly bathochromic enamine (158) was examined, as this in combination with the croconic residue should give an exceptionally bathochromic dye, i.e. (208). The reaction occurred readily, and the dye was purified by column chromatography, although it appeared to suffer slight decomposition on the column [as did (207)]. The dye was obtained as brown crystals and gave the expected

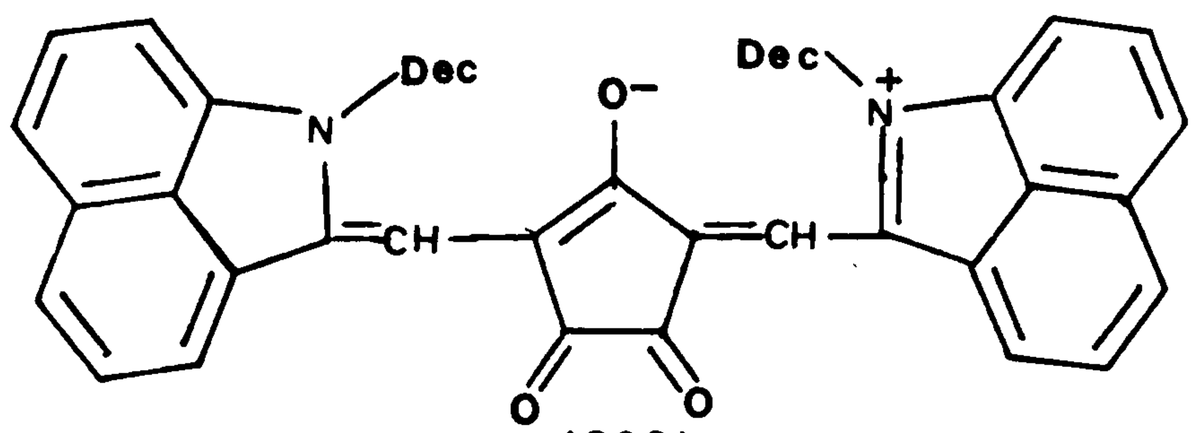

(208)

M+1 peak by FAB-mass spectrometry. As expected it was exceptionally bathochromic with an absorption maximum near 1000nm.

2.3.2.3 Light Absorption Properties of the Croconium Dyes

The spectroscopic properties of the croconium dyes were measured in toluene and dichloromethane. The results are summarised in Tables 34 and 35.

From the data of Table 34 it can be seen how the croconium system is particularly useful for effecting near-infrared absorption using only moderately powerful electron donor residues, such as 3-hydroxy-N,N-dialkylanilines. In fact it would seem that every croconium dye that can be synthesised using currently known procedures will inevitably be near-infrared absorbing.

Dyes (203) and (204) exhibited an almost negligible positive solvatochromism whereas the more bathochromic dye (207) exhibited negative solvatochromism. As expected, dye (204) absorbed at a longer

Table 34: Absorption spectra of the croconium dyes

Dye	λ_{max}/nm (CH_2Cl_2)	(Toluene)	ε_{max}/$lmol^{-1}cm^{-1}$ (CH_2Cl_2)	$\Delta\lambda_{max}$/nm (CH_2Cl_2-Tol)
(203)	822	820	214,000	+2
(204)	854	853	203,500	+1
(205)	— 882(a)	—	—	—
(207)	886	900	186,300	-14
(208)	— 1014(b)	—	—	—

(a) - hot DMF,(very low solubility in CH_2Cl_2 and toluene)
(b) - measured in trichloroethane : acetone (12:1)

wavelength than (203), demonstrating the enhanced electron donor strength of the julolidine system.

The extinction coefficients, where it was possible to record them, were extremely high, which is a reflection of the extensively delocalised nature of these dye molecules coupled with a high degree of electronic symmetry. These characteristics also lead to dyes that have very narrow band widths. This is demonstrated by Fig. 17, which shows the visible - near-infrared spectrum of dye (203). It is also

Fig. 17: Visible - near-infrared spectrum of dye (203) in dichloromethane

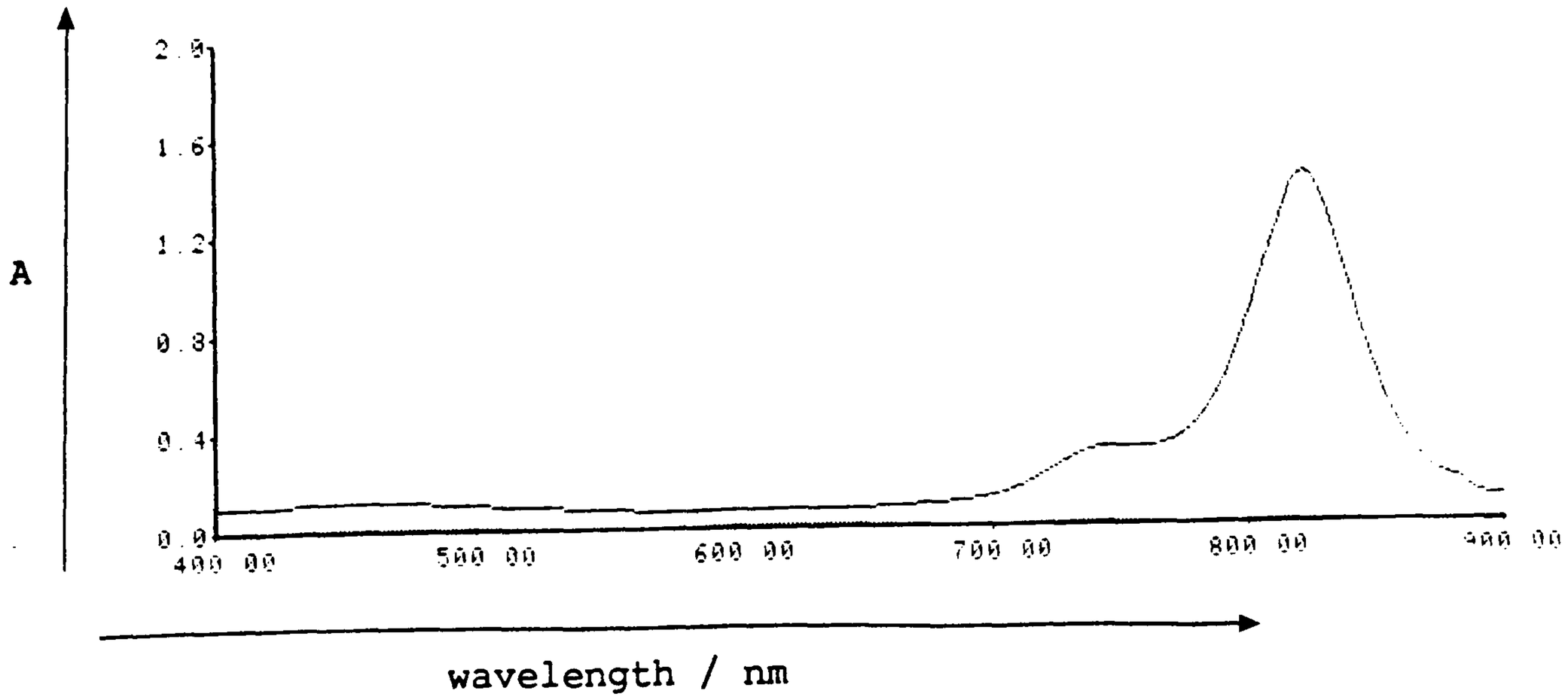

A - absorbance

noteworthy that, as with the squarylium dyes, the croconium dyes possess minimal visible absorption between 400 - 700nm.

The PPP-MO method was then applied to the calculation of the spectra of representative dyes, and the results are summarised in Table 35. For the 3-hydroxy-substituted dyes, eg. (203), and the analogous acylamino dye (207) it was assumed that two of the croconium carbonyl groups were hydrogen bonded to the adjacent -OH or -NH protons.

Table 35: Comparison of PPP-MO calculated and experimental values for representative croconium dyes

Dye	λ_{max}/nm (Calc)	λ_{max}/nm (Toluene)	$\Delta\lambda_{max}$/nm (Tol-Calc)	Oscillator strength (f)(Calc)
(203)	833	820	+13	1.34
(207)	922	900	+22	1.26
(208)	1155	1014[a]	+141	2.26

(a) - solvent = trichloroethane : acetone (12:1)

It can be seen from Table 35 that good agreement between theory and experiment was found for (203) and (207). The calculated λ_{max} value for dye (208) was less satisfactory, being much higher than the observed value. For this dye the VSIP and electron affinity parameter values of 17.75eV and 7.75eV respectively for the benzindole nitrogen atom were those described previously in Section 2.1.3.2. This overestimation of the λ_{max} value may, in part, be due to the assumed planarity of the dye chromophore, whereas in fact the n-decyl group will cause loss of planarity due to steric crowding.

The calculated ground state charge density and the π-electron density changes for the visible absorption bands of dyes (203) and (208) are summarised in Figures 18 and 19 respectively.

Fig. 18: <u>(a) Ground state electron densities and (b) π-electron density changes for the first absorption band of dye (203)</u>

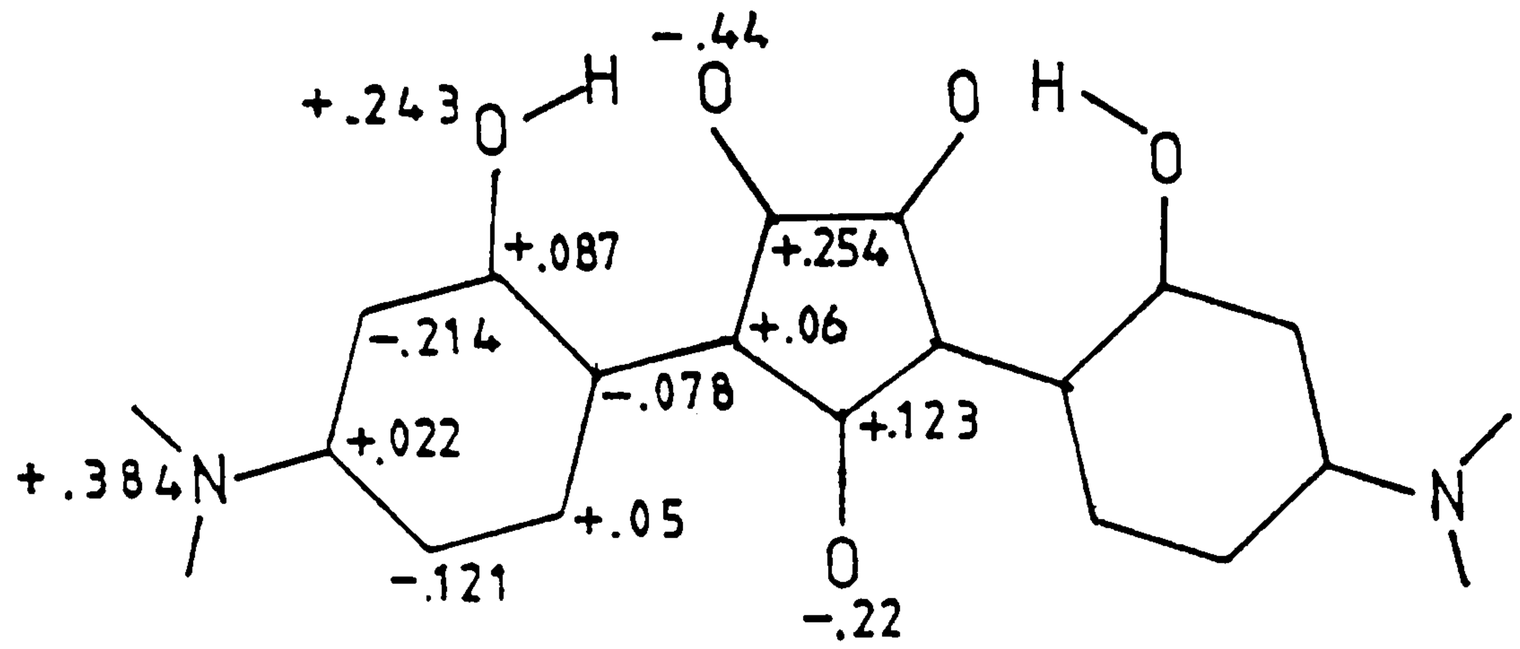

(a)

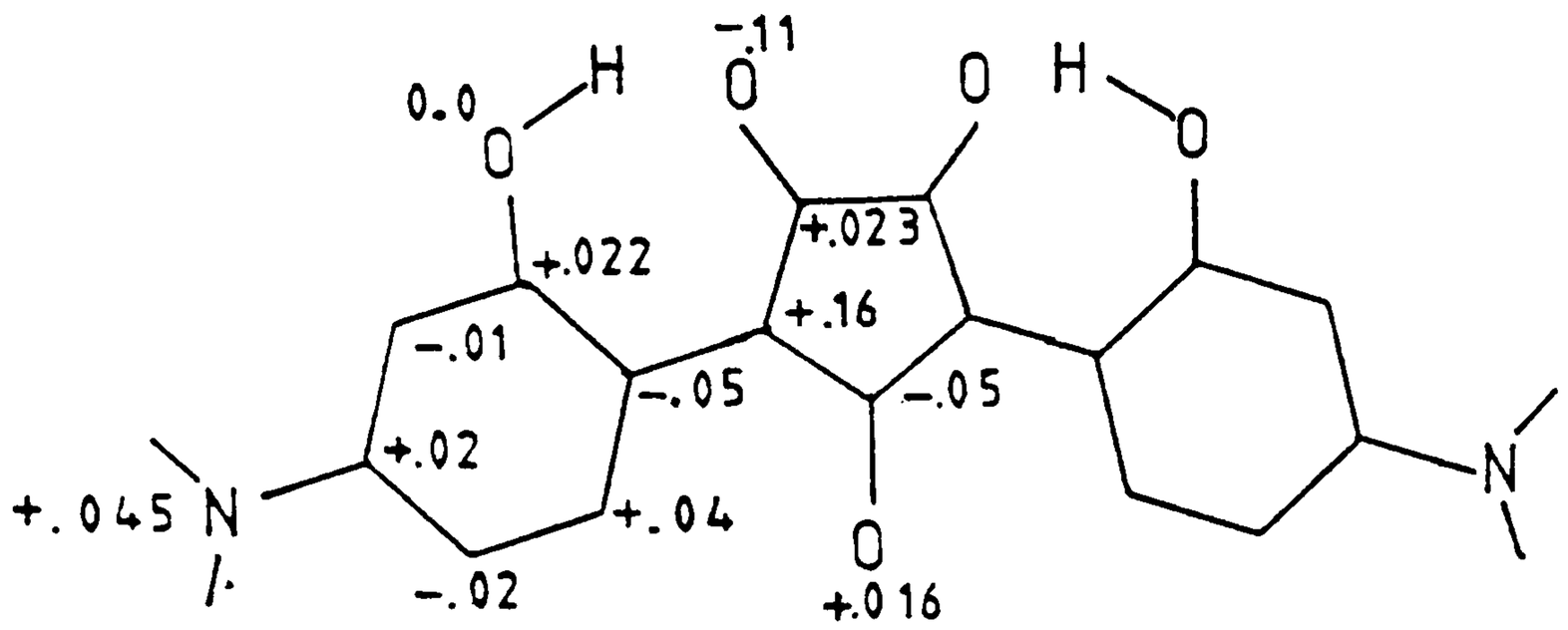

(b)

λ_{max} (calc) = 833nm

λ_{max} (toluene) = 820nm

From the ground state charge densities of both (203) and (208) it is apparent that the systems are typical donor-acceptor chromophores. Thus the nitrogen atoms are electron deficient and electron density is transferred extensively to the three central carbonyl groups.

The chromophores have nearly complete electronic symmetry as shown by Figs. 18(b) and 19(b). Thus a relatively small redistribution of electron density occurs after electronic excitation. As stated previously, this high degree of electronic symmetry is synonymous with narrow absorption bands.

It is notable from Fig. 18(a) that the hydroxyl group in the donor aryl residues also donate a significant amount of electron density to

Fig. 19: <u>(a) Ground state electron densities and (b) π-electron density changes for the first absorption band of dye (208)</u>

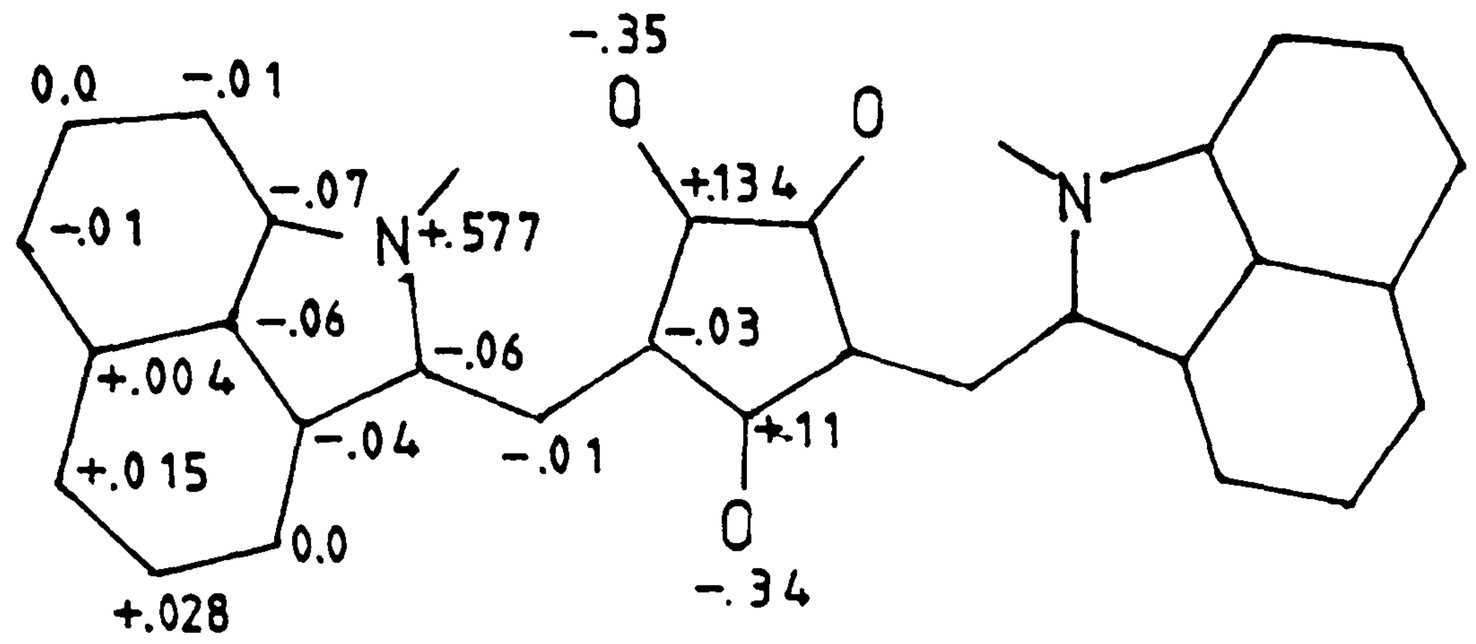

(a)

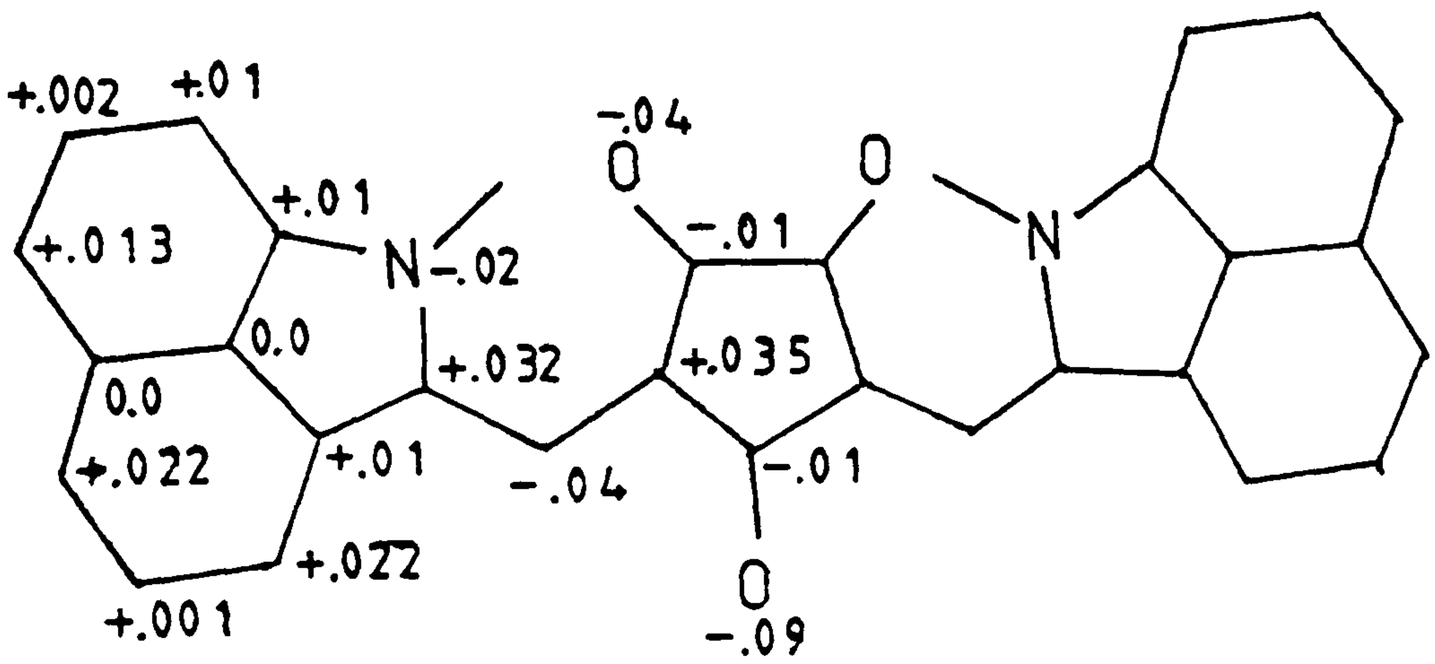

(b)

λ_{max} (calc) = 1155nm

λ_{max}* = 1014nm

* measured in trichloroethane : acetone (12:1)

the croconium ring in the ground state but the groups make no contribution to the electron density changes accompanying electron excitation [Fig. 18(b)].

In Fig. 19(b) it is also interesting to note that the migration of electron density is not as might be expected. Thus, rather than migration of electron density from the donor nitrogen atoms to the acceptor carbonyl groups, there is a loss of electron density from

both amino and carbonyl groups with a build up of electron density in the aromatic rings.

2.3.2.4 Stability Properties of the Croconium Dyes

The stability properties of the croconium dyes were assessed in cellulose acetate film by the techniques described previously in Section 2.2.1.4. The results are summarised in Table 36. The simple monoazo dye (148) was taken as the standard as in previous stability tests.

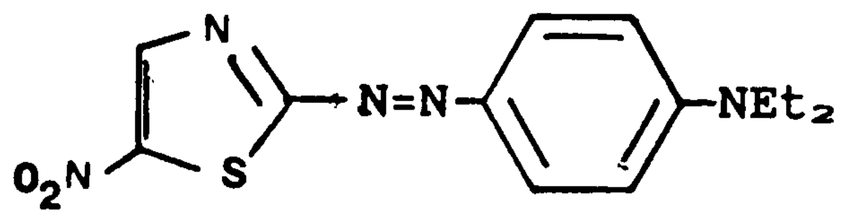

(148)

Table 36 : Stability properties of selected croconium dyes in cellulose acetate films

Dye	Photo stability (% loss)	Thermal stability (% loss)
Standard (148)	8	5
(203)	66	87
(204)	30	90
(207)	65	total decomposition
(208)	21	total decomposition

It was not possible to assess the stability properties of dye (205) as it was too insoluble to be effectively cast into the film.

Unlike the squarylium dyes discussed in Section 2.3.1.4 the stability properties of the croconium dyes do not appear to follow any specific trends. For example, if thermal stability is considered then the usual trend of decreasing stability with increasing bathochromic shift of the dye is observed. Thus the stabilities of (207) and (208)

are so low that total decomposition of the dye on the cellulose acetate film occurred during the test period (190°C for 60 minutes), whereas the dyes (203) and (204) were rather more stable. On the other hand, the lightfastness properties are less predictable and the most bathochromic dye (208) was also the most stable. Surprisingly the julolidine dye (204) was more photostable than (203), the reverse of the situation normally found with julolidine-based systems in other dye classes[6a].

On the whole the croconium dyes had very poor thermal stability properties and significantly poorer lightfastness properties when compared to the standard.

A comparison of the stability properties of (208) with the analogous squarylium dye (194) (Table 33; Section 2.3.1.4) shows the croconium dye to have only slightly lower photochemical stability, but much inferior heat stability than its squarylium counterpart. It is interesting to note however that the photochemical stability of (194) is significantly better than that observed for the other infrared absorbing squarylium dyes and that of (208) is much better than those obtained for the other croconium dyes. It would appear that, as well as imparting a significant bathochromic shift, the benzindole residue (158) also lends itself to infrared absorbing dyes of greater photostability than would perhaps be expected.

2.3.2.5 An Examination of the Mechanism of the Condensation Reaction Between Croconic Acid and Arylamines

The mechanism of the reaction between squaric acid and tertiary arylamines has been investigated[61,62], and shown to involve initial formation of a squarate half-ester with the alcohol component of the solvent. This then reacts with the arylamine (see Section 1.3.5.1). No such investigations have been undertaken for the analogous

reactions with croconic acid, and thus a series of experiments were devised to try and define the parameters that control this condensation reaction.

When examining the synthesis of dye (204) it was noted that 8-hydroxyjulolidine and croconic acid reacted readily in ethanol at room temperature to give (204). Unlike the corresponding squaric acid

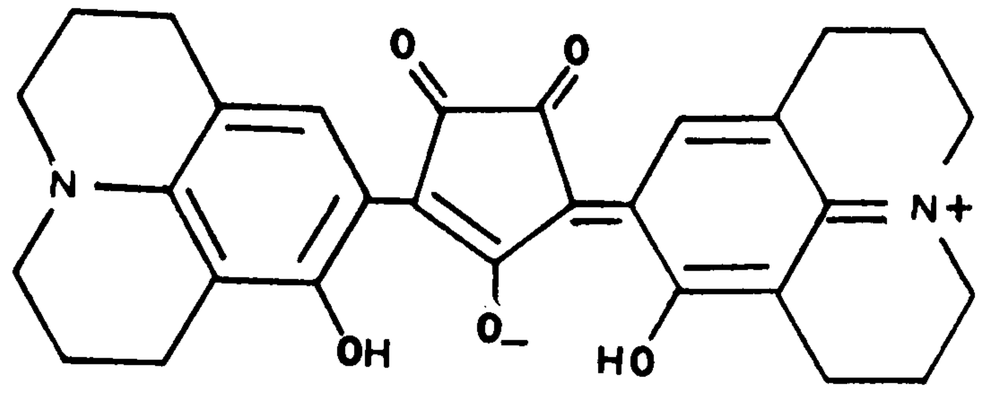

(204)

reaction, azeotropic removal of water was unnecessary for the reaction to proceed to completion. This reaction was therefore very useful for mechanistic studies, particularly as the formation of (204) could be monitored readily by absorption spectroscopy.

The reaction was studied kinetically and the effects of different solvent systems, acids, and base catalysts on the reaction rate were determined.

Solvent effects were examined by rapidly mixing equal volumes of a solution of croconic acid and a solution of 8-hydroxyjulolidine in the appropriate solvent system to give a solution containing 0.88×10^{-4}mol of croconic acid and 1.76×10^{-4}mol of 8-hydroxyjulolidine in 10ml of solvent. The solution was then transferred to a 1mm pathlength quartz cell and held at the appropriate temperature, while the absorbance at the λ_{max} of the dye (204) was measured at various intervals of time. Zero time was taken as the moment of mixing the two solutions.

The reaction showed an induction period, during which little conversion to (204) occurred, and then reaction commenced at a steady rate until almost complete. A typical rate profile is shown in Fig. 20 for the reaction in n-propanol. The gradient of the linear

Fig. 20: Rate of formation of dye (204) in n-propanol at 30°C

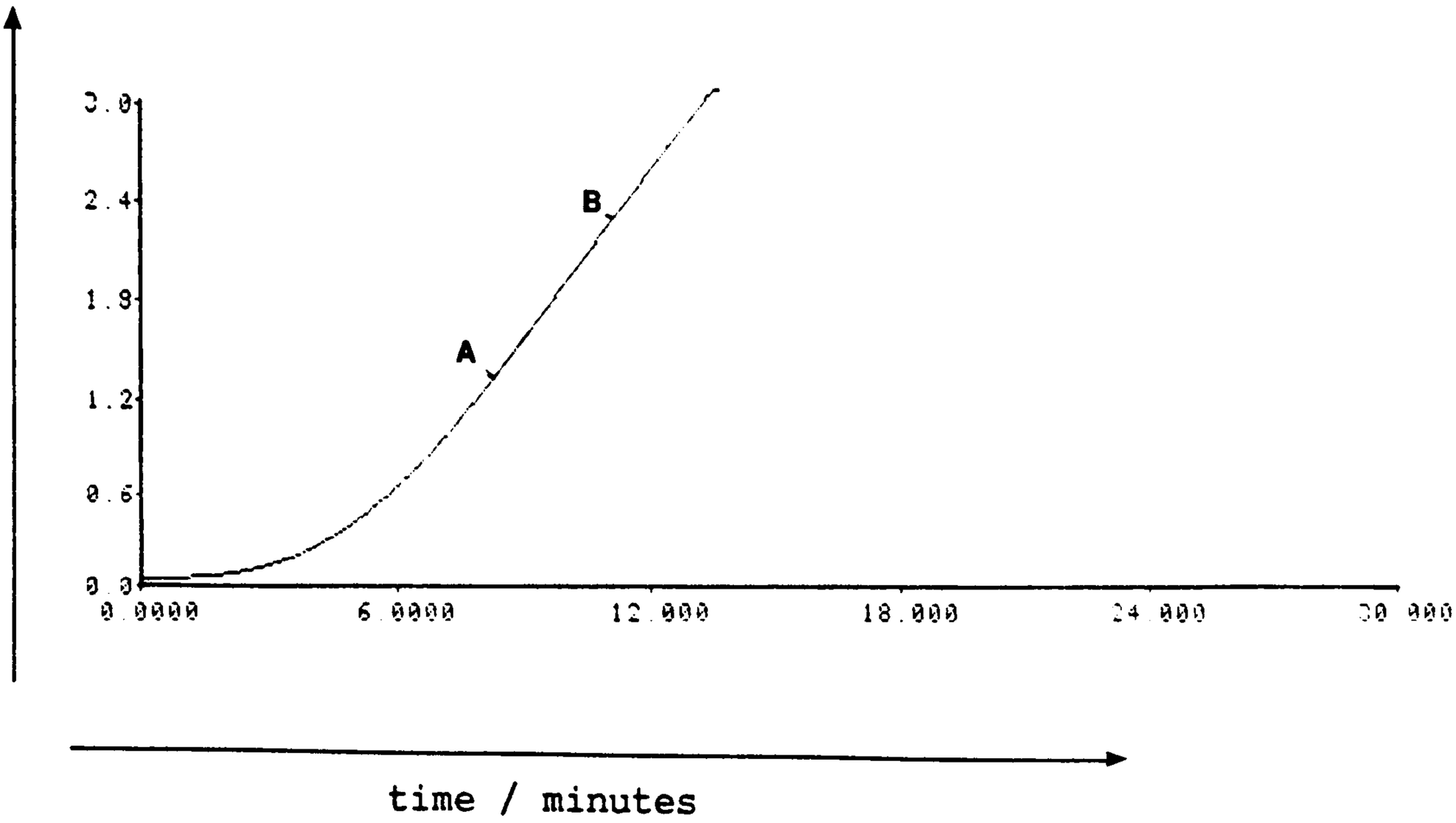

A - absorbance

part of the curve (i.e. between A and B) was taken as a measure of the reaction rate.

Initially, pure solvents were considered, namely methanol, ethanol, n-propanol, n-butanol, n-pentanol, isopropyl alcohol, 2-methyl-1-propanol, dimethylformamide, and acetonitrile. The calculated gradients of the rate curves are summarised in Table 37. Dielectric constants of the relevant solvents are also listed. The reactions were all carried out at 30°C over a 30 minute time period, recording the absorbance at λ_{max} in each solvent at 30 second intervals.

Attempts to carry out dye synthesis in solvents other than those given in Table 37 were hampered by the low solubility of croconic acid in such solvents at room temperature. Thus it was not possible to dissolve croconic acid in n-hexanol or any higher alcohols, nor was it sufficiently soluble in ethyl acetate, dichloromethane, toluene, or diethyl ether.

The results in Table 37 show that dye formation does not occur significantly in acetonitrile or dimethylformamide during the

Table 37: The rates of formation of dye (204) in selected pure solvents at 30°C

Solvent	Dielectric constant Σ	Gradient/absorbance units per second
methanol	32.7	0.15
ethanol	24.6	0.17
n-propanol	20.3	0.34
n-butanol	17.5	0.37
n-pentanol	13.9	0.38
iso-propanol	19.9	0.32
2-methyl-1-propanol	17.7	0.45
dimethylformamide	36.7	0.00
acetonitrile	37.5	0.00

30 minute time period set for this experiment. However, after leaving for 5 hours in the dark at room temperature a small amount of dye could be detected in each solution. Therefore, although reaction does occur in these two solvents, they are far less effective than alcohol solvents.

From Table 37 it is apparent that in alcohols the reaction rate increases with increasing chain length in the series methanol to n-pentanol. At first sight this would seem to be related to the decrease in dielectric constant as the chain length increases. However, other factors such as solvation of the reactants or of a reactive intermediate appear to play a role in the reaction. For example, the rate of dye formation is only slightly enhanced in ethanol relative to methanol, even though the decrease in dielectric constant in ethanol is very large. On the other hand, on passing from ethanol to n-propanol, where there is a much smaller decrease in dielectric constant, the rate of dye formation doubles. It is

probable that in methanol and ethanol there is strong solvation of the reactants, so retarding the reaction. With longer aliphatic chains, solvation will be less effective and dielectric effects become more significant. This theory would also help explain why 2-methyl-1-propanol showed the highest rate of reaction, even though its dielectric constant is higher than that of n-butanol and n-pentanol. Steric effects would make 2-methyl-1-propanol even less effective as a solvating species than n-butanol or n-pentanol.

As alcohols are clearly important in the dye forming process, it was of interest to examine the influence of the concentration of the alcohol in an inert solvent on reaction rate. The alcohol chosen for this series of experiments was n-propanol. Various diluent co-solvents were then examined in conjunction with this alcohol. Water was examined as an example of a highly polar protic solvent, dimethylformamide and acetonitrile as examples of polar aprotic solvents, and toluene as representative of a non-polar aprotic solvent. These solvents were mixed with n-propanol to give proportions of n-propanol ranging from 10% to 90%, and the rate of formation of dye (204) was measured as before.

The experimental measurements for the water and toluene systems were taken over 30 minutes, at 30 second time intervals because of the high reaction rate. For the dimethylformamide and acetonitrile systems, reactions were carried out over 1 hour, monitoring at 1 minute intervals. The results are summarised in Table 38.

It is clear from Table 38 that in the case of water the rate of dye formation decreases as the percentage of water increases, until no dye is formed over the time period of the experiment when 50% water is present. This may be due, in part, to the progressive increase in dielectric constant as the proportion of water is increased. The dipolar aprotic solvents, namely dimethylformamide and acetonitrile

Table 38: Relative rates of formation of (204) in mixed solvent systems at 31°C

% n-propanol	% co-solvent	Reaction rate of dye formation / absorbance units sec^{-1}			
		water	toluene	dimethyl-formamide	acetonitrile
100	0	0.34	0.34	0.34	0.34
95	5	0.31[a]	0.33	0.091[c]	0.13[c]
90	10	0.22[a]	0.33	0.064[c]	0.12[c]
85	15	0.19[a]	0.32	0.042[d]	0.10[d]
80	20	0.15[a]	0.34	0.029[d]	0.09[e]
50	50	0.00[b]	0.51	0.00[d]	0.06[d]
25	75	——	0.53[a]	——	——
10	90	——	0.63[b]	——	——

(a) - recorded at 30°C
(b) - recorded at 32°C
(c) - recorded at 24°C
(d) - recorded at 26°C
(e) - recorded at 25°C

also appear to severely retard the rate of reaction even when present in low proportions. In the case of toluene as co-solvent, a different effect is observed. From zero to 20% toluene in the solvent system there is little change in the rate of dye formation. However, as the proportion of toluene is increased from 50% to 90% there is a marked increase in the rate of dye formation.

These results show that the alcohol is important in the reaction mechanism and that any factor that increases the dielectric constant of the medium depresses the rate of reaction.

It was noted that in solvents in which the reaction rate is low the solution of croconic acid was noticeably more yellow in colour. This was shown to be due to the dissociation of croconic acid (λ_{max} ca. 300nm), which is virtually colourless, into its monoanion (λ_{max} ca.

370nm) which is yellow. Thus it is probable that the anion is unreactive in the condensation process, and thus the greater the degree of dissociation of croconic acid the lower the rate of reaction.

The relative degrees of dissociation of croconic acid in different toluene - n-propanol mixtures can be seen from Fig. 21. Only at n-propanol proportions below 50% is the concentration of the croconate anion appreciably depressed.

Fig. 21: <u>UV/visible spectrum of croconic acid in toluene : n-propanol solvent mixtures</u>

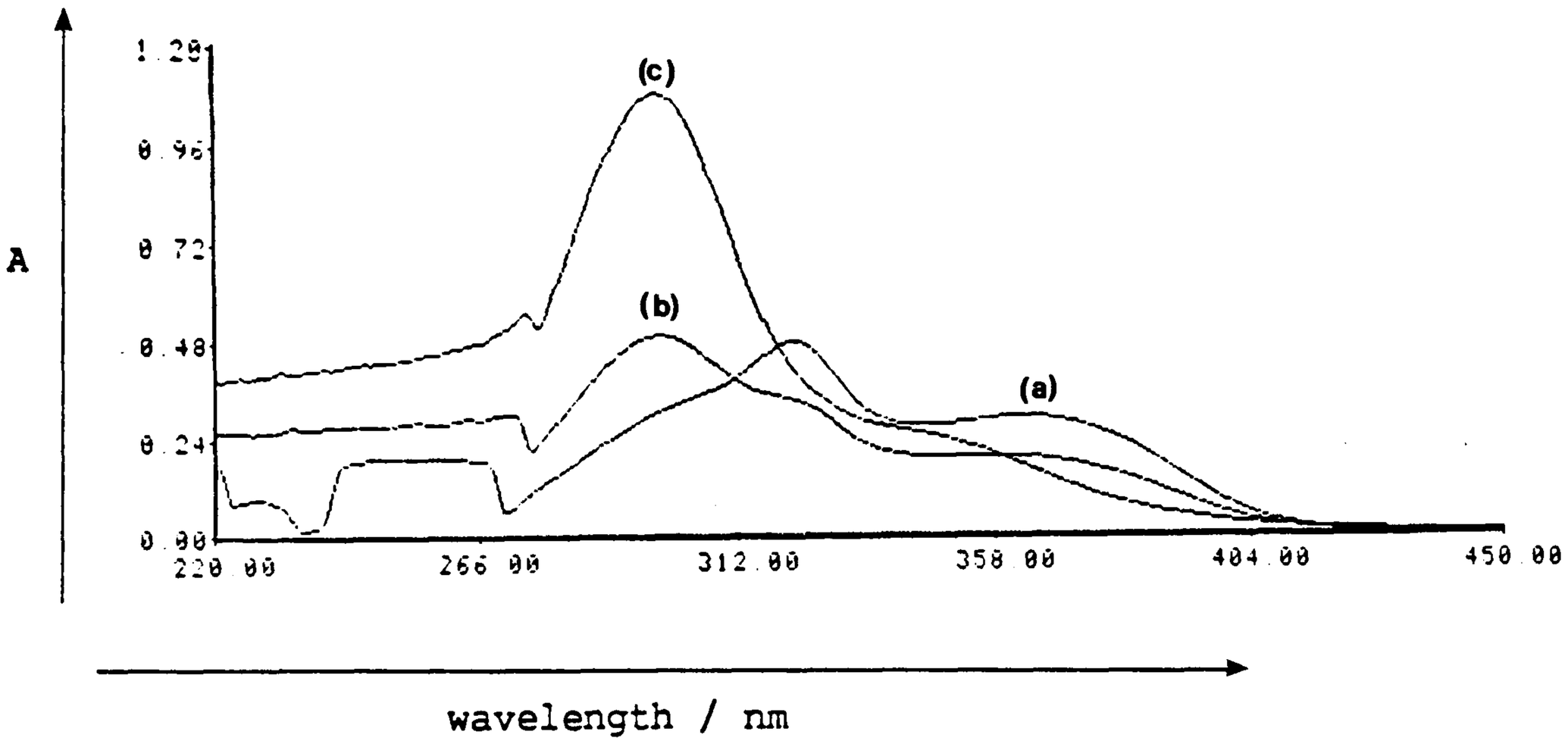

A - absorbance
(a) - 5% toluene : 95% n-propanol
(b) - 50% toluene : 50% n-propanol
(c) - 90% toluene : 10% n-propanol

The effects of acid and base on the rate of reaction confirmed this suggestion. Thus a solvent mixture comprising 90% toluene and 10% n-propanol was used and, after mixing the croconic acid and 8-hydroxyjulolidine reactants in this solvent one drop of a solution of acid or base was added to $2cm^3$ of the reaction solution in a spectrophotometer cuvette. The reaction was then monitored spectroscopically in the usual way. Relative reaction rates for the addition of various acids and bases are summarised in Table 39.

Table 39: The effects of additives on the rate of formation of (204) (90% toluene : 10% n-propanol at 26°C)

Additive (1 drop per $2cm^3$)	Relative rate/ absorbance units per min.	Additive (1 drop per $2cm^3$)	Relative rate/ absorbance units per min.
none	0.44	45% BF_3 etherate in ether	0.048
HCl(10M;aqueous)	0.00	DABCO (1M;ethanolic)	0.00
HCl (1M;ethanolic)	0.11(a)	KOH (1M;ethanolic)	0.00
acetic acid glacial	0.61		

(a) - recorded at 28°C

From Table 39 it is evident that small amounts of mineral acid inhibit or retard the rate of reaction whereas the relatively weak acetic acid accelerates the reaction. The reaction is completely inhibited by base, which supports the earlier suggestion that the

Fig. 22: Effects of acid and base on the uv/visible absorption spectrum of croconic acid (90% toluene : 10% n-propanol)

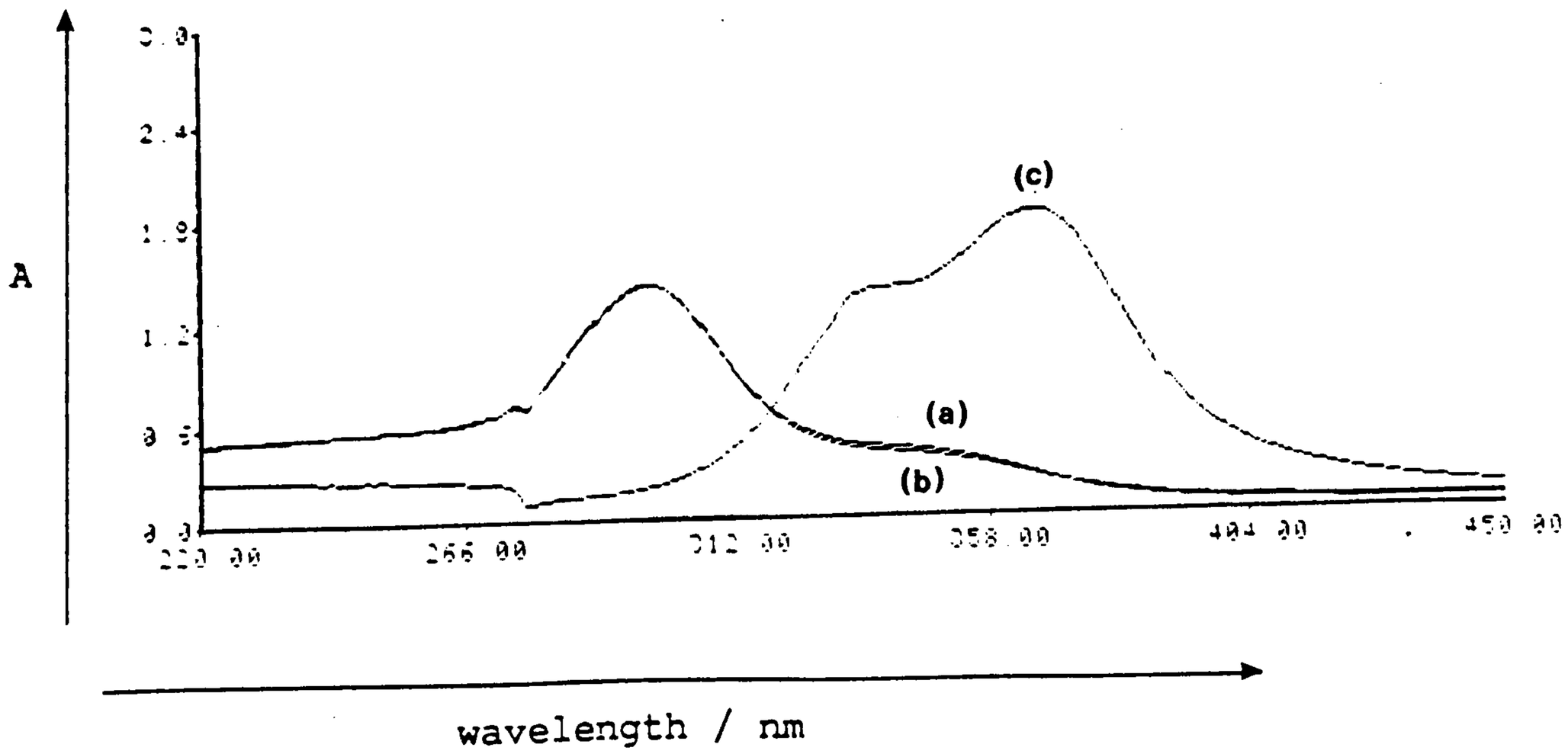

A - absorbance
(a) - no additive
(b) - 1 drop of glacial acetic acid
(c) - 1 drop of 1M ethanilic DABCO

anion of croconic acid is not reactive towards hydroxyjulolidine. As can be seen from Fig. 22, the addition of DABCO at the level indicated in Table 39 causes complete ionisation of the croconic acid. It can also be seen from Fig. 22 that acetic acid has little effect on dissociation.

It is known that the condensation reaction between dialkylarylamines and squaric acid to give squarylium dyes involves the dialkyl 'ester' intermediate of the squaric acid. It was therefore a possibility that the analogous reaction with croconic acid in the presence of alcohols could involve the croconate diester (209).

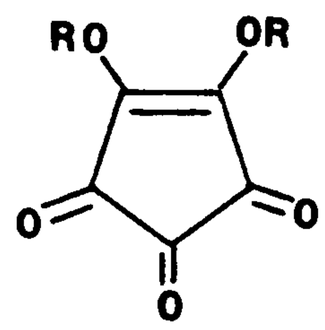

(209)

To examine this possibility diethyl croconate (209; R = Et) was synthesised and its reaction with 8-hydroxyjulolidine carried out.

Thus the diethyl ester was dissolved in a 90% toluene : 10% n-propanol mixture at the same concentration as used for the croconic acid reactions. This solution was then mixed with a similar solution of 8-hydroxyjulolidine and the formation of dye (204) was monitored spectroscopically over a 30 minute time period. However, no absorption at ca. 850nm could be detected at the end of this period. This reaction mixture was then heated on a water bath at 80°C for 20 minutes. A very small amount of dye (204) was detected. Thus it would seem that the diester is not an important intermediate in the reaction of croconic acid with 8-hydroxyjulolidine.

That the alcohol co-solvent is not strictly essential for the reaction was demonstrated by heating the two components in distilled, dry toluene under reflux. A significant amount of (204) was detected

spectroscopically. However, the reaction was very slow and of little preparative value, partly because of the low solubility of croconic acid in toluene. Thus the alcohol may play two roles in the reaction, namely as a specific reactant and as a good solvent for croconic acid.

In summary, the reaction between croconic acid and 8-hydroxyjulolidine proceeds more rapidly in the presence of an alcohol solvent, diluted extensively with a non-polar solvent such as toluene. The reaction is catalysed by traces of a weak acid such as glacial acetic acid, but is inhibited by strong acids, bases and polar solvents.

The evidence suggests that any factor that causes increased dissociation of croconic acid into its mono- and di-anion will inhibit the condensation reaction and thus the reaction involves croconic acid in its undissociated form. The role of the alcohol solvent in the reaction is uncertain, but does not involve the intermediate formation of the croconate diester. Two possible alternatives are the hemi-ketal [e.g. (210) in Scheme 28] and the half-ester [e.g. (211) in Scheme 28], but there are of course other possible tautomeric structures.

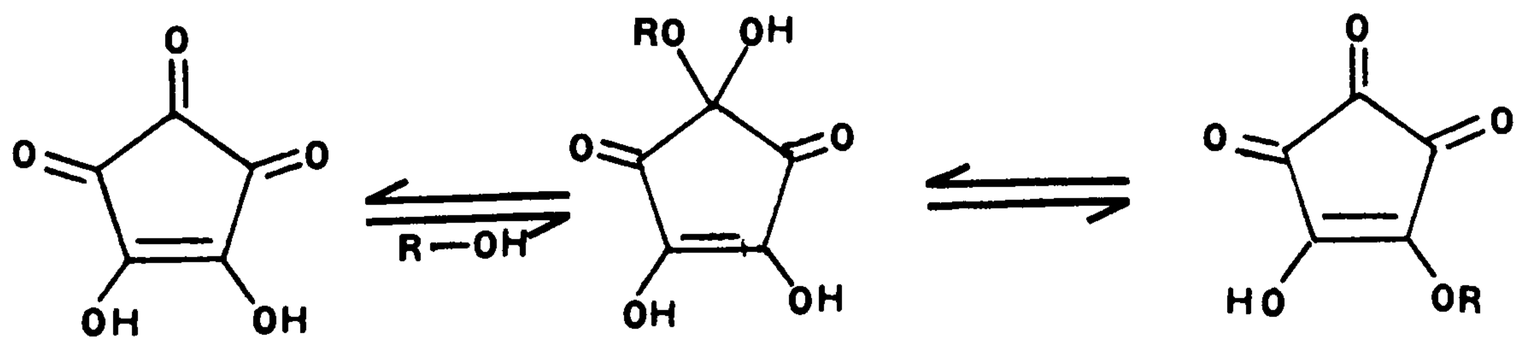

(210) (211)

Scheme 28

The kinetic results suggest the intermediacy of a species such as (210) or (211). Thus the induction period observed in the reaction studies indicate that there is a build up of a colourless intermediate in the early stages of the reaction until formation of the dye becomes apparent.

2.3.3 Conclusions : The Oxocarbon Dyes as Infrared Absorbers

The spectroscopic data in Tables 31 and 34 indicates that with the use of suitably powerful electron donor residues it is possible to shift the visible absorption band of squarylium and croconium dyes into the near-infrared region of the spectrum. Table 34 shows that only moderate nucleophilic arylamines are needed to effect near-infrared absorption in the case of the croconium dyes.

Both the squarylium and croconium dyes have narrow intense bands which makes them suitable for use in optical data recording systems employing diode lasers.

The infrared dyes also have the rare property of being virtually colourless to the human eye [at concentrations giving strong absorption (>80%) at 800nm]. This is a desirable feature for some applications, e.g. security coding systems.

The main disadvantage of these dyes is their generally poor stability, the general trend being the more bathochromic the dye, the more unstable the dye to heat and light. However, for some applications the stability would be adequate, and photostability could be enhanced further by using ultraviolet screens.

2.4 HIGHLY BATHOCHROMIC DYES DERIVED FROM ELECTRONEGATIVE CHLORO-COMPOUNDS

In donor-acceptor dyes, the electronegative acceptor residue is often introduced by converting it to a carbanion, if it contains a suitable active methylene group. This is then condensed to an electron rich aldehyde or nitroso compound, which provides the electron donor residue. This method is invaluable for the dicyanovinyl, pyridone, pyrazalone and other electron acceptor systems. A different approach to donor-acceptor dyes is to use a halo-derivative of an electronegative residue, e.g. 2,4-dinitro-

chlorobenzene. This can then be condensed with an electron rich arylamine, or enamine. An example of such a reaction is shown in Scheme 29, studied in detail by Blackburn[141].

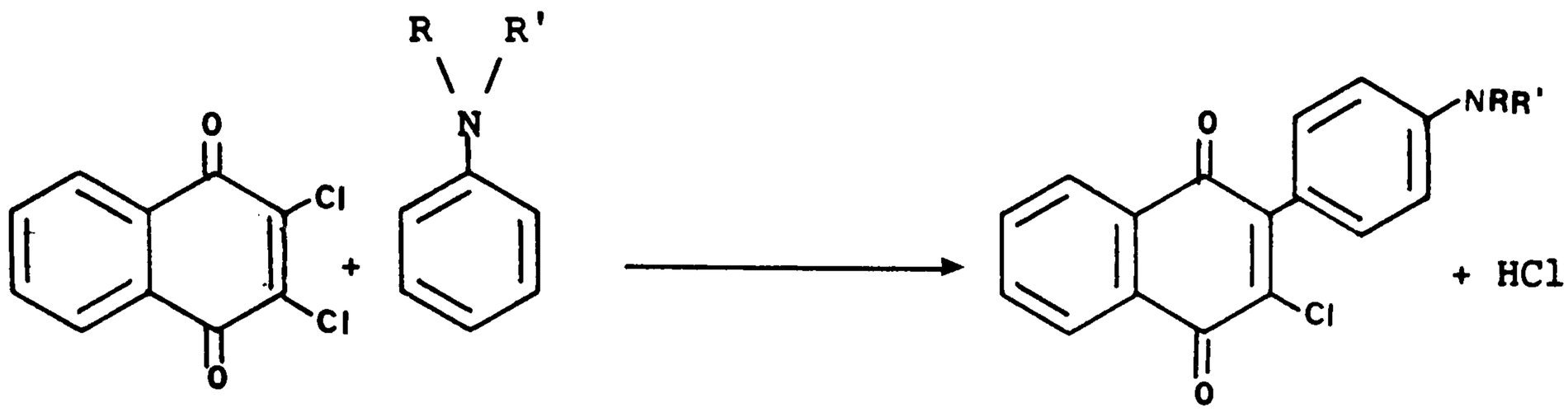

Scheme 29

This is a useful general way of making donor-acceptor dyes, where the acceptor residue is directly attached to the aromatic ring of the donor residue.

For such reactions to work there must be strong electron withdrawing groups present in order to make the chlorine atom particularly susceptible to nucleophilic substitution.

The active chloro compounds used in this work were the pyrroline derivative (212) and the thiophene derivative (213).

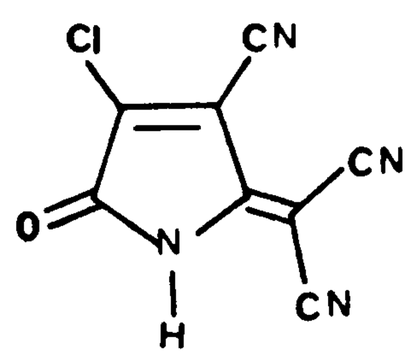

(212)

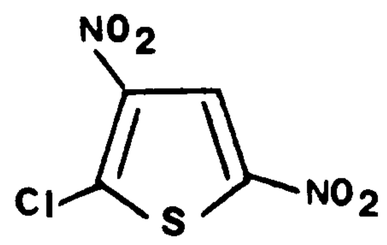

(213)

2.4.1. Synthesis of Dyes and Intermediates

The pyrroline derivative (212) was synthesised by the literature method[142,143], but the final chlorination stage was carried out more effectively with thionyl chloride instead of the quoted oxalyl chloride.

The thiophene derivative (213) was available from work carried out previously in this department[144].

The dihydroperimidine and perimidine intermediates, Michler's ethylene, and 1-decyl-2(1H)-methyl-benz[c,d]indolium iodide used in this work have been described previously.

The pyrroline active chlorine compound (212) was reacted with the appropriate dihydroperimidine and perimidine in ethyl acetate at room temperature to give dyes (214) and (215) respectively. The dyes were

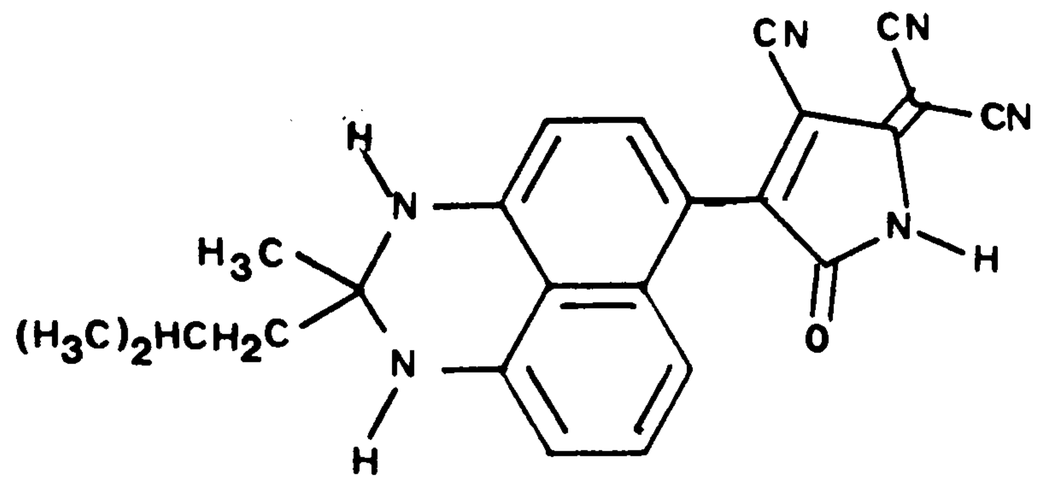

(214)

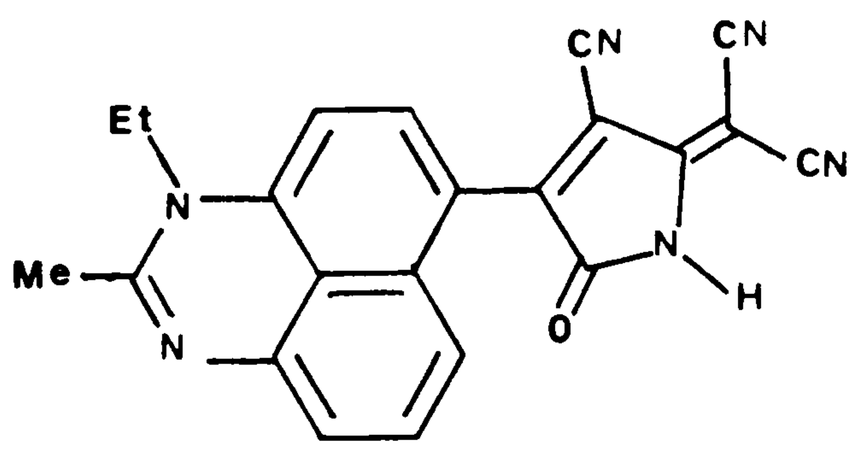

(215)

purified by recrystallisation and were characterised by microanalysis.

The analogous Michler's ethylene derivative (216) was prepared by stirring Michler's ethylene with pyrroline (212) in ethyl acetate at

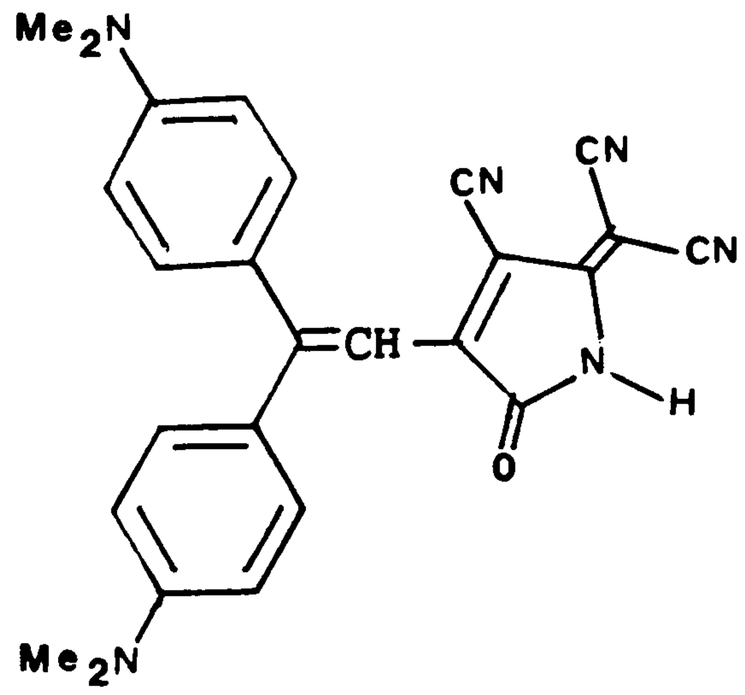

(216)

room temperature. The dye was characterised by mass spectrometry.

The synthesis of the benzindole derivative (217) was effected by

stirring 1-decyl-2(1H)-methyl-benz[c,d]indolium iodide (158) with (212) in ethanol at room temperature. Ethyl acetate was not utilised

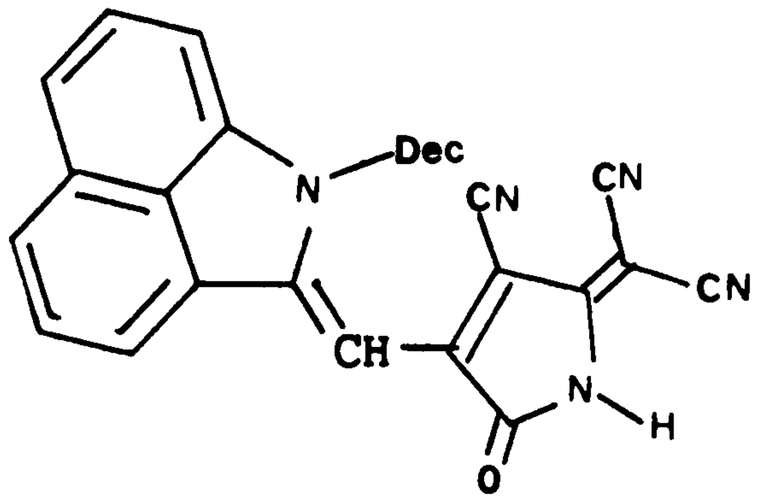

(217)

as the reaction solvent due to the low solubility of (158) in this medium. Even after recrystallisation from ethanol and preparative scale t.l.c., satisfactory microanalytical data could not be obtained for this product. Structural confirmation was therefore obtained by mass spectrometry. Unsatisfactory microanalytical results were generally obtained for the dyes derived from (158) described in this work.

The pyrroline dye (218) was obtained from the reaction of (212) with 2-amino-3-carboxyethyl-4-phenyl-thiophene in acetic acid. This was effected by stirring the solution at room temperature for 2 hours. The blue dye was obtained as bronzy/gold crystals that gave a

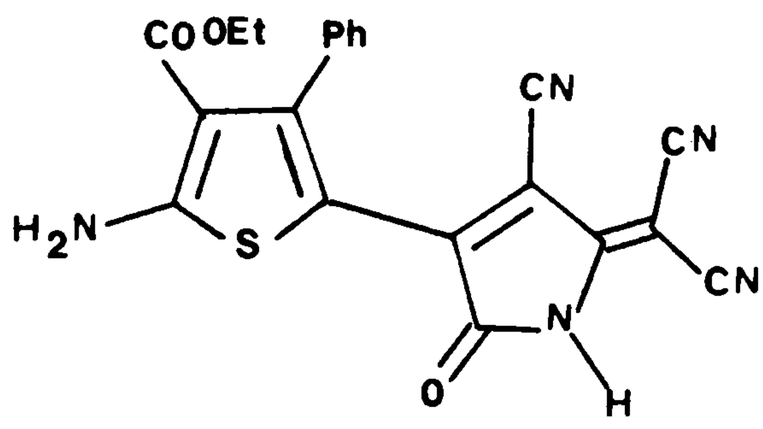

(218)

satisfactory microanalysis. It is interesting that the reaction involves formation of a C-C bond, rather than reaction of the amino group of the thiophene to give a secondary amine.

Attempts were made to diazotise and couple (218) to N,N-diethylaniline to give a dye of formula (219), but the coupling

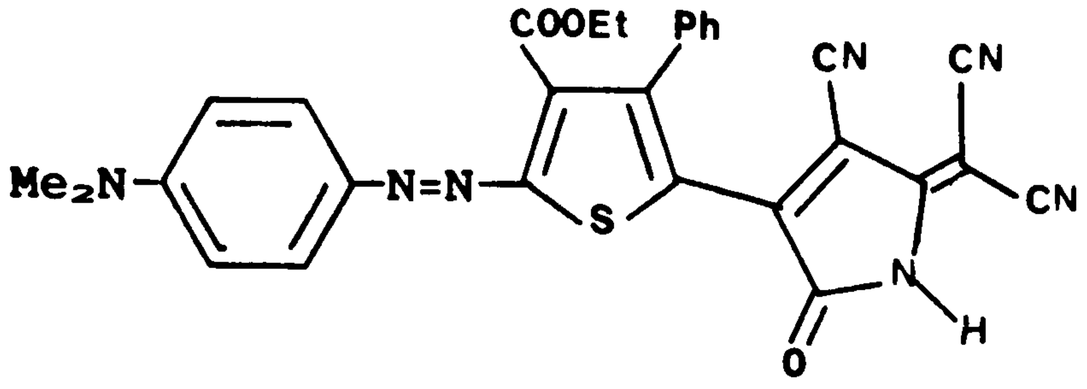

(219)

reaction was very inefficient. The crude reaction product showed a λ_{max} of 630nm, which represents a bathochromic shift of only 20nm relative to (218). The complex nature of the reaction mixture precluded isolation and purification of the dye.

Although attempts were made to synthesise dyes from 2-chloro-3,5-dinitrothiophene (213) analogous to those derived from the pyrroline (212), problems were encountered in isolation and purification of the products. This was somewhat surprising as reactions of the chlorothiophene with the appropriate nucleophile occurred readily at room temperature, with minimal formation of by-products, as shown by t.l.c. analysis.

Thus only the dyes (220) and (221) could be isolated satisfactorily, and these were characterised by mass spectrometry.

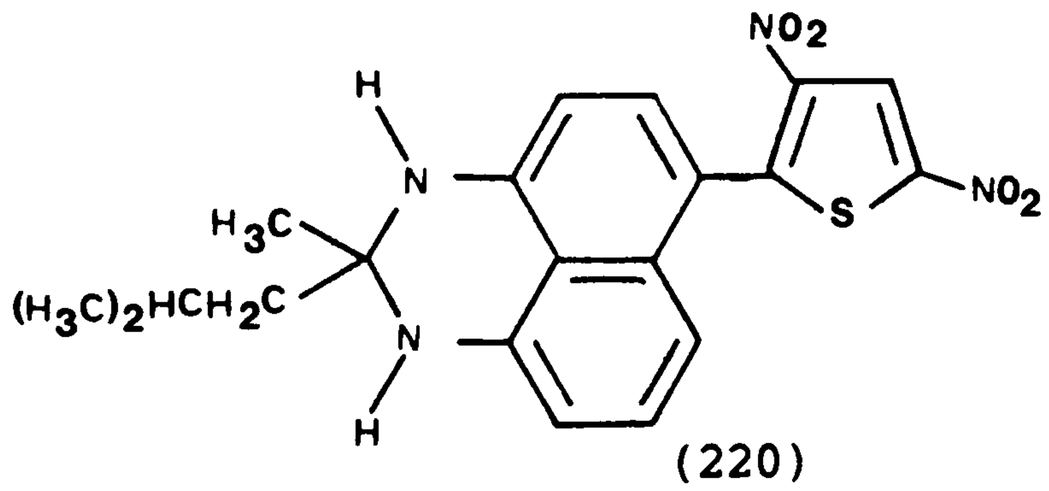

(220)

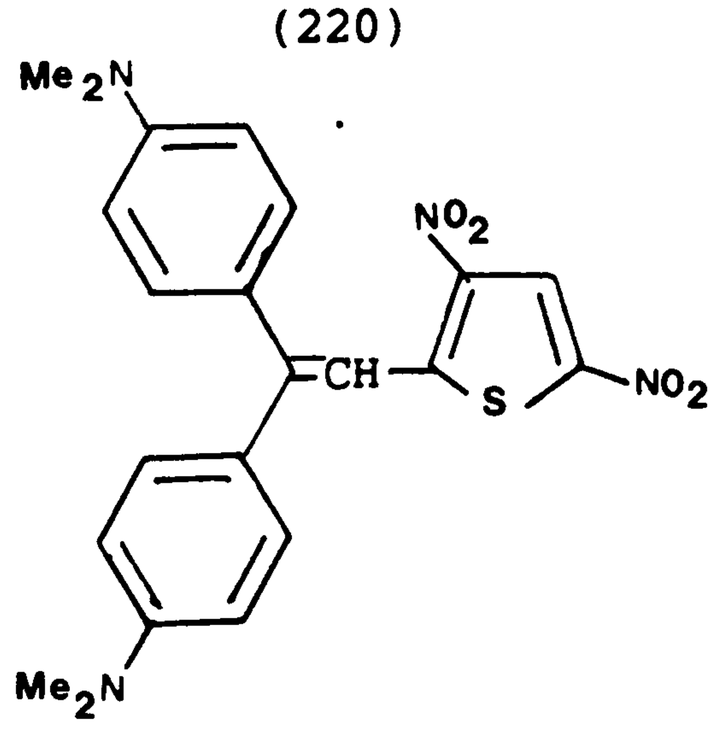

(221)

Both dyes were synthesised by stirring the appropriate nucleophile with (213) in ethyl acetate at room temperature for 2 hours. The dyes were purified by column chromatography over silica gel 60, and (220) was obtained as black, glass-like crystals and (221) as golden brown needles.

2.4.2. Light Absorption Properties

Absorption spectroscopic properties of the dyes (214) - (218), (220) and (221) were measured in acetone and toluene, the former solvent being used to determine molar absorption coefficients (low solubility of the dyes precluded the use of dichloromethane). The results are summarised in Tables 40 - 43.

Table 40: Visible absorption spectroscopic properties of dyes derived from (212)

Dye	λ_{max}/nm (acetone)	λ_{max}/nm (Toluene)	ε_{max}/ $lmol^{-1}cm^{-1}$ (acetone)	$\Delta\lambda_{max}$/nm (acetone-Tol)
(214)	727	702	25,500	+25
(215)	736	745	86,300	-9
(216)	729	713	28,000	+16
(217)	693	692	44,500	+1
(218)	610	595	15,000	+15

Table 41: Visible absorption spectroscopic properties of dyes derived from 2-chloro-3,5-dinitro-thiophene

Dye	λ_{max}/nm (acetone)	λ_{max}/nm (Toluene)	ε_{max}/ $lmol^{-1}cm^{-1}$ (acetone)	$\Delta\lambda_{max}$/nm (acetone-Tol)
(220)	530	515	27,700	+15
(221)	573	550	27,700	+23

Comparison of dyes (214) and (216) with dyes (220) and (221) respectively (Tables 40 and 41) shows the much greater electron accepting ability and thus bathochromic effect of the pyrroline residue (212) relative to the dinitrothiophene (213).

The data of Table 40 also demonstrates the powerful electron donating effect of the donor groups used throughout this work, and for example dyes (214) - (217) are shown to absorb at much longer wavelengths than the thiophene dye (218). Such thiophene residues are generally regarded as strong electron donors in their own right.

Again, from the data of Table 40, it is interesting to note that the perimidine system in (215) absorbs at longer wavelengths than the dihydroperimidine dye (214). This observation is confirmed by the PPP-MO calculated absorption maxima for the two dyes (Table 42). This relative bathochromicity has been found for all the dyes described in this thesis, with the notable exception of the squarylium system. Dye (215) was also the most bathochromic of all the dyes listed in Tables 40 and 41 and was the only one with a sufficiently polar ground state to exhibit a negative solvatochromism.

Fig. 23: Visible - near-infrared spectrum of dye (217) in dichloromethane

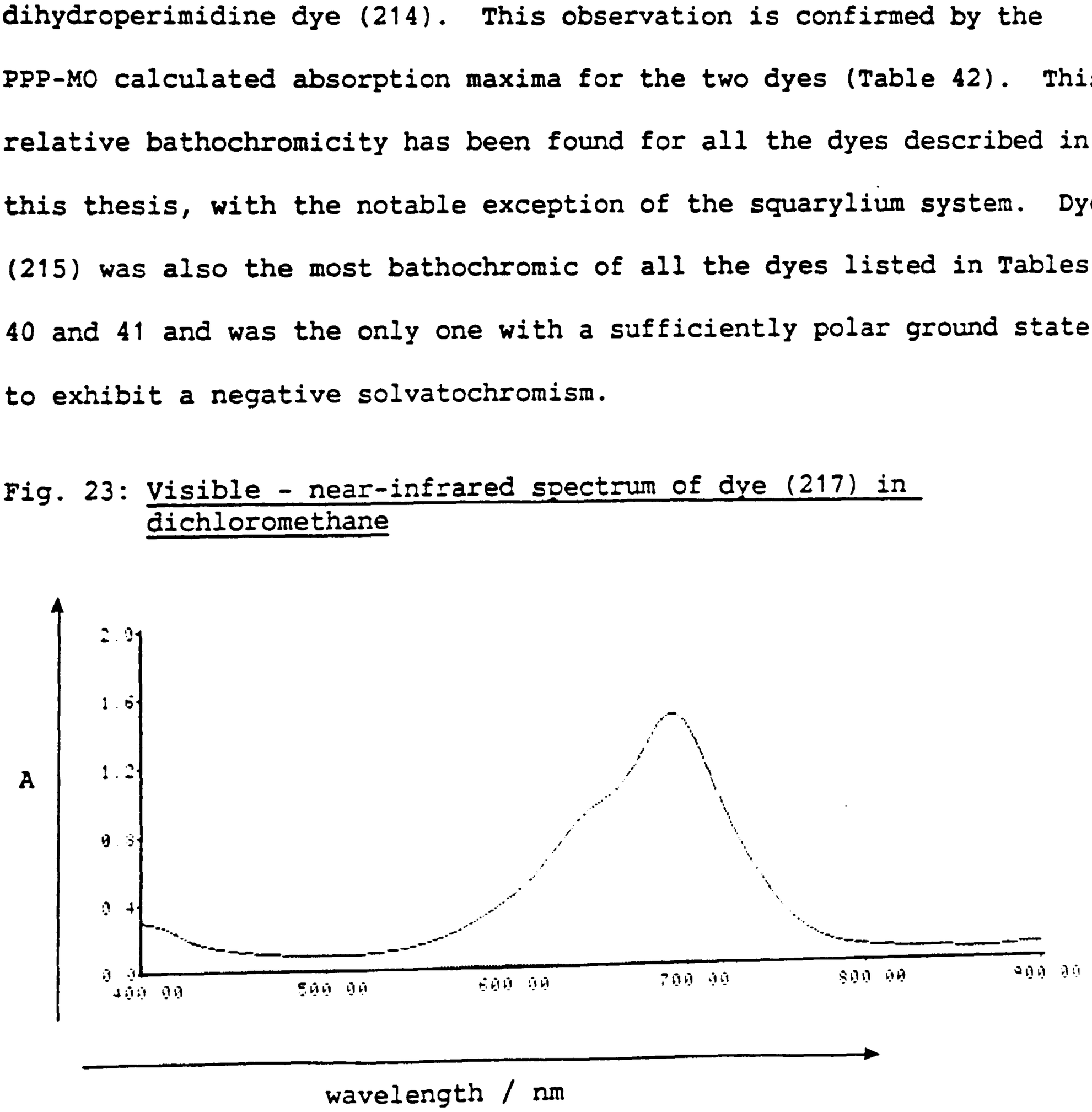

A - absorbance

Near-infrared absorption (λ_{max} > 700nm) was observed with dyes (214), (215), and (216), with dye (217) absorbing just short of 700nm. It should be noted that the absorption curves of all the dyes were very broad, so making the dyes strongly coloured to the human eye. The absorption spectrum of dye (217), shown in Fig. 23 is typical of this series.

With the exception of (215) and (217) the dyes possessed relatively low molar extinction coefficients, which is suggestive of reduced planarity caused by steric crowding. This non-planarity also accounts for the broad absorption bands.

The absorption spectra of the dyes were then calculated by the PPP-MO method. Parameters relevant to the donor parts of the molecule were those previously used in earlier sections. For the acceptor residues in (212) best results were obtained with an electron affinity value of 4.5eV for the cyano nitrogen atoms, in accordance with previously published work[136]. For all other atoms, conventional parameters previously listed were used. The results of MO calculations are summarised in Tables 42 and 43.

Table 42: Comparison of PPP-calculated and experimental absorption spectra of dyes derived from (212)

Dye	λ_{max}/nm (Calc)	λ_{max}/nm (Toluene)	$\Delta\lambda_{max}$/nm (Tol-Calc)	Oscillator strength (f)(Calc)
(214)	756	702	+54	0.84
(215)	758	745	+13	0.46
(216)	752	713	+39	1.1
(217)	674	692	-18	1.1
(218)	632	595	+37	1.2

Table 43: Comparison of PPP-calculated and experimental absorption spectra of dyes derived from (213)

Dye	λ_{max}/nm (Calc)	λ_{max}/nm (Toluene)	$\Delta\lambda_{max}$/nm (Tol-Calc)	Oscillator strength (f)(Calc)
(220)	563	513	+50	0.91
(221)	558	550	+8	0.76

Although the calculated and experimental λ_{max} values are in reasonable agreement, the agreement is not as good as with other dye classes. This will be largely due to the greater degree of steric hindrance present in these dyes. As the PPP-method was used for assumed planar structures the poorer agreement is not surprising. This is exemplified by dyes (220) and (221). In (220) there will be strong steric interaction between the nitrothiophene residue and the peri-hydrogen atom on the dihydroperimidine ring. This will result in twisting of the thiophene ring out of plane, so reducing the absorption wavelength of the dye, and thus the MO-calculated λ_{max} value is overestimated by some 50nm. Such peri steric interactions will be markedly less in (221) and so the observed λ_{max} value is much closer to the calculated value (λ_{max} = +8nm).

The π-electronic characteristics of these chromophores were examined by the PPP-MO method, using (215) and (221) as representative examples. The ground state charge densities and the π-electron density changes for the visible transitions of these dyes are shown in Figs. 24 and 25 respectively.

It can be seen from Fig. 24(a) that in the ground state, dye (215) shows a build up of negative charge on the cyano nitrogens and the carbonyl group of the pyrroline ring and a loss of electron density from the perimidine nitrogen atoms. The high degree of charge separation shows the powerful donor-acceptor character of the

Fig. 24: (a) Ground state charge densities and (b) π-electron density changes for the first absorption band of dye (215)

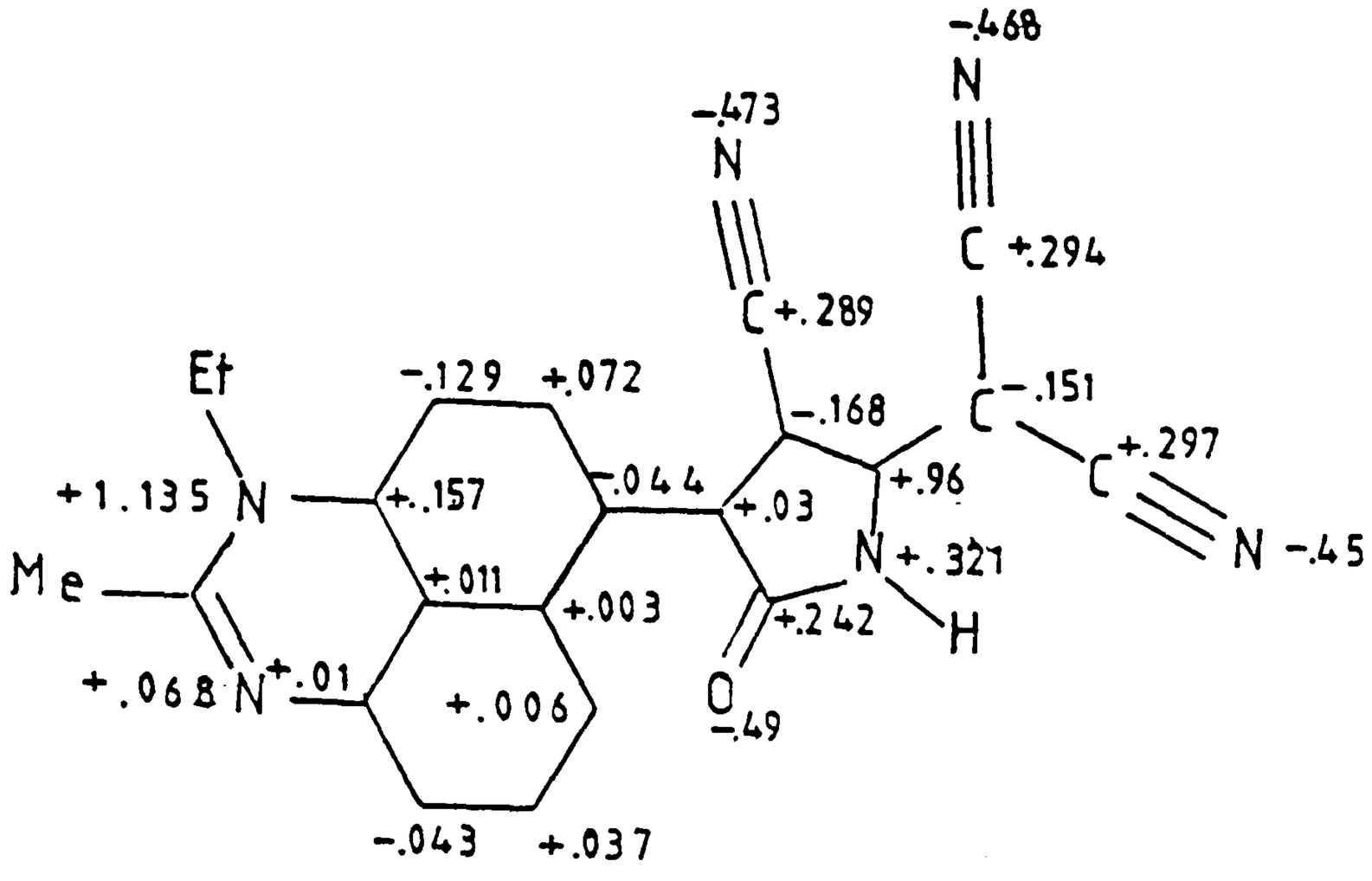

λ_{max} (calc) = 758nm

λ_{max} (toluene) = 745nm

chromophore. Light absorption to give the first excited singlet state results in migration of electron density from the donor atoms to the acceptor part of the molecule, as expected for such a system [Fig. 25(b)]. This trend is mirrored with the dye (221), as shown by Figures 25(a) and (b). Thus it can be seen from Fig. 25(a) that in

Fig. 25: (a) Ground state charge densities and (b) π-electron density changes for the visible transition of dye (221)

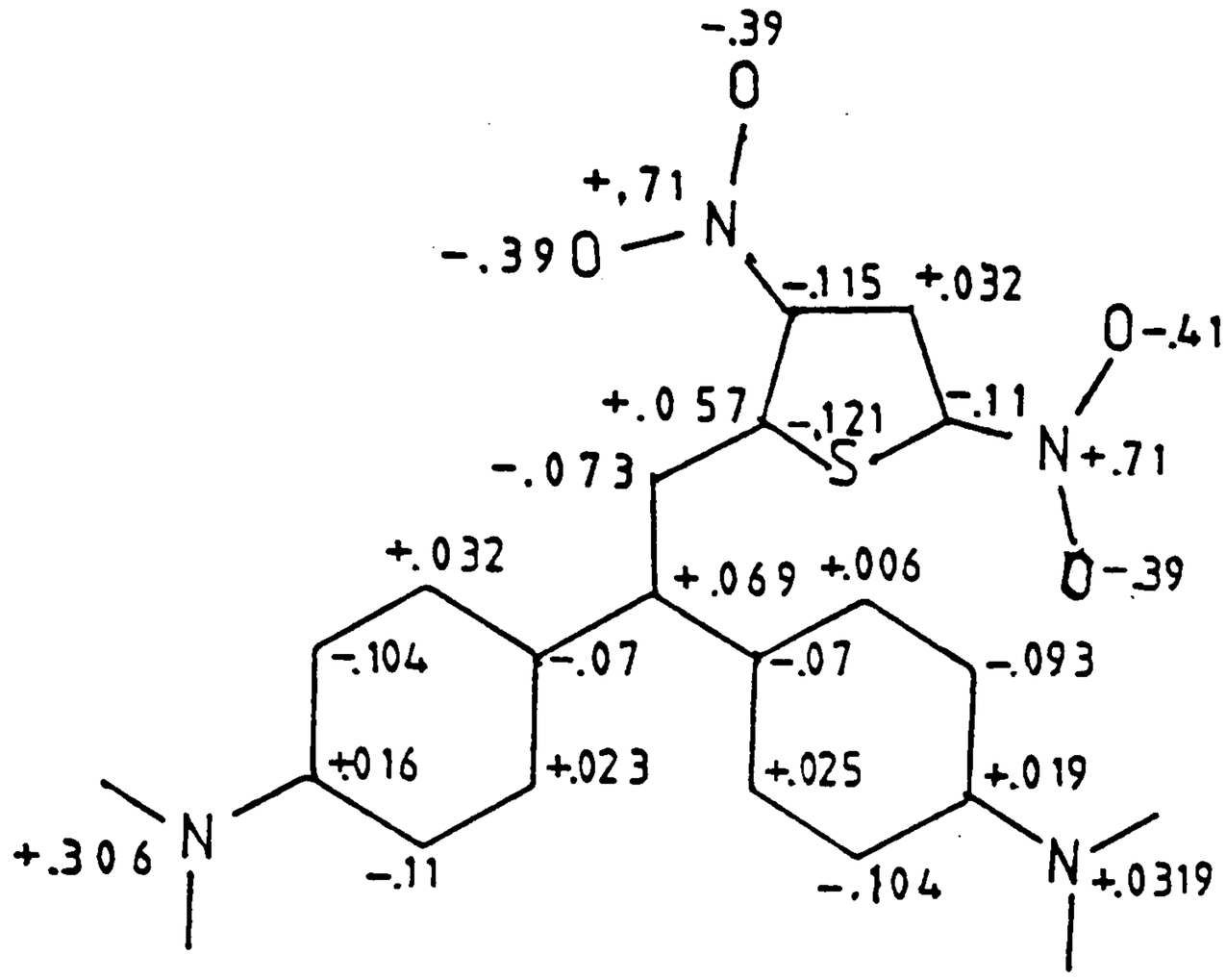

(a)

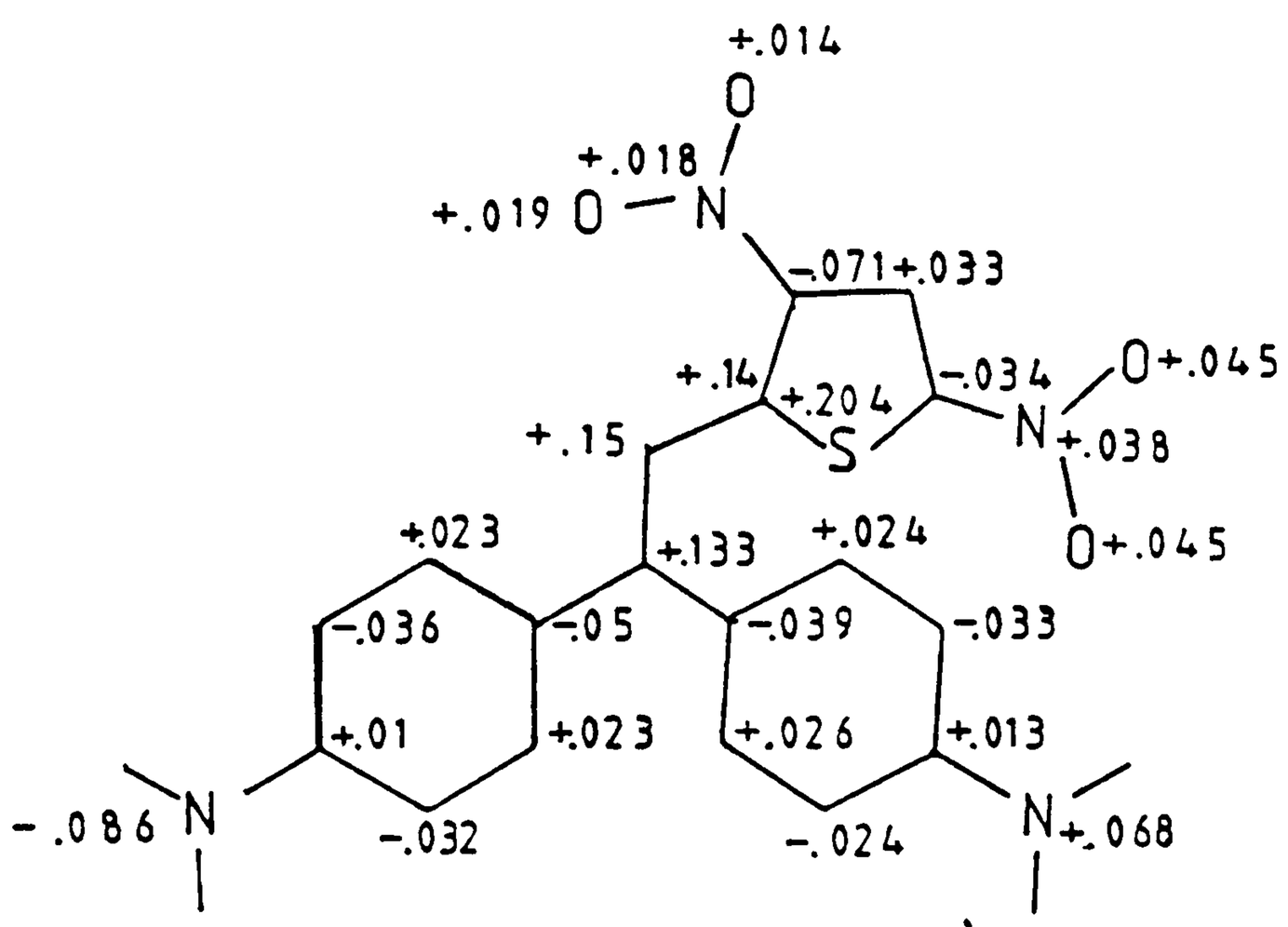

(b)

λ_{max} (calc) = 558

λ_{max} (toluene) = 550

the ground state there is a build up of electron density on the nitro-groups of the thiophene residue and a loss of density from the electron donating dimethylamino groups in the Michler's ethylene part of the molecule. Fig. 25(b) again shows the characteristic migration of electron density from the donor to the acceptor part of the molecule.

2.4.3. Stability Properties

The stability properties of the dyes were assessed by the methods described in Section 2.1.2.4. Thus the dyes were cast into cellulose acetate film and their lightfastness and thermal stability properties assessed relative to the blue standard (148). The results are summarised in Tables 44 and 45.

Table 44: Stability properties of pyrroline based dyes

Dye	Photo stability (% loss)	Thermal stability (% loss)
Standard (148)	8	5
(214)	68	11
(215)	15	2
(216)	39	1
(217)	75	4
(218)	87	27

Table 45: Stability properties of thiophene based dyes

Dye	Photo stability (% loss)	Thermal stability (% loss)
Standard (148)	8	5
(220)	Total Decomposition	27
(221)	Total Decomposition	15

Compared to the standard dye, the lightfastness properties of the dyes in Tables 44 and 45, with the exception of (215) were very poor, and the dinitrothiophene dyes in Table 45 were totally destroyed during the period of the test. The photo- and thermal stabilities of (215) were surprisingly high, particularly as this dye was the most

bathochromic of the dyes in this section.

The thermal stabilities of the dyes were generally much better, however, and dyes (215) - (217) were more stable than the standard dye.

By comparing (214) and (216) with (220) and (221) respectively it is clear that the pyrroline dyes possess both better lightfastness and thermal stabilities than the dinitrothiophene dyes. This is a promising result, as the pyrrolines are far more bathochromic than the analogous thiophene dyes.

2.4.4 Conclusions

This work has proved that by simple room temperature condensation reactions using active chloro compounds it is possible to obtain donor-acceptor dyes that possess near-infrared absorption. The dyes however have broad absorption bands which renders them intensely coloured and they are thus unsuitable for some applications. The solubility of such dyes is generally low in solvents less polar than acetone which restricts their practical value, and although their photochemical stability properties are poor their thermal stabilities are surprisingly good in most cases.

Thus the dyes may show adequate all-round stability if protection from u.v. light is provided, or if photostabilisers are included in media containing the dyes.

3. EXPERIMENTAL

Melting Points

These were determined on an Electrothermal melting point apparatus and are uncorrected. In some instances melting points were measured by differential scanning calorimetry, using a Du Pont Instruments Thermal Analyst 2,000.

Spectra

Infrared spectra were recorded on a Perkin-Elmer 1720 Series Infrared Fourier Transform Spectrometer. Visible and ultraviolet spectra were recorded on a Perkin-Elmer Lambda 15 UV/Visible Spectrophotometer. The instrument was set up according to the parameters cited in Table 46. The visible - near-infrared spectrum of dye (208) was recorded using a Perkin-Elmer Lambda 9 UV/Visible/Near-infrared Spectrophotometer. The uv/visible spectrum in Fig. 9 was recorded using a Unicam SP800 Spectrophotometer, using the 'fast scan' mode, and a slit width of 0.02mm.

Table 46: Spectrometer settings used for recording uv-visible spectra

ordinate mode	ABS
slit	2nm
scan speed	480nm/min
response	0.5s
lamp	UV/VIS
cycles/time	1/0.05min
peak threshold	0.02A
recorder	ON
ordinate min/max	0.000/3.000
abscissa min/max	190.0/900.0

Chromatography

Thin layer chromatography was carried out on either plastic sheets coated with Kieselgel 60 (Merck) (without fluorescent indicator) or aluminium sheets coated with aluminium oxide F_{254} neutral (Merck, type E). Preparative layer chromatography sheets were prepared on glass sheets using Kieselgel 60H. Chromatography columns were prepared with Kieselgel 60 (70-230 mesh ASTM) or with aluminium oxide (M&B) (neutral).

N.M.R. Spectra

Proton and ^{13}C magnetic resonance spectra were recorded using a WH400 n.m.r. instrument.

Mass Spectra

The low resolution spectra were recorded on a VG 12-253 Quadrupole Spectrometer. The fast-atom bombardment spectra were recorded on a VG ZAB-E Spectrometer.

Elemental Analysis (C,H,N)

These were carried out on a Technicon CHN Autoanalyser.

Experimental Procedures

Preparation of dye-containing cellulose acetate film

Cellulose acetate (2.5g) was added to a mixture of dichloromethane/methanol ($25cm^3$ 9:1) containing the calculated amount of dye in a beaker covered with a watch glass. The mixture was thoroughly stirred with a magnetic stirrer for at least 1½ hours at room temperature until a clear solution was obtained. The film was cast onto a glass sheet with a t.l.c. spreader adjusted to a thickness of 5mm. Immediately after casting a similarly sized glass sheet was placed over the wet film a few mm from its surface, by using

microscope slides as spacers, to prevent the film from 'clouding' caused by too rapid evaporation of the solvent.

After drying in the dark at room temperature for 12 hours the film was peeled off the glass and kept in a vacuum dessicator for at least three days. The film was cut into pieces which were then mounted in a slide frame. Such films could then be subjected to heat or photochemical treatment and degradation of the dye assessed directly by visible absorption spectroscopy. (Details of the thermal and photochemical exposure conditions are summarised in Section 2.1.2.4)

Recrystallisation of 1.8-diaminonaphthalene (1,8-DAN)(121)

Excess commercial 1,8-DAN (97.5%) was heated in refluxing ligroin (b.p. 100-120°C) for 10 minutes, and the supernatant solution decanted from the undissolved residue. After cooling to room temperature, the deposited 1,8-DAN was filtered off as salmon pink needles, m.p. 59-61°C,(lit[145] 61.5-64°C).

Synthesis of 2-methylperimidine (120a)

Finely ground recrystallised 1,8-DAN (2g) was added to acetic anhydride (20cm^3) and the solution was stirred at room temperature for 10 minutes and then the temperature raised, over 25 minutes, until refluxing occurred. After refluxing for 5 minutes the solution was allowed to cool to room temperature whereupon the 2-methylperimidine acetate salt was deposited as yellow crystals. These were filtered off, washed with a little acetic anhydride and recrystallised from acetic anhydride (10ml) to give pale yellow crystals. These were dissolved in cold water (5ml) and aqueous ammonia added to give a pH of 7.5. At this pH pale yellow crystals of the free 2-methylperimidine (120a) rapidly deposited and these were filtered off and washed with water, (1.36g : 59.3%) m.p. 213-215°C, (lit[146], 215-216°C).

1-Ethyl-2-methylperimidine (120b)

Ethyl-p-toluene sulphonate (2.0g) and 2-methylperimidine (1.8g) were mixed and heated up to 160°C over 1 hour and kept at this temperature for a further 45 minutes. After cooling, the light brown solid was dissolved in hot DMF and poured into aqueous ammonia solution (o.g. 0.880)(ca. 50ml). The resultant oily suspension was heated, with stirring, for 15 minutes, and the mixture then extracted with dichloromethane. The deep green dichloromethane solution was then separated, washed with water and dried over sodium sulphate (anhydrous) and the dichloromethane removed by rotary evaporation. This gave a green tar which was redissolved in dichloromethane and chromatographed over neutral alumina in dichloromethane. 1-Ethyl-2-methylperimidine was eluted off the column first as a pale yellow band and after solvent removal gave pale yellow crystals (0.90g : 43%), m.p. 108-112°C (lit[109], 115°C).

General Procedures for the synthesis of 2,2-dialkyl-2,2-dihydro-1H-perimidines

Procedure (A)

To a mixture of 1,8-DAN (10g) and sulphuric acid (9g, 96%) in water (300ml) was added the appropriate ketone (0.1mol) dropwise and the mixture heated at 60°C for 1 hour. After cooling, the solution was neutralised with sodium hydroxide solution and the white precipitate filtered off. The dihydroperimidines were purified by chromatography over silica gel 60. Dyes made by this procedure, and their properties are summarised in Table 47.

from n-propanol. Dyes made by this method and their characterisation data are summarised in Table 47.

Synthesis of dihydroperimidine (124)

Recrystallised 1,8-DAN (10.35g, 0.066mol) and diethyl malonate (42g, 45ml) were heated together at 150°C for 4 hours. After cooling the light brown solid was filtered off and washed with ethanol. Purification was carried out by column chromatography (silica gel 60/CH_2Cl_2), evaporation of the eluent giving (124) as white crystals, (16.2g, 97%), m.p. 147-150°, (found: C, 70.6; H, 5.50; N, 10.85%. $C_{15}H_{14}N_2O_2$ requires C,70.87; H,5.51; N,11.02%).

Synthesis of dihydroperimidine (125)

The dihydroperimidine (123g), (1.25g, 4mmol) and p-toluene sulphonic acid (0.07g) were heated in toluene with conditions of azeotropic removal of water using a Dean-Stark trap for 16 hours. Removal of the solvent under vacuum gave a tarry solid. This was dissolved in dichloromethane and chromatographed over silica gel 60 to give (125) as pale yellow leaflets, (0.5g, 53%) m.p. 137 - 140°C, (found : C, 75.75; H, 6.0; N, 11.30%. $C_{15}H_{14}N_2O$ requires C, 75.63; H, 5.9; N; 11.76%).

Generalised procedure for the diazotisation and coupling of 4-nitroaniline to perimidines and dihydroperimidines.

A mixture of sodium nitrite (0.7g, 0.01mol) was cooled to 0°C by addition of ice (Solution A). The ice slurry was used immediately.

4-Nitroaniline (1.38g, 0.01mol) was dissolved in a mixture of concentrated hydrochloric acid (5ml) and glacial acetic acid (10ml)

with heating. The hot, clear solution was poured onto the ice slurry (Solution A) and the mixture stirred at 0°C for 15 minutes. This gave a clear solution of the diazonium salt (Solution B).

The perimidine or dihydroperimidine (10mmol) was dissolved in dimethylformamide (60cm^3) and sodium acetate (5g) dissolved in water(20ml) added. This solution was then cooled to <5°C and solution B was added dropwise. After stirring for 10 minutes the resultant suspension was then rotary evaporated to as near dryness as possible, and the crude dye extracted into dichloromethane. The dried CH_2Cl_2 solution was then column chromatographed over silica gel 60 to give first the <u>para</u> and then the <u>ortho</u> azo dye isomers. Characterisation data for dyes prepared in this way are summarised in Tables 48 and 49.

Table 48: <u>Characterisation data for the ortho coupled perimidine and dihydroperimidine monoazo dyes</u>

Dye	Appearance of crystals and melting point	Characterisation data
(130f)	metallic green 191-193°C	$C_{24}H_{27}N_5O_2$ calc:C,69.06;H,6.48;N,16.79% found:C,68.95;H,6.50;N,16.80%
(130g)	deep red/green 202-204°C	m/e = 462
(130h)	metallic green 199-201°C	$C_{30}H_{25}N_5O_2$ calc:C,71.5 ;H,4,97;N,13.91% found:C,71.35;H,4.78;N,13.75%
(130i)	deep red 275°C	$C_{30}H_{21}N_5O_3$ calc:C,74.2 ;H,4.74;N,14.43% found:C,74.05;H,4.45;N,14.55%
(134b)	violet 74-75°C	m/e = 360 (= M+1)

Table 49: Characterisation data for the para coupled perimidine and dihydroperimidine monoazo dyes

Dye	Appearance of crystals and melting point	Characterisation data
(131f)	metallic green 182-185°C	$C_{24}H_{27}N_5O_2$ calc:C,69.06;H,6.48;N,16.79% found:C,69.10;H,6.35;N,16.52%
(131g)	dull green 194°C	m/e = 462
(131h)	dull purple 155-157°C	$C_{30}H_{25}N_5O_2$ calc:C,71.5 ;H,4,97;N,13.91% found:C,71.45;H,5.00;N,13.79%
(131i)	dull green 152-154°C	$C_{30}H_{21}N_5O_3$ calc:C,74.2 ;H,4.74;N,14.43% found:C,73.95;H,4.90;N,14.10%
(132)	dull green 273-275°C	$C_{21}H_{17}N_5O_3$ calc:C,65.12;H,4.4 ;N,18.1 % found:C,64.9 ;H,4.65;N,18.55%
(133)	pale yellow 242-245°C	$C_{21}H_{17}N_5O_4$ calc:C,62.5 ;H,4.2 ;N,17.36% found:C,62.45;H,4.15;N,17.40%
(135b)	metallic green 100-102°C	m/e = 359

Synthesis of Michler's Ethylene (149)

Iodomethane (25ml) and dry magnesium turnings (4.2g) were added separately to dry diethyl ether (20ml). The suspension was stirred and when vigorous effervescence had started a further aliquot of diethyl ether (80ml) was added. The reaction mixture was stirred for a further 20 - 25 minutes until the effervescence and self-refluxing had ceased, leaving a grey suspension. To this was added a previously prepared solution of Michler's Ketone (9g) (recrystallised twice from toluene) in toluene (250ml) in a steady stream. [The Michler's Ketone was dissolved in toluene by heating. Cooling to room temperature gave a small amount of precipitation, which was ignored]. The resulting deep orange suspension was stirred vigorously for 22 hours with the

exclusion of light. Water (200ml) was then added dropwise (vigorous effervescence) and the suspension stirred for 5 minutes. A solution of glacial acetic acid (15ml) and ammonium chloride (30g) in water (150ml) was then added and the pale green suspension was stirred for 3½ hours after which the magnesium hydroxide was removed by filtration. The organic layer was separated, dried over anhydrous sodium sulphate, and evaporated to dryness under vacuum. The residue was recrystallised twice from ethanol to give (149) as pale green lustrous needles, (2.49g, 28%), m.p. 116 - 120°C (lit[128], 121 - 122°C).

Preparation of benz[c,d]indol-2(1H)-one (156)

Anhydrous aluminium chloride (72g, 0.54mol) was powdered and added immediately to anhydrous o-dichlorobenzene (426g, 327ml). Dissolution was effected by heating to 160°C.

To this solution was added over 1 hour a previously prepared solution of 1-naphthylisocyanate (36g, 0.21mol, 42.4ml) in anhydrous o-dichlorobenzene (108g, 83ml), maintaining the temperature at 160°C. The reaction mixture was then stirred at 160°C for a further 1 hour. Finely ground sodium chloride (35g, 0.6mol) was then added at 150 - 160°C and the mixture stirred at this temperature for 15 minutes.

After cooling to 100°C as much solvent as possible was distilled off under vacuum, and the resulting tar was mixed with water (400ml) and stirred at 90°C for 1 hour. The water was then removed under vacuum and the resultant tar steam-distilled for 8 hours which eventually afforded (156) as pale yellow platelets, (15g, 42%), m.p. 172 - 176°C (lit[129], 180 - 181°C).

Preparation of 1-decyl-benz[c,d]indol-2(1H)-one (157)

Benz[c,d]indol-2(1H)-one (1.69g, 0.01mol) was dissolved in hot

o-dichlorobenzene (60ml) and sodium hydroxide solution (45%w/v, 50ml) was added. To this solution was added 18-crown-6 (0.05g) followed by n-decyl bromide (2.75g, 0.0125mol). The mixture was then heated under reflux for 2 hours during which time the precipitated benzindole turned a deeper yellow and re-dissolved. The solution was cooled and filtered through cellulose powder to give two distinct layers, and the upper organic yellow layer was isolated and steam distilled to remove all the o-dichlorobenzene. This gave (157) as a pale yellow solid, (2.19g, 71%), m.p. 43 - 45°C.

Preparation of 1-decyl-2(1H)-methyl-benz[c,d]indolium iodide (158)

Iodomethane (14.2g, 0.1mol) was added to a mixture of dry diethyl ether (20ml) and dry magnesium turnings (2.4g). When effervescence started more dry diethyl ether (60ml) was added. The reaction mixture was stirred until effervescence and self-refluxing ceased. One tenth of this Grignard solution by volume was then added dropwise at -5 - 0°C to a previously prepared and well stirred solution of finely powdered (157) (2g, 7mmol) in dry diethyl ether (25ml). The suspension was stirred at 0°C for 15 minutes then heated under reflux for 1 hour. The mixture was cooled to <10°C and a solution of concentrated hydrochloric acid (1.4g) in water (11ml) added dropwise, ensuring that the temperature remained below 20°C. The deep orange/red suspension was stirred for 5 minutes and then filtered to give (158) as an orange powder, (2.27g, 96%), [found, $^m/e$ = 308; $C_{22}H_{30}N$ (for the product minus I^-), requires $^m/e$ = 308].

General procedure for the preparation of azo dyes (162) and (163)

(149) or (158) (1mmol) was dissolved in ethanol (10ml) and 4-nitrobenzenediazonium chloride (0.24g, 1mmol) added. The solution

was stirred at room temperature for 1 hour and the resulting solid filtered off and washed with water.

Dye (162): was recrystallised from ethanol and was obtained as metallic green needles, (0.38g, 31%), m.p. 216 - 218°C, (found $^m/e$ = 415, $C_{24}H_{25}N_5O_2$ requires $^m/e$ = 415).

Dye (163): was isolated by thick layer chromatography as metallic green needles, (0.2g, 6%), m.p. 75 - 78°C, (found, $^m/e$ = 456; $C_{28}H_{32}N_4O_2$ requires $^m/e$ = 456).

Preparation of 3-cyano-6-hydroxy-4-methyl-2-pyridone

Aqueous ammonia (33%, 76ml) was added with stirring to a mixture of water (125ml) and ethyl cyanoacetate (29.9g, 0.264mol), and stirring was continued for 12 hours. The solution was then mixed with ethyl acetoacetate (40g, 0.308mol) and water (65ml) and the mixture heated in an autoclave with stirring at 120°C for 6 hours. After cooling to room temperature the mixture was transferred to a 1 litre three necked flask and heated to 60°C to dissolve the solid. Water (400ml) was then added dropwise whilst maintaining the temperature at 60°C. The solution was strongly acidified with hydrochloric acid and the pale brown solid filtered off and washed acid free with, initially, hot, then cold water. The product was obtained as white needles, (44g, 90%), m.p. >300°C.

Formylation of 3-cyano-6-hydroxy-4-methyl-2-pyridone

Dimethylformamide was cooled to 0°C and phosphorous oxychloride (16.9g, 10.2ml, 0.11mol) added with stirring at <10°C. 3-Cyano-6-hydroxy-4-methyl-2-pyridone (17.6g; 0.11mol) was then added portionwise and as the mixture thickened during addition so more dimethylformamide (50ml) was added to maintain stirring. The stiff white paste was stirred at a temperature below 10°C for 2 hours, and the temperature then allowed

to rise to ca. 20°C overnight. The mixture was then heated to 55 - 60°C and maintained at this temperature for 2 hours, after which it was poured into water (800ml) at 60°C. The suspension was then cooled to 15°C with ice addition, and the dull yellow crystals of 3-cyano-5-formyl-6-hydroxy-4-methyl-2-pyridone were filtered off, washed with ice-cold water and dried in a dessicator, (14.2g, 85%), m.p. 212 - 214°C.

Nitrosation of 3-cyano-6-hydroxy-4-methyl-2-pyridone

3-Cyano-6-hydroxy-4-methyl-2-pyridone (3.75g, 0.025mol), sodium nitrite (1.9g, 0.025mol), water (37.5ml) and aqueous sodium hydroxide (40% w/v; 2.5ml) were mixed together and stirred until a clear solution was obtained. This was added slowly to a previously prepared mixture of water (100ml) and concentrated hydrochloric acid (10ml), cooled to 0°C. Stirring was continued for 1 hour at 0 - 5°C and the pale yellow crystals of 3-cyano-6-hydroxy-4-methyl-5-nitroso-2-pyridone filtered off, washed with water and then dried, (3.96g, 89%), m.p. 194 - 195°C.

Condensation of (149) and (158) with various 3-cyano-5-formyl-6-hydroxy-4-methyl-2-pyridones

Derivative (149) or (158) (0.5mmol) was dissolved in ethanol (5ml), and a solution of the formyl-pyridone (0.5mmol) in ethanol (5ml) was added. The mixture was then heated under reflux for 30 minutes. After cooling to room temperature the resultant solid was filtered off to give the crude dye. The dyes were purified either by recrystallisation or column chromatography, and characterisation data are summarised in Table 50.

Table 50: Characterisation data for dyes derived from 5-formyl- and 5-nitroso-2-pyridones

Structure	Yield %	Appearance of crystals and melting point	Characterisation data
(178a)[a]	52	metallic green 261-263°C	$C_{26}H_{26}N_4O_2$ calc:C,73.20;H,6.10;N,13.10% found:C,73.05;H,6.15;N,12.70%
(180a)[a]	47	green/blue powder >300°C	$C_{25}H_{25}N_5O_2$ calc:C,70.25;H,5.85;N,16.39% found:C,70.05;H,5.80;N,16.45%
(178b)[a]	68	metallic green 251-253°C	$C_{28}H_{30}N_4O_2$ calc:C,74.00;H,6.6 ;N,12.3 % found:C,74.3 ;H,6.8 ;N,12.3 %
(180b)[a]	40	pale blue powder >350°C	$C_{27}H_{29}N_5O_2$ calc:C,71.2 ;H,6.4 ;N,15.40% found:C,70.9 ;H,6.55;N,15.65%
(178c)[b]	55	dull green needles 217-219°C	$C_{31}H_{37}N_5O_2$ calc:C,72.7 ;H,7.24;N,13.69% found:C,73.0 ;H,7.20;N,13.51%
(180c)[b]	41	dull green powder 255-258°C	$C_{30}H_{38}N_6O_2$ calc:C,70.3 ;H,7.03;N,16.4 % found:C,70.05;H,6.95;N,16.3 %
(179a)[a]	72	dull blue powder 220-221°C	m/e = 468 (= M+1)
(181a)[a]	84	deep green needles 198-200°C	m/e = 468
(179b)[c]	14	dull blue/green 210-215°C	m/e = 495
(181b)[c]	46	deep green needles 191-194°C	m/e = 496
(179c)[d]	51	blue powder >300°C	m/e = 552
(181c)[d]	83	dull green needles >300°C	m/e = 553

(a) - recrystallised from ethanol
(b) - purified by column chromatography over silica gel 60
(c) - recrystallised from ethyl acetate
(d) - purified by column chromatography over aluminium oxide

Condensation of (149) and (158) with various 3-cyano-6-hydroxy-4-methyl-5-nitroso-2-pyridones

The same procedure was used as for the formyl-pyridones and the reaction could be carried out by stirring at room temperature for 1 hour. The results are summarised in Table 50.

General procedures for the synthesis of squarylium dyes

Procedure A

Squaric acid (2mmol) and the arylamine or enamine (4mmol) were refluxed, with stirring in a mixture of n-butanol (40ml) and toluene (20ml) for 20minutes-32hours and the water formed was removed azeotropically by using a Dean-Stark trap. The mixture was cooled and the precipitated dye filtered off, washed with toluene and purified by column chromatography over silica gel 60. Yields, m.p., and characterisation data are summarised in Table 51.

Procedure B

This method was similar to Procedure A except that n-propanol (40ml) was substituted for the n-butanol. This had the advantage that for dyes that did not crystallise out on cooling it was possible to remove the alcohol by washing with water, then drying the separated toluene layer over anhydrous sodium sulphate. This dried toluene layer could then be directly column chromatographed over silica gel 60. Yields, m.p., and characterisation date of dyes made according to this procedure are summarised in Table 51.

Table 51: Yields and characterisation data for squarylium dyes

Structure	Yield %	Appearance of crystals and melting point	Characterisation data
(189a)*	80	dull green needles >300°C	$^{m}/e$ = 531 (= M+1)
(189b)*	70	dark green needles 158-159°C	$^{m}/e$ = 558
(189c)*,**	80	lustrous blue 119-120°C	$^{m}/e$ = 614
(189d)**	33	dull green 176-180°C	$C_{52}H_{34}N_4O_4$ calc:C,80.21;H,4.37;N,7.20 % found:C,80.30;H,4.45;N,6.95 %
(189e)**	41	dull blue >300°C	$C_{52}H_{38}N_4O_2$ calc:C,83.2 ;H,5.10;N,7.5 % found:C,82.95;H,5.35;N,7.15 %
(189f)**	81	pale green 86-88°C	$C_{42}H_{46}N_4O_6$ calc:C,71.79;H,6.55;N,8.0 % found:C,71.8 ;H,6.80;N,7.65 %
(192)*	85	metallic green needles >300°C	$C_{32}H_{26}N_4O_2$ calc:C,77.10;H,5.22;N,11.25% found:C,76.9 ;H,5.3 ;N,11.1 %
(193)**	5	dull green needles 121-122°C	$^{m}/e$ = 610
(194)**	80	very deep green 82-84°C	$^{m}/e$ = 693 (= M+1)

* - Procedure (A)
** - Procedure (B)

Synthesis of anhydrous croconic acid

a. Preparation of tetramethoxy-p-benzoquinone (198)

Sodium hydroxide (16.25g, 0.4mol) was dissolved in methanol (600ml) and cooled to below 10°C. Chloranil (25g, 0.1mol) was added, with stirring, over 20 minutes, ensuring that the temperature remained below 10°C. The suspension was then heated under reflux for 50 minutes. The reaction mixture was filtered off and, on cooling,

orange needles of (198) were deposited, (9.59g, 42%), m.p. 135 - 138°C (lit[140] 135°C).

b. Preparation of tetrahydroxy-p-benzoquinone (199)

(198) (10g, 43mmol) was refluxed for 1 hour in a mixture of glacial acetic acid (100ml) and hydrobromic acid (48%, 100ml). The reaction mixture was then evaporated to dryness under vacuum and the residue recrystallised from hot hydrochloric acid (2M). This gave tetrahydroxy-p-benzoquinone as deep red platelets, (5.64g, 76%), m.p.>300°C, (lit[140]>300°C).

c. Preparation of barium croconate hydrate (200)

To a solution of sodium hydroxide (4.8g, 0.12mol) in water (120ml) was added tetrahydroxy-p-benzoquinone (2.1g, 0.012mol) and active manganese dioxide (Aldrich Chemicals), (5.5g). This mixture was stirred at room temperature for five minutes and then refluxed for 45 minutes. The reaction mixture was then filtered hot to remove the manganese dioxide which was then washed with hot water (2 x 40ml). To the combined washings and filtrate was added concentrated hydrochloric acid (21ml) dropwise, giving a bright yellow solution. A hot solution (ca. 90°C) of barium chloride trihydrate (5g) in water (15ml) was then added dropwise, to give bright yellow platelets of the barium croconate salt. The suspension was heated to 85 - 90°C and cooled to room temperature, filtration gave (200) as lustrous yellow platelets (2.49g, 70%).

d. Preparation of anhydrous croconic acid

Barium croconate hydrate (2.75g, 9mmol) was added portionwise to a hot (60°C) mixture of water (10ml) and sulphuric acid (98%; 1ml). The resultant pale yellow suspension was stirred at this temperature for

40 minutes and filtered hot to remove the insoluble barium sulphate. The precipitate was washed with hot water (ca. 20ml) and the combined washings and filtrate were evaporated to dryness under vacuum. The residual tarry solid was slurried with acetone, giving anhydrous croconic acid as pale yellow crystals (1.09g, 85%).

General procedure for the synthesis of croconium dyes

Croconic acid (2mmol) and the 3-hydroxyarylamine or enamine (4mmol) were refluxed, with stirring, in a mixture of n-propanol (40ml) and toluene (20ml) for 11minutes-1hour and the water formed was removed azeotropically by using a Dean-Stark trap. The mixture was cooled and, when the dye precipitated out, the product was filtered and washed with toluene. Where the dye did not crystallise out, the alcohol was removed by washing with water, the separated toluene layer dried over anhydrous sodium sulphate and then directly column chromatographed over silica gel 60. Yields, m.p., and characterisation data are summarised in Table 52.

Table 52: Characterisation data for the croconium dyes

Structure	Yield %	Appearance of crystals and melting point	Characterisation data
(203)	83	olive green metallic 219-221°C	$C_{25}H_{28}N_2O_5$ calc:C,68.80;H,6.42;N,6.42 % found:C,68.70;H,6.65;N,6.15 %
(204)	89	dull brown 245-247°C	$C_{29}H_{28}N_2O_5$ calc:C,71.9 ;H,5.8 ;N,5.80 % found:C,71.6 ;H,5.75;N,5.50 %
(205)	75	dull green/yellow 244-245°C	$^m/e$ =465 (= M+1)
(207)	4	dull brown 168-170°C	$^m/e$ = 655 (= M+1)
(208)	26	dull brown 69-72°C	$^m/e$ = 721 (= M+1)

Procedures used in the kinetic studies of the reaction of croconic acid with 8-hydroxyjulolidine

a. Preparation of alcoholic solutions

Croconic acid (25mg, 1.76 x 10^{-4}mol) was dissolved in the appropriate, distilled, alcohol by placing on a sonic bath for 30 minutes, after which the alcohol was made up to 50ml in a graduated flask. This solution was stored in the dark until required.

The corresponding 8-hydroxyjulolidine solution was prepared in a similar manner using (0.0665g, 3.52 x 10^{-4}mol) of the amine.

An aliquot (5ml) of the alcohol solution of croconic acid was mixed with the same amount of the 8-hydroxyjulolidine solution at a known temperature. This reaction mixture was transferred to a 1mm quartz cell and placed in the spectrophotometer. One minute after mixing the solutions the rate of dye formation was recorded at 30 second time intervals over a 30 minute time period, the temperature inside the spectrophotometer being recorded throughout the experiment.

b. Preparation of solutions involving mixed solvents

Croconic acid (25mg, 1.76 x 10^{-4}mol) was dissolved in the minimum volume possible of n-propanol in a 50 ml graduated flask by placing on a sonic bath for 30 minutes, after which the solution was made up to the mark by additions of the required volumes of n-propanol and the second solvent (e.g. 90% n-propanol:10% toluene required 45ml n-propanol:5ml toluene). This solution was then stored in the dark until required.

The corresponding 8-hydroxyjulolidine solution was prepared in a similar manner using (0.0665g, 3.52 x 10^{-4}mol) of the amine.

An aliquot (5ml) of the mixed solvent solution of croconic acid was mixed with 5ml of the corresponding 8-hydroxyjulolidine mixed solvent

solution at a known temperature. This reaction mixture was transferred to a 1mm quartz cell and placed in the spectrophotometer. The rate of dye formation was recorded at either 1 minute intervals for 1 hour (when the co-solvent was either dimethylformamide or acetonitrile) or 30 second time intervals for 30 minutes (when the co-solvent was either water or toluene) starting after 1 minute had elapsed from mixing. The temperature inside the spectrophotometer was recorded throughout the experiment.

c. Experiments involving added acids and bases

The solutions of croconic acid and 8-hydroxyjulolidine in 90% toluene : 10% n-propanol were prepared in a manner identical to that described in (a) and (b) above.

To 1ml of the croconic acid solution, in a spectrophotometer cuvette, was added a 1ml aliquot of the 8-hydroxyjulolidine solution and to this mixture was added one drop of hydrochloric acid (10M; aqueous). The contents of the cuvette were then transferred to a 1mm quartz cell and the rate of dye formation recorded in the spectrophotometer, at known temperature, at 30 second intervals for 30 minutes. This procedure was repeated for the following acids and bases; hydrochloric acid (1M; ethanolic); glacial acetic acid; 45% boron trifluoride etherate in ether; DABCO (1M; ethanolic); and potassium hydroxide (1M; ethanolic).

Synthesis of diethyl croconate

a. Preparation of silver croconate

To a stirred solution of croconic acid (1.42g, 0.01mol) and water (10ml) was added a solution of silver nitrate (3.4g, 0.02mol) and water (30ml). The resulting bright orange suspension was stirred in

the absence of light for 20 minutes. The precipitate was filtered off and dried in a dessicator in the dark, (3.24g, 91%).

b. Preparation of diethyl croconate monohydrate

A solution of silver croconate (9g, 0.025mol) and iodoethane (8.1g, 0.052mol) in dry diethyl ether (30ml) was stirred in the absence of light for 4 hours. A further aliquot of iodoethane (0.9g, 5.7mmol) was added and stirring continued for a further 12 hours, after which the diethyl ether was removed under vacuum. The resultant tarry pale yellow residue was dissolved in dichloromethane and washed with water to remove any residual croconic acid. After separation, the dichloromethane layer was dried over anhydrous sodium sulphate and column chromatographed directly over silica gel 60, with acetone as eluent. Diethyl croconate monohydrate was eluted as the only yellow band and, after solvent removal, was afforded as a golden yellow oil, (0.5g, 0.1%), (found $^{m}/e$ = 216; $C_9H_{12}O_6$ requires $^{m}/e$ = 216).

Kinetic aspects of rate of formulation of (204) from diethyl croconate and 8-hydroxyjulolidine

Diethyl croconate monohydrate (38mg, 1.7 x 10^{-4}mol) was added to n-propanol (5ml), in a 50ml graduated flask and solution effected by treatment in a sonic bath for 30 minutes. The flask was then made up to the mark with toluene.

The corresponding 8-hydroxyjulolidine solution was prepared in a similar manner to the diethyl croconate solution using (0.0665g, 3.52 x 10^{-4}mol) of 8-hydroxyjulolidine.

An aliquot (5ml) of the diethyl croconate solution was mixed with an equal volume of the 8-hydroxyjulolidine solution at known temperature. The reaction mixture was transferred to a 1mm quartz cell and the rate of dye formation was recorded over 30 minutes at

30 second time intervals, starting 1 minute after mixing. The internal temperature of the spectrophotometer was recorded throughout the duration of the experiment.

Preparation of 3-chloro-4-cyano-5-dicyanomethylene-2-oxo-3-pyrroline (212)

a. Malononitrile dimer

To xylene (120ml) and 1 drop of alkyl benzene sulphonate, in an inert atmosphere and with external cooling from an ice-water bath, was added sodium (10.4g) portionwise. The reaction mixture was heated to 120°C with vigorous stirring and then allowed to cool to 20°C without stirring. To this solution was then added a solution of methanol (0.15ml) and xylene (10ml) followed by a solution of malononitrile (75g, 1.13mol) in tetrahydrofuran (50ml), the latter solution being added portionwise over 10 minutes. The resultant reaction mixture was then heated to 40°C over 20 minutes and maintained at that temperature for 4 hours. Methanol was then added dropwise, ensuring that the temperature was maintained between 30 - 50°C (NB. much heat was evolved due to destruction of excess sodium). After 30 minutes, toluene (100ml) was added, the crude product filtered off and air dried for 5 minutes. The crude product was then added to an ice(200g) : water(300ml) mixture which was diluted to 1400ml with water. This mixture was then acidified with concentrated hydrochloric acid (35ml) and stirred for 20 minutes. The final white product was then filtered off, washed with water and dried, (30.4g, 20%), m.p. 172 - 174°C.

b. Preparation of the sodium salt of 4-cyano-3-dicyanomethylene-3-hydroxy-2-oxo-3-pyrroline

To a solution of malononitrile dimer (13.2g, 0.1mol) in methanol (prepared by heating) was added diethyl oxalate (16g, 15ml) dropwise. This solution was then added to a previously prepared methanolic solution of sodium methoxide made by dissolving sodium (4.7g, 0.2mol) in methanol (75ml), under nitrogen, with cooling.

After warming gently (to a maximum of 32°C), the clear yellow solution was cooled, with stirring, to ca. 20°C over 2 hours and one third of the methanol was removed under vacuum. Toluene (2 x 50ml) was added whereupon the gel rapidly crystallised. Stirring was maintained for 15 minutes and the resultant yellow crystals were then filtered off, washed with toluene, then petrol, and then dried at 50°C for 1 hour. The product was then dissolved in water (400ml), and acetic acid added to give a pH 4.5 . The resulting suspension was stirred for 30 minutes and the yellow product filtered off and dried at 50°C, (21g,31.3%).

c. Preparation of 3-chloro-4-cyano-5-dicyanomethylene-2-oxo-3-pyrroline (212)

To a solution of the sodium salt of 4-cyano-3-dicyanomethylene-3-hydroxy-2-oxo-3-pyrroline (10g, 0.043mol) in acetonitrile (20ml) was added thionyl chloride (10ml) dropwise. The mixture was then refluxed for 30 minutes and cooled to 5°C over 1 hour. The product was then filtered off, washed with dichloromethane, then cyclohexane and dried under reduced pressure at 50°C. (20g, 84.5%)

Synthesis of dyes (214) - (216)

The chloro compound (212) (0.2g, 1mmol) and the appropriate reactant (1mmol) were dissolved in ethyl acetate (15ml) and stirred

without heating for 1 hour. The resulting dyes were filtered off, washed with water and dried. Yields, m.p., and characterisation data are summarised in Table 53.

Table 53: Characterisation data for dyes (214) - (218)

Structure	Yield %	Appearance of crystals and melting point	Characterisation data
(214)[a]	24	dull blue/grey 252-255°C	$C_{24}H_{20}N_6O$ calc:C,70.58;H,4.90;N,20.58% found:C,70.80;H,5.05;N,20.55%
(215)[b]	98	dull blue/green >300°C	$C_{21}H_{14}N_6O$ calc:C,68.85;H,3.82;N,22.95% found:C,69.1 ;H,3.68;N,22.87%
(216)[c]	74	dull green >300°C	$C_{26}H_{22}N_6O$ calc:C,71.88;H,5.10;N,19.4 % found:C,72.0 ;H,4.8 ;N,19.8 %
(217)[d]	13	metallic green needles 260-261°C	$^m/e$ = 475
(218)	76	bronzy/gold 248-250°C	$C_{21}H_{14}N_5O_3S$ calc:C,60.57;H,3.3 ;N,16.82% found:C,60.25;H,3.0 ;N,16.65%

(a) - recrystallised from toluene after hot filtration
(b) - recrystallised from o-dichlorobenzene
(c) - purified by column chromatography over silica gel 60
(d) - recrystallised from ethanol after hot filtration

Synthesis of dye (217)

1-Decyl-2(1H)-methyl-benz[c,d]indolium iodide (0.44g, 1mmol) and (212) (0.2g, 1mmol) were dissolved in ethanol (20ml) and stirred without heating for 30 minutes. The product was then filtered off, washed with water and dried. Characterisation data for (217) is contained in Table 53.

Synthesis of (218)

2-Amino-3-carboxyethyl-4-phenyl-thiophene (3.02g, 0.0122mol) and

(212) (2.5g, 0.0122mol) were dissolved in glacial acetic acid (100ml) and stirred without heating for 2 hours. The resultant bronzy/gold crystals of (218) were filtered off and washed with water. The product gave a satisfactory microanalysis without further purification. Characterisation data for (218) is summarised in Table 53.

Procedure for synthesis of dyes (220) and (221)

2-Chloro-3,5-dinitrothiophene (0.208g, 1mmol) and (123a) or (149) (1mmol) were mixed in ethyl acetate (10ml) and stirred, without additional heating, for 2 hours. The precipitated crystals were then filtered off. Purification was achieved by column chromatography over silica gel 60.

Dye 220: was obtained as lustrous black platelets, (0.18g, 43%), m.p. 150-152°C. (found: $^{m}/e$ = 412; $C_{20}H_{20}N_4O_4S$ requires $^{m}/e$ = 412).

Dye 221: was obtained as golden brown needles (0.14g, 32%), m.p. 262 - 265°C. (found: $^{m}/e$ = 438; $C_{22}H_{22}N_4O_4S$ requires $^{m}/e$ = 438).

REFERENCES

1. J.A. Pople, Trans. Faraday Soc., 49, 1375, (1953).
2. R. Pariser, R.G. Parr, J.Chem.Phys., 21, 466, (1953).
3. J. Griffiths, "Colour and Constitution of Organic Molecules", (London : Academic Press, 1976).
4. C. Greville Williams, Trans. Roy. Soc. Edinburgh, 21, 377, (1857).
5. W. H. Mills, R. S. Wishart, J. Chem. Soc., 117, 579, (1920).
6. L. G. S. Brooker et al, J. Am. Chem. Soc., 62, 1116, (1940).
7. L. G. S. Brooker et al, J. Am. Chem. Soc., 63, 3192, (1941).
8. L. G. S. Brooker, R. H. Sprague, J. Am. Chem. Soc., 63, 3203, (1941).
9. L. G. S. Brooker, R. H. Sprague, J. Am. Chem. Soc., 63, 3214, (1941).
10. K. Venkataraman (Ed), "Chemistry of Synthetic Dyes", Vol.VIII (London : Academic Press, 1978).
11. R. Fabian, H. Hartman, "Light Absorption of Organic Colourants", (Berlin : Springer Verlag, 1980).
12. L. G. S. Brooker et al, J. Am. Chem. Soc., 67, 1875, (1945).
13. Kodak Chemical Catalogue.
14. A. Barker, C. C. Barker, J. Chem. Soc., 1307, (1954).
15. S. Akiyama et al, Chem. Lett., 311, (1981).
16. G. Hallas, J. S. D. C., 86, 238, (1970).
17. S. Akiyama et al, J. Chem. Soc. Perkin Trans. I, 3155, (1988).
18. S. Akiyama et al, Chem. Lett., 329, (1986).
19. S. Akiyama et al, J. Chem. Soc. Chem. Commun., 710, (1987).
20. S. Akiyama et al, Dyes and Pigments, 9, 454, (1988).
21. S. Akiyama et al, Bull. Chem. Soc. Jpn., 61, 2253, (1988).
22. G. A. Reynolds, K. H. Drexhage, J. Org. Chem., 42, 885, (1977).
23. A. I. Tolmachev et al, Dyes and Pigments, 9, 443, (1988).

24. S. Watanbe, H. Nakazumi, S. Kado, T. Kitao, J. Chem. Soc., in press.

25. T. G. Deligeorgieu, N. I. Gadjev, Dyes and Pigments, 12, 157, (1990).

26. P. F. Gordon, P. Gregory, "Organic Chemistry in Colour", (New York : Springer-Verlag, 1983).

27. S. S. Malhotra, M. C. Whiting, J. Chem. Soc., 3812, (1960).

28. K. Y. Chu, J. Griffiths, J. Chem. Research, (M)2319, (S)180, (1978).

29. K. Y. Chu, J. Griffiths, J. Chem. Soc. Perkin Trans., 1083, (1978); 696, (1979).

30. G. G. Buckley, J. Griffiths, J. Chem. Soc. Perkin Trans., 702, (1979).

31. K. Tagaki, M. Matsuoka, Y. Kubo, T. Kitao, J. S. D. C., 101, 140, (1985).

32. M. Matsuoka, S. H. Kim, Y. Yubo, K. Kitao, J. S. D. C., 102, 232, (1986).

33. Japanese Patent 01,66,288 (1989) : Chem. Abs., III, 164373K.

34. D. Heard, G. G. Roberts, M. J. Goringe, J. Griffiths, Thin Solid Films, 180, 305, (1989).

35. M. Matsuoka et al, Dyes and Pigments, 7, 93, (1986).

36. M. Matsuoka, T. Kitao, Chem. Letters, 1351, (1985).

37. S. Matsumoto, K. M. Zunoya, H. Hatou, H. Tomi, Mol. Cryst. Liq. Cryst., 122, 285, (1985).

38. Japanese Patent 60,49,063 (1985): Chem. Abs., 103, 55427.

39. P. Griess, Liebigs. Ann. Chem., 106, 123, (1858).

40. J. B. Dickey, et al, J. S. D. C., 74, 123, (1958).

41. J. B. Dickey, et al, J. Org. Chem., 24, 187, (1959).

42. K. A. Bello, J. Griffiths, J. Chem. Soc. Chem. Commun., 1639, (1986).

43. P. Gregory, European Patent 280,434 (1988): Chem. Abs., 110, 116654K.

44. D. Scheltz, Hel. Chim. Acta., 58, 1207, (1975).

45. K. A. Bello, L. Cheng, J. Griffiths, J. Chem. Soc. Perkin Trans. (II), 815, (1987).

46. M. J. S. Dewar, J. Chem. Soc., 2329, (1950).

47. J. D. Park, S. Cohen, J. R. Lacher, J. Am. Chem. Soc., 81, 3480, (1959).

48. J. D. Park, S. Cohen, J. R. Lacher, J. Am. Chem. Soc., 84, 2919, (1962).

49. R. West, H. Y. Niu, J. Am. Chem. Soc., 84, 1324, (1962).

50. R. West, H. Y. Niu, D. I. Powell, M. V. Evans, J. Am. Chem. Soc., 82, 6204, (1960).

51. M. Ito, R. West, J. Am. Chem. Soc., 85, 2580, (1963).

52. W. M. McIntyre, M. S. Werkerna, J. Chem. Phys., 42, 3563, (1964).

53. N. C. Baezinger, J. J. Hegenbarth, J. Am. Chem. Soc., 86, 3250, (1964).

54. M. A. Neuman, Diss. Abstr., 26, 6394, (1966).

55. A. H. Schmidt, W. Ried, Synthesis, 869, (1978).

56. G. Maahs, P. Hengenberg, Angew. Chem., 78, 927, (1966).

57. U. S. Patent 4,097,530.

58. A. Treibs, K. Jacob, Angew. Chem. Int. Ed. Engl., 4, 694, (1965).

59. U. K. Patent 2,097,013.

60. R. D. Loutfy, C. K. Hsiao, P. M. Kazmaier, Photogr. Sci., 27, 5, (1983).

61. K - Y Law, F. C. Bailey, Can. J. Chem., 64, 2267, (1986).

62. N. Kuramoto, K. Natsukawa, K. Asao, Dyes and Pigments, 11, 21, (1989).

63. A. Treibs, K. Jacob, Justus Liebigs Ann. Chem., 699, 153, (1966).

64. A. Treibs, K. Jacob, Justus Liebigs Ann. Chem., 741, 101, (1970).

65. U. S. Patent 3,617,270 (1971).

66. K - Y Law, S. Caplan, R. K. Crandall, Dyes and Pigments, 9, 187, (1988).

67. K - Y Law, F. C. Bailey, J. Chem. Soc., In Press.

68. K. A. Bello, Ph.D. Thesis, University of Leeds (1986).

69. C. Brunner, Schweigger's J., 38, 517, (1823).

70. L. Gmelin, Ann. Phys. (Leipzig)[2], 4, 1, (1825).

71. K. Yamada, M. Mizuno, Y. Hirata, Bull. Chem. Soc. Jpn., 31, 543, (1958).

72. A. J. Fatiadi, H. S. Isbell, W. F. Sagar, J. of Res., 67A, 153, (1963).

73. R. Nietzki, Ber. Dtsch. Chem. Ges., 20, 1617, 2114, (1887).

74. K. K. Hartley, A. R. Wolff, L. D. Travis, Icarus, 77, 382, (1989): Chem. Abs., 110, 196685j.

75. Y. Hirata, K. Inukai, T. Tsujuichi, J. Chem. Soc. Jpn., Pure Chem., 69, 63, (1948): Chem. Abs., 47, 5902, (1953).

76. A Treibs, L. Schulze, Liebigs Ann. Chem., 201, (1971).

77. A. Voelkl, G. Quadbeck, Aerztl. Lab, 19(2), 45, (1973): Chem. Abs., 72, 29233v.

78. A. J. Fatiadi, J. Am. Chem. Soc., 100, 2586, (1978).

79. R. West, "Oxocarbons", (New York : Academic Press, 1980).

80. For example:-

Japanese Patent 61,34,092, (1986): Chem. Abs., 106, 41718r.

Japanese Patent 59,14,150, (1984): Chem. Abs., 102, 15216y.

Japanese Patent 61,30,590, (1984): Chem. Abs., 105, 124354z.

Japanese Patent 58,173,696, (1983): Chem. Abs., 100, 94591b.

81. S. Yasui, M. Matsuoka, T. Kitao, Dyes and Pigments, 10, 13, (1988).

82. U. K. Patent 322,169.

83. For example:-

Japanese Patent 01,34,791, (1989): Chem. Abs., 111, 164314s.

Japanese Patent 63,242,682, (1988): Chem. Abs., 111, 31421c.

Japanese Patent 63,267,592, (1988): Chem. Abs., 111, 31426h.

Japanese Patent 63,306,091, (1988): Chem. Abs., 111, 87536m.

Japanese Patent 64,00,569, (1989): Chem. Abs., 111, 87544n.

Japanese Patent 01,08,093, (1989): Chem. Abs., 111, 68049p.

84. W. S. Chan, J. F. Marshall, R. Svensen, D. Phillips, I. R. Holt, Photochem. and Photobiol., 45, 757, (1987).

85. R. L. Wheeler, G. Nagasubramanian, A. J. Bard, L. A. Schechtmann, D. R. Dininny, M. F. Kennedy, J. Am. Chem. Soc., 106, 7404, (1984).

86. Private communication.

87. J. Silver, P. J. Lukes, P. K. Hey, J. M. O'Connor, Polyhedron, 8, 13, (1989): Chem. Abs., 111, 162880z.

88. Japanese Patents 61,152,685 and 61,152,769, (1986): Chem. Abs., 106, 19999t, 20000u.

89. L. Mikhalenko, I. Solovara, J. Gen. Chem. U.S.S.R., 986, (1985).

90. German Patent 3,446,418 A1 (1986).

91. European Patent 155,780 (1985).

92. European Patent 313,943 (1989).

93. For example:-

Japanese Patent 63,301,261 (1988): Chem. Abs., 111, 116825n.

Japanese Patent 63,227,386 (1988): Chem. Abs., 111, 31437n.

Japanese Patent 63,227,387 (1988): Chem. Abs., 111, 31438p.

Japanese Patent 63,274,591 (1988): Chem. Abs., 111, 87541j.

94. W. H. Mills, R. E. D. Clark, J. Chem. Soc., 175, (1936).

95. A. J. Lowe, J. Chem. Soc., 1258, (1940).

96. G. N. Schauzer, V. Mayweg, J. Am. Chem. Soc., 84, (1962).

97. G. N. Schauzer et al, Angew. Chem. Int. Edn. Eng., 3, 381, (1964).

98. S. H. Kim, M. Matsuoka, M. Yomoto, Y. Tsuchiya, T. Kitao, Dyes and Pigments, 8, 381, (1987).

99. J. Griffiths, C. Hawkins, J. Chem. Soc. Perkin Trans. (II), 747, (1977).

100. N. Kuramoto, T. Kitao, J. S. D. C., 98, 334, (1982).

101. N. Nakazumi, E. Hamada, T. Ishiguro, H. Shiozaki, T. Kitao, J. S. D. C., 105, 26, (1989).

102. For example:-

German Patent 3,716,734 (1988): Chem. Abs., 111, 31419h.

Japanese Patent 63,209,890 (1988): Chem. Abs., 111, 31420b.

Japanese Patent 63,288,785 (1988): Chem. Abs., 111, 87548s.

Japanese Patent 63,288,786 (1988): Chem. Abs., 111, 87549t.

103. Y. Kubo, S. Sasaki, K. Yoshida, Chem. Lett., 1563, (1987).

104. Y. Kubo, K. Sasaki, H. Kataoka, K. Yoshida, J. Chem. Soc. Perkin Trans.(I), 1469, (1982).

105. Y. Kubo, H. Kataoka, Y. Yoshida, J. Chem. Soc. Chem. Commun., 1457, (1988).

106. Y. Kubo, H. Kataoka, M. Ikezawa, K. Yoshida, J. Chem. Soc. Perkin Trans. (I), in press.

107. A. F. Pozharskii, V. V. Dal'nikouskaya, Russian Chemical Reviews, 50(9), 816, (1981).

108. J. H. Richmond, "Six-membered Heterocyclic Nitrogen Compounds with Three Condensed Rings", (New York: Academic Press, 1958).

109. R. A. Jeffreys, J. Chem. Soc., 2394, (1955).

110. M. Allum, N. Y. Abou-Zeid, Egypt J. Chem., 4, 339, (1972).

111. The Colour Index.

112. U. Pfüller, H. Franz, A. Preiss, Histochemistry, 54, 237, (1977).

113. H. Yamamoto, K. Maruoka, J. Am. Chem. Soc., 103, 4186, (1981).

114. European Patent 0 071 197A1, (1983).

115. S. N. Corns, J. Griffiths - Unpublished observations.

116. M. Ellwood, Ph.D. Thesis, University of Leeds, (1982).

117. A. Hantzsch, Chem. Ber., 52, 509, (1919).

118. F. Ketrmann, S. Hempel, Chem. Ber., 50, 856, (1917).

119. M. T. Rogers, T. W. Campbell, R. W. Meatman, J. Am. Chem. Soc., 73, 5122, (1951).

120. C. R. Bury, J. Am. Chem. Soc., 57, 2115, (1935).

121. I. M. Klotz, H. A. Fries, J. Y. Chem Ho, M. Mellody, J. Am. Chem. Soc., 76, 5136, (1954).

122. W. S. McGuire, T. F. Izzo, F. Zuffanti, J. Org. Chem., 21, 632, (1956).

123. H. H. Jaffé, J. Chem. Phys., 21, 415, (1953).

124. L. Pentimalli, Tetrahedron, 5, 27, (1959).

125. T. Horiike, M. Mondo, S. Kwon, N. Kuroki, Dyes and Pigments, 6, 321, (1984).

126. G. Hallas, J. S. D. C., 86, 238, (1970).

127. K. Venkataraman (Ed.), "The Chemistry of Synthetic Dyes", Vol. IV, (London: Academic Press, 1979).

128. P. Pfeiffer, R. Wizinger, Liebigs Ann. Chem., 461, 132, (1928).

129. German Patent, 3,422,075, (1986).

130. German Patent, 3,445,252, (1986): Chem. Abs., 105, 133748h.

131. U. S. Patent, 3,299,892, (1967).

132. U. S. Patent, 3,362,953, (1968).

133. U. K. Patent, 1,055,831, (1964).

134. S. Hünig, H. Schwarz, Liebigs Ann. Chem., 599, 131, (1956).

135. European Patent 319,234, (1989); Chem. Abs., 112, 22278e.

136. K. A. Bello, J. Griffiths, Dyes and Pigments, 11, 65, (1988).

137. W. Ziebenbein, H. E. Sprenger, Angew. Chem. Int. Ed. Eng., 5, 893, (1966).

138. H. E. Sprenger, W. Ziebenbein, Angew. Chem. Int. Ed. Eng., 5, 894, (1966).

139. German Patent 3,631, 843A1, (1988).

140. H. J. Bernd, U. Peltzmann, R. Peltzmann, Z. Naturforsch, 33(B), (10), 1201, (1978).

141. C. Blackburn, Ph.D Thesis, University of Leeds 1982.

142. U.S. Patent 2,719,861.

143. U.S. Patent 3,013,013.

144. L. F. Dixon, Internal Paper.

145. Aldrich Catalogue of Fine Chemicals.

146. J. S. Whitehurst, J. Chem. Soc., 226, (1951).